

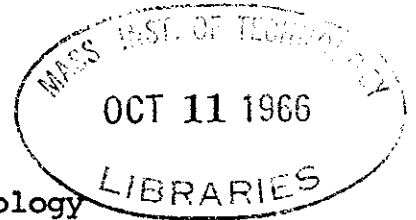
PLANE-STRAIN DEFORMATION ANALYSIS OF SOIL

by

JOHN THOMAS CHRISTIAN

SB, Massachusetts Institute of Technology  
(1958)

SM, Massachusetts Institute of Technology  
(1959)



Submitted in partial fulfillment  
of the requirements for the degree of  
Doctor of Philosophy in Civil Engineering

at the

Massachusetts Institute of Technology  
(1966)

Signature of Author . . . . .  
Department of Civil Engineering, August 22, 1966

Certified by . . . . .  
Thesis Co-Supervisor

Certified by . . . . .  
Thesis Co-Supervisor

Accepted by . . . . .  
Chairman, Departmental Committee on Graduate Students

ABSTRACT

PLANE-STRAIN DEFORMATION ANALYSIS OF SOIL

by

JOHN THOMAS CHRISTIAN

Submitted to the Department of Civil Engineering on August 22, 1966, in partial fulfillment of the requirements for the degree of Doctor of Philosophy in Civil Engineering.

A major problem in soil mechanics is the prediction of stresses and displacements under loads applied to soil masses. Such predictions have usually been made from solutions to classical problems in the theory of linear elasticity even though neither the boundary conditions or the material properties agree with the theory.

The applicability of the theory of plasticity to soil mechanics is examined. Four different yield criteria are proposed: Tresca's, Hencky's and von Mises', Drucker and Prager's generalization of the Mohr-Coulomb law, and a strain-hardening model which allows plastic compression. The large volume changes predicted by the Drucker-Prager criterion are described, and the development of more reasonable strain-hardening models by Roscoe and his associates is summarized. The strain-hardening model used is based on Roscoe's but is simplified for computational reasons.

Analysis leading to incremental stress-strain relations for the four yield criteria is presented. A lumped parameter mathematical model, originally proposed by Ang and Harper (1964), is described and the stress-strain relations are developed in terms of it. A special relation for elastically and plastically incompressible material yielding according to Tresca's or Hencky's and von Mises' criterion, is developed. Computer programs for all five of

these relations and for purely elastic relations were written.

Results of twelve runs on an embankment loading problem are shown. These indicate that the boundary conditions, initial stress state, and yield criterion affect the displacements and stresses in various ways. Vertical stresses are not much affected, but horizontal and shear stresses are greatly dependent on all factors. The final failure load for non-frictional materials agreed in all cases with theoretical predictions. Increasing the horizontal initial compressive stress or using an expansive plastic relation like the Drucker-Prager made the load-displacement curves resemble those for general shear, even though much of the soil might be plastic before the displacements became large. Lower initial horizontal compressive stress or use of the strain-hardening relation gave curves resembling those for local shear. The pattern of plastic yielding is consistent but is much larger than that necessary for limiting equilibrium.

Descriptions of the program use and of the analysis are presented. Suggestions are made for further research in this area and for coordination of laboratory and field measurements with this effort.

Thesis Co-Supervisor: T. William Lambe  
Title: Professor of Civil Engineering

Thesis Co-Supervisor: Robert V. Whitman  
Title: Professor of Civil Engineering

## ACKNOWLEDGMENT

The author is grateful for the efforts of many who have assisted him in his graduate work and on his thesis.

Professor T. William Lambe, Head of the Soil Mechanics Division of the Department of Civil Engineering at M.I.T., was the author's faculty advisor and co-supervisor of his thesis. His encouragement of the writer's studies and research and his continuing interest in his professional development have been invaluable during the past three years.

Professor Robert V. Whitman was co-supervisor of the thesis and first suggested the present line of investigation. He has continued to follow closely the research. His penetrating questions and imaginative suggestions were indispensable in its completion.

Many other members of the faculty and staff of M.I.T. have helped the author. In particular, he must remember several discussions with Professor Kaare Höeg, whose skepticism toward unsupported conclusions has illuminated the work in progress. Mr. H. A. Balakrishna Rao, Research Assistant, and Mr. Carlos Lorente de No have done research in related areas and have made useful comments on the present work. Others too numerous to mention have also helped.

The National Science Foundation provided financial support to the writer by a Graduate Fellowship. Without this support he could not have pursued his graduate studies.

Funds for computer time and some other expenses were provided by contract DA-22-079-eng-427 with the U.S. Army Waterways Experiment Station, Vicksburg, Mississippi. Some of the computer time was bought from the M.I.T. Civil Engineering Systems Laboratory for the IBM 360/40. Most of the work was done on the IBM 7094 at the Computation Center at M.I.T., Cambridge, Massachusetts.

Mrs. Loretta McMaster typed the final draft, and Miss Jacqueline Perry drew most of the figures.

Finally, the author is grateful to his wife, Lynda, for her patience and support during his graduate studies. Her application of classical erudition to his equations and of English scholarship to deciphering his text will be remembered by the writer.

## CONTENTS

	<u>Page</u>
LIST OF FIGURES	9
LIST OF TABLES	12
CHAPTER 1 INTRODUCTION	13
CHAPTER 2 CURRENT PROCEDURE AND PREVIOUS WORK	15
2.1 Present Methods of Analysis	15
2.2 Improvements in Stress Distribution	18
CHAPTER 3 THEORETICAL CONSIDERATIONS	21
3.1 Initial Assumptions	21
3.2 Notation	21
3.3 Elastic Relations	22
3.4 General Forms of Plastic Relations	23
3.5 Elastic-Plastic Relationships	28
3.6 Non-Frictional Material	30
3.6.1 Conventions and Invariants	30
3.6.2 Yield Criteria	34
3.6.3 Incompressible Material	39
3.7 Frictional Materials	40
3.7.1 Drucker and Prager's Generalized Criterion	40
3.7.2 Validity of Drucker-Prager Yield Criterion	43
3.7.3 Capped Yield Criteria	46
3.7.4 Elliptical Cap	49
3.8 Other Stress-Strain Relations	50

	<u>Page</u>
CHAPTER 4    MATHEMATICAL PROCEDURES	52
4.1    Solution of Lumped Parameter Model	52
4.2    Programs Developed	55
4.2.1    General	55
4.2.2    Tresca Material	56
4.2.3    Prandtl-Reuss Material	57
4.2.4    Undrained Material	58
4.2.5    Drucker-Prager Material	59
4.2.6    Strain Hardening Material	60
4.3    Other Comments	61
4.3.1    Errors	61
4.3.2    Initial Stresses	63
CHAPTER 5    RESULTS AND DISCUSSION	65
5.1    General	65
5.2    Effects of Poisson's Ratio	66
5.3    Effects of Boundary and Initial Stress	71
5.4    Effects of Other Yield Criteria	76
5.5    Discussion of Mathematical Model	80
CHAPTER 6    CONCLUSIONS AND FUTURE WORK	83
6.1    Conclusions	83
6.2    Future Work	88
REFERENCES	90
APPENDICES	
A.    List and Definitions of Symbols Used	98

	<u>Page</u>
B. Notation	102
C. Computer Program Use	106
D. Material With No Change of Volume	114
E. Incremental Plastic Stress Strain Relations	123
F. Conversion From $\phi$ and C to $\alpha$ and K	154
 BIOGRAPHY	 159
 FIGURES	 160
 TABLES	 250



## LIST OF FIGURES

	<u>Page</u>
1. TYPES OF PLASTIC BEHAVIOR	160
2. NORMALITY OF PLASTIC STRAIN RATE	161
3. NON-FRICTIONAL YIELD CRITERIA	162
4. MOHR-COULOMB LAW	163
5. FRICTIONAL YIELD CRITERIA	164
6. COULOMB FRICTION FROM DRUCKER-PRAGER CONSTANTS	165
7. COULOMB COHESION FROM DRUCKER-PRAGER CONSTANTS	166
8. STRAIN RATES FOR FRICTIONAL MATERIALS	167
9. CAPPED SURFACES	168
10. ELLIPTICAL SURFACE	169
11. LUMPED PARAMETER MODEL	170
12. FORCE CONVENTION	171
13. STANDARD PROBLEM	172
14. DISPLACEMENTS IN RUNS 1,3, and 4	173
15a,b,c SPREAD OF PLASTIC ZONE-Run 1	174
15d,e,f SPREAD OF PLASTIC ZONE-Run 1	175
16a,b,c SPREAD OF PLASTIC ZONE-Run 2	176
16d,e,f SPREAD OF PLASTIC ZONE-Run 2	177
17a,b,c SPREAD OF PLASTIC ZONE-Run 3	178
17d,e,f SPREAD OF PLASTIC ZONE-Run 3	179
18a,b,c SPREAD OF PLASTIC ZONE-Run 4	180
18d,e,f SPREAD OF PLASTIC ZONE-Run 4	181
19. CONVENTIONS IN STRESS FIGURES	182
20. NORMALIZED ELASTIC STRESSES-Run 1	183

	<u>Page</u>
21. NORMALIZED STRESSES-Run 1	184
22. NORMALIZED ELASTIC STRESSES-Run 2	185
23. NORMALIZED STRESSES-Run 2	186
24. NORMALIZED STRESSES-Run 2	187
25. NORMALIZED ELASTIC STRESSES-Run 3	188
26. NORMALIZED STRESSES-Run 3	189
27. DISPLACEMENT FIELDS-Run 1	190
28. DISPLACEMENT FIELDS-Run 2	191
29. DISPLACEMENT FIELDS-Run 3	192
30. INCREMENTAL DISPLACEMENTS-Run 5	193
31. INCREMENTAL DISPLACEMENTS-Run 5	194
32. INCREMENTAL DISPLACEMENTS-Run 5	195
33. FINAL DISPLACEMENTS-Run 5	196
34. DISPLACEMENTS IN RUN 5	197
35a,b,c SPREAD OF PLASTIC ZONE-Run 5	198
35d,e,f SPREAD OF PLASTIC ZONE-Run 5	199
36. NORMALIZED STRESSES-Run 5	200
37. NORMALIZED STRESSES-Run 5	201
38. NORMALIZED STRESSES-Run 5	202
39. NORMALIZED STRESSES-Run 5	203
40. NORMALIZED STRESSES-Run 5	204
41. NORMALIZED STRESSES-Run 5	205
42. DISPLACEMENTS IN RUN 6	206
43a,b,c SPREAD OF PLASTIC ZONE-Run 6	207
43d,e,f SPREAD OF PLASTIC ZONE-Run 6	208
44. NORMALIZED STRESSES-Run 6	209
45. NORMALIZED STRESSES-Run 6	210

	<u>Page</u>
46. NORMALIZED STRESSES-Run 6	211
47. NORMALIZED STRESSES-Run 6	212
48. NORMALIZED STRESSES-Run 6	213
49. NORMALIZED STRESSES-Run 6	214
50. INCREMENTAL DISPLACEMENTS-Run 6	215
51. INCREMENTAL DISPLACEMENTS-Run 6	216
52. DISPLACEMENTS IN RUN 7	217
53. SPREAD OF PLASTIC ZONE-Run 7	218
54. NORMALIZED STRESSES-Run 7	219
55. NORMALIZED STRESSES-Run 7	220
56. INCREMENTAL DISPLACEMENTS-Run 7	221
57. FINAL DISPLACEMENTS-Run 7	222
58. DISPLACEMENTS IN RUNS 5 AND 8	223
59a,b,c SPREAD OF PLASTIC ZONE-Run 8	224
59d,e,f SPREAD OF PLASTIC ZONE-Run 8	225
60. NORMALIZED STRESSES-Run 8	226
61. NORMALIZED STRESSES-Run 8	227
62. INCREMENTAL DISPLACEMENTS-Run 8	228
63. INCREMENTAL DISPLACEMENTS-Run 8	229
64. DISPLACEMENTS IN RUNS 5 AND 10	230
65a,b,c SPREAD OF PLASTIC ZONE-Run 10	231
65d,e,f SPREAD OF PLASTIC ZONE-Run 10	232
66. NORMALIZED STRESSES-Run 10	233
67. NORMALIZED STRESSES-Run 10	234
68. INCREMENTAL DISPLACEMENTS-Run 10	235
69. INCREMENTAL DISPLACEMENTS-Run 10	236

	<u>Page</u>
70. COMPARISON OF TRESCA AND PRANDTL-REUSS DISPLACEMENTS	237
71. SPREAD OF PLASTIC ZONE-Run 9	238
72. NORMALIZED STRESSES-Run 9	239
73. INCREMENTAL DISPLACEMENTS-Run 9	240
74. DRUCKER-PRAGER DISPLACEMENTS	241
75. SPREAD OF PLASTIC ZONE-Run 12	242
76. NORMALIZED STRESSES-Run 12	243
77. DISPLACEMENTS-Run 12	244
78. VERTICAL DISPLACEMENTS-Run 11	245
79. NORMALIZED STRESSES-Run 11	246
80. STRESS PATHS-Run 11	247
81. DISPLACEMENT FIELDS-Run 11	248
82. INCREMENTAL DISPLACEMENTS-Run 11	249

#### LIST OF TABLES

I	COMPUTER PROGRAMS	250
II	RUNS MADE	251

## CHAPTER 1

### INTRODUCTION

The deformation of soil masses under applied loads is important in the design of almost all civil engineering structures. Like most such problems it requires for its solution a knowledge of material properties, a mathematical solution of equilibrium and continuity equations, and the results of field measurements to verify and refine the first two items. All three of these must exist together.

The recent proliferation of computers and expansion in their capacities has made possible an attack on a large number of problems that were before unsolvable by traditional methods. The present work represents the use of computer approaches to the solution of one common type of soil deformation problem, that involving plane strain, using stress-strain properties predicted by plasticity theory. It is part of a continuing research effort at M.I.T. into analysis of soil deformations. Previous reports have been made by Christian (1965) and Whitman and Hoeg (1965).

The immediate motivation for this work is the necessity to understand the behavior of soil and structure systems under dynamic loads. However, the results are also directly useful in static applications. There is now a concerted effort at M.I.T. to investigate the performance of actual engineering structures by field measurements,

laboratory studies, model studies, and theoretical analyses. The research reported here fits into both these over all efforts.

Conditions of plane strain were assumed and a lumped parameter mathematical model was used to analyze the behavior of a soil layer under an embankment load. Five types of stress-strain behavior were used under various boundary conditions. The programs can be used for any plane rectangular strain geometry and loads can be specified by forces or displacements at any mass point in the lumped parameter array. Only one type of loading was used here, but input requirements for a general loading are described in Appendix C.

## CHAPTER 2

### CURRENT PROCEDURE AND PREVIOUS WORK

#### 2.1 Present Methods of Analysis

It is now the practice to consider that deformation of soils under loads, particularly loads imposed by foundations, can be divided into three stages. First, the soil deforms with no movement of pore water; this is called immediate or "elastic" settlement. Next there is additional, time-dependent movement as the pore water flows out of the soil to relieve the hydraulic pressure built up by the loading. This is the "primary" consolidation. Finally, there is a "secondary" consolidation, which is not well understood and can be construed as including everything that did not happen in the first two stages. Obviously, if the soil has a high permeability, the first two stages will occur rapidly and become indistinguishable, but even in cases of low permeability there is bound to be some vagueness in the demarcation between the three stages.

Almost all analyses based on the above assumptions must begin with a determination of the stresses in the soil. Most such calculations of stress use the linear theory of elasticity or use prepared solutions which are based on it. In particular, a commonly applied solution is that of the problem of Boussinesq, which considers the effect of a vertical point load on the surface of a semi-infinite, homogeneous, isotropic, linearly elastic half space. The

expressions for stress are in a convenient algebraic form that can be found in most books on elasticity theory (e.g.: Timoshenko and Goodier, 1951, Sokolnikoff, 1956, or Love, 1944). Integrations of this solution for vertical stresses under distributed vertical surface loads have been developed into charts (Taylor, 1948, Newmark, 1942, Kondner and Krizek, 1965) or computer programs (Stoll, 1960).

Elasticity theory has also been employed to obtain solutions for cases on the half plane and for circular loadings (Jurgenson, 1934, Terzaghi, 1943). Burmister (1956) has solved the difficult problem of the finite elastic layer loaded on the surface, and his expressions have been integrated by Davis and Poulos (1965). Many other problems can be approximated by results from the theory of linear elasticity.

If the engineer feels confidence in the values of the elastic constants he is using, he can compute displacements directly from an available elastic solution. This approach is usually used for immediate settlements, although Ladd (1964) has shown that Young's modulus is dependent on the stress history of the soil and on the stress level to which the soil is loaded. A further inaccuracy arises because most footing loads are applied at some depth below the surface of the soil. Janbu, Bjerrum, and Kjaernsli (1956) have proposed a chart for correcting the solutions for depth of burial.

Consolidation settlements are usually computed by the Terzaghi one-dimensional consolidation theory (Taylor, 1948).



This requires that the compressibility of the soil be measured in a laterally confined test and then be used under the assumption that the vertical stresses in the field will have the same effect. That the vertical stresses obtained from Boussinesq's problem do not depend on the elastic constants makes this procedure attractive, but the stress and strain conditions in the field and in the laboratory compression test are still only coincidentally the same.

Since the Terzaghi theory states that the consolidation settlement results from dissipation of excess pore pressures, Skempton and Bjerrum (1957) proposed the consolidation settlement be corrected by using the empirical factor,  $A$ , (Skempton, 1954) which describes the tendency of the stresses in the undrained soil to become pore pressures. It is defined for undrained soils by

$$A = \frac{\Delta p - \Delta \sigma_3}{\Delta \sigma_1 - \Delta \sigma_3} , \quad (1)$$

where  $\Delta p$  = change of fluid pressure,

$\Delta \sigma_1$  = change of largest compressive stress,

$\Delta \sigma_3$  = change of smallest compressive stress,

and, for this case, compression is considered positive.

The correction involves reducing the calculated settlements according to a chart as a function of  $A$ .  $A$  is considered a material property even though it can be shown to be

dependent on loading pattern (Appendix D), stress history (Brinch Hansen, 1957), and magnitude of shear stress in relation to failure stress (Ladd, 1964).

Lambe (1964) proposed that these corrections could be avoided by the stress path method of estimating settlements. This involves first calculating, by elastic theory, stresses caused by the load under consideration. Next, triaxial tests are run on samples of similar soil consolidated to the same initial stresses as those in the ground and loaded in the triaxial cell by increments of stress identical to those calculated. The undrained, primary consolidation, and secondary consolidation strains can be measured and displacements calculated by integrating the strains over the depth represented by the sample. Davis and Poulos (1963) have presented a similar technique. Both of these procedures require that the sample of soil be chosen and loaded so it is representative of the entire soil layer.

## 2.2 Improvements in Stress Distribution

In all the methods described above the stress distributions are based on linear, isotropic, homogeneous elastic theory for relatively simple boundary conditions. One of the first improvements was proposed by Biot (1941 a, b, c), who described soil as a two phase system composed of a porous elastic skeleton and a fluid, which is assumed incompressible in all solutions known to the

author. Although this is an idealized picture of soil, solutions to specific problems have been few and are usually rather complicated (McNamee and Gibson, 1960a,b). The solutions do show that the stress pattern changes with consolidation, sometimes dramatically (Gibson, Knight, and Taylor, 1963, Josselin de Jong, 1965). Davis and Poulos (1965) have developed an approximate technique for solving some problems by ignoring certain coupling effects.

Developments in computation methods have made possible the analysis of more complicated problems than those that could be treated with closed form analytic techniques. Finite differences have been used for complicated loadings on linearly elastic bodies. Examples include solution for the Airy stress function in plane strain (Allen, 1954, Dingwall and Scrivner, 1954) and direct solution of the finite difference forms of the partial differential equations of equilibrium for plane strain (Schjødt, 1958) or for axially symmetric loadings (Wilson, 1948). Bendel (1962) has applied such techniques to an elastic-perfectly-plastic frictional material under plane strain conditions in the cross-section of a dam.

A second technique involves dividing the body into many discrete "finite elements" whose strains can be approximated from the displacement of a few points around each element. These have been used to solve problems in linear elasticity for plane stress conditions (Clough, 1960), for conditions of axial symmetry (Clough and Rashid, 1965), and for three-dimensional situations (Argyris, 1965

a,b). Non-elastic problems have been treated by Argyris (1965a,b) using deformation theories of plasticity and by Reyes (1965) using incremental plasticity for a frictional material in plane strain.

The mathematical model used here was developed by Ang and Harper (1965). Whitman (1964) proposed using it to investigate the behavior of soil under various assumptions of elastic and plastic stress-strain behavior. A special case of the model for undrained elastic soils under plane strain conditions was developed by Christian (1965) and is described briefly in Appendix D. The initial results of the elastic-plastic calculations were presented by Whitman and Hoeg (1965).

## CHAPTER 3

### THEORETICAL CONSIDERATIONS

#### 3.1 Initial Assumptions

Soil is a complicated material, and any mathematical representation of a stress-strain law is bound to be a stark idealization. In this work certain reasonable assumptions and simplifications were made in all analyses. They could be changed in further developments of the research effort.

First, the soil was assumed to be non-viscous; that is, the mechanical behavior was not time dependent. Second, the soil was made isotropic and homogeneous except for anisotropies or inhomogeneities induced by plastic flow. Third, the stress-strain behavior was described by the incremental theory of plasticity.

#### 3.2 Notation

In the remainder of the exposition the notation conventions are compromises between traditional soil mechanics usage and continuum mechanics usage. Appendix B contains a description of the differences between soil mechanics notation and that adopted here. The most important features are mentioned below.

All stresses are positive in tension, and all strains are positive in extension. Subscripts refer to orthogonal

Cartesian axes. Stresses are represented by a subscripted  $\sigma$ , and strains are represented by a subscripted  $\epsilon$ . The same symbols without subscripts refer to volumetric stresses and strains, respectively. The deviatoric stresses and strains are represented by subscripted  $s$  and  $e$ , respectively.

The Einstein summation convention over repeated subscripts is used whenever the subscripts are the letters  $i$  through  $n$ . The Kronecker delta is used.

A dot over a symbol indicates the rate of the quantity; that is, its time derivative, or, if it is not time-dependent, its incremental increase during the loading process. The superscripts (e) and (p) over strain quantities indicate the elastic and plastic components, respectively. A symbol without a superscript is the total of elastic and plastic strain when both exist.

### 3.3 Elastic Relations

The constitutive relationships of linear elasticity (Timoshenko and Goodier, 1951, or Sokolnikoff, 1956) can be expressed for an isotropic body as

$$\epsilon_{ij} = \frac{1+\nu}{E} \sigma_{ij} - \frac{\nu}{E} \sigma_{kk} \delta_{ij}, \quad (2)$$

or, in more conventional notation,

$$\epsilon_{xx} = \frac{1}{E} [\sigma_{xx} - \nu(\sigma_{yy} - \sigma_{zz})], \text{ etc.}$$

and

$$\gamma_{xy} = 2 \epsilon_{xy} = \frac{1}{G} \sigma_{xy} = \frac{1}{G} \tau_{xy}, \text{ etc.} \quad (2a)$$

In the case of plane strain  $\epsilon_{xz}$ ,  $\epsilon_{yz}$ , and  $\epsilon_{zz}$  are all equal to zero, so equation (2) can be converted into

$$\sigma_{xx} = \frac{E}{(1-2\nu)(1+\nu)} [(1-\nu)\epsilon_{xx} + \nu\epsilon_{yy}], \text{ etc.}$$

and

$$\sigma_{xy} = \frac{E}{2(1+\nu)} \gamma_{xy}. \quad (3)$$

These relations apply to a body that has not yielded plastically.

### 3.4 General Forms of Plastic Relations

There are two theories of plasticity: the deformation theory, and the incremental theory (Hill, 1950). The difference between them arises from the way they relate plastic strains to stresses. In the deformation theory the plastic strains are dependent directly on the stresses, but in the incremental theory the basic relationship is between strain rate and existing stresses and stress rate. Both assume the soil is elastic or rigid until the

stresses satisfy a yield criterion, after which the material is plastic. When the loading involves a constant ratio of applied loads, the two theories can be made identical (Fung, 1965), but Hill(1950) has shown that there are mathematical inconsistencies in the deformation theory for general loading patterns. Because the deformation theory leads to more convenient stress-strain relationships, it has been favored by those working with finite elements (Clough, 1965, Argyris, 1965a,b).

Within the incremental theory materials can be divided into perfectly plastic ones and strain hardening ones. Incremental perfect plasticity has been described mathematically by several authors (Hill, 1950, Prager, 1959). It postulates that the material yields when the stresses satisfy the yield function or yield criterion,  $f$ , so that

$$f(\sigma_{ij}) = 0 \quad (4)$$

In the absence of any further constraint the body would then flow plastically. Figure 1a shows a stress-strain diagram for a tension specimen of a rigid-plastic material, for which there is no strain below yield. Figure 1b shows such a diagram for an elastic-perfectly-plastic material, which has elastic strains below yield.

Figure 1c demonstrates strain hardening behavior. In this case the material starts yielding when the stresses reach a critical value defined by a yield function,  $f$ ,



but now the yield function changes as plastic strain occurs, so  $f$  is defined by

$$f(\sigma_{ij}, \epsilon_{ij}^{(P)}, K) = 0, \quad (5)$$

where  $K$  is a term dependent on the plastic strain and

$\epsilon_{ij}^{(P)}$  is the plastic strain.

Drucker (1950, 1951, 1954) has described the general concept of a stable material as one on which an increment of load does positive or zero work during a full cycle of loading and unloading. He has shown that, if such a material has plastic strain increments whose principal axes coincide with the principal axes of stress, there must follow that the yield function is convex around the origin when plotted in coordinates of stress and that the plastic strain increment is a vector normal to this yield surface. Drucker's stability definition can be regarded as a way of prescribing that the material must not collapse during yielding or, in other words, that its strength must not decrease during failure under increasing loads.

The results of Drucker's theoretical work are shown in Figure 2. The curve,  $f$ , is the yield function plotted in stress coordinates,  $\sigma_{ij}$  is the stress at plastic yielding, and  $\dot{\epsilon}_{ij}^{(P)}$  is the plastic strain increment. It follows that  $\dot{\epsilon}_{ij}^*$  is not an admissible plastic strain increment. The

same result has been demonstrated from thermodynamic considerations by Ziegler (1963) and Aldrich (1966). The conclusion is known as the normality condition.

A mathematical statement of the normality condition follows from the recognition that both the plastic strain increment and the gradient of the convex yield function are normal to it. Drucker (1951) shows that for a perfectly plastic material the two must be proportional:

$$\dot{\epsilon}_{ij}^{(P)} = \lambda \frac{\partial f}{\partial \sigma_{ij}} \quad (6)$$

In this expression  $\lambda$  is a constant to be determined. The equation states the theory of the plastic potential, which is basic to much of plasticity theory (Hill, 1950, Prager, 1959).

Because the function,  $f$ , depends only on the stress, equation (6) can also be written

$$\dot{\epsilon}_{ij}^{(P)} = \lambda g(\sigma_{ij}), \quad (7)$$

where  $g$  is a function of stress and is the gradient of  $f$ . Equation (7) resembles the equation of Newtonian viscosity, and  $\lambda$  does indeed have the dimensions of a viscosity. The relation is not, however, a viscous one because the dot over the epsilon does not denote differentiation with

respect to time but merely indicates that the relation applies to some infinitesimally small strain increment. The strain can occur slowly or rapidly so long as it is the same increment. This distinction must be borne in mind, for the incremental stresses and strains are often referred to as stress or strain rates without implication that the phenomena involved are dependent on time. Similarly, incremental displacements are often referred to as velocities.

For the strain hardening materials the expressions of the plastic potential theory can be derived by differentiating equation (5) to obtain

$$\dot{f} = \frac{\partial}{\partial \sigma_{ij}} \dot{\sigma}_{ij} + \frac{\partial f}{\partial \epsilon_{ij}^{(P)}} \dot{\epsilon}_{ij}^{(P)} + \frac{\partial f}{\partial K} \frac{\partial K}{\partial \epsilon_{ij}^{(P)}} \dot{\epsilon}_{ij}^{(P)} = 0 \quad (8)$$

If normality holds, terms can be collected to give

$$\dot{\epsilon}_{ij}^{(P)} = \Lambda \frac{\partial f}{\partial \sigma_{ij}} \quad (9)$$

and

$$\Lambda = - \frac{\frac{\partial f}{\partial \sigma_{kl}} \dot{\sigma}_{kl}}{\frac{\partial f}{\partial \epsilon_{ij}^{(P)}} + \frac{\partial f}{\partial K} \frac{\partial K}{\partial \epsilon_{ij}^{(P)}} \frac{\partial f}{\partial \sigma_{ij}}} \quad (10)$$

These can be written in another form, which is often more

convenient,

$$\dot{\epsilon}_{ij}^{(P)} = \hat{G} \frac{\partial f}{\partial \sigma_{ij}} \frac{\partial f}{\partial \sigma_{kl}} \dot{\sigma}_{kl} \quad (11)$$

and

$$\hat{G} = - \frac{1}{\left( \frac{\partial f}{\partial \epsilon_{mn}}^{(P)} + \frac{\partial f}{\partial K} \frac{\partial K}{\partial \epsilon_{mn}}^{(P)} \right) \frac{\partial f}{\partial \sigma_{mn}}} \quad (12)$$

The expression for  $\hat{G}$  is a scalar function which can be evaluated algebraically.

### 3.5 Elastic-Plastic Relationships

When a material has yielded and is flowing plastically, it also continues to undergo elastic strains. If the stresses should become less than those required to satisfy the yield criterion, the strains will become elastic only. No stress state is allowed which exceeds the yield criterion. These three rules can be summarized thus:

$$\begin{aligned} \dot{\epsilon}_{ij} &= \dot{\epsilon}_{ij}^{(e)} & \text{if } f < 0, \\ \dot{\epsilon}_{ij} &= \dot{\epsilon}_{ij}^{(e)} + \dot{\epsilon}_{ij}^{(p)} & \text{if } f = 0, \end{aligned} \quad (13)$$

and  $f > 0$  is inadmissible.

The elastic relations of stress and strain are stated in section 3.3. The relations for elastic-plastic materials can be of two forms, depending on whether the material is perfectly plastic or strain hardening.

The elastic-perfectly-plastic relations are

$$\dot{\epsilon}_{ij} = \dot{\epsilon}_{ij}^{(e)} + \lambda \frac{\partial f}{\partial \sigma_{ij}} \quad (14)$$

or

$$\dot{\epsilon}_{ij} = \frac{1+\nu}{E} \dot{\sigma}_{ij} - \frac{\nu}{E} \dot{\sigma}_{kk} \delta_{ij} + \lambda \frac{\partial f}{\partial \sigma_{ij}} \quad (15)$$

In these equations  $\lambda$  must be determined from the additional condition that the stresses cannot violate equation (4).

The relations for the strain hardening material will be

$$\dot{\epsilon}_{ij} = \frac{1+\nu}{E} \dot{\sigma}_{ij} - \frac{\nu}{E} \dot{\sigma}_{kk} \delta_{ij} + \hat{G} \frac{\partial f}{\partial \sigma_{ij}} \frac{\partial f}{\partial \sigma_{kl}} \dot{\sigma}_{kl} \quad (16)$$

In this equation the  $\hat{G}$  is determined from equation (12).

In subsequent sections these relations are specialized for the various yield criteria considered. Nevertheless, in all cases the general forms are those of equation (15) or equation (16).

### 3.6 Non-Frictional Material

#### 3.6.1 Conventions and Invariants

The stress,  $\sigma_{ij}$ , acting on a point can be written as a three by three array

$$\sigma_{ij} = \begin{bmatrix} \sigma_{11} & \sigma_{12} & \sigma_{13} \\ \sigma_{21} & \sigma_{22} & \sigma_{23} \\ \sigma_{31} & \sigma_{32} & \sigma_{33} \end{bmatrix} \quad (17)$$

the elements of which change values as the coordinates change. The array transforms according to the rules for a second order tensor (Sokolnikoff, 1956), so  $\sigma_{ij}$  is called the stress tensor. It is also known that this tensor is symmetrical, i.e.  $\sigma_{xy} = \sigma_{yx}$ . In the coordinate system  $(x,y,z)$  the stress tensor is

$$\sigma_{ij} = \begin{bmatrix} \sigma_{xx} & \sigma_{xy} & \sigma_{xz} \\ \sigma_{xy} & \sigma_{yy} & \sigma_{yz} \\ \sigma_{xz} & \sigma_{yz} & \sigma_{zz} \end{bmatrix} = \begin{bmatrix} \sigma_{xx} & \tau_{xy} & \tau_{xz} \\ \tau_{xy} & \sigma_{yy} & \tau_{yz} \\ \tau_{xz} & \tau_{yz} & \sigma_{zz} \end{bmatrix} \quad (18)$$

It is a fundamental result of the theories of tensor algebra and matrix algebra that such an array has three invariants, or algebraic functions of the elements of the

array that do not change even though the elements change value as the coordinates transform. These are defined by the three relations

$$I_1 = \sigma_{11} + \sigma_{22} + \sigma_{33} = \sigma_{ii} \quad (19)$$

$$I_2 = \begin{vmatrix} \sigma_{11} & \sigma_{12} \\ \sigma_{12} & \sigma_{22} \end{vmatrix} + \begin{vmatrix} \sigma_{11} & \sigma_{13} \\ \sigma_{13} & \sigma_{33} \end{vmatrix} + \begin{vmatrix} \sigma_{22} & \sigma_{23} \\ \sigma_{23} & \sigma_{33} \end{vmatrix} \quad (20)$$

$$I_3 = \begin{vmatrix} \sigma_{11} & \sigma_{12} & \sigma_{13} \\ \sigma_{12} & \sigma_{22} & \sigma_{23} \\ \sigma_{13} & \sigma_{23} & \sigma_{33} \end{vmatrix} \quad (21)$$

Another important result is that there must be some coordinate directions such that when the stress tensor is transformed into those coordinates only the diagonal elements are non-zero. These are the principal stresses, designated by  $\sigma_1, \sigma_2, \sigma_3$ . In terms of the principal stresses the invariants become

$$I_1 = \sigma_1 + \sigma_2 + \sigma_3 \quad (22)$$

$$I_2 = \sigma_1\sigma_2 + \sigma_1\sigma_3 + \sigma_2\sigma_3 \quad (23)$$

$$I_3 = \sigma_1\sigma_2\sigma_3 \quad (24)$$

One third of the first invariant of stress is the hydrostatic component of the stress or the volumetric stress,  $\sigma$ . It is a tensor with the elementary form

$$\sigma = \begin{bmatrix} \sigma & 0 & 0 \\ 0 & \sigma & 0 \\ 0 & 0 & \sigma \end{bmatrix} \quad (25)$$

which does not change when the coordinates change.

If the volumetric stress tensor,  $\sigma$ , is subtracted from the stress tensor,  $\sigma_{ij}$ , a new tensor,  $s_{ij}$ , results:

$$s_{ij} = \sigma_{ij} - \sigma \delta_{ij}, \quad (26)$$

or

$$s_{ij} = \begin{bmatrix} \sigma_{11} - \sigma & \sigma_{12} & \sigma_{13} \\ \sigma_{12} & \sigma_{22} - \sigma & \sigma_{23} \\ \sigma_{13} & \sigma_{23} & \sigma_{33} - \sigma \end{bmatrix} \quad (26a)$$

$$= \begin{bmatrix} s_{11} & s_{12} & s_{13} \\ s_{12} & s_{22} & s_{23} \\ s_{13} & s_{23} & s_{33} \end{bmatrix} \quad (26b)$$



This is called the stress deviator tensor or the deviatoric stress tensor, and it is not the same as the deviator stress used in triaxial testing of soil. Since it is a tensor, it too possesses invariants, which will be designated  $J_1$ ,  $J_2$ , and  $J_3$  to distinguish them from  $I_1$ ,  $I_2$ , and  $I_3$ .

The first invariant of the deviator stress

$$J_1 = \sigma_{11} - \sigma + \sigma_{22} - \sigma + \sigma_{33} - \sigma = I_1 - 3\sigma = 0. \quad (27)$$

Thus, the deviator stress tensor has no hydrostatic component but represents purely deformational stress, while the volumetric stress has only a hydrostatic component. This division of the tensor is a convenient way to separate the effects of these two components of stress. The three tensors,  $\sigma_{ij}$ ,  $s_{ij}$ , and  $\sigma$ , all have the same principal directions.

A similar analysis can be performed on the symmetrical infinitesimal strain tensor,  $\epsilon_{ij}$ . This leads to a total strain tensor,

$$\epsilon_{ij} = \begin{bmatrix} \epsilon_{11} & \epsilon_{12} & \epsilon_{13} \\ \epsilon_{12} & \epsilon_{22} & \epsilon_{23} \\ \epsilon_{13} & \epsilon_{23} & \epsilon_{33} \end{bmatrix} \quad (28)$$

a volumetric strain tensor or dilatation,

$$\epsilon = \begin{bmatrix} \epsilon & 0 & 0 \\ 0 & \epsilon & 0 \\ 0 & 0 & \epsilon \end{bmatrix} \quad (29)$$

and a deviator strain tensor,

$$e_{ij} = \begin{bmatrix} e_{11} & e_{12} & e_{13} \\ e_{12} & e_{22} & e_{23} \\ e_{13} & e_{23} & e_{33} \end{bmatrix} \quad (30)$$

Again

$$\epsilon_{ij} = \epsilon \delta_{ij} + e_{ij} \quad (31)$$

These strain tensors possess invariants and principal directions like those of the stress tensors, but they will not be used in what follows.

### 3.6.2 Yield Criteria

A non-frictional material is one whose strength or yield criterion does not depend on volumetric stress or strain. Many engineering materials are included in this definition, and saturated clays are often considered unaffected by volumetric stress in the " $\phi = 0$ " analysis (Skempton, 1948). Since the yielding does not depend on the volumetric stress, the yield function will not depend

on  $I_1$ , or

$$\frac{\partial f}{\partial I_1} = \frac{\partial f}{\partial \sigma_{ii}} = 0 \quad (32)$$

The plastic volumetric strain rate is, therefore,

$$3\dot{\epsilon}^{(p)} = \dot{\epsilon}_{ii}^{(p)} = \lambda \frac{\partial f}{\partial \sigma_{ii}} = 0 \quad (33)$$

There are two generally recognized yield criteria for non-frictional materials, one named after Tresca and the other after von Mises and Hencky. The Tresca criterion specifies that yielding occurs when the maximum shear stress exceeds a critical value,  $k$ . If it is known that the major and minor principal stresses are in the plane  $(x,y)$ , this criterion can be stated

$$\left( \frac{\sigma_{xx} - \sigma_{yy}}{2} \right)^2 + \tau_{xy}^2 = k^2 \quad (34)$$

The Hencky-von Mises criterion is stated by the equation

$$J_2 = k^2 \quad (35)$$

This expression accounts for all the principal stresses and is much simpler for mathematical purposes, but its physical meaning is not immediately clear. Novozhilov

(1952) has obtained the criterion by considering a sphere as it deforms elastically. Such a body has all orientations of faces distributed equally. If a limit is set on the root mean square of the shear strain on all orientations of faces, the controlling stress function becomes proportional to the Hencky-von Mises criterion.

When these two yield functions are plotted in coordinates of principal stress, they appear as a hexagonal prism and a right circular cylinder, respectively. The common central axis is the line of volumetric stress ( $\sigma_1 = \sigma_2 = \sigma_3$ ). Figure 3a shows this representation. Since there is no change along the volumetric stress line, the figure can be equally well represented by a cross section perpendicular to that line which is shown in Figure 3b as seen by an observer looking down that line toward the origin. Distances in this figure measured from the origin parallel to the  $\sigma_1$ ,  $\sigma_2$ , and  $\sigma_3$  axes are proportional to the  $s_1$ ,  $s_2$ , and  $s_3$  components of the stress, respectively.

Stress-strain relationships for the elastic-plastic materials which yield according to these criteria are derived in Appendix E. Both derivations follow similar lines. For the material that follows the Hencky-von Mises criterion a rate of deformational work is defined by

$$\dot{W} = s_{ij} \dot{e}_{ij}. \quad (35)$$

There being no volumetric plastic strain, equation (6) can be written

$$\dot{\epsilon}_{ij}^{(p)} = \lambda \frac{\partial f}{\partial s_{ij}} \quad (36)$$

The unknown constant,  $\lambda$ , is then found to be

$$\lambda = \frac{G\dot{W}}{k^2} \quad (37)$$

The difference between the stress-strain relations resulting from the two criteria involves the effect of the intermediate principal stress, strain, and strain rate. Since the Tresca criterion is independent of the intermediate principal stress, there must be no plastic strain in the direction of intermediate principal stress. For plane strain conditions this will usually be the direction normal to the plane.

A graphical view of this can be seen in Figure 3b, where a strain rate,  $\dot{\epsilon}_{ij}^{(p)}$ , normal to the Tresca surface at a point C, is seen to be normal to the axis labelled  $\sigma_2$ , which actually represents  $s_2$ . Therefore, there is no component of the deviatoric strain rate in the  $\sigma_2$  direction, and it has been shown previously that there is no volumetric plastic strain. The total plastic strain rate must have no component in the  $\sigma_2$  direction.

If the Hencky-von Mises criterion applies, the situation is quite different. A strain rate,  $\dot{\epsilon}_{ij}^{(p)}$ , drawn

at point D in Figure 3b obviously does have a component in the  $\sigma_2$  direction. There will be plastic straining normal to the plane, which must be countered by equal and opposite elastic strains to maintain zero total normal strain. The intermediate principal stress,  $\sigma_2$ , will necessarily increase more rapidly than it would if the material were still elastic. The resulting movement of the stresses from point D to point A in Figure 3b has been demonstrated analytically by Hill (1950). When the stresses are at point A, the strain rate is again normal to  $\sigma_2$ , and no more plastic strain normal to the plane of plane strain occurs.

It is possible for a material obeying the Hencky-von Mises criterion and loaded under plane strain conditions to have no plastic strain normal to the plane under two special conditions. The first is that the elastic strains are so small that the material is considered rigid before yielding. Then all strains are plastic, so the normal plastic strain must be zero. Such a material is called a von Mises material by Prager and Hodge (1951) to distinguish it from the elastic-plastic material obeying the same yield criterion, which is usually called the Prandtl-Reuss material. It will be called that here.

The second special case occurs when the Poisson's ratio for the elastic portion of the behavior is equal to one-half. For plane strain conditions the elastic stress

normal to the plane will be equal to the volumetric stress, and the corresponding deviatoric stress component will be zero. The stresses must therefore meet the yield criterion at point A or point A' in Figure 3b, where the strain rate has no component in the  $\sigma_2$  direction. It should be noted that, for an elastically incompressible material, both the Tresca and Prandtl-Reuss materials give the same results in plane strain.

### 3.6.3 Incompressible Material

Soil loaded so rapidly that pore fluid cannot escape is often considered elastically incompressible, and it is necessary to have solutions for stress distributions in such a material. When closed form solutions exist for a general isotropic, linearly elastic body, they can be made to apply to the incompressible case by setting Poisson's ratio to one half, making the bulk modulus infinite. Davis and Poulos (1965) have applied this approach to the Burmister (1956) solutions of an elastic layer in cylindrical coordinates.

When finite difference or finite element methods are used, the problem cannot be so easily treated. Such techniques involve the calculation of stresses from displacements, and it can be seen from equation (3) that directly setting Poisson's ratio to one half would make the denominator of the elastic expression equal to zero. This

results from the special problem that the volumetric stresses are independent of the volumetric strains, so some modification is necessary in formulating the mathematical model.

The modifications were developed from the effective stress principle of soil mechanics. This states that soil is a two-phase system, one phase a soil skeleton and the other a pore fluid. The two phases have different stress-strain properties, but, if no flow of the pore fluid occurs, the strains must be identical in the two phases. Any stress applied to the material as a whole is carried partly by the skeleton as "effective stress" and partly by the pore fluid as "pore pressure". This allows the creation of a model similar to Biot's (1941a,b,c) porous elastic consolidation model.

The skeleton of the soil is considered here an elastic-perfectly-plastic porous material whose behavior is described by the elastic constants  $E$  and  $\nu$  and by the plastic yield stress,  $k$ . The pore fluid is incompressible and has no shear strength. In other words, the skeleton has finite values of bulk modulus,  $K$ , and shear modulus,  $G$ , and the pore fluid has an infinite  $K$  and zero  $G$ . The two phases deform together so that their strains are compatible. A more detailed description of the analysis for this material is in Appendix D.

### 3.7 Frictional Materials

#### 3.7.1 Drucker and Prager's Generalized Criterion

The yield criteria considered above require that the



strength of the material not be dependent on the volumetric stress. For rapid, undrained loading of soil this may be close to the truth (Skempton, 1954), but it is not generally so for slower, drained loadings. The shear strength then increases with normal stress on the failure plane according to the Mohr-Coulomb law:

$$\tau = c + \sigma \tan \phi, \quad (44)$$

where  $\tau$  is the shear strength on the surface of failure,  
 $c$  is a physical constant called "cohesion"  
 $\sigma$  is the normal stress on the surface of failure, and  
 $\phi$  is a physical constant called the "angle of friction"

This law is generally accepted as valid for failure conditions even though experimental determination of  $c$  and  $\phi$  is the subject of controversy and the two physical constants can vary with void ratio of the soil, relative density, previous consolidation history, and perhaps the stress system. The relation can be plotted as shown in Figure 4, where tensile stresses are positive.

Use of Mohr's circle in Figure 4 allows the law to be written in the form

$$\frac{\sigma_1 - \sigma_3}{2} + \frac{\sigma_1 + \sigma_3}{2} \cos \phi = c \cos \phi, \quad (45)$$

where  $\sigma_1$  and  $\sigma_3$  are major and minor principal stresses,

and in the form

$$\left(\frac{\sigma_{yy} - \sigma_{xx}}{2}\right)^2 + \tau_{xy}^2 + \frac{\sigma_{xx} + \sigma_{yy}}{2} \cos \phi = c \cos \phi \quad (46)$$

Two questions arise from examination of these relations:

- a) How, if at all, should the effect of the stresses out of the  $(\sigma_1, \sigma_3)$  plane be considered?
- b) Is this a yield criterion?

If the effects of intermediate stress are ignored, the relation can be plotted in Figure 5a against axes of principal stress, and a cross-section normal to the volumetric stress line can be plotted as in Figure 5b. The surface is an irregular, hexagonal pyramid. These plots assume that when  $\sigma_2$  becomes a major or minor principal stress it is substituted for the appropriate quantity in the equation (45).

Prager and Drucker (1952) have suggested the following generalization of the Mohr-Coulomb law to account for all principal stresses:

$$\alpha I_1 + J_2^{\frac{1}{2}} = k, \quad (47)$$

where  $\alpha$  and  $k$  are physical constants. It plots as a right circular cone in Figure 5.

The constants  $\alpha$  and  $k$  are not uniquely related to  $c$  and  $\phi$  because of the effect of the intermediate principal stress. In Appendix F relations between these terms are derived for conditions of plane strain, axially symmetric compression, and axially symmetric extension. The results, plotted in Figures 6 and 7, show that the Mohr-Coulomb surface must be adjusted to touch the Prager-Drucker surface at a line corresponding to the stress conditions. In Figure 5 points A and A' correspond to axial compression, point B to axial extension, and points C and C' to plane strain. Points C and C' will move along their respective yield surfaces as Poisson's ratio for the elastic behavior varies.

Which of these two frictional criteria to use is difficult to decide, in part because, as is explained in the next section, there is ground for doubting the validity of either as a yield criterion. Since the Prager-Drucker form does not have "corners", it has been chosen here for mathematical convenience.

### 3.7.2 Validity of Drucker-Prager Yield Criterion

Prager and Drucker (1952) showed that their generalization of the Mohr-Coulomb law in combination with the normality rule predicts plastic volumetric strains according to the equation

$$\dot{\epsilon}^{(p)} = \lambda \frac{\partial f}{\partial \sigma} = 3\lambda\alpha \quad (48)$$

This means there must be positive (expansive) volume changes during drained plastic strain. The same result can be seen from Figure 8, in which the outward normal to the Prager-Drucker surface clearly has a positive volumetric component. The same conclusion would also apply to the Mohr-Coulomb law if it were used as a yield criterion.

It is a well established fact of soil mechanics (Henkel, 1958, Ladd, 1964) that some soils, such as over-consolidated clays and dense sands, do expand at the early stages of shear. Others, such as normally consolidated clays and loose sands, compress during shear. Inorganic clays tend to arrive at a stable volume after shear so that further distortion continues with no volume change. This behavior is obviously in conflict with Prager and Drucker's predictions from the generalized Mohr-Coulomb law, and they clearly recognized this.

There are several possible solutions for the dilemma. First, the material may be yielding on a number of discrete surfaces. Second, the normality rule may not apply. Third, the Mohr-Coulomb and Drucker-Prager laws may not be yield criteria in the sense meant by plasticity theory. Finally, plasticity theory may not apply to soils.

The first objection, that the soil may not yield as a mass, is certainly valid in many cases, as Prager and Drucker (1952) and Brinch Hansen (1953) have pointed out. The soil, failing along separate surfaces, behaves essentially

as two or more solids sliding past each other. Since the thickness of these zones is vanishingly small, there is a small volume of yielding material and no measurable volume change. Drucker (1954) has demonstrated that an assemblage of sliding masses is not necessarily stable, so the limit theorems of plasticity theory cannot be shown to apply to such an assemblage. The bearing capacity formulas of soil mechanics (Terzaghi, 1943) are applications of the limit theorems, and they also assume a yielding mass rather than an arrangement of blocks. Further, it is reasonable that some soft soils must flow in a mass, especially under contained flow conditions. For these reasons this objection cannot be the only explanation of the problem. The mathematical model adopted here for computations cannot at this time be used for cases of thin line failures, and this mode of yielding is not considered further.

The proposition that normality may not apply has been advanced by several writers. Brinch Hansen (1953) and Takagi (1962), for example, have solved problems of limiting equilibrium or plastic flow by assuming the Mohr-Coulomb criterion is valid but normality is not. The stresses satisfy the Mohr-Coulomb law, but the strains and strain rates satisfy boundary conditions or assumed conditions of no volume change. If it were possible to determine beforehand what sort of volume change could be expected, this type of approach could also be used for contained flow.

Rowe's (1962) stress-dilatancy relations are possibly useful for such an empirical approach.

The major difficulty arising from discarding normality is that it eliminates the proof of the limiting equilibrium theories of plasticity, leaving them only intuitively supported (Drucker and Prager, 1952). These are among the most useful results of the theory and are widely used in soil mechanics for analysis of bearing capacity, lateral earth pressures, and slope stability. In addition, lack of normality implies the material is unstable in Drucker's sense or becomes instantaneously anisotropic with respect to strain rates. Both of these are unreasonable as general assumptions.

The last two possible alternatives to the consequences of the frictional yield criteria are discussed in the following sections.

### 3.7.3 Capped Yield Surfaces

Because the consequences of abandoning normality seem to be as unpleasant as those of retaining it for the frictional criteria, it is attractive to consider the possibility of another yield criterion. The techniques developed for computation in plastic flow problems in which the stresses satisfy the Mohr-Coulomb law and the strain rates do not remain normal to its surface may still be valid if it turns out there is another yield surface which intersects the

Mohr-Coulomb surface at the stress in question but at an angle. Such a situation is illustrated in Figure 8. The curved surface intersects the Drucker-Prager surface at point A. The normal to the curved surface is not normal to the Drucker-Prager surface. Thus, normality is satisfied if the curved surface is the yield surface, but it is not if the Drucker-Prager or Mohr-Coulomb laws are the yield surfaces. Drucker, Henkel, and Gibson (1957) suggested such a solution to the normality problem.

These authors proposed that the yield surface for soils should look like the Mohr-Coulomb surface except that it should be capped at the open end by a dome which would expand and contract as the volume of the soil changed. The dome was assumed spherical for simplicity. Figure 9a shows a cross-section through such a surface cut by a plane on which  $\sigma_2$  is equal to  $\sigma_3$ , that is, a plane of stresses possible in a triaxial test.

If a triaxial sample were consolidated isotropically from point A to point B, the cap would move along the isotropic line with the stress. The effective stress path for subsequent undrained shearing would follow the cap of the yield surface from B to C. The normal to this surface has a negative (compressive) volumetric strain rate component, which would be countered by an increase in compressive pore pressure. This would decrease the effective compressive volumetric stress to allow elastic expansion to balance the plastic compression. The net effect

would be no volume change. At point C the normal would have no volumetric component, and further tendency for volume change would cease.

Experimental results (Henkel, 1958) indicate that this theory is too simple for soils because, among other things, it predicts strain rates which do not agree with the data from laboratory triaxial shear tests. Since then the more accurate definition of the plastic behavior of soils has concerned Roscoe and his associates (1958, 1963), who have made several modifications to the basic capped yield criterion theory.

First, they have shown that the yield criterion moves during shear to make the soil a strain hardening or softening material. The position of the surface is assumed to be a function of the plastic volumetric strain. Second, they have described a bullet-shaped yield surface, pointed at the isotropic end, like that shown in Figure 9b. Third, they have assumed all deviatoric strains are plastic, which makes the material rigid with respect to deformation in the elastic range. The only elastic strains are volumetric. This is not a necessary assumption, but it greatly simplifies the analysis of the soil behavior while still being fairly reasonable.

A sample of soil consolidated isotropically would be represented by the point A in Figure 9b. The yield surface would be the line AB. As the soil was sheared, the yield surface would move out until the stresses reached point C,



where the normal to the yield surface would have no volumetric component. This is called the "critical voids ratio line" by Roscoe.

A heavily over-consolidated soil might be initially at a point such as D in Figure 9b, but there is very little evidence about the plastic behavior of such a soil. It can be assumed intuitively that an over-consolidated soil would be strain softening. Its stresses would move elastically from D to some point E, whereupon plastic yielding would start and the yield surface would collapse. The stresses would finally reach the critical voids ratio line at a point F. Such a material would be unstable and would probably develop failure along discrete cracks rather than in the mass.

#### 3.7.4 Elliptical Cap

For the purposes of this research a simplified, composite mathematical model was adopted. The soil was assumed elastic-plastic with strain hardening as a result of plastic volumetric strain. The yield surface was assumed to be elliptical when plotted as in Figure 10. The position of the ellipse is defined by its center (points A and B), and the movement of the ellipse during plastic strain is linearly dependent on the plastic volumetric strain. Thus, if the stresses move from A' to B', the surface will move along with them, and the plastic volume change will be proportional to the change in stress. It would be more in accordance with the known compression behavior of soil for the plastic volume change to be logarithmically related

to stress, but this idealization makes the analysis simpler without changing the essential character of the yield criterion.

Further assumptions are that the ratio of the principal axes of the ellipse is a constant and that when the soil stress moves below the yield surface (as from C to D) it does not move. If the stresses return to the surface (as at point E), the surface can then move out during further plastic strain.

The heavily over-consolidated case was not of primary interest here, but it happens that the analysis indicates that the ellipse will collapse if stresses occur on it between F and G. Although this is reasonable, the behavior is open to question, so the model is not intended to serve for heavily over-consolidated clays or dense sands.

The derivations of incremental stress-strain relations for the Drucker-Prager criterion and for the elliptical strain hardening criterion are described in Appendix E.

### 3.8 Other Stress-Strain Relations

The computational techniques described in the next chapter can be applied with almost any stress-strain law. This would allow the use of empirical relations for predicting soil deformation under load. This has not been done here largely because the aim of this work was the investigation of incremental plasticity theory and its applications, but nothing should be inferred about the possible

validity or lack of validity of other stress-strain relations.

In particular, the results of Rowe's (1962) work has already been mentioned, and correlations such as those presented by Brinch Hansen (1965) could also be used. Experimentally determined relations between stress level and stress-strain moduli (Ladd, 1964) could similarly be included.

The major problem in using such equations is that it is not always clear how they can be generalized for stress systems other than those under which they were obtained, usually those of the triaxial compression test. The most direct approach would be to use an apparent Young's modulus,  $E$ , dependent on the stress level. In any case, such extrapolations are likely to be very intuitive and will lack much of the mathematical justification inherent in plasticity theory. Nevertheless, it is to be hoped that future developments of this research effort will include consideration of such empirical stress-strain laws.

## CHAPTER 4

### MATHEMATICAL PROCEDURES

#### 4.1 Solution of Lumped Parameter Model

The Ang model has been described extensively elsewhere (Ang and Harper, 1964, Whitman, 1964, Christian, 1965), so only its main features are summarized here. The model is basically a physically reasonable way of representing a continuum in such a manner that there result linear algebraic equations identical to those resulting from central finite difference analysis.

The plane continuum is approximated by discrete points called mass points and stress points, which are shown in Figure 11. The coordinate directions,  $x$  and  $y$ , and the corresponding displacement components,  $u$  and  $v$ , are defined at each mass point in the positive sense shown in the figure.

Strains can then be calculated at the stress points as differences between the displacements of the surrounding mass points. If the subscripts UR, UL, LR, and LL stand for "upper right", "upper left", "lower right", and "lower left", respectively, the three strains become

$$\begin{aligned}\epsilon_{xx} &= (u_{LR} - u_{UL})/\delta \\ \epsilon_{yy} &= (v_{LL} - v_{UR})/\delta \\ \gamma_{xy} &= (u_{LL} - u_{UR} + v_{LR} - v_{UL})/\delta\end{aligned}\tag{49}$$

where  $\delta$  is the diagonal distance between mass points. This is clearly a first order central difference approximation to the relations

$$\begin{aligned}\epsilon_{xx} &= \frac{\partial u}{\partial x} \\ \epsilon_{yy} &= \frac{\partial v}{\partial y} \\ \gamma_{xy} &= \frac{\partial u}{\partial y} + \frac{\partial v}{\partial x}.\end{aligned}\tag{50}$$

If a stress-strain law is known, the stresses,  $\sigma_{xx}$ ,  $\sigma_{yy}$ , and  $\sigma_{xy}$ , can be computed from the strains. These stresses must now exert forces on the surrounding mass points, and the forces are

$$\begin{aligned}F_x &= \sigma_{xx} \frac{\delta}{2} \\ F_y &= \sigma_{yy} \frac{\delta}{2} \\ F_{xy} &= \sigma_{xy} \frac{\delta}{2}\end{aligned}\tag{51}$$

The positive directions in which the forces act on neighboring mass points are shown in Figure 12. It should be noted that extensional strains and tensile stresses are positive.

The model is loaded by applying forces or displacements to any chosen mass points. The resulting displacements at all mass points are computed by an iteration procedure. The computer program calculates the forces exerted on each mass point by the surrounding stress points and by applied forces at the mass point and adds the forces to find whether it is in equilibrium. If it is not, the displacements of the mass point are adjusted to eliminate the unbalanced forces. The process continues throughout the array of mass points repetitively until the unbalanced force at each mass point is less than a convergence criterion. The displacements are then the solution. From them can be calculated the strains, stresses, and forces in the stress points or on the mass points.

The convergence criterion requires that the magnitude of the unbalanced force in each direction at each mass point be less than the sum of the absolute magnitude of the forces exerted in that direction multiplied by a small number,  $\epsilon$ , plus the existing displacement in that direction divided by the flexibility in that direction and multiplied by  $\epsilon$ . Values of  $\epsilon$  have ranged from  $10^{-4}$  to  $10^{-6}$  in this research, but  $10^{-5}$  has generally been the most satisfactory compromise between computational speed and accuracy.

Only rectangular boundaries have been included in the programs, although the basic square grid could be fitted to geometries with rectangular inclusions or stepped boundaries. The boundary conditions are restricted to

four types: free, fixed, reflected, and "smooth". The free boundary has no displacement restraint, and the fixed boundary has full displacement restraint. The reflected boundary occurs on the center line of a symmetrical problem. The last boundary condition is an approximation of the conditions far from the loaded zone. It requires points on the boundary to move only parallel to the boundary and by the same amount as the parallel component of the motion of points one step in from the boundary. All boundaries must be composed of mass points. Displacements can be prescribed on any boundary, as they can be at any other mass point. Any boundary can be of any type, except that the bottom can be fixed or smooth only.

Plastic relations or otherwise non-linear stress-strain laws can be used by solving the problem incrementally. That is, a small load is applied, the problem is solved, new stress-strain relations are calculated, and a new increment of load is applied. This continues until the desired load or displacement level is reached.

## 4.2 Programs Developed

### 4.2.1 General

Six basic programs were written for six different stress-strain relations. Table I lists them and summarizes their salient features. Appendix C describes the use of the programs and the input required for each. The following paragraphs describe the important points about them.

#### 4.2.2 Tresca Material

The basic program for this material was originally called PERPLAS and is the program described by Whitman and Hoeg (1965). Some slight modifications have since been made to convert it to the M.I.T. Computation Center I.B.M. 7094 machine. It is now called MASS-TR, which is an acronym for Multi-dimensional Analysis of Stress and Strain - Tresca. The analysis for the elastic-perfectly-plastic Tresca material is presented in Appendix E.

The iterations are carried out by row. At each internal mass point forces must be computed from each of four surrounding stress points, two of which are common with the previous mass point on the row. The forces in the two common stress points are not calculated again as the program moves from one mass point to another along a row: instead, the previously computed values are used. When the program moves to the next row, it does compute new values for forces from stress points in common with the previous row. This means that the iteration is essentially a total step process within a row and a single step process from row to row.

There is a searching subroutine that estimates the increment of load required to make one additional point yield. It is also possible to advance by fixed increments of load. The most satisfactory procedure seems to be to use the searching subroutine to find the load required to cause the first stress point to yield and then to use fixed



increments (see Whitman and Hoeg, 1965).

After the iteration has converged, the stresses are checked to be sure none exceed the yield criterion. If any one stress point does have stresses above the yield criterion, the stresses are corrected according to Appendix E. Further iterations are then carried out to put the system in equilibrium. Final convergence is not satisfied until all plastic stress points have stresses at the yield criterion and equilibrium is satisfied.

Early in the research effort it became evident that some method was needed for preserving the status of a problem after a computer run so the problem could be started again later. The program now includes instructions to dump the status on a magnetic tape after each load increment has been solved. Since the M.I.T. Computation Center has a rigid timing control on jobs, a time check is included in the program to prevent the dump if there is not enough time left in the run to complete the dump. The problem is started again by the same program if an input quantity is properly set. The status is read back from the tape, and calculations proceed.

#### 4.2.3 Prandtl-Reuss Material

The program for this material is called MASS-PR, which stands for Multi-dimensional Analysis of Stress and Strain - Prandtl-Reuss. The analysis is in Appendix E. In most

respects the program is very similar to MASS-TR, except that it uses the Prandtl-Reuss relations.

The speed of convergence was improved for this material by including the correction for forces in excess of the yield criterion directly in the calculation of forces at each cycle of iteration.

#### 4.2.4 Undrained Material

Two programs were written for undrained material: one for purely elastic material, and the other for elastic-perfectly-plastic material. The first, called PLANE for PLANE Elastic, is an improved version of the routine described by the author in a previous report (Christian, 1965). The second is called PLUSS for PLANE Undrained Stress and Strain. The analysis for both is in Appendix D, where it is shown that the Tresca and Hencky-von Mises criteria give the same results for an incompressible solid. PLUSS is, therefore, based on MASS-TR, the simpler of the two elastic-perfectly-plastic programs above.

The main change from MASS-TR is the addition of a routine for calculation of the pore pressures after each increment. The convergence criterion for pore pressures is that the required change must be less than the existing pore pressure multiplied by  $\epsilon$ .

The iteration procedure for displacements was converted from the partially total step, partially single step arrangement in MASS-TR to a fully single step method. The change

was made because the technique used in MASS-TR usually would not converge when used with the pore pressure routine for eliminating volume change.

Program PLUSS, for elastic-perfectly-plastic material, allows initial stresses to be specified in the soil. These are specified as some fraction of the yield stress. An initial vertical effective stress in compression and horizontal effective stress in tension provide the required shear stress. To insure vertical equilibrium a tensile pore pressure is included to balance the vertical compression. These stresses must be subtracted from the stresses under load to obtain the incremental behavior patterns, but they do permit problems to be started from states other than unstressed ones.

The program uses the same technique as does MASS-TR to preserve the status of a problem and to start it again.

#### 4.2.5 Drucker-Prager Material

The program for the analysis of problems using the Mohr-Coulomb failure law as generalized by Drucker and Prager is called MASS-DP, for MASS - Drucker-Prager. The analysis is in Appendix E, and the same dump and restart techniques as the other programs.

The program uses a single step iteration procedure. It checks periodically throughout the calculation whether the strains of all stress points agree with the assumptions

about their elastic or plastic status. If a stress point is found whose stresses are, say, in the plastic range, but whose strains indicate it should be unloading, the point is changed from plastic to elastic. This allows points to yield and return to the plastic state as they need to during the incremental loading of the soil mass. Convergence is satisfied when forces are in equilibrium and all stresses and strains agree with the assumed state of the stress points.

The correction to prevent forces' exceeding the yield criterion is made when the forces are calculated in the iteration process. The flexibility is also calculated each time for the mass point so its displacement correction will be more accurate.

For a frictional material the weight of the soil is important. This program calculates the weight at each mass point and uses it as one of the forces to be included in the equilibrium equation. Initial stresses are computed from the weight and from a specified ratio of horizontal to vertical stress.

#### 4.2.6 Strain Hardening Material

The program for the strain hardening material is called MASS-SH and follows the analysis presented in Appendix E. It uses the same dump and restart procedure as the other plastic programs.

Although the program is quite similar to the other plastic programs, there is a distinction in that the points are all plastic at the start of loading. Some points must become elastic as loading progresses, so there must be the same sort of ability for points to yield or become elastic as exists in the MASS-DP program. The yield surface moves as a point strains plastically. Therefore, no correction routine has been included in the iteration, but, after each incremental solution, each plastic stress point acquires a new position of the yield surface which is based on the stresses developed in that point up to that time.

#### 4.3 Other Comments

##### 4.3.1 Errors

The errors involved in calculation procedures such as these are of two types: truncation and round off. The first is the error induced by approximation a continuous problem with a finite system. The second is the error involved in solving the simultaneous algebraic equations numerically.

The round off error has been minimized by using a rather stringent convergence test and small convergence criteria. The effects of varying the convergence criterion from  $10^{-4}$  to  $10^{-6}$  were not important. Reproducible results

were obtained from different types of computing machines. The general experience with finite elements and finite difference techniques is that the round off error is less important than the truncation error. For these reasons the round off is not the major problem, but it is evident that some must exist.

The truncation error is a far more serious problem. It should be greatest where the stress and strain gradients are largest because the model does not allow for reduction of point spacing in these regions. Figure 20, for example, shows that the vertical stresses oscillate between tension and compression outside of the loaded area at the surface. This is caused by truncation error, specifically the elimination of higher order terms from the solution.

Comparison of the stress distributions in the elastic range with closed form solution for the half plane indicate good agreement except at the bottom, where the boundary changes their distribution (Whitman and Hoeg, 1965). Also, comparisons between theoretically predicted final failure loads and loads at which the calculations appear to continue indefinitely indicate agreement within one or two per cent (Whitman and Hoeg, 1965). These two facts suggest that, although the truncation error may be serious for certain regions, the general pattern of the results is correct and can be relied on for research purposes.

### 4.3.2 Initial Stresses

It is highly desirable to be able to run problems with initial stresses other than zero, but this raises certain problems in computational technique and analysis. The initial stresses can be stored in the machine memory and all additional stresses added to them to give the stress at any time. This incremental technique has to be employed in any case for the plastic stress points, and it can be used just as easily for elastic points. One must be careful to remember that the stresses in such elastic points are no longer linear functions of the strains alone but are linear functions of the strains added to some initial value. The difficulty arises in determining what the initial stresses will be.

An initial approach is to calculate them from elastic theory, which predicts that a linearly elastic, isotropic, homogeneous material, loaded vertically with a stress,  $\sigma_v$ , with no lateral displacement allowed, will have lateral stresses,  $\sigma_h$ , given by

$$\sigma_h = \frac{\nu}{1-\nu} \sigma_v = K_o \sigma_v \quad (52)$$

This equation predicts values of  $K_o$  of 0.25 for  $\nu$  of 0.2.

Now, a cohesionless material can be shown to have a ratio of  $\sigma_h$  to  $\sigma_v$  at failure ( $K_f$ ) defined by

$$K_f = \frac{\sigma_h}{\sigma_v} = \frac{1 - \sin \phi}{1 + \sin \phi} \quad (53)$$

If  $\phi$  is  $30^\circ$ , this means  $K_f$  is 0.333. In other words, the material is presumed to be beyond the failure state before loading unless a restriction is placed on allowable values of  $\nu$ .

The computer programs for the frictional materials (MASS-DP and MASS-SH) avoid this problem by allowing an initial value of  $K_0$  to be specified as independent input data. The internal forces in the stress points implied by this value and by the weight of the material are calculated and stored as initial forces. The solution then proceeds from these initial values.

The frictionless material cannot be handled in this way because the shear stresses must increase linearly with depth if the  $K_0$  is constant. At some depth they must ultimately exceed the yield stress, making the material plastic under its own weight. In the program for an undrained elastic-plastic material (PLUSS) the initial stress is specified as a fraction of the yield stress and is constant with depth.



## CHAPTER 5

### RESULTS AND DISCUSSION

#### 5.1 General

After the computer programs were debugged and tested, the problem shown in Figure 13 was analyzed under various boundary conditions for differing material properties. The loading was always force controlled and simulated the effect of a long embankment on a layer of soil. The lateral boundary of the soil was between 280 feet and 300 feet from the center line of the load. The change was the result of the use of three computers (an IBM 7040, an IBM 7094, and an IBM 360/40) during the course of the research. The IBM 360/40 had stringent limitations on the allowable size of COMMON storage, which limited the size of arrays that could be handled by the programs. Therefore, several runs were made with lateral boundaries at 280 feet, while the previous work of Whitman and Hoeg (1965) had used 300 feet. In some of the test runs on the frictional material the lateral boundary was at 320 feet. The salient features of the runs are summarized in Table II.

In the following discussion it is convenient to refer to points by number. The convention is found in Figure 13. Row numbers are given first. Thus, mass point 1-4 is the rightmost loaded point. Stress points are identified by the mass point above and to the left of them.

The previous work of Whitman and Hoeg (1965) showed from runs with PERFPLAS on a single material that the model performs well, giving elastic stresses and displacements that agree reasonably well with available analytic solutions. The vertical stresses were less in error than the horizontal. The highest attainable load is within a few percent of the theoretically predicted Prandtl failure load of  $(2 + \pi)$  times  $k$ . The effect of moving both the lateral and bottom boundaries together was to increase displacements but not to change the load of initial yield or final failure. However, the lateral boundary does have a confining effect so that moving it closer to the load without moving the bottom retarded the first yield without affecting the final load. Although finer mesh sizes gave better results, the spacing used here gave result quite close to those from finer meshes. The greatest error is near the corner of the load, where the stress gradients are high. A convergence criterion of  $10^{-5}$  seemed to be the best compromise between accuracy and speed of solution. These results were considered as starting points for the present research.

## 5.2 Effects of Poisson's Ratio

Examination of the incremental stress-strain relations of Appendix E reveals that Young's modulus,  $E$ , can be factored out of them. This means that the effect of changing  $E$  can be achieved by changing all displacements for a

given load proportionally. The effect of changing the yield stress,  $k$ , can be simulated by changing all stresses and Young's modulus proportionally and then adjusting for the change in Young's modulus. This is essentially the same thing as adjusting for a change in units. The only remaining material property for non-frictional material whose effect must be determined from actual computer runs is Poisson's ratio.

Runs 1 through 4 were made with essentially the same boundary conditions and material properties except for changing Poisson's ratios. Run 2, which is the same as run XIV of Whitman and Hoeg, had the lateral boundary 20 feet further out than the other runs, but the effect is minor. All runs had  $E$  of 3,000 TSF and  $k$  of 1.75 TSF, this being achieved in run 4 by an effective stress  $E$  of 2,600 TSF and an effective stress Poisson's ratio of 0.3.

The surface displacements plotted in Figure 14 show that the material with low values of Poisson's ratio compresses more vertically and moves less to the side. All runs showed excessive convergence times at a load of about 9 TSF, which is the Prandtl failure load. In all cases the plastic zone tends to move down before it moves out to the side. The major effects of the change in Poisson's ratio are to change the load at first yield and to alter the pattern of the plastic zone near the bottom of the layer of soil. The load at initial yield increases

from 4.05 TSF for Poisson's ratio of 0.2 to 4.93 TSF for Poisson's ratio of 0.5. Figures 15 through 18 show that the plastic zone tends to reach the bottom increasingly farther from the center line as Poisson's ratio increases and that for values of 0.4 to 0.5 the zone does not reach the center line by the time of ultimate failure. Besides these two points the pattern of the yielded zones is very similar for the range of values of Poisson's ratio used.

The conventions used in the stress distribution diagrams are illustrated by Figure 19. The space for the pore pressure is left blank for the non-frictional runs on material with Poisson's ratio not equal to 0.5. The plots for the runs on frictional material (runs 11 and 12) use this space for the stress normal to the plane of the problem.

The stress distributions for runs 1 through 3 are shown in Figures 20 through 26. Stress distributions for the material with Poisson's ratio of 0.5 are shown for run 5 in Figures 36 through 41, which will serve for run 4 also. These figures, and all similar figures presented later, represent the normalized stresses, that is, the stresses divided by the applied surface load. They are presented as percentages so that -99 means 99% compressive stress.

The elastic stresses are shown in Figures 20, 22, 25, and 36. The vertical stresses are not much affected by changes in Poisson's ratio, which is in agreement with the results of most closed form solutions to elastic stress

distribution problems. The horizontal stresses, however, become increasingly compressive as Poisson's ratio increases. This increased compressive stress explains the higher load at first yield for the material with higher Poisson's ratio.

The plastic stress distributions in Figures 21, 24, 26, and 41, which show the situation at the highest load attained in each run, show that the vertical stresses may become somewhat more compressive as yielding progresses, but the changes from the elastic case are small. The horizontal stresses, however, become markedly more compressive as yielding progresses. The horizontal stresses near the lateral boundary are more compressive for higher values of Poisson's ratio than for lower values. Near the load the variation is much less pronounced between materials with different Poisson's ratios. It is evident the lateral boundary acts as a strong restraint on lateral movement during failure. Figure 23 shows an intermediate stage during the development of the plastic zone and is plotted primarily for comparison with later runs with different yield criteria.

In Figures 36 through 41 the pore pressure reflects the increasing compressive stress as yielding spreads. The pore pressure for this material does not depend on the shear stress and so therefore will not increase as yielding occurs. This is contrary to the behavior of soil, and as a result the mathematical model must be regarded as a total stress model even though it uses the effective stress

principle to handle incompressible materials. There is, of course, no reason why a similar model could not be set up which would compute pore pressures dependent on deviatoric stress or strain if a valid relation were developed experimentally.

The displacements under elastic conditions and at the final load are shown in Figures 27, 28, and 29 for runs 1, 2, and 3. It can be seen that the general patterns of displacement are quite similar for all three materials. The materials with the higher Poisson's ratios do have more upward movement at the surface outside the loaded area at failure. It is also evident that point 2-4, directly under the corner of the loaded area and one row beneath the surface develops large displacements during plastic strain. This is caused partly by errors in the lumped parameter model, but it also reflects the failure of the corner of the load. Since each loaded mass point can move independently, the failure actually involves the displacement of the outside portion of the load.

The development of the failure is seen in more detail for the incompressible material in Figures 30 through 33. The final displacements (Figure 33) are reasonably similar in pattern to the elastic ones (Figure 30a) but much larger. Point 2-2 has moved somewhat less strongly to the right, and point 2-4 again has large displacements at failure. Figures 30b through 32 show the increments of displacement between successive loads. In effect, these are velocities. They show the marked increase in vertical

movement directly outside the loaded area as failure is approached. Also point 1-3 tends to move inward at early stages of yielding, but its velocity changes near failure. The increase in displacement of point 2-4 is remarkable in Figure 32. It should be remembered that the displacements in Figures 30 through 33 are for run 5, which used a lower E than run 4. The patterns are the same even though the magnitudes are not.

The effect of increasing Poisson's ratio is to increase the lateral stresses at all stages of loading, and as a result the load at first yield is increased. There is more upward movement outside the loaded area and less downward movement directly under the load for higher values of Poisson's ratio.

### 5.3 Effects of Boundary and Initial Stress

Runs 5 through 8 and run 10 were run on an incompressible material with the same yield stress as the previous runs. Young's modulus (with respect to total stress) was 865 TSF for all runs except run 6, for which it was 3,000 TSF. The effective stress parameters were 705 TSF and 0.3, respectively, for most runs, and 2,600 TSF and 0.3, respectively, for run 6.

The displacement fields for run 5 are shown in Figures 30 through 33 and have been described in the previous section. Figure 34 shows the vertical displacements of some points on the surface. Since the material

is incompressible, the points outside the loaded area must move up as the loaded area moves down. Failure seems to occur near the Prandtl failure load of 9 TSF. Point 1-4, which is at the edge of the loaded area, moves very little, while at failure point 1-3 seems to accelerate as the edge of the load fails.

Figure 35 shows the spread of the plastic zone. Differences between this and Figure 18 are the result of plotting at different stress levels. The patterns are identical if the same stresses are picked. Figures 36 through 41, which show the stress distributions have already been discussed.

Run 6 was done for a material having a smooth interface at the bottom of the layer. Comparison of the surface displacements in Figure 42 with those in Figure 14 shows that the smooth bottom causes larger displacements at the surface, as might be expected from a reduction in stiffness of the system. Figure 42 suggests that failure is occurring at a lower load than the Prandtl load, and, from the behavior of point 1-4, that something unusual is happening at loads immediately above 8 TSF.

Figure 43 shows that the plastic zone starts to spread quite similarly to the way it did for run 5, except that the initial yield load is 4.75 TSF rather than 4.93 TSF because of reduced rigidity. However, at a load of 7.93 TSF another plastic zone starts to spread out from the side boundary. The material is being pushed out laterally against the boundary until it yields there. This



effect of the lateral boundary was observed during testing of the program for incompressible material. A run with lateral boundaries 140 feet from the center line and with a fixed bottom developed a similar yield zone near the outer boundary. The lateral boundary has an increasing influence on the yield pattern as the material becomes less compressible and as the boundary becomes more necessary for static equilibrium in the lateral direction.

The stress patterns in Figures 44 through 49 show the marked increase in lateral horizontal stress near the boundary compared to the patterns in Figures 36 through 41. However, the fixed bottom causes much higher horizontal stresses near the bottom. The displacements and incremental displacements in Figures 50 and 51 are much larger outside the loaded area than they are for a problem with a fixed bottom. They are what would be expected.

The problem of the plastic failure of a plane material on a smooth base is described by Hill (1950), who presents on page 257 a figure relating the ratio of width of loaded area to depth to the failure load. This applies to a rigid load on a layer infinitely wide, but the results were used to check the program. Run 7 had a smooth bottom and a free side. The surface displacements in Figure 52 indicate failure occurs at about 4.5 TSF of load. Hill's figure indicates, for the present geometry, that the failure load should be about 4.6 TSF. This is a remarkable agreement, which confirms confidence in the program.

Figure 52 shows that the failure occurs rapidly when there is no lateral restraint. The plastic zone spreads to the bottom in Figure 53, and final failure happens soon thereafter. The initial yield load is reduced by the absence of restraint from 4.75 TSF to 3.70 TSF. The stresses in Figures 54 and 55 show little difference between vertical stresses for the two runs 6 and 7 but a sizeable difference in horizontal stresses. Obviously, the greatly reduced compression in run 7 allows yielding to occur at lower loads than before. The displacements in Figures 56 and 57 are predominantly in the horizontal direction, which confirms Hill's picture of the mode of failure.

Run 8 started from an initial stress distribution in which the horizontal stresses were in tension and equal to the yield stress. This means the soil would have initial shear stresses equal one-half the yield stress. The distribution would simulate the situation in most normally consolidated deposits, where the horizontal stresses before loading are less compressive than the vertical stresses.

Figure 58 compares the surface displacements from run 8 with those from run 5, which was identical except for the lack of initial stress. The effect of the initial stress is to make the material act softer. The vertical displacements are all increased, and the yielding occurs at lower load so as to make the curve flatter. At the theoretical failure load the curves of displacement for points 1-1 and 1-3 do not appear to be vertical, but the number of iterations for convergence was increasing as it

does near failure. The over-all effect of initial stress is to make the displacement curve look more like that for "local shear" rather than "general shear" (Taylor, 1948).

The plastic zone spreads in Figure 59 in much the same way as it does in run 5, except that it starts spreading at a lower stress. The load at initial yield is reduced by one half to 2.48 TSF. In Figures 60 and 61 are plotted the changes in stress at two points in the plastic range, that is, the normalized difference between the initial stresses and the calculated stresses at that load. The stress increment during the elastic portion of the run is identical to that for run 5. The vertical stresses are little affected by the initial stress, but the horizontal stress increment is greatly increased in run 8, especially near the lateral boundary, where the increment is nearly doubled. This phenomenon arises because at failure the material outside of the loaded area must fail with greater horizontal than vertical compressive stress and this can only happen if large changes in horizontal compression overcome the initial stress in the other direction. The displacements in Figures 62 and 63 show that the mode of failure is the same as that for run 5 but with larger displacements.

Run 10 was started from the opposite stress state. The horizontal initial stresses were made compressive and equal to the yield stress to create initial shear stresses equal to one-half the yield stress and in the opposite direction to that of run 8. Figure 64 compares the surface

displacements to those from run 5. The effect of the initial stresses is to make the material act more as though it were failing in general shear and to reduce the displacements during plastic flow. As would be expected, the effect is precisely the reverse of that in run 8.

Figure 65 shows the spread of the plastic zone from the initial yield load of 6.89 TSF. That the first yield should occur away from the center line is not surprising, but the pattern of the plastic zone is. The lateral and bottom boundaries have a significant effect, as they do for most of the runs on stiffer material. It should be noted that the plastic zone does not spread as far down below the load and never reaches the bottom there.

The normalized stress increments are shown in Figures 66 and 67 for two stages in the plastic range. The horizontal stress increments are reduced from those in run 8 while the vertical ones are not much affected. The displacements, plotted in Figures 68 and 69, show the same general patterns of motion as in the previous runs, but there appears to be a more erratic motion near the corner of the loaded area.

#### 5.4 Effects of Other Yield Criteria

Run 9 was made with the Prandtl-Reuss material but with otherwise identical properties and geometry to run 2. Despite several changes in the computational technique the

program for the Prandtl-Reuss material converges much less rapidly than the program for the Tresca material. It is not clear why this is so. To avoid excessive computer use the run with the Prandtl-Reuss material was cut short at a load of 5.22 TSF.

The displacements at the surface for run 9 and the corresponding portion of run 2 are compared in Figure 70. At this early stage of the load history there is not much change between the two, but the Prandtl-Reuss material is the softer. The load at initial yield is reduced from 4.43 TSF in run 2 to 4.09 TSF in run 9. These effects result from the consideration of the intermediate principal stress, which can be seen graphically in Figure 3 to cause yielding at lower loads than those predicted by Tresca's criterion.

The plastic zone develops according to Figure 71. Comparison with Figure 16 reveals that at comparable loads the pattern of yielding is identical for the two materials. The stress distribution at the final load is shown in Figure 72 and is virtually identical to the distribution at nearly equal applied load in run 2, which is shown in Figure 23. The incremental displacements at the final load and the final displacements are plotted in Figure 73. These conform to the pattern of run 2.

Runs 11 and 12 were made with frictional material. Both had no cohesion ( $k = 0$ ) and had the coefficient  $\alpha$  equal to 0.165, which corresponds to a Coulomb friction

angle,  $\phi$ , in triaxial compression of  $21.8^\circ$ . The initial ratio of lateral to vertical stress,  $K_0$ , was 0.5. In both runs the elastic properties were selected to equal those in run 2.

Results of run 12 are shown in Figures 74 through 77. The run was stopped at an applied load of 5.30 TSF because the convergence times were increasing and an excessive amount of computer time was being used. The surface displacements (Figure 74) are nearly linear until the load has nearly reached 5.00 TSF, where the curves begin to bend. This marks the beginning of the heave of the material being pushed up by the failure. Such heave must precede the failure because the criterion requires volume change during yield.

The plastic zone spreads downward in Figure 75 as would be expected from the spread observed in non-frictional runs. There is more lateral extent to the zone than occurs for non-frictional materials. The tongue-shaped plastic area at the surface outside the loaded area results from the very small confining stress at the surface and directly beneath it. This is probably caused more by numerical inaccuracies in the solution than by anything else.

Figure 76 shows the increments of stress at the final load of 5.30 TSF. These are the differences between the calculated stresses and the initial stresses. The increments are remarkably similar to those shown in Figure 23 for the Tresca material at a load of 5.31 TSF. Of course, this load does not imply that the plastic failure has

developed to a corresponding degree, for the two materials behave quite differently. The main difference between the two stress distributions is in the horizontal stresses, which are more compressive for the Drucker-Prager material. This results from the expansion of the material as it yields. There must be a counter action because of the restraint of the lateral boundary, so the horizontal stresses become more compressive.

The displacements in Figure 77b are in the same general pattern as those previously computed in run 2, but the increments shown in Figure 77a indicate that considerable expansion is beginning to happen at the edge of the loaded area.

Run 11 was made with the strain hardening material. The material constants were the same as for run 12 where similar constants could be defined. In addition, plastic compressibility and the shape of the ellipse were defined as in Table II. The results in Figures 78 through 81 show a markedly different behavior. The vertical displacements at the surface (Figure 78) are almost ten times those in Figure 74, and they show a continually curving downward trend which will soon pass the curves in Figure 74.

Since the material starts out entirely plastic and there is almost no return to the elastic state, no plots of the formation of the plastic zone are given. The initial portion of the loading is clearly largely taken up by plastic volumetric compression. Figure 79 shows that the

lateral stresses and stresses normal to the plane are much larger than in previous runs. This Figure shows incremental stresses beyond the initial stresses.

The general stress paths followed by two typical points are shown in Figure 80. This also illustrates the increase in volumetric stress followed by increase in deviatoric stress as measured by  $J_2$ . In plotting this figure it was observed that the stress paths often moved erratically while following similar general patterns. The erratic motion is caused by rounding error in calculating the stresses from differences in displacements and by truncation error from taking load increments too large. The stability limits for size of load increments require more investigation in the future.

The displacement patterns in Figures 81 and 82 indicate that at the load level reached there is relatively little displacement outside the loaded area and that lateral shear movement is just beginning.

### 5.5 Discussion of Mathematical Model

The results and discussion presented in the previous sections indicate that the model developed by Harper and Ang can be usefully extended to treat a wide range of constitutive relations. It is still true that there must be errors in any numerical technique. The most persistent systematic error found in this research is a tendency for values of stress or displacement to oscillate from point



to point. The vertical stress at the surface just outside the loaded area should be zero, but in all the stress distribution figures there is an oscillation of the vertical stress in the top stress point which decreases with distance from the load. The large displacements of mass point 2-4 in the plastic zone have already been commented on.

Some of this error results from ignoring several modes of deformation. For example, in Figure 12, if the mass point at the upper left were to move some distance up to the right in the negative y direction with no x component of motion and if the upper right mass point to move down to the right an equal amount in the positive x direction with no y component, there would be no stress calculated in the stress point. There would, however, be stress induced in an actual square piece of the continuum by these motions, which correspond to an applied bending moment. The ignoring of this type of behavior must cause error.

This type of error can also be predicted by considering that there are eight independent components of displacement of the four mass points around each stress point. Three of these components will suffice to define the rigid body motion of the stress point and mass points. The remaining five can be used to describe five independent deformation modes, which can in turn be used to calculate stresses. In the present model only three deformation modes are used, the two neglected ones being the two bending modes.

Another difficulty in using the model is that it is very difficult, and often impossible, to provide more small grids in areas of large displacement or stress gradients. A triangular array would be much more convenient from this point of view.

For these two reasons it would seem that further extensions of the work to more complicated geometries should be done with a more sophisticated model. The present model is extremely easy to use and allows a very simple form of computer input, but it does have limitations.

The ultimate check on the displacement predictions made by the model must come from experimental and field measurements. The latter are particularly promising because it is often possible to find conditions in which plane strain is very closely approximated, as in the case of long highway embankments. There are now in progress several research projects to make such measurements, and it is hoped that they will give information on the usefulness of the model as a design tool. At the same time the predictions of the model will make the collection of significant data more certain by indicating expected displacement and stress distributions.

## CHAPTER 6

### CONCLUSIONS AND FUTURE WORK

#### 6.1 Conclusions

First, the research has demonstrated a useful technique for predicting displacements and stresses under plane strain conditions. In particular, deformation modes with no change of volume and two modes of frictional behavior have been studied. The results can be obtained from quite simple inputs to computer programs. The errors on the results are largely caused by the approximations inherent in the finite difference approach.

Several runs on material obeying Tresca's yield criterion show that increase of Poisson's ratio while keeping other parameters constant makes the material behave more stiffly and reduces displacements. For the material with no volume change initial stresses differing from zero have a sharp effect on the stress and displacement field but do not affect the failure load. The effect of lower initial horizontal than vertical stress is to increase the displacement under load and to reduce the load at first yield. The reverse effects are noted for the case of higher horizontal stresses than vertical.

Two types of frictional material were examined. One, the Drucker-Prager material, expanded during yield, and the other contracted during yield. The results of the runs

showed the two materials to develop quite different stress fields, the Drucker-Prager material having much lower lateral stresses. The displacement fields indicated that the Drucker-Prager material had displacements that increased almost linearly with load until near failure. The other material had displacements that increased more rapidly than the load.

The surface displacements for the two frictional materials closely resemble the displacements for local and general shear. The strain hardening material shows a continually increasing rate of displacement with no obvious break from an initial straight line load-displacement relation. This is similar to the curve expected for local shear, where progressive failure occurs. The Drucker-Prager material does show a straight line initial load-displacement relation which curves at higher loads. This recalls the general shear pattern, where the material fails almost all at once.

However, in both the strain-hardening and Drucker-Prager cases the material under the load is largely plastic throughout the loading. Thus, the difference between these curves is not the result of progressive as opposed to sudden failure but of the plastic stress-strain properties of the material. Expansive materials, such as the Drucker-Prager material, have displacement curves of the general shear form, but contracting materials have curves of the local shear form.

The incompressible material with initial stress can have curves of either form, depending on the initial stress. Higher horizontal than vertical initial compressive stress tends to retard yielding and to cause a general shear type of failure. Lower horizontal compressive stress tends to cause local shear failure. The ultimate load is not affected by initial stress.

These results indicate that the difference between local and general shear is not so much the pattern of yielding and formation of the plastic zone as it is a reflection of the plastic stress-strain properties of the material or the initial stresses.

The stress distributions all reveal that changes of material properties, initial conditions, and boundary conditions do not have significant effects on the normalized vertical stress distribution, which remains relatively unchanged even during the development of plastic flow. Therefore, the engineering use of quite simple methods of predicting vertical stresses, such as the several charts available, is quite justified. On the other hand, horizontal and shear stresses are greatly affected by all these factors. These last stresses therefore control the maximum shear or maximum deviatoric stress on the soil and determine whether it is plastic. Engineering use of horizontal stresses and shear stresses (and, hence, of principal stresses) derived from simple solutions, such as those of Boussinesq's problem, does not appear justified without

field experience, experimental verification, or considerable engineering judgement. This does not mean to imply that simple solutions should not be used but only that they should be used in the knowledge that the horizontal stresses and shear stresses will be the ones in error. Exactly what sort of approximation or correction should be used in engineering design is a question to be answered from the results of field measurements in conjunction with calculations like those presented here.

The effect of the lateral boundaries is mainly to restrict lateral motion. This can greatly affect the pattern of the spread of the plastic zone for the stiffer materials such as those with high initial compressive horizontal stresses. When the bottom boundary is smooth, the effect of the lateral boundary is also more noticeable than when the bottom is fixed. The completely different behavior of runs 6 and 7 illustrates this. If the lateral boundary is close, enough the plastic zone often develops in part at the boundary.

The two frictional materials used represent drained behavior and apply primarily to sands. A clay could also be treated by them if the loading were slow enough to allow drainage. The same sort of changes which converted the MASS-TR program into the PLUSS program for undrained, incompressible material could be applied to MASS-SH to describe the behavior of a saturated clay. Such a programming effort in conjunction with experimental work to describe better the stress-strain behavior of clay should be undertaken.

These computer programs demonstrate that it is possible to treat analytically the deformation behavior of rather complicated materials. The stress-strain relations used in the last two programs are certainly not the correct ones for a true soil, but there is still very little known about the general stress-strain law for soils. This is a subject which requires much further research, both in the laboratory and in the field. Computer programs like the present ones will be very useful in relating laboratory observations to field measurements and predictions. There is no apparent reason why almost any experimentally observed stress-strain relation cannot be used in a similar program.

One of the important advantages of plasticity theory in calculation of stresses and displacements is that it automatically allows treatment of rotation of the principal stresses. This certainly occurs as loading and yielding progresses, but it is ignored by most relations between principal stresses and strains. In particular, empirical relations generally ignore it. The development of better laboratory knowledge of the general stress-strain relation for soil, including effects of rotation of stress, will greatly improve the accuracy of computations like those presented here. Together with field verification these should increase the general understanding of the load displacement behavior of soil masses.

## 6.2 Future Work

The present effort is part of a research project into the dynamic behavior of structures and soil. This work is continuing and represents the first and most obvious area of expansion.

The errors mentioned in the discussion of the results and the desire to distribute more elements in areas of stress concentration indicate that more sophisticated mathematical models and ones allowing finer elements may have to be used for future static applications of the work. The insights gained from the simple model used here will be useful in such research. In particular, the knowledge of how to treat incompressible material will be important. Software for analysis of finite element systems of triangular shape has been developed at M.I.T. and will be used in some of the future developments. Such finite elements will also allow consideration of axially symmetric cases after some additional programming effort.

There are several additional stress-strain relations which could be used with very little more effort. The empirical relations of Brinch Hansen (1965) and the deformation theory of plasticity would both seem promising. Rowe's (1962) stress-dilatancy relations may also be used. Elastic solutions for incompressible and compressible materials with Young's modulus varying with depth would be a simple way of simulating real soil deposits.



The availability of a technique for handling undrained (incompressible) material and drained (compressible) material having the same effective stress parameters suggests that these methods could be used to solve two and three dimensional consolidation problems in accordance with Biot's (1941 a,b,c) theory. The analytical solution of such problems is quite difficult, so a numerical procedure could become a useful design tool.

Finally, the availability of this and other computational schemes makes it possible to use complicated stress-strain relations. This suggests that laboratory and theoretical research into the stress-strain behavior of soil aimed at developing general models is important and that the results of such research can be used in calculations on real soil masses and models. The coordination of laboratory, theory, and field is necessary for expansion of knowledge about soil behavior.

## REFERENCES

1. Aldrich, Stephen C., (1966). "Constitutive Theory for Plastic Continua with Application to Soil Mechanics," S.M. Thesis, M.I.T.
2. Allen, C. N. de G., (1954). Relaxation Methods in Engineering and Science. (New York: McGraw-Hill).
3. Ang, Alfredo H.S., and Harper, Goin N., (1964). "Analysis of Contained Plastic Flow in Plane Solids," Proceedings, ASCE, Journal of the Engineering Mechanics Division, Vol. 90, No. EM2, pp. 195-223.
4. Argyris, J. H., (1965a). "Matrix Analysis of Three-Dimensional Elastic Media Small and Large Displacements", AIAA Journal, Vol. 3, No. 1, pp. 45-51.
5. Argyris, J. H., (1965b). "Three-Dimensional Anisotropic and Inhomogeneous Elastic Media Matrix Analysis for Small and Large Displacements," Ingenieur-Archiv, Vol. 34, No. 1, pp. 33-55.
6. Bendel, H., (1962). "Die Berechnung von Spannungen und Verschiebungen in Erddammen," Mittellilungen der Versuchsanstalt fur Wasserbau und Erdbau, Zurich, No. 55.
7. Biot, Maurice A., (1941a). "General Tehory of Three-Dimensional Consolidation", Journal of Applied Physics, Vol. 12, pp. 155-164.
8. Biot, Maurice A., (1941b). "Consolidation Settlement under a Rectangular Load Distribution", Journal of Applied Physics, Vol. 12, pp. 426-430.

9. Biot, Maurice A., and Clingan, F.M., (1941c). "Consolidation Settlement of a Soil with an Impervious Top Surface," Journal of Applied Physics, Vol. 12, pp. 578-581.
10. Bishop, Allen W., (1966). "The Strength of Soils as Engineering Materials," Sixth Rankine Lecture, Geotechnique, Vol. 16, No. 2, pp. 91-128.
11. Burmister, D.M., (1956). "Stresses and Displacement Characteristics of a Two-Layer Rigid Base Soil System: Influence Diagrams and Practical Applications," Proceedings, Highway Research Board, Vo. 35, pp. 773-814.
12. Christian, John T., (1965). "Two-Dimensional Analysis of Stress and Strain in Soils," Report No. 1: "Iteration Procedure for Saturated Elastic Porous Material," U.S. Army Waterways Experiment Station, Contract No. DA-22-079-eng-427.
13. Clough, Ray W., (1960). "The Finite Element Method in Plane Stress Analysis," Proceedings, Second Conference on Electronic Computation, ASCE, pp. 345-378.
14. Clough, Ray W., (1965). "The Finite Element Method in Structural Mechanics," in Stress Analysis, edited by O.C. Zienkiewicz and G.S. Holister. (New York: Wiley).
15. Clough, Ray W., and Rashid, Yusef, (1965). "Finite Element Analysis of Axi-Symmetric Solids," Proceedings, ASCE, Journal of the Engineering Mechanics Division, Vol. 91, No. EM<sup>1</sup>, pp. 71-85.
16. Davis, E.H., and Poulos, H.G., (1963). "Triaxial Testing and Three-Dimensional Settlement Analysis," Proceedings, Fourth Australia-New Zealand Conference on Soil Mechanics and Foundation Engineering, pp. 233-243.

17. Davis, E.H., and Poulos, H.G., (1965). "The Analysis of Settlement under Three-Dimensional Conditions," Symposium on Soft Ground Engineering, Brisbane.
18. Dingwall, J.C., and Scrivner, F.H., (1954). "Application of Elastic Theory to Highway Embankments by Use of Difference Equations," Proceedings, Highway Research Board, Vol. 33, pp. 476-481.
19. Drucker, Daniel C., (1950). "Some Implications of Work Hardening and Ideal Plasticity," Quarterly of Applied Mathematics, Vol. 7, No. 4, pp. 411-418.
20. Drucker, Daniel C., (1951). "A More Fundamental Approach to Plastic Stress-Strain Relations," Proceedings, First U.S. National Congress of Applied Mechanics, pp. 487-491.
21. Drucker, Daniel C., (1954). "Coulomb Friction, Plasticity, and Limit Loads," Transactions, ASME, Journal of Applied Mechanics, Vol. 21, No. 1, pp. 71-74.
22. Drucker, Daniel C., Gibson, R. E., and Henkel, D. J., (1957). "Soil Mechanics and Work-Hardening Theories of Plasticity," Transactions, ASCE, Vol. 122, pp. 338-346.
23. Drucker, Daniel C., and Prager, William, (1952). "Soil Mechanics and Plastic Analysis or Limit Design," Quarterly of Applied Mathematics, Vol. 10, No. 2, pp. 157-165.
24. Fung, Y. C. (1965). Foundations of Solid Mechanics, (Englewood Cliffs, N. J.: Prentice-Hall).
25. Gibson, R.E., Knight, K., and Taylor, P.W., (1963). "A Critical Experiment to Examine Theories of Three-Dimensional Consolidation," Proceedings, European Conference on Soil Mechanics and Foundation Engineering, pp. 69-76.

26. Hansen, Jorgen Brinch, (1953). Earth Pressure Calculation, (Copenhagen: Danish Technical Press).
27. Hansen, Jorgen Brinch, (1957). "Calculation of Settlements by Means of Pore Pressure Coefficients," Acta Polytechnica 235, Civil Engineering and Building Construction Series, Vol. 4, No. 8.
28. Hansen, Jorgen Brinch, (1965). "Some Stress-Strain Relationships for Soils," Proceedings, Sixth International Conference on Soil Mechanics and Foundation Engineering, Vol. 1, pp. 231-234.
29. Harper, Goin Neil, (1963). "A Numerical Procedure for the Analysis of Contained Plastic Flow Problems," Ph. D. Thesis, University of Illinois.
30. Henkel, D. J., (1958). "The Correlation between Deformation, Pore Water Pressure, and Strength Characteristics of Saturated Clays," Ph.D. Thesis, University of London.
31. Hill, R., (1950). The Mathematical Theory of Plasticity, (Oxford: Clarendon Press).
32. Janbu, N., Bjerrum, L., and Kjaernsli, B., (1956). "Veiledning ved losning av fundamenteringsoppgaver (Soil Mechanics Applied to Some Engineering Problems)," (in Norwegian with English summary), Norwegian Geotechnical Institute, Publication No. 16.
33. de Josselin de Jong, G., and Verruijt, A., (1965). "Primary and Secondary Consolidation of a Spherical Clay Sample," Proceedings, Sixth International Conference on Soil Mechanics and Foundation Engineering, Vol. 1, pp. 254-258.
34. Jurgenson, Leo, (1934). "The Application of Theories of Elasticity and Plasticity to Foundation Problems," in Contributions to Soil Mechanics, 1925-1940, Boston Society of Civil Engineers, pp. 148-183.

35. Kondner, Robert L., and Krizek, Raymond J., (1965), "Calculation of the Vertical Stress Distribution Beneath Groups of Footings," Geotechnique, Vol. 15, No. 4, pp. 396-408.
36. Ladd, Charles C., (1964). "Stress-Strain Modulus of Clay in Undrained Shear," Proceedings, ASCE Journal of the Soil Mechanics and Foundations Division, Vol. 90, No. SM5, pp. 103-132.
37. Lambe, T. William, (1964). "Methods of Estimating Settlement," Proceedings, ASCE, Journal of the Soil Mechanics and Foundations Division, Vol. 90, No. SM5, pp. 43-67.
38. Love, A.E.H., (1944). A Treatise on the Mathematical Theory of Elasticity, (New York: Dover).
39. McNamee, J., and Gibson, R.E., (1960a). "Displacement Functions and Linear Transforms Applied to Diffusion through Porous Media," Quarterly Journal of Mechanics and Applied Mathematics, Vol. 13, pp. 98-111.
40. McNamee, J., and Gibson, R.E., (1960b). "Plane Strain and Axially Symmetric Problems of the Consolidation of a Semi-Infinite Clay Stratum," Quarterly Journal of Mechanics and Applied Mathematics, Vol. 13, pp. 210-227.
41. Newmark, Nathan M., (1942). "Influence Charts for Computation of Stresses in Elastic Foundations," University of Illinois, Engineering Experiment Station, Bulletin Series, No. 338.
42. Novozhilov, V.V., (1952). "O fixicheskom smisle invariantov napryazheniya, ispol'zuyemikh v teoriy plastichnosti (On the Physical Significance of the Invariants of Stress Used in the Theory of Plasticity)," Prikladnaya Matematika i Mekhanika, Vol. 16, No. 5, pp. 617-619. Translation courtesy of Prof. Charles A. Berg.

43. Prager, William, (1959). An Introduction to Plasticity, (Reading, Mass.: Addison-Wesley).
44. Prager, William, and Hodge, P. G., Jr., (1951). Theory of Perfectly Plastic Solids, (New York: Wiley).
45. Reyes, Salvador Faustino, (1966). "Elastic-Plastic Analysis of Underground Openings by the Finite Element Method," Ph.D. Thesis, University of Illinois.
46. Roscoe, K. H., Scofield, A. N., and Worth, C. P., (1958). "On the Yielding of Soils," Geotechnique, Vol. 8, No. 1, pp. 25-53.
47. Roscoe, K. H., Scofield, A. N., and Thurairajah, A., (1963). "Yielding of Soils in States Wetter than Critical," Geotechnique, Vol. 13, No. 3, pp. 211-240.
48. Rowe, P. W., (1962). "The Stress-Dilatancy Relation for Static Equilibrium of an Assembly of Particles in Contact," Proceedings, Royal Society, A269, pp. 500-527.
49. Schjodt, R., (1958). "Stresses in an Excavation with a Vertical Wall Subjected to its Own Weight," Proceedings, Brussels Conference 58 on Earth Pressure Problems, Vol. 1, pp. 89-93.
50. Skempton, A. W., (1954). "The Pore Pressure Coefficients A and B," Geotechnique, Vol. 4, No. 4, pp. 143-147.
51. Skempton, A. W., and Bjerrum, L., (1957). "A Contribution to the Settlement Analysis of Foundations on Clay," Geotechnique, Vol. 7, No. 4, pp. 168-178.
52. Skempton, A. W. (1948). "The  $\phi=0$  Analysis of Stability and its Theoretical Basis," Proceedings, Second International Conference on Soil Mechanics and Foundation Engineering, Vol. 1, pp. 72-78.

53. Sokolnokoff, I.S., (1956). Mathematical Theory of Elasticity, (New York: McGraw-Hill).
54. Stoll, U.W., (1960). "Computer Solution of Pressure Distribution Problem," Proceedings, ASCE, Journal of the Soil Mechanics and Foundations Division, Vol. 86, No. SM6, pp. 1-9.
55. Takagi, Shunsuke, (1962). "Plane Plastic Deformation of Soils," Proceedings, ASCE, Journal of the Engineering Mechanics Division, Vol. 88, No. EM3, pp. 107-151.
56. Taylor, Donald W., (1948). Fundamentals of Soil Mechanics, (New York: Wiley).
57. Terzaghi, Karl, (1943). Theoretical Soil Mechanics, (New York: Wiley).
58. Timoshenko, S., and Goodier, J.N., (1951). Theory of Elasticity, (New York: McGraw-Hill).
59. Whitman, Robert V., (1964). "Multidimensional Analysis of Stress and Strain in Soils," Stanford Research Institute Report to the Defense Atomic Support Agency, DASA No. 1558.
60. Whitman, Robert V., and Hoeg, Kaare, (1965). "Two-Dimensional Analysis of Stress and Strain in Soils," Report No. 2: "Development of Plastic Zone Beneath a Footing," U.S. Army Waterways Experiment Station, Contract No. DA-22-079-eng-427.
61. Wilson, Guthlac, (1948). "A Relaxation Method for the Solution of Problems Concerning Axially Symmetrical Distributions of Load in an Elastic Medium," Journal of the Institution of Civil Engineers, Vol. 30, pp. 149-166.



62. Ziegler, Hans, (1963). "Some Extremum Principles in Irreversible Thermodynamics with Application to Continuum Mechanics," in Progress in Solid Mechanics, edited by I.N. Sneddon and R. Hill, (New York: Wiley), Vol. 4, pp. 91-193.

APPENDIX A

LIST AND DEFINITIONS OF SYMBOLS USED

- A Skempton's A factor  
Coefficient in Drucker-Prager stress-strain relations  
Coefficient in Tresca stress-strain relations
- B Coefficient in Drucker-Prager stress-strain relations  
Coefficient in Tresca stress-strain relations
- C Coefficient in Tresca stress-strain relations  
Ratio between plastic volumetric strain and  
volumetric stress for strain hardening material
- D Ratio of half axes of elliptical yield surface  
Coefficient in Tresca stress-strain relations
- E Young's modulus
- F Derivative of strain hardening yield function  
with respect to volumetric strain
- $F_x, F_y$  Normal forces in x and y directions, respectively,  
in stress point
- $F_{xy}$  Shear force in stress point
- G Shear modulus =  $\frac{E}{2(1+\nu)}$
- $\hat{G}$  Invariant term in expression relating plastic strain  
rate and stress rate for strain hardening material

$I_1$	First stress invariant
$J_2$	Second deviatoric stress invariant
$K_0$	Coefficient of earth pressure at rest
$K_f$	Coefficient of earth pressure at failure
$K$	Bulk modulus = $\frac{E}{3(1-2\nu)}$
$[K], [K^{(p)}], [K^{(e)}]$	Stiffness matrices for strain hardening material
$T$	Ratio used in correcting stresses for Drucker-Prager material
$T_{ij}$	Derivative of strain hardening yield function with respect to stress, $\sigma_{ij}$
$\dot{W}$	Work rate
$a$	Minor half-axis of elliptical yield surface
$b$	Major half-axis of elliptical yield surface
$c$	Coulomb cohesion
$e_{ij}$	Deviatoric strain tensor
$f$	Yield function
$i, j, k, l, m, n$	Subscripts used to indicate coordinate directions
$k$	Constant in various yield functions
$k_t$	Temporary value to be corrected to $k$
$p$	Pore pressure

$p_o, p_c$	Stress states used in strain hardening derivation
$s_{ij}$	Deviatoric stress tensor
$u, v$	Displacement of mass point in x and y directions, respectively
$x, y$	Coordinate axes for each mass point in the plane
$z$	Coordinate axis normal to plane
$\alpha$	Frictional coefficient in Drucker-Prager and strain hardening yield criteria
$\Delta$	Symbol to indicate finite increment
$\delta_{xy}$	Engineering shear strain in (x,y) plane = $2\epsilon_{xy}$
$\delta$	Diagonal distance between mass points
$\delta_{ij}$	Kronecker delta (= 1 when $k = j$ ; = 0 when $i \neq j$ )
$\epsilon$	Volumetric strain = $(\epsilon_{11} + \epsilon_{22} + \epsilon_{33})/3$ Convergence criterion
$e_{ij}$	Total strain tensor = $\frac{1}{2}(\frac{\partial u_i}{\partial x_j} + \frac{\partial u_j}{\partial x_i})$ , where $u_i$ and $x_i$ are displacements and coordinates, respectively, and i varies from 1 to 3
$\lambda$	Coefficient in plastic stress-strain laws to be found Horizontal distance between mass points

$\lambda'$	Coefficient in plastic stress-strain laws to be found
$\nu$	Poisson's ratio
$\sigma$	Volumetric stress = $(\sigma_{11} + \sigma_{22} + \sigma_{33})/3$
$\sigma_{ij}$	Total stress tensor
$\tau_{xy}$	Shear stress in (x,y) directions in plane
$\phi$	Coulomb angle of friction

- Notes:
1. A dot (·) over a quantity indicates the incremental rate of that quantity.
  2. The superscript (P) over a strain term indicates the plastic component of the quantity.
  3. The superscript (e) over a strain term indicates the elastic component of the quantity.
  4. A bar over a stress is used to distinguish effective from total stress where such distinction is necessary.

## APPENDIX B

### NOTATION

Most of the notation used in the mathematical derivations is standard in all mechanics, including soil mechanics, but there are some specific uses which are unusual. The following comments describe those points.

#### 1. Sign Convention

All stresses are considered positive in tension, and all strains are considered positive in extension. This is contrary to the usual soil mechanics usage but agrees with continuum mechanics conventions. Shear stresses and strains are positive when they are in a positive coordinate direction on a surface whose outward normal is in a positive direction. For example,  $\sigma_{xy}$  is positive if the stress is in the +x direction on a face whose outward normal is in the +y direction. The convention is illustrated in Figures 11 and 12.

#### 2. Subscripts and Summation Convention

Subscripts consist of two letters which refer to two of three Cartesian axes. When specific axes are meant, the letters x, y, or z are used. When a general expression is being stated without reference to the specific x, y,

and z system, subscripts i through n, representing a coordinate system  $x_1, x_2, x_3$ , are used.

The repeated subscript summation convention is used with subscripts i through n. This means that whenever a subscript is repeated in a product or single term that term is summed as the subscripts vary from 1 to 3.

For example,

$$s_{ii} = s_{11} + s_{22} + s_{33},$$

$$\begin{aligned} s_{ij}s_{ij} &= s_{11}s_{11} + s_{12}s_{12} + s_{13}s_{13} \\ &+ s_{21}s_{21} + s_{22}s_{22} + s_{23}s_{23} \\ &+ s_{33}s_{33} + s_{31}s_{31} + s_{32}s_{32} \\ &+ s_{33}s_{33}. \end{aligned}$$

In connection with this convention the Kronecker delta is used. This is defined by

$$\delta_{ij} = \begin{cases} 0 & \text{if } i \neq j \\ 1 & \text{if } i = j \end{cases}$$

### 3. Stress and Strain Notation

Stresses are denoted by a subscripted  $\sigma$ , i.e.,  $\sigma_{ij}$ , or  $\sigma_{xy}$ .  $\tau$  and  $\sigma$  can be considered interchangeable.

Volumetric stress is described by an unsubscripted  $\sigma$ . Deviatoric stress is described by a subscripted  $s$ , i.e.,  $s_{ij}$  or  $s_{xy}$ .

Displacements are represented by  $u$  and  $v$  in the  $x$  and  $y$  directions, respectively. Strains are denoted by a subscripted  $\epsilon$ , and volumetric strains by an unsubscripted  $\epsilon$ . Deviatoric strains are represented by a subscripted  $e$ . It should be noted that volumetric strain is taken to mean one third of the sum of the normal strains.

When the shear strain is described by  $\epsilon_{xy}$ , for example, it is meant as

$$\epsilon_{xy} = \frac{1}{2} \left( \frac{\partial u}{\partial y} + \frac{\partial v}{\partial x} \right)$$

This differs from the usual engineering strain,  $\gamma_{xy}$ , which is defined by

$$\gamma_{xy} = \frac{\partial u}{\partial y} + \frac{\partial v}{\partial x}$$

Whenever  $\gamma_{xy}$  is used, it follows that

$$\gamma_{xy} = 2 \epsilon_{xy}$$

#### 4. Other Conventions

Whenever a symbol has a dot over it, the symbol is understood to represent the rate of change of the quantity



or its change during an increment of loading. A superscript (e) is used to indicate the elastic portion of a quantity. A superscript (p) indicates the plastic portion. These are used over strain symbols when the distinction between elastic and plastic components is not plain from the context. When they are used, the symbol without superscript indicates total strain, elastic and plastic.

The following elastic constants are used:

$E$  = Young's modulus

$\nu$  = Poisson's ratio

$G$  = Shear modulus =  $\frac{E}{2(1+\nu)}$

$K$  = Bulk modulus =  $\frac{E}{3(1-2\nu)}$

## APPENDIX C

### COMPUTER PROGRAM USE

#### 1. General

All the programs described here are written to be run on the M.I.T. Computation Center IBM 7094 computer. Certain timer routines are used which are not available elsewhere. All programs except PLANE (for elastic drained and undrained material) must be run with a user tape mounted on tape mount B5. This tape is used to store data for restarting a problem. For all programs except PLANE there are two available versions of the output subroutine: one for regular runs (5 minutes), and one for long runs (15 minutes). The programs are available as source programs in FORTRAN and FAP and as binary decks.

#### 2. Input

##### 2.1 Input for MASS-TR

There are ten groups of cards or individual cards required, as follows:

1. A card supplied with the deck which contains words used in printing the boundary condition in the output.
2. An arbitrary comment in columns 2 through 72. This is printed at the head of the output.
3. Format (2I5) - two integers. The first is an arbitrary problem identification number. The

second can have three values: 0 if the loading is by applied forces, 1 if the loading is by specified displacements, 2 if this is a restart of a previous problem.

4. Format (2I5) - two integers. First is the number of rows of mass points in the array; second is the number of columns.
5. Format (5E10.3) - five real numbers. These are, in order, Young's modulus, Poisson's ratio, the horizontal distance between mass points, the convergence criterion, and the convergence criterion for specified load levels.
6. Format (2E10.3) - two real numbers. These are the yield stress and the size of the desired load increment, which should correspond to the loads input by cards under number eight below.
7. Format (4E5) - four integers. These are the boundary conditions in the order left, right, top, and bottom. There can be four choices for each: 1 for free, 2 for fixed, 3 for reflected, and 4 for smooth or infinite. At present the bottom must be fixed or smooth.
8. Format (2I5,2E10.3) - Applied loads or displacements. Each card specifies the loading of one mass point. The first two fields are the row and column of the point, respectively. The last two are the load or displacement in the x and y

directions, respectively. After all loaded points are specified, there must be a blank card to end this group.

9. Format (3I5) - three integers. These specify the manner of incrementing the load. The first one can have two values: 1 to indicate a constant, standard increment of load or displacement, 2 to indicate the increment will be calculated each time to make only one stress point yield. The second applies only when a standard increment is used, and it can have two values: 1 for an increment that is standard even through the elastic range, 2 to indicate the increment to cause first yield will be calculated and the standard increment will be used after that. The last one applies to whether a downgrade routine will be used to reduce the applied load if it should stress an elastic point beyond the yield stress. The number one indicates no downgrading, and the number two indicates downgrading.
10. Format (7E10.3) - There can be up to seven of these cards, which list specific loads at which there must be a solution.

If it is desired to restart a problem, cards one through three must be submitted along with cards in group ten. No further input is needed.

## 2.2 Input for MASS-PR

The input for MASS-PR is identical to that for MASS-TR with one exception. In runs which restart a problem one additional card must be submitted after card three. This, in format (E10.3), must contain the value of the standard load increment to be used in the restarted run.

## 2.3 Input for PLUSS

The input for PLUSS is almost identical to that for MASS-TR. Cards one through five are identical. The  $E$  and  $\nu$  are specified with respect to effective stress. Card six has four real numbers (format 4E10.3). The first is the yield stress, the second is the magnitude of the standard increment of load or displacement to be used, the third is the magnitude of the initial load, and the fourth is the decimal portion of the yield stress which is to be the initial shear stress.

Card nine has only one integer, format (I5), which has the value one to indicate a constant increment of load and the value two to indicate the increment to cause first yield is calculated and the standard increment is used thereafter. There is no provision for calculated increments during plastic flow.

## 2.4 Input for MASS-DP

The first four cards are identical to those for MASS-TR. Cards five and six are as follows:

5. Format (5E10.3) - The five real numbers are:  
Young's modulus, Poisson's ratio,  $k$  in the Drucker-Prager equation,  $\alpha$  in the Drucker-Prager equation, and the unit weight of the soil.
6. Format (5E10.3) - The five real numbers are:  
the horizontal distance between mass points, the standard increment of load, the initial load magnitude, the convergence criterion, and  $K_0$ .  
Cards seven and eight are the same as those for MASS-TR. Card nine is the same except that it does not require the specification of the downgrade option, which does not exist in MASS-DP.  
Card ten is the same.

Restart problems have input similar to that for MASS-TR except that the increment of load to be used must be specified by a card in format (E10.3) after card three.

## 2.5 Input for MASS-SH

The first four cards are identical to those for MASS-TR. Cards five and six are as follows:

5. Format (5E10.3) - The five fields are: Young's modulus, Poisson's ratio, the horizontal distance between mass points, the convergence criterion, and the unit weight of soil.
6. Format (6E10.3) - The six fields are  $\alpha$ ,  $k$ ,  $D$ ,  $C$ , the standard load increment, and  $K_0$ .

Cards seven and eight are the same as before. Cards in group nine are the loads at which specific solution is desired, which are called group ten in the previous programs. There is no option other than that of a standard load.

Restart problems are handled identically to those in MASS-TR, except that the load increment must be specified after card three by one card in format (E10.3).

## 2.6 Input for PLANE

There are six groups of cards for PLANE. This program does not require a restart tape as it has no restart capability. Several problems can be run consecutively by submitting cards two through six for each problem as successive data cards. The cards are as follows:

1. A card supplied with the deck similar to card one in MASS-TR. It is not repeated in successive problems.
2. A comment card as in MASS-TR.
3. Format (4I5) - four integers. The first is the number of rows in the problem, and the second is the number of columns. The third indicates whether forces or displacements will be specified. The number one indicates displacements; the number zero indicates forces. The last number is one if the problem is to be run undrained (no volume change) and zero if it is to be drained.

4. Format (4I5) - four intergers. These are the boundary conditions as in card seven for MASS-TR. At present the top boundary must be free, and no other boundary may be free.
5. Format (4E15.5) - four real numbers. The first two are Young's modulus and Poisson's ratio with respect to effective stress. The third is the horizontal distance between mass points, and the fourth is the convergence criterion.
6. These are the applied loads or displacements, one card per loaded mass point. The format is the same as in cards eight of MASS-TR. However, the third field specifies the vertical load or displacement, and the fourth specifies the horizontal. The last card must be blank.

### 3. Output

The output from all these programs is in the form of listings. At the head of the output is a description of the input data. For each convergence at a load or displacement the programs put out a list of all displacements boundary forces, vertical stresses, horizontal stresses, shear stresses on the horizontal plane, and stresses normal to the plane or pore pressures where those are calculated in the solution. For all but MASS-SH they put out the ratio between the stress level at each stress point and the yield



stress. For MASS-SH the square root of  $J_2$  is listed for each stress point. All plastic programs except MASS-SH provide a small map of the stress point array containing a zero for each elastic point, a one for each plastic point, and a two for each newly-yielded point. The corresponding array for MASS-SH uses a one for an elastic point and a zero for a plastic point because of the internal logic of the program.

PLANE gives the same sort of listings and in addition provides listings of the principal stresses at each stress point and their orientation. An optional output package for PLANE provides normalized values of all stresses arranged on the page so the decimal point falls on the stress point. This package works only for arrays of stress points which have fifteen or less points on a row.

## APPENDIX D

### MATERIAL WITH NO CHANGE OF VOLUME

#### 1. Difficulties in Use of $\nu = 0.5$

The material considered here is an elastic or elastic-perfectly-plastic one whose yield criterion does not imply volumetric plastic strain. It is often a reasonable approximation to the actual behavior of undrained clay to assume that there is no volume change in the elastic range either. This is done by setting Poisson's ratio,  $\nu$ , equal to one half, for then the bulk modulus,  $K$ , is infinite. The closed form solutions to many standard problems of elasticity then give useful numerical results, and, in particular, the solutions for vertical stress in Boussinesq's problem do so because they do not depend on Poisson's ratio.

Unfortunately, the direct use of Poisson's ratio of one-half is not possible in the mathematical model used here since the term  $(1-2\nu)$  appears in the denominator of equations (E18) and (E35). The model tries to calculate stresses from strains, but the volumetric stresses can have any value in an element so long as the volumetric strains are zero, so the calculation cannot be made. In other words, the finite values of volumetric stress which satisfy equilibrium and the boundary conditions are specified by a multiplication of an infinite quantity (the bulk modulus) by a zero quantity (the volumetric strain).

An initial approach was to make Poisson's ratio as close to one half as possible. This caused exorbitantly long running times in the elastic range for  $\nu$  over about 0.4, as Figure 13 by Christian (1965) shows. As Poisson's ratio becomes close to one half, the terms with  $(1-2\nu)$  in the denominator become quite large; large stresses result from small displacements. The adjustments in displacement at each mass point in each cycle become so small and so dependent on minor errors in values of strain that many more cycles are needed for convergence.

## 2. Porous Elastic and Porous Elastic-Plastic Materials

The soil may be considered a system with two phases: the solid soil skeleton and the pore fluid. The pore fluid is assumed incompressible and unable to carry any shear stress. All deviatoric rigidity must lie in the soil skeleton. It is further assumed that the strains in the two phases must be identical.

If the soil skeleton is linearly elastic and isotropic, the material is the "poro-elastic" solid, described by Biot (1941 a,b,c). It is the material for which most two- and three-dimensional consolidation work has been done and is also the material used one-dimensionally in the Terzaghi consolidation theory (Taylor, 1948).

Now, there will be no plastic volumetric strain for a material obeying Tresca's or Hencky's and von Mises' yield criterion. The elastic behavior of the skeleton

can be defined with respect to effective stresses by

$$\epsilon_{ij} = \frac{1+\nu}{E} \bar{\sigma}_{ij} - \frac{\nu}{E} \bar{\sigma}_{kk} \delta_{ij}, \quad (D1)$$

where  $\bar{\sigma}_{ij}$  is the effective stress and  $E$  and  $\nu$  are the elastic constants with respect to effective stress. The volumetric strain will be defined by

$$\epsilon = \frac{1-2\nu}{E} \bar{\sigma}, \quad (D2)$$

if  $\bar{\sigma}$  is the effective volumetric stress. The pore fluid pressure is represented by  $p$  to avoid confusion with the displacement  $u$ , and, by definition of total stress,  $\sigma$ ,

$$\bar{\sigma} = \sigma - p. \quad (D3)$$

The problem is to reduce  $\epsilon$  to zero and, hence,  $\bar{\sigma}$  to zero. At some stage in an iterative procedure there may be some volumetric strain,  $\epsilon$ , and some volumetric stress,  $\bar{\sigma}$ . If the pore pressure is now increased by  $\bar{\sigma}$  while  $\sigma$  is constant, the effective stress will reduce to zero, as will the volumetric strain. This suggests the following process:

- 1) All effective stresses are defined in terms of strains, and the computer proceeds through one cycle of the iteration without worrying about pore pressures. This will cause volume change.

It must be remembered that already existing pore pressures must be considered in the equilibrium equations.

- 2) The volumetric strains are calculated and the pore pressures increased in accordance with

$$\Delta p = \frac{E}{(1-2\nu)} \epsilon. \quad (D4)$$

- 3) Steps one and two are repeated until the displacements converge and further  $\Delta p$ 's are smaller than the convergence criterion.

This routine is convenient in the program for the undrained plastic material (PLUSS) since the updated forces in the stress points are not stored until convergence has occurred. The volumetric strain is the most easily calculated measure of the effective volumetric stress. In the actual program the calculation is done by evaluating the bulk strain, which is three times  $\epsilon$  and equal to the sum of  $\epsilon_{xx}$  and  $\epsilon_{yy}$ , and dividing it by the bulk modulus,  $K$ .

A previous report (Christian, 1965) describes a program for a purely elastic porous material. In this program the updated forces are stored as the iteration is carried out, so some further analysis is helpful. The expressions for normal strain in such a porous elastic material are

$$E\Delta\epsilon_{xx} = \Delta\bar{\sigma}_{xx} - \nu(\Delta\bar{\sigma}_{yy} + \Delta\bar{\sigma}_{zz}) \quad (D5)$$

and two others obtained by permutation of subscripts. For plane strain conditions

$$\Delta\epsilon_{zz} = 0, \quad (D6)$$

and

$$\Delta\bar{\sigma} = \nu(\Delta\bar{\sigma}_{xx} + \Delta\bar{\sigma}_{yy}). \quad (D7)$$

The requirement of no volume change is

$$\Delta\epsilon_{xx} + \Delta\epsilon_{yy} + \Delta\epsilon_{zz} = \Delta\epsilon_{xx} + \Delta\epsilon_{yy} = 0 \quad (D8)$$

From these equations it follows that

$$(1 - 2\nu)(\Delta\bar{\sigma}_{xx} + \Delta\bar{\sigma}_{yy}) = 0. \quad (D9)$$

$$\Delta\bar{\sigma}_{xx} + \Delta\bar{\sigma}_{yy} = 0. \quad (D10)$$

$$\Delta\sigma_{xx} + \Delta\sigma_{yy} - 2\Delta p = 0. \quad (D11)$$

$$\Delta p = (\Delta\sigma_{xx} + \Delta\sigma_{yy})/2. \quad (D12)$$

Since in each cycle of the iteration described above the effective stresses are initially computed without reference to changes in pore pressure occurring simultaneously, the changes are changes in total stress also. The iteration can then proceed by adding one half their sum to the pore pressure, and the process is repeated until convergence occurs.

### 3. Skempton's A Factor

The A factor (Skempton, 1954) for an incompressible material is defined by

$$A = \frac{\Delta p - \Delta\sigma_3}{\Delta\sigma_1 - \Delta\sigma_3}, \quad (D13)$$

if  $\Delta\sigma_1$  is the greatest compressive stress change and  $\Delta\sigma_3$  is the smallest compressive stress change. From equation (D11) one can write

$$\Delta\sigma_1 - \Delta\sigma_3 = 2\Delta p - 2\Delta\sigma_3. \quad (D14)$$

This leads to

$$A = 0.5 \quad (D15)$$

For axially symmetric stress systems there are two extreme cases: extension and compression. In extension  $\Delta\sigma_2 = \Delta\sigma_1$ , and in compression  $\Delta\sigma_2 = \Delta\sigma_3$ . The previous analysis assumes the pore pressure is the volumetric stress, so, in triaxial compression,

$$\begin{aligned} \Delta p &= (\Delta\sigma_1 + \Delta\sigma_2 + \Delta\sigma_3)/3 \\ &= (2\Delta\sigma_3 + \Delta\sigma_1)/3. \end{aligned} \quad (D16)$$

This can easily be converted into

$$\Delta\sigma_1 - \Delta\sigma_3 = 3\Delta p - 3\Delta\sigma_3, \quad (D17)$$

or

$$A = 1/3. \quad (D18)$$

In triaxial extension the equation corresponding to equation (D16) is

$$\Delta p = (2\Delta\sigma_1 + \Delta\sigma_3)/3. \quad (D19)$$

This leads to

$$2\Delta\sigma_1 - 2\Delta\sigma_3 = 3\Delta p - 3\Delta\sigma_3, \quad (D20)$$

and

$$A = 2/3. \quad (D21)$$

These results demonstrate that the A factor is very much a function of the applied stress system even for this simple material whose pore pressures are not affected by shear stresses. The extrapolation of pore pressure measurements from triaxial test results to conditions with other stress systems on the basis of the A factor would seem to have a considerable danger of error.

#### 4. Total Stress Elastic Constants

It is useful to be able to convert the effective stress elastic constants, E and  $\nu$ , to total stress elastic constants, E\* and  $\nu^*$ . Since there is no elastic volume change,  $\nu^*$  is



one-half. The shear strains must be identical whether total or effective stresses are used, and also total shear stresses must equal effective shear stresses. This means that the shear moduli,  $G$  and  $G^*$ , relating effective and total stress, respectively, to shear strain must be equal.

$$\frac{E}{1 + \nu} = \frac{E^*}{1 + .5'} \quad (D22)$$

and

$$E^* = \frac{1.5}{1 + \nu} E. \quad (D23)$$

This expression has also been derived by Davis and Poulos (1963).

### 5. Yield Criterion

Under undrained, plane strain conditions Tresca's and Hencky's and von Mises' yield criteria give identical results. This follows because the total stress normal to the plane must be given by

$$\sigma_{zz} = 0.5 (\sigma_{xx} + \sigma_{yy}). \quad (D24)$$

This means that the normal stress,  $\sigma_{zz}$ , is the average total stress, which is equal to the pore pressure. Subtraction of the pore pressure from equation (D24) leads to

$$\bar{\sigma}_{zz} = 0 = 0.5(\bar{\sigma}_{xx} + \bar{\sigma}_{yy}). \quad (D25)$$

The second invariant of deviator stress,  $J_2$ , which is the critical term for the Hencky-von Mises criterion, can be written in terms of principal stresses as

$$J_2 = [(\sigma_1 - \sigma_2)^2 + (\sigma_1 - \sigma_3)^2 + (\sigma_2 - \sigma_3)^2]/6. \quad (D26)$$

If the x and y axes are chosen to coincide with those of principal stress and either of equations (D24) or (D25) is substituted into equation (D26), the result is

$$J_2 = (\sigma_1 - \sigma_3)^2/4. \quad (D27)$$

Equation (D27) means that the Hencky-von Mises criterion reduces to

$$|0.5 (\sigma_1 - \sigma_3)| = k, \quad (D28)$$

which is the Tresca criterion of maximum shear stress. For this reason the program for the undrained elastic-perfectly-plastic material obeying Tresca's criterion serves for the undrained Prandtl-Reuss material as well.

## APPENDIX E

### INCREMENTAL PLASTIC STRESS STRAIN RELATIONS

#### 1. Tresca Yield Criterion

A similar analysis was originally presented by Harper (1963) and Whitman (1964) and is included here for completeness. Dots over stresses and strains indicate rates. The yield criterion, for plane strain, is defined by

$$f = \left( \frac{\sigma_{xx} - \sigma_{yy}}{2} \right)^2 + \tau_{xy}^2 - k^2 = 0 \quad (E1)$$

if it is assumed all yielding will occur parallel to the plane of plane strain. The theory of the plastic potential requires that

$$\dot{\epsilon}_{ij}^{(P)} = \lambda' \frac{\partial f}{\partial \sigma_{ij}} \quad (E2)$$

Since there is no volumetric plastic strain rate ( $\dot{\epsilon}^{(P)} \equiv 0$ ), it follows that the deviatoric plastic strain is

$$\dot{\epsilon}_{ij}^{(P)} = \lambda' \frac{\partial f}{\partial s_{ij}} \quad (E3)$$

Further, the yield criterion can be expressed in terms of the deviator as

$$f = \left( \frac{s_{xx} - s_{yy}}{2} \right)^2 + \tau_{xy}^2 - k^2 = 0. \quad (E4)$$

From equations (E3) and (E4)

$$\begin{aligned} \dot{\epsilon}_{xx}^{(P)} &= \lambda' (s_{xx} - s_{yy}) \\ \dot{\epsilon}_{yy}^{(P)} &= -\lambda' (s_{xx} - s_{yy}) \\ \dot{\epsilon}_{xy}^{(P)} &= 2\lambda' \tau_{xy} \end{aligned} \tag{E5}$$

Now both sides can be multiplied by  $2G$  and a new constant,  $\lambda$ , defined as  $4G\lambda'$  to give

$$\begin{aligned} 2G \dot{\epsilon}_{xx}^{(P)} &= \lambda \left( \frac{s_{xx} - s_{yy}}{2} \right) \\ 2G \dot{\epsilon}_{yy}^{(P)} &= \lambda \left( \frac{s_{yy} - s_{xx}}{2} \right) \\ 2G \dot{\epsilon}_{xy}^{(P)} &= G \dot{\gamma}_{xy}^{(P)} = \lambda \tau_{xy} \end{aligned} \tag{E6}$$

From the equations of elasticity the elastic strain rates can be defined as

$$\begin{aligned} 2G \dot{\epsilon}_{xx}^{(e)} &= \dot{s}_{xx} \\ 2G \dot{\epsilon}_{yy}^{(e)} &= \dot{s}_{yy} \end{aligned}$$

$$2G \dot{\epsilon}_{xy}^{(e)} = G \dot{\gamma}_{xy}^{(e)} = \dot{\tau}_{xy} \quad (E7)$$

Since the total strain rate must be the sum of the elastic and plastic strain rates, equations (E6) and (E7) can be combined to give

$$2G \dot{\epsilon}_{xx} = \dot{s}_{xx} + \lambda \left( \frac{s_{xx} - s_{yy}}{2} \right)$$

$$2G \dot{\epsilon}_{yy} = \dot{s}_{yy} + \lambda \left( \frac{s_{yy} - s_{xx}}{2} \right) \quad (E8)$$

$$G \dot{\gamma}_{xy} = \dot{\tau}_{xy} + \lambda \tau_{xy}.$$

A term,  $\dot{W}$ , can be defined

$$\begin{aligned} \dot{W} &= \left( \frac{s_{xx} - s_{yy}}{2} \right) (\dot{\epsilon}_{xx} - \dot{\epsilon}_{yy}) + \tau_{xy} \dot{\gamma}_{xy} \\ &= \left( \frac{s_{xx} - s_{yy}}{2} \right) \dot{\epsilon}_{xx} + \left( \frac{s_{yy} - s_{xx}}{2} \right) \dot{\epsilon}_{yy} + \tau_{xy} \dot{\gamma}_{xy} \end{aligned} \quad (E9)$$

Now the first of equation (8) is multiplied by  $\left( \frac{s_{xx} - s_{yy}}{2} \right)$ , the second by  $\left( \frac{s_{yy} - s_{xx}}{2} \right)$ , and the third by  $2\tau_{xy}$ , and the results are added to give

$$\begin{aligned} 2G\dot{W} &= \left( \frac{s_{xx} - s_{yy}}{2} \right) \dot{s}_{xx} + \lambda \left( \frac{s_{xx} - s_{yy}}{2} \right)^2 + \left( \frac{s_{yy} - s_{xx}}{2} \right) \dot{s}_{yy} \\ &\quad + \lambda \left( \frac{s_{yy} - s_{xx}}{2} \right)^2 + 2\tau_{xy} \dot{\tau}_{xy} + 2\lambda \tau_{xy}^2 \end{aligned}$$

$$\begin{aligned}
&= \left( \frac{s_{xx} - s_{yy}}{2} \right) \dot{s}_{xx} + \left( \frac{s_{yy} - s_{xx}}{2} \right) \dot{s}_{yy} + 2\tau_{xy} \dot{\tau}_{xy} \\
&\quad + 2\lambda \left[ \left( \frac{s_{xx} - s_{yy}}{2} \right)^2 + \tau_{xy}^2 \right] \\
&= \dot{f} + 2\lambda k^2 = 2\lambda k^2 \tag{E10}
\end{aligned}$$

Therefore,

$$\lambda = \frac{G\dot{W}}{k} \tag{E11}$$

Substitution of equation (E11) into equation (E8) and rearrangement of terms give

$$\begin{aligned}
\dot{s}_{xx} &= 2G \left( \dot{e}_{xx} - \frac{\dot{W}}{2k^2} \frac{(s_{xx} - s_{yy})}{2} \right) \\
\dot{s}_{yy} &= 2G \left( \dot{e}_{yy} - \frac{\dot{W}}{2k^2} \frac{(s_{yy} - s_{xx})}{2} \right) \\
\dot{\tau}_{xy} &= G \left( \dot{\gamma}_{xy} - \frac{\dot{W}}{k} \tau_{xy} \right). \tag{E12}
\end{aligned}$$

The total stress rates are

$$\begin{aligned}
\dot{\sigma}_{xx} &= 2G \left( \dot{e}_{xx} - \frac{\dot{W}}{2k^2} \frac{(s_{xx} - s_{yy})}{2} \right) + 3K\dot{e} \\
\dot{\sigma}_{yy} &= 2G \left( \dot{e}_{yy} - \frac{\dot{W}}{2k^2} \frac{(s_{xx} - s_{yy})}{2} \right) + 3K\dot{e} \\
\dot{\tau}_{xy} &= G \left( \dot{\gamma}_{xy} - \frac{\dot{W}}{k^2} \tau_{xy} \right). \tag{E13}
\end{aligned}$$

These equations can be converted into incremental form by making all rate terms, such as  $\dot{\sigma}_{xx}$ , into small increments, such as  $\Delta\sigma_{xx}$ . The term  $\dot{W}$  can first be expressed incrementally as

$$\Delta W = \left( \frac{\sigma_x - \sigma_y}{2} \right) (\Delta\epsilon_x - \Delta\epsilon_y) + \tau_{xy} \Delta\gamma_{xy}. \quad (E14)$$

The equation (E13) then becomes, after some algebraic manipulation,

$$\begin{aligned} \Delta\sigma_{xx} = & \left[ \frac{4G + 3K}{3} - \frac{G}{k^2} \left( \frac{\sigma_{xx} - \sigma_{yy}}{2} \right)^2 \right] \Delta\epsilon_{xx} \\ & + \left[ \frac{-2G + 3K}{3} + \frac{G}{k^2} \left( \frac{\sigma_{xx} - \sigma_{yy}}{2} \right)^2 \right] \Delta\epsilon_{yy} \\ & + \left[ -\frac{G\tau_{xy}}{k^2} - \frac{\sigma_x - \sigma_y}{2} \right] \Delta\gamma_{xy} \\ \Delta\sigma_{yy} = & \left[ \frac{-2G + 3K}{3} + \frac{G}{k^2} \left( \frac{\sigma_{xx} - \sigma_{yy}}{2} \right)^2 \right] \Delta\epsilon_{xx} \\ & + \left[ \frac{4G + 3K}{3} - \frac{G}{k^2} \left( \frac{\sigma_{xx} - \sigma_{yy}}{2} \right)^2 \right] \Delta\epsilon_{yy} \\ & + \left[ \frac{G\tau_{xy}}{k^2} - \frac{\sigma_x - \sigma_y}{2} \right] \Delta\gamma_{xy} \end{aligned} \quad (E15)$$

$$\begin{aligned} \Delta \tau_{xy} = & \left[ -\frac{G}{k^2} \tau_{xy} \left( \frac{\sigma_x - \sigma_y}{2} \right) \right] \Delta \epsilon_{xx} \\ & + \left[ \frac{G}{k^2} \tau_{xy} \left( \frac{\sigma_x - \sigma_y}{2} \right) \right] \Delta \epsilon_{yy} \\ & + \left[ G \left( 1 - \frac{\tau_{xy}^2}{k^2} \right) \right] \Delta \gamma_{xy} . \end{aligned}$$

The computer program uses forces and displacements rather than stresses and strains. If  $\delta$  is the diagonal distance between points and the abbreviations UL, UR, LL, LR stand for upper left, upper right, lower left, and lower right, respectively, following approximations can be used:

$$F_x = \sigma_{xx} \frac{\delta}{2}$$

$$F_y = \sigma_{yy} \frac{\delta}{2}$$

$$F_{xy} = \tau_{xy} \frac{\delta}{2} \tag{E16}$$

and

$$\delta \cdot \epsilon_{xx} = u_{LR} - u_{UL}$$

$$\delta \cdot \epsilon_{yy} = v_{LL} - v_{UR}$$

$$\delta \cdot \epsilon_{xy} = u_{LL} - u_{UR} + v_{LR} - v_{UL} \tag{E17}$$



In these expressions the F's are forces in a stress point and u and v are the two components of displacements at surrounding mass points.

Then,

$$\begin{aligned}
 \Delta F_x &= A(\Delta u_{LR} - \Delta u_{UL}) + B(\Delta v_{LL} - \Delta v_{UR}) \\
 &\quad - C(\Delta u_{LL} - \Delta u_{UR} + \Delta v_{LR} - \Delta v_{UL}) \\
 \Delta F_y &= B(\Delta u_{LR} - \Delta u_{UL}) + A(\Delta v_{LL} - \Delta v_{UR}) \\
 &\quad + C(\Delta u_{LL} - \Delta u_{UR} + \Delta v_{LR} - \Delta v_{UL}) \\
 \Delta F_{xy} &= -C(\Delta u_{LR} - \Delta u_{UL}) + C(\Delta v_{LL} - \Delta v_{UR}) \\
 &\quad + D(\Delta u_{LL} - \Delta u_{UR} + \Delta v_{LR} - \Delta v_{UL})
 \end{aligned} \tag{E18}$$

where

$$\begin{aligned}
 A &= \frac{1}{2} \left[ \frac{4G + 3K}{3} - \frac{G}{k^2 \delta^2} (F_x - F_y)^2 \right] \\
 B &= \frac{1}{2} \left[ \frac{-2G + 3K}{3} + \frac{G}{k^2 \delta^2} (F_x - F_y)^2 \right] \\
 C &= \frac{G}{k^2 \delta^2} F_{xy} (F_x - F_y) \\
 D &= \frac{1}{2} \left[ G - \frac{4G}{k^2 \delta^2} (F_{xy})^2 \right].
 \end{aligned} \tag{E19}$$

These equations will provide a finite approximation to the actual differential behavior of the stresses. After several increments the stresses may have departed markedly from the yield surface because of accumulated errors. To prevent this it is desirable to have a correction to the above results.

It is assumed that during the correction the average stress does not change. After application of equations (E18) and (E19) a set of forces  $F'_x$ ,  $F'_y$ , and  $F'_{xy}$ , will have been calculated. These should satisfy the equation

$$\left(\frac{F_x - F_y}{2}\right)^2 + F_{xy}^2 = \frac{k^2 \delta^2}{4} \quad (\text{E20})$$

In fact the relation will be

$$\left(\frac{F_x - F_y}{2}\right)^2 + F_{xy}^2 = \frac{k_t^2 \delta^2}{4} \quad (\text{E21})$$

A reasonable correction would be to reduce both components,  $\frac{F_x - F_y}{2}$  and  $F_{xy}$ , by an equal ratio. This leads to new

values

$$\frac{F'_x - F'_y}{2} = \frac{F_x - F_y}{2} \cdot \frac{k}{k_t}$$

$$F'_{xy} = F_{xy} \cdot \frac{k}{k_t} \quad (\text{E22})$$

By the assumption of constant average stress

$$\frac{F'_x + F'_y}{2} = \frac{F_x + F_y}{2}, \quad (\text{E23})$$

Therefore,

$$F'_x = \frac{F_x}{2} \left(1 + \frac{k}{k_t}\right) + \frac{F_y}{2} \left(1 - \frac{k}{k_t}\right)$$
$$F'_y = \frac{F_x}{2} \left(1 - \frac{k}{k_t}\right) + \frac{F_y}{2} \left(1 + \frac{k}{k_t}\right). \quad (\text{E24})$$

## 2. Prandtl-Reuss Material

The Prandtl-Reuss material is linearly elastic up to the yield criterion and yields according to the von Mises criterion,

$$f = J_2 - k^2 = 0 \quad (\text{E25})$$

The second invariant of the deviatoric stress tensor can be expressed, using the summation convention, as

$$J_2 = \frac{1}{2} s_{ij} s_{ij} \quad (\text{E26})$$

As in the case of the Tresca material, there is no volumetric plastic strain, and the plastic potential gives

a set of nine equations,

$$\overset{(P)}{\dot{e}_{ij}} = \lambda' s_{ij} \quad (E27)$$

These can be combined with the elastic stress-strain relation (E7) to give

$$2G \dot{e}_{ij} = \dot{s}_{ij} + \lambda s_{ij} \quad (E28)$$

The rate of deviatoric work is now defined as

$$\dot{W} = s_{ij} \dot{e}_{ij} \quad (E29) \quad (E29)$$

Multiplication of each equation of (E28) by  $s_{ij}$  and addition of all equations (contraction) gives

$$\begin{aligned} 2G \dot{W} &= s_{ij} \dot{s}_{ij} + \lambda s_{ij} s_{ij} \\ &= \dot{J}_2 + 2\lambda J_2 = 2\lambda k^2 \end{aligned} \quad (E30)$$

Therefore,

$$\lambda = \frac{G\dot{W}}{k^2} \quad (E31)$$

By a process similar to that which led to equations (E13), it follows that

$$\dot{\sigma}_{ij} = 2G (\dot{\epsilon}_{ij} - \frac{\dot{W}}{2k} s_{ij}) + 3K \dot{\epsilon} \delta_{ij} \quad (E32)$$

For plane strain,  $\tau_{xz}$ ,  $\tau_{yz}$ , and  $\epsilon_{zz}$  are zero, but  $\sigma_{zz}$  is not, nor is  $\dot{\sigma}_{zz}$ . The equations (E32) can be converted directly into incremental form, but it is first convenient to eliminate  $\sigma_{zz}$ . The volumetric stress,  $\sigma$ , is entirely elastic, so

$$\sigma = 3K \epsilon = K(\epsilon_{xx} + \epsilon_{yy}), \quad (E33)$$

and

$$s_{xx} = \sigma_{xx} - K(\epsilon_{xx} + \epsilon_{yy})$$

$$s_{yy} = \sigma_{yy} - K(\epsilon_{xx} + \epsilon_{yy}) \quad (E34)$$

$$s_{zz} = -s_{xx} - s_{yy} = 2K(\epsilon_{xx} + \epsilon_{yy}) - \sigma_{xx} - \sigma_{yy}.$$

These can now be used to obtain the equations

$$\begin{aligned} \Delta \sigma_{xx} = & \left[ \frac{4G + 3K}{3} - \frac{G}{k} (\sigma_{xx} - \sigma)^2 \right] \Delta \epsilon_{xx} \\ & + \left[ \frac{-2G + 3K}{3} - \frac{G}{k} (\sigma_{xx} - \sigma)(\sigma_{yy} - \sigma) \right] \Delta \epsilon_{yy} \\ & + \left[ -\frac{G\tau_{xy}}{k^2} (\sigma_{xx} - \sigma) \right] \Delta \gamma_{xy} \end{aligned}$$

$$\begin{aligned}
\Delta\sigma_{yy} &= \left[ \frac{-2G + 3K}{3} - \frac{G}{k^2} (\sigma_{xx} - \sigma)(\sigma_{yy} - \sigma) \right] \Delta\epsilon_{xx} \\
&+ \left[ \frac{4G + 3K}{3} - \frac{G}{k^2} (\sigma_{yy} - \sigma)^2 \right] \Delta\epsilon_{yy} \\
&+ \left[ -\frac{G\tau_{xy}}{k^2} (\sigma_{yy} - \sigma) \right] \Delta\gamma_{xy} \\
\Delta\tau_{xy} &= \left[ \frac{G\tau_{xy}}{k^2} (\sigma - \sigma_{xx}) \right] \Delta\epsilon_{xx} + \left[ \frac{G\tau_{xy}}{k^2} (\sigma - \sigma_{yy}) \right] \Delta\epsilon_{yy} \\
&+ \left[ G - \frac{\tau_{xy}^2}{k^2} \right] \Delta\gamma_{xy} \tag{E35}
\end{aligned}$$

These equations can be converted into displacement form to obtain relations analogous to equations (E18) and (E19).

The correction procedure for bringing the stresses back to the yield surface is much more complicated for this material than for the Tresca material. After an incremental deformation there is a new set of stresses  $\sigma_{xx}$ ,  $\sigma_{yy}$ ,  $\sigma_{zz}$  and  $\tau_{xy}$ . These are the non-zero elements of the stress tensor  $\sigma_{ij}$ , which will have a volumetric component  $\sigma$  and a deviatoric component  $s_{ij}$ . The actual value of the second invariant will be

$$k_t = \frac{1}{2} s_{ij} s_{ij}, \tag{E36}$$

and  $k_t > k$  (E37)

The most obvious way to obtain new values of stress,  $\sigma'_{ij}$ , would be to reduce each of the components  $s_{ij}$  so that

$$s_{ij} = \frac{k}{k_t} s'_{ij} \quad (E38)$$

and  $\sigma' = \sigma. \quad (E39)$

However, this implies a change in  $\epsilon_{zz}$  because

$$\Delta\epsilon_{zz} = \frac{1}{3K} \Delta\sigma + \frac{1}{2G} \Delta s_{zz} \quad (E40)$$

To prevent a change in normal strain, which would violate the conditions of plane strain, it is necessary to change  $\sigma$  also. This means that

$$(1 - 2\nu)\Delta\sigma + (1 + \nu)\Delta s_{zz} = 0 \quad (E41)$$

and  $\Delta\sigma = \frac{1+\nu}{1-2\nu} s_{zz} \left(1 - \frac{k}{k_t}\right) \quad (E42)$

Equation (E42) replaces equation (E39).

Now, the new value of  $\sigma'_{xx}$  can be found, thus:

$$\begin{aligned} \sigma'_{xx} &= s'_{xx} + \sigma' = s_{xx} \frac{k}{k_t} + \sigma - \frac{(1+\nu)}{(1-2\nu)} (s_{xx} + s_{yy}) \left(1 - \frac{k}{k_t}\right) \\ &= \sigma_{xx} \frac{k}{k_t} - \frac{(1+\nu)}{(1-2\nu)} (\sigma_{xx} + \sigma_{yy}) \left(1 - \frac{k}{k_t}\right) \\ &\quad + \sigma \frac{3}{1-2\nu} \left(1 - \frac{k}{k_t}\right) \end{aligned} \quad (E43)$$

The volumetric stress,  $\sigma$ , is purely elastic, so it can be calculated from the volumetric strains:

$$\sigma = K(\epsilon_{xx} + \epsilon_{yy}) \quad (E44)$$

This can be used with equation (E43) to correct the values of  $\sigma_{xx}$ , and a similar expression holds for correcting  $\sigma_{yy}$ . The shear stress  $\tau_{xy}$  is corrected directly from equation (E46).

### 3. Drucker-Prager Yield Criterion

The analysis presented here follows that presented by Reyes(1966), whose work came to the author's attention as he was debugging and correcting a program based on a slightly different analysis. As in the Prandtl-Reuss case the summation convention is used.

The Drucker-Prager (1952) generalization of the Mohr-Coulomb yield criterion states that

$$f = \alpha I_1 + J_2^{\frac{1}{2}} - k = 0 \quad (E45)$$

where the first stress invariant,  $I_1$ , is defined by

$$I_1 = \sigma_{kk} \quad (E46)$$

and the second deviatoric stress invariant,  $J_2$ , is defined



by

$$J_2 = \frac{1}{2} s_{ij} s_{ij} \quad (E47)$$

The theory of the plastic potential then predicts that in the plastic range

$$\dot{\epsilon}_{ij}^{(P)} = \lambda \frac{\partial f}{\partial \sigma_{ij}} = \lambda \left[ \alpha \delta_{ij} + \frac{s_{ij}}{2J_2^{\frac{1}{2}}} \right], \quad (E48)$$

and

$$\dot{\epsilon}_{ij} = \frac{1+\nu}{E} \dot{\sigma}_{ij} - \frac{\nu}{E} \dot{I}_1 \delta_{ij} + \lambda \left[ \alpha \delta_{ij} + \frac{s_{ij}}{2J_2^{\frac{1}{2}}} \right]. \quad (E49)$$

To obtain  $\lambda$ , it is convenient to define the rate of doing work,  $\dot{W}$ , by

$$\dot{W} = \sigma_{ij} \dot{\epsilon}_{ij} \quad (E50)$$

Then,

$$\begin{aligned} \dot{W} &= \frac{1+\nu}{E} \sigma_{ij} \dot{\sigma}_{ij} - \frac{\nu}{E} \dot{I}_1 \sigma_{ij} \delta_{ij} + \lambda \left[ \alpha \delta_{ij} + \frac{s_{ij}}{2J_2^{\frac{1}{2}}} \right] \sigma_{ij} \\ &= \frac{1+\nu}{E} \sigma_{ij} \dot{\sigma}_{ij} - \frac{\nu}{E} I_1 \dot{I}_1 + \lambda \left[ \alpha I_1 + \frac{s_{ij} (s_{ij} + \frac{1}{3} I_1 \delta_{ij})}{2J_2^{\frac{1}{2}}} \right] \\ &= \frac{1}{2G} \sigma_{ij} \dot{\sigma}_{ij} - \frac{\nu}{E} I_1 \dot{I}_1 + \lambda k, \end{aligned} \quad (E51)$$

and

$$\lambda = \frac{1}{k} \left[ \dot{W} - \frac{1}{2G} \sigma_{ij} \dot{\sigma}_{ij} + \frac{v}{E} I_1 \dot{i}_1 \right] \quad (E52)$$

A further simplification is obtained by recognizing that

$$\dot{f} = \alpha \dot{i}_1 + (\dot{J}_2)^{\frac{1}{2}} = \alpha \dot{i}_1 + \frac{1}{2} \frac{\dot{J}_2}{J_2^{\frac{1}{2}}} = 0 \quad (E53)$$

so

$$\dot{J}_2 = -2\alpha \dot{i}_1 J_2^{\frac{1}{2}} \quad (E54)$$

Then,

$$\begin{aligned} \frac{\sigma_{ij} \dot{\sigma}_{ij}}{2G} &= \frac{1}{2G} \left[ s_{ij} + \frac{1}{3} I_1 \delta_{ij} \right] \left[ \dot{s}_{ij} + \frac{1}{3} \dot{i}_1 \delta_{ij} \right] \\ &= \frac{1}{2G} \left[ \dot{J}_2 + \frac{1}{3} I_1 \dot{i}_1 \right] \\ &= \frac{1}{2G} \left[ \frac{I_1}{3} - 2\alpha J_2^{\frac{1}{2}} \right] \dot{i}_1 \end{aligned} \quad (E55)$$

This can be substituted into Equation (E52) to give

$$\lambda = \frac{1}{k} \left[ \dot{W} - \left( \frac{I_1}{9K} - \frac{\alpha J_2^{\frac{1}{2}}}{G} \right) \dot{i}_1 \right] \quad (E56)$$

Equation (E49) becomes

$$\begin{aligned}
\dot{\epsilon}_{ij} &= \frac{\dot{\sigma}_{ij}}{2G} - \frac{\nu}{E} \dot{I}_1 \delta_{ij} \\
&+ \frac{1}{k} \left[ \dot{W} - \frac{I_1}{9K} \dot{I}_1 - \frac{\alpha J_2^{\frac{1}{2}}}{G} I_1 \right] \cdot \left[ \alpha \delta_{ij} + \frac{\sigma_{ij}}{2J_2^{\frac{1}{2}}} \right] \\
&= \frac{\sigma_{ij}}{2G} - \frac{3\nu K}{E} \left( \frac{\dot{I}_1}{3K} \right) \delta_{ij} \\
&+ \frac{1}{k} \left[ \dot{W} - \frac{\dot{I}_1}{3K} \left( \frac{I_1}{3} - \frac{3\alpha K J_2^{\frac{1}{2}}}{G} \right) \right] \cdot \\
&\left[ \alpha \delta_{ij} + \frac{\sigma_{ij}}{2J_2^{\frac{1}{2}}} - \frac{I_1}{6J_2^{\frac{1}{2}}} \delta_{ij} \right] \tag{E57}
\end{aligned}$$

It is now necessary to get expressions for  $\dot{\sigma}_{ij}$  in terms of  $\dot{\epsilon}_{ij}$  and  $\sigma_{ij}$ . First, the first form of equation (E57) is contracted to give

$$\begin{aligned}
\dot{\epsilon}_{kk} &= \frac{1+\nu}{E} \dot{I}_1 - \frac{3\nu}{E} \dot{I}_1 + \frac{3\alpha}{k} \left[ \dot{W} - \frac{I_1 \dot{I}_1}{9K} - \frac{\alpha J_2^{\frac{1}{2}}}{G} \dot{I}_1 \right] \\
&= \frac{\dot{I}_1}{3K} \left[ 1 + \frac{9\alpha^2 J_2^{\frac{1}{2}}}{k} \frac{K}{G} - \frac{\alpha I_1}{k} \right] + \frac{3\alpha \dot{W}}{k} \tag{E58}
\end{aligned}$$

Since

$$I_1 = \frac{k - J_2^{\frac{1}{2}}}{\alpha}, \tag{E59}$$

equation (E58) becomes

$$\dot{\epsilon}_{kk} = \frac{\dot{I}_1}{3K} \cdot \frac{J_2^{1/2}}{k} \left[ 1 + \frac{9\alpha^2 K}{G} \right] + \frac{3\alpha \dot{W}}{k} \quad (E60)$$

Now a variable  $p$  is defined as

$$p = \frac{J_2^{1/2}}{k} \left[ 1 + \frac{9\alpha^2 K}{G} \right] \quad (E61)$$

Then, equation (E60) leads to

$$\frac{\dot{I}_1}{3K} = \frac{1}{p} \left[ \dot{\epsilon}_{kk} - \frac{3\alpha \dot{W}}{k} \right] \quad (E62)$$

This can be used in equation (E57) to give

$$\begin{aligned} \dot{\epsilon}_{ij} = & \frac{\sigma_{ij}}{2G} - \frac{3\nu K}{E} \frac{1}{p} \left[ \dot{\epsilon}_{kk} - \frac{3\alpha \dot{W}}{k} \right] \delta_{ij} \\ & + \frac{1}{k} \left[ \dot{W} - \frac{1}{p} \left( \dot{\epsilon}_{kk} - \frac{3\alpha \dot{W}}{k} \right) \cdot \left( \frac{k}{3\alpha} \right) \cdot (1-p) \right] \cdot \\ & \left[ \left( \alpha - \frac{I_1}{6J_2^{1/2}} \right) \delta_{ij} + \frac{\sigma_{ij}}{2J_2^{1/2}} \right] \quad (E63) \end{aligned}$$

If this is expanded algebraically and terms are collected, it becomes

$$\begin{aligned} \dot{\epsilon}_{ij} = & \frac{\dot{\sigma}_{ij}}{2G} + \frac{\dot{W}}{kp} \left[ \left\{ \left( 1 + \frac{9\nu K}{E} \right) \alpha - \frac{I_1}{6J_2^{1/2}} \right\} \delta_{ij} + \frac{\sigma_{ij}}{2J_2^{1/2}} \right] \\ & + \dot{\epsilon}_{kk} \left[ \left\{ \left( \alpha - \frac{I_1}{6J_2^{1/2}} \right) \left( \frac{p-1}{3\alpha p} \right) - \frac{3\nu K}{E p} \right\} \delta_{ij} + \frac{p-1}{3\alpha p} \frac{\sigma_{ij}}{2J_2^{1/2}} \right] \end{aligned} \quad (E64)$$

Three other variables,  $h$ ,  $A$ , and  $B$ , can be defined by

$$h = \alpha \left( 1 + \frac{9\nu K}{E} \right) - \frac{I_1}{6J_2^{1/2}} \quad (E65)$$

$$= \frac{3}{2} \alpha \frac{K}{G} - \frac{I_1}{6J_2^{1/2}}$$

$$A = \frac{p-1}{6 \alpha p J_2^{1/2}} \quad (E66)$$

and

$$B = \left( \alpha - \frac{I_1}{6J_2^{1/2}} \right) \left( \frac{p-1}{3\alpha p} \right) - \frac{3\nu K}{E p} \quad (E67)$$

The last two terms can be simplified. First, it can be shown that

$$A = \frac{p-1}{6\alpha p J_2^{1/2}} = \frac{h}{pk} \quad (E68)$$

Second, it can also be shown that

$$\frac{p-1}{3\alpha p} = \frac{2h}{[1+9\alpha^2 \frac{K}{G}]} \quad (E69)$$

so

$$B = \frac{2h}{[1+9\alpha^2 \frac{K}{G}]} \left( \alpha - \frac{I_1}{6J_2^{\frac{1}{2}}} \right) - \frac{3\nu K}{E_p} \quad (E70)$$

These terms now allow simplification of equation (E64) into

$$\frac{\dot{\sigma}_{ij}}{2G} = \dot{\epsilon}_{ij} - \frac{\dot{W}}{kp} \left[ h\delta_{ij} + \frac{\sigma_{ij}}{2J_2^{\frac{1}{2}}} \right] - \dot{\epsilon}_{kk} [B\delta_{ij} + A\sigma_{ij}] \quad (E71)$$

Under plane strain conditions this is, for  $\dot{\sigma}_{xx}$ ,

$$\begin{aligned} \frac{\dot{\sigma}_{xx}}{2G} = \dot{\epsilon}_{xx} - \frac{\sigma_{xx}\dot{\epsilon}_{xx} + \sigma_{yy}\dot{\epsilon}_{yy} + \tau_{xy}\dot{\gamma}_{xy}}{kp} \left[ h + \frac{\sigma_{xx}}{2J_2^{\frac{1}{2}}} \right] \\ - (\dot{\epsilon}_{xx} + \dot{\epsilon}_{yy}) [B + A\sigma_{xx}] \end{aligned} \quad (E72)$$

A new variable, C, is now defined as

$$C = \frac{1}{2kpJ_2^{\frac{1}{2}}} = \frac{1}{2J_2(1+9\alpha^2 \frac{K}{G})} \quad (E73)$$

The final form is

$$\begin{aligned}
 \dot{\sigma}_{xx} &= 2G[1 - B - 2A\sigma_{xx} - C\sigma_{xx}^2] \dot{\epsilon}_{xx} \\
 &+ 2G[-B - (\sigma_{xx} + \sigma_{yy})A - C\sigma_{xx}\sigma_{yy}] \dot{\epsilon}_{yy} \\
 &+ 2G[-A\tau_{xy} - C\sigma_{xx}\tau_{xy}] \dot{\gamma}_{xy}
 \end{aligned} \tag{E74}$$

Similarly,

$$\begin{aligned}
 \dot{\sigma}_{yy} &= 2G[-B - (\sigma_{xx} + \sigma_{yy})A - C\sigma_{xx}\sigma_{yy}] \dot{\epsilon}_{xx} \\
 &+ 2G[1 - B - 2A\sigma_{yy} - C\sigma_{yy}^2] \dot{\epsilon}_{yy} \\
 &+ 2G[-A\tau_{xy} - C\sigma_{yy}\tau_{xy}] \dot{\gamma}_{xy}
 \end{aligned} \tag{E75}$$

$$\begin{aligned}
 \dot{\tau}_{xy} &= 2G[-A\tau_{xy} - C\sigma_{xx}\tau_{xy}] \dot{\epsilon}_{xx} \\
 &+ 2G[-A\tau_{xy} - C\sigma_{yy}\tau_{xy}] \dot{\epsilon}_{yy} \\
 &+ 2G\left[\frac{1}{2} - C\tau_{xy}^2\right] \dot{\gamma}_{xy}
 \end{aligned} \tag{E76}$$

and

$$\begin{aligned}
 \dot{\sigma}_{zz} = & 2G[ - B - (\sigma_{xx} + \sigma_{zz})A - C\sigma_{zz}\sigma_{xx} ] \dot{\epsilon}_{xx} \\
 & + 2G[ - B - (\sigma_{yy} + \sigma_{zz})A - C\sigma_{zz}\sigma_{yy} ] \dot{\epsilon}_{yy} \\
 & + 2G[ - A\tau_{xy} - C\sigma_{zz}\tau_{xy} ] \dot{\gamma}_{xy}
 \end{aligned} \tag{E77}$$

These expressions can be easily converted into incremental form.

The correction to bring stresses back to the yield surface is quite complicated for the Drucker-Prager yield criterion, so an approximate correction was developed. This assumes the volumetric stress (or  $I_1$ ), remains constant. A measure of the amount by which the yield criterion is exceeded is

$$\frac{k - \alpha I_1}{\sqrt{J_2}} = T \tag{E78}$$

This term,  $T$ , will be unity when the yield criterion is satisfied and otherwise will be less than unity. The approximate correction involves changing  $(\sigma_{xx} - \sigma_{yy})$  and  $\tau_{xy}$  by a ratio to  $T$ , leading to the expressions

$$\sigma'_{xx} = \frac{\sigma_{xx}}{2} (1 + T) + \frac{\sigma_{yy}}{2} (1 - T)$$



$$\sigma'_{YY} = \frac{\sigma_{XX}}{2} (1 - T) + \frac{\sigma_{YY}}{2} (1 + T)$$

$$\tau'_{xy} = \tau_{xy}(T) \quad (E79)$$

The new stresses are then used to reevaluate T from equation (E78). The new T then leads to new values of the stresses from equations (E79). The process continues until the correction ratio differs from unity by less than a convergence criterion.

#### 4. Strain Hardening Material

The yield surface for the strain hardening material is assumed to be the ellipsoid shown in Figure 10. Certain parameters are to be constant regardless of the position of the ellipsoid and are given as data. They include  $\alpha$ ,  $k$ , and the ratio of half-axis AA' to half-axis AF, which is called D. The straight sided cone is defined by the relation

$$\alpha I_1 + J_2 = k, \quad (E80)$$

which is the Drucker-Prager equation. If the axes AA' and AF are denoted by  $a$  and  $b$ , respectively, and the stress at A is  $p_0$ , the yield surface is represented by

$$\frac{(I_1/3 - p_0)^2}{a^2} + \frac{J_2}{b^2} = 1 \quad (E81)$$

Equation (E81) is the equation of the yield criterion for known values of  $a$  and  $p_0$ .

It is now necessary to define how the yield surface moves as a function of plastic strain. If the yield surface depends only on plastic volumetric strain and if the plastic volumetric strain depends linearly on volumetric stress for a "virgin" compression, a final constant,  $C$ , can be defined for isotropic stress,  $p_c$ , by

$$C \epsilon^{(P)} = p_c = p_0 - a, \quad (E82)$$

since  $a$  and  $b$  are always taken as positive. In fact the plastic volumetric strain is more likely to depend on the logarithm of  $p_c$ , but the linear assumption is used here for simplicity.

The first problem is to find the yield surface for a given state of stress, at point E, for example, if the material is plastic. From equation (E80) it follows that

$$b = k - 3\alpha p_0 \quad (E83)$$

and

$$a = Db = D(k - 3\alpha p_0) \quad (E84)$$

Equation (E81) can then be expressed as

$$\left(\frac{I_1}{3} - p_0\right)^2 + D^2 J_2 = D^2 (k - 3\alpha p_0)^2, \quad (E85)$$

which is a quadratic equation in  $p_0$ . If coefficients  $A, B,$

and C are defined by

$$\begin{aligned}
 A &= 1 - 9 D^2 \alpha^2 \\
 B &= -\frac{2}{3} I_1 + 6 D^2 k \alpha \\
 C &= \frac{I_1^2}{9} + D^2 J_2 - D^2 k^2,
 \end{aligned}
 \tag{E86}$$

the solution becomes

$$p_o = \frac{-B + \sqrt{B^2 - 4AC}}{2A}
 \tag{E87}$$

the optional sign being taken as positive after examining the geometry of the problem.

The major problem is to derive stress-strain relations for this material. When the summation convection is used, it can be shown that the plastic strains are defined by

$$\begin{aligned}
 \dot{\epsilon}_{ij}^{(P)} &= \hat{G} \frac{\partial f}{\partial \sigma_{ij}} \frac{\partial f}{\partial \sigma_{kl}} \dot{\sigma}_{kl} \\
 \hat{G} &= - \frac{1}{\frac{\partial f}{\partial \epsilon_{mn}^{(P)}} \frac{\partial f}{\partial \sigma_{mn}}}
 \end{aligned}
 \tag{E88}$$

The term  $f$  in these equations is the yield function derived from equation (E81):

$$f(\sigma_{ij}, \epsilon_{ij}^{(P)}) = b^2 (I_1/3 - p_0)^2 + a^2 J_2 - a^2 b^2 = 0 \quad (E89)$$

Then

$$\frac{\partial f}{\partial \sigma_{ij}} = \frac{2}{3} b^2 (I_1/3 - p_0) \delta_{ij} + a^2 s_{ij} \quad (E90)$$

The derivatives with respect to plastic strain can be found by first finding the derivatives of  $p_0$ ,  $a$ , and  $b$ .

The first of these is

$$\frac{\partial p_0}{\partial \epsilon_{ij}^{(P)}} = \frac{\partial}{\partial \epsilon_{ij}^{(P)}} \left( \frac{C \epsilon^{(P)} + Dk}{1 + 3D \alpha} \right) \quad (E91)$$

$$\frac{\partial p_0}{\partial \epsilon_{ij}^{(P)}} = \frac{1}{3} \frac{C}{1 + 3D \alpha} \delta_{ij} \quad (E92)$$

The next one is

$$\begin{aligned} \frac{\partial a}{\partial \epsilon_{ij}^{(P)}} &= \frac{\partial}{\partial \epsilon_{ij}^{(P)}} \left( - \frac{3D \alpha p_0}{1 + 3D \alpha} \right) \\ &= - \frac{D \alpha C}{1 + 3D \alpha} \delta_{ij} \end{aligned} \quad (E93)$$

Finally,

$$\frac{\partial b}{\partial \epsilon_{ij}} (P) = - \frac{\partial C}{1+3D\alpha} \delta_{ij} \quad (E94)$$

Now,

$$\begin{aligned} \frac{\partial f}{\partial \epsilon_{ij}} (P) = & 2 b^2 (I_1/3 - p_o) \frac{\partial p_o}{\partial \epsilon_{ij}} (P) + 2 (I_1/3 - p_o)^2 b \frac{\partial b}{\partial \epsilon_{ij}} (P) \\ & + 2J_2 a \frac{\partial a}{\partial \epsilon_{ij}} (P) - 2ab^2 \frac{\partial a}{\partial \epsilon_{ij}} (P) - 2a^2 b \frac{\partial b}{\partial \epsilon_{ij}} (P) \end{aligned}$$

(E95)

This equation becomes, after substitution and algebraic simplification,

$$\begin{aligned} \frac{\partial f}{\partial \epsilon_{ij}} (P) = & - \frac{2C}{3(1+3D\alpha)} \left[ b \left( \frac{I_1}{3} - p_o \right) \left\{ b + 3\alpha \left( \frac{I_1}{3} - p_o \right) \right\} \right. \\ & \left. + 3\alpha b D^2 (J_2 - 2b^2) \right] \delta_{ij} \end{aligned} \quad (E96)$$

To evaluate  $\hat{G}$ , equations (E90) and (E96) must be multiplied and added. From equation (E96) it is evident that only terms with  $i = j$  will contribute and for all such cases

$\frac{\partial f}{\partial \epsilon_{ij}^{(P)}}$  will be the same, regardless of values of  $i$  and  $j$ .

If this term is called  $F$ , the result is

$$\begin{aligned} \frac{\partial f}{\partial \epsilon_{mn}^{(P)}} \cdot \frac{\partial f}{\partial \sigma_{mn}} &= F \left[ a^2 (s_{kk}) + 2b^2 \left( \frac{I_1}{3} - p_o \right) \right] \\ &= 2 b^2 \left( \frac{I_1}{3} - p_o \right) F. \end{aligned} \quad (E97)$$

This expression can be evaluated and its negative reciprocal found to obtain  $\hat{G}$ .

For a more concise notation, the times  $T_{ij}$  can be defined as

$$T_{ij} = \frac{\partial f}{\partial \sigma_{ij}} = \left[ s_{ij} + \frac{2}{3D^2} (I_{1/3} - p_o) \delta_{ij} \right] a^2 \quad (E98)$$

Then the conditions of plane strain can be invoked to eliminate the terms  $\epsilon_{23}$ ,  $\epsilon_{32}$ ,  $\epsilon_{13}$ ,  $\sigma_{23}$ ,  $\sigma_{32}$ ,  $\sigma_{13}$ , and  $\sigma_{31}$ , all of which are zero. The remainder of the analysis is then carried out most conveniently by matrix notation. The strain rates are defined by a column matrix  $\{ \dot{\epsilon}_{ij}^{(P)} \}$ :

$$\{ \dot{\epsilon}_{ij}^{(P)} \} = \{ \dot{\epsilon}_{11}^{(P)} \quad \dot{\epsilon}_{22}^{(P)} \quad \dot{\epsilon}_{33}^{(P)} \quad \dot{\epsilon}_{12}^{(P)} \quad \dot{\epsilon}_{21}^{(P)} \} \quad (E99)$$

The stress rates are similarly represented by

$$\{ \dot{\sigma}_{ij} \} = \{ \dot{\sigma}_{11} \quad \dot{\sigma}_{22} \quad \dot{\sigma}_{33} \quad \dot{\sigma}_{12} \quad \dot{\sigma}_{21} \} \quad (E100)$$

Then, equation (E88) becomes

$$\left\{ \begin{array}{l} \text{(P)} \\ \dot{\epsilon}_{11} \\ \text{(P)} \\ \dot{\epsilon}_{22} \\ \text{(P)} \\ \dot{\epsilon}_{33} \\ \text{(P)} \\ \dot{\epsilon}_{12} \\ \text{(P)} \\ \dot{\epsilon}_{21} \end{array} \right\} = \hat{G} \left[ \begin{array}{ccccc} T_{11}^2 & T_{11} \cdot T_{22} & T_{11} \cdot T_{33} & T_{11} \cdot T_{12} & T_{11} \cdot T_{21} \\ T_{11} \cdot T_{22} & T_{22}^2 & T_{22} \cdot T_{33} & T_{22} \cdot T_{12} & T_{22} \cdot T_{21} \\ T_{11} \cdot T_{33} & T_{22} \cdot T_{33} & T_{33}^2 & T_{33} \cdot T_{12} & T_{33} \cdot T_{21} \\ T_{11} \cdot T_{12} & T_{22} \cdot T_{12} & T_{33} \cdot T_{12} & T_{12}^2 & T_{12} \cdot T_{21} \\ T_{11} \cdot T_{21} & T_{22} \cdot T_{21} & T_{33} \cdot T_{21} & T_{12} \cdot T_{21} & T_{21}^2 \end{array} \right] \left\{ \begin{array}{l} \dot{\sigma}_{11} \\ \dot{\sigma}_{22} \\ \dot{\sigma}_{33} \\ \dot{\sigma}_{12} \\ \dot{\sigma}_{21} \end{array} \right\} \quad (E101)$$

Since  $\dot{\epsilon}_{12}^{(P)} = \dot{\epsilon}_{21}^{(P)} = \frac{1}{2} \dot{\gamma}_{12}^{(P)}$  and  $\dot{\sigma}_{12} = \dot{\sigma}_{21}$ , the equation can

be written more conveniently

$$\begin{Bmatrix} \dot{\epsilon}_{11}^{(P)} \\ \dot{\epsilon}_{22}^{(P)} \\ \dot{\epsilon}_{33}^{(P)} \\ \dot{\gamma}_{12}^{(P)} \end{Bmatrix} = \hat{G} \begin{bmatrix} T_{11}^2 & T_{11} \cdot T_{22} & T_{11} \cdot T_{33} & 2T_{11} \cdot T_{12} \\ T_{11} \cdot T_{22} & T_{22}^2 & T_{22} \cdot T_{33} & 2T_{22} \cdot T_{12} \\ T_{11} \cdot T_{33} & T_{22} \cdot T_{33} & T_{33}^2 & 2T_{33} \cdot T_{12} \\ 2T_{11} \cdot T_{12} & 2T_{22} \cdot T_{12} & 2T_{33} \cdot T_{12} & 4T_{12}^2 \end{bmatrix} \begin{Bmatrix} \dot{\sigma}_{11} \\ \dot{\sigma}_{22} \\ \dot{\sigma}_{33} \\ \dot{\sigma}_{12} \end{Bmatrix} \quad (E102)$$

or

$$\{ \dot{\epsilon}_{ij}^{(P)} \} = [K^{(P)}] \{ \dot{\sigma}_{ij} \} \quad (E103)$$

The elastic strain rates can be expressed by

$$\begin{Bmatrix} \dot{\epsilon}_{11}^{(P)} \\ \dot{\epsilon}_{22}^{(P)} \\ \dot{\epsilon}_{33}^{(P)} \\ \dot{\gamma}_{12}^{(P)} \end{Bmatrix} = \frac{1}{E} \begin{bmatrix} 1 & -\nu & -\nu & 0 \\ -\nu & 1 & -\nu & 0 \\ -\nu & -\nu & 1 & 0 \\ 0 & 0 & 0 & 2(1+\nu) \end{bmatrix} \begin{Bmatrix} \dot{\sigma}_{11} \\ \dot{\sigma}_{22} \\ \dot{\sigma}_{33} \\ \dot{\sigma}_{12} \end{Bmatrix} \quad (E104)$$

or

$$\{ \dot{\epsilon}_{ij}^{(e)} \} = [K^{(e)}] \{ \dot{\sigma}_{ij} \} \quad (E105)$$



Adding equations (E103) and (E105) will give

$$\begin{aligned}\{\dot{\epsilon}_{ij}\} &= \{\dot{\epsilon}_{ij}^{(P)}\} + \{\dot{\epsilon}_{ij}^{(P)}\} = [K^{(P)} + K^{(e)}] \{\dot{\sigma}_{ij}\} \\ &= [K] \{\dot{\sigma}_{ij}\}.\end{aligned}\tag{E106}$$

The incremental stresses can then be found by inverting [K] to satisfy the equation

$$\{\dot{\sigma}_{ij}\} = [K]^{-1} \{\dot{\epsilon}_{ij}\}\tag{E107}$$

The computer program calculates the terms of [K] and inverts the matrix to provide the required coefficients to compute the incremental changes in stress.

No correction routine is used because the program calculates a new position for the yield surface for each plastic point after the iteration for a loading step has converged.

APPENDIX F

CONVERSION FROM  $\phi$  AND  $c$  TO  $\alpha$  AND  $k$

The Mohr-Coulomb law can be written in the form

$$\frac{\sigma_1 - \sigma_3}{2} + \frac{\sigma_1 + \sigma_3}{2} \cos \phi = c \cos \phi, \quad (F1a)$$

if tensile stresses are positive. (Reference to Figure 4 will help clarify this expression.) Equation (F1a) can be rewritten

$$\sigma_1 - \sigma_3 \frac{1 - \sin \phi}{1 + \sin \phi} = \frac{2 c \cos \phi}{1 + \sin \phi} \quad (F1)$$

The Drucker-Prager (1952) relation is

$$\alpha I_1 + J_2^{1/2} = k. \quad (F2)$$

The last expression does not allow the constants  $\alpha$  and  $k$  to be expressed in terms of  $c$  and  $\phi$  unless some assumption or restriction is made about the intermediate principal stress. Drucker and Prager (1952) assumed a rigid-perfectly plastic material under plane strain and obtained

$$\alpha = \frac{\tan \phi}{(9 + 12 \tan^2 \phi)^{1/2}}$$

$$k = \frac{3 c}{(9 + 12 \tan^2 \phi)^{1/2}}$$

$$\varphi = \tan^{-1} \frac{3\alpha}{(1-12\alpha^2)^{\frac{1}{2}}}$$

$$c = \frac{k}{(1 - 12\alpha^2)^{\frac{1}{2}}} \quad (\text{F3})$$

Analogous relations can be derived for the conditions of the triaxial compression test and triaxial extension test. The stress conditions for the compression test are

$$\sigma_2 = \sigma_1, \quad (\text{F4})$$

since tension is defined as positive and the subscripts 1, 2, and 3 indicate decreasing positive or increasing negative value. Then

$$\begin{aligned} I_1 &= 2\sigma_1 + \sigma_3 \\ J_2 &= \frac{1}{6} \left[ (\sigma_1 - \sigma_3)^2 + (\sigma_2 - \sigma_3)^2 + (\sigma_1 - \sigma_2)^2 \right] \\ &= \frac{1}{6} \left[ (\sigma_1 - \sigma_3)^2 \cdot 2 \right] = \frac{1}{3} (\sigma_1 - \sigma_3)^2. \end{aligned} \quad (\text{F5})$$

Substitution into equation (F2) gives

$$\alpha(2\sigma_1 + \sigma_3) + \frac{1}{\sqrt{3}} (\sigma_1 - \sigma_3) = k, \quad (\text{F6})$$

and hence,

$$\sigma_1 - \sigma_3 \frac{1 - \sqrt{3}\alpha}{1 + 2\sqrt{3}\alpha} = \frac{\sqrt{3} k}{1 + 2\sqrt{3}\alpha} \quad (\text{F7})$$

Equating corresponding coefficients in equations (F1) and (F7) and solution of the resulting simultaneous equations give

$$\alpha = \frac{2 \sin \varphi}{\sqrt{3}(3 - \sin \varphi)}$$

$$k = \frac{6 c \cos \varphi}{\sqrt{3}(3 - \sin \varphi)}$$

$$\varphi = \sin^{-1} \frac{3\sqrt{3}\alpha}{2 + \sqrt{3}\alpha}$$

$$c = \frac{\sqrt{3} k}{2[(1 - \sqrt{3}\alpha)(1 + 2\sqrt{3}\alpha)]^{\frac{1}{2}}} \quad (\text{F8})$$

In triaxial extension

$$\sigma_2 = \sigma_3, \quad (\text{F9})$$

and

$$I_1 = \sigma_1 + 2\sigma_3$$

$$J_2 = \frac{1}{3} (\sigma_1 - \sigma_3)^2 \quad (\text{F10})$$

A similar substitution into equation (F2) gives

$$\alpha(\sigma_1 + 2\sigma_3) + \frac{1}{\sqrt{3}} (\sigma_1 - \sigma_3) = k, \quad (\text{F11})$$

and

$$\sigma_1 - \sigma_3 \frac{1 - 2\sqrt{3}\alpha}{1 + \sqrt{3}\alpha} = \frac{\sqrt{3} k}{1 + \sqrt{3}\alpha}. \quad (\text{F12})$$

Solving the simultaneous equations results in

$$\alpha = \frac{2 \sin \varphi}{\sqrt{3}(3 + \sin \varphi)}$$

$$k = \frac{6 c \cos \varphi}{\sqrt{3}(3 + \sin \varphi)} \quad (\text{F13})$$

$$\varphi = \sin^{-1} \frac{3\sqrt{3}\alpha}{2 - \sqrt{3}\alpha}$$

$$c = \frac{\sqrt{3} k}{2[(1 + \sqrt{3}\alpha)(1 - 2\sqrt{3}\alpha)]^{\frac{1}{2}}}$$

Equations (F3), (F8), and (F13) are plotted in Figures 6 and 7. These predict much higher values of  $c$  and  $\varphi$  for plane strain and extension than for compression. The plane strain curve would be different if a different assumption were made from that of rigid-plastic behavior. For example,  $\sigma_2$  can be assumed some ratio of the sum of

the sum of  $\sigma_1$  and  $\sigma_3$  between the limiting cases of triaxial compression and extension. The difference in values of  $m$  between extension and compression is not observed experimentally (Bishop, 1966), so the Drucker-Prager generalization remains a mathematical convenience which probably will be abandoned when a better understanding of the effect of  $\sigma_2$  on the strength of soil is obtained by experiment.

Equation (F8) has been derived independently by Reyes (1966), but he presents incorrect forms for the first two of equations (F13).

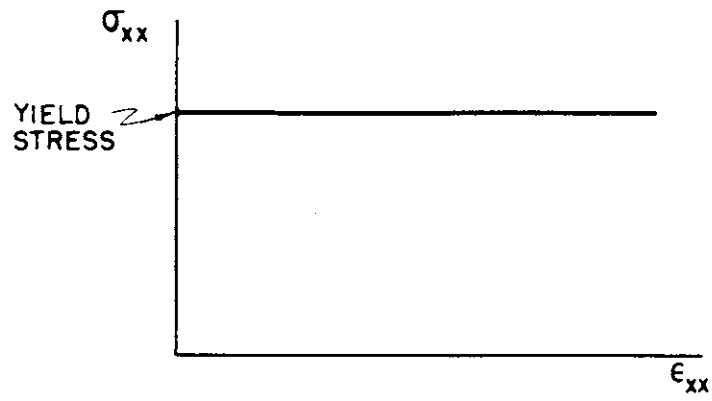
## BIOGRAPHY

John Thomas Christian was born on November 2, 1936, in New York, N. Y. His early education was at the Escola Americana do Rio de Janeiro, Brazil, and The McCallie School, Chattanooga, Tennessee. He entered the Massachusetts Institute of Technology in September, 1953, and received the S.B. degree in September, 1958, and the S.M. degree in September, 1959.

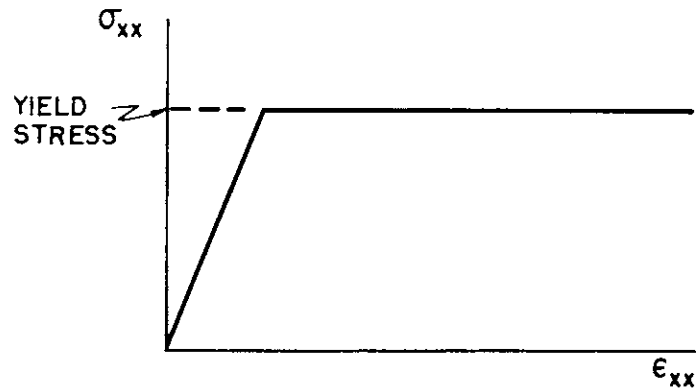
From September, 1959, to August, 1963, he served as a Lieutenant in the United States Air Force, working in civil engineering offices. He received the U.S.A. F. Commendation Medal for his work.

In addition to his military service and summer jobs in Brazil and Canada during his undergraduate career, his professional experience includes work as a soil engineer on various projects in Venezuela and elsewhere.

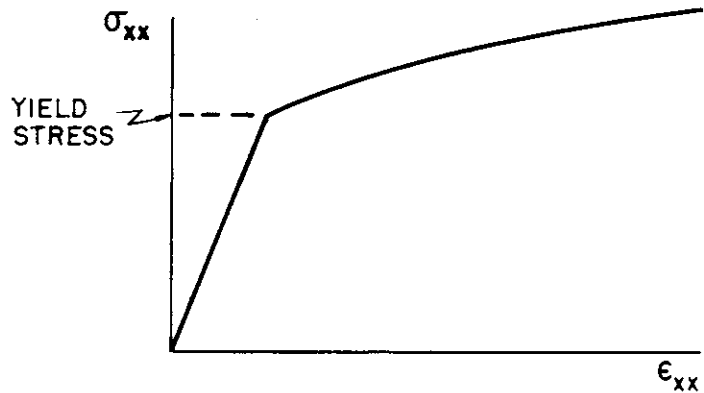
He is a member of Tau Beta Pi, Sigma Xi, and Chi Epsilon, honorary societies. He is also a member of the American Society of Civil Engineers and the International Society of Soil Mechanics and Foundation Engineering.



RIGID-PERFECTLY-PLASTIC  
(a)



ELASTIC-PERFECTLY-PLASTIC  
(b)



ELASTIC-STRAIN-HARDENING  
(c)

FIG. 1 TYPES OF PLASTIC BEHAVIOR



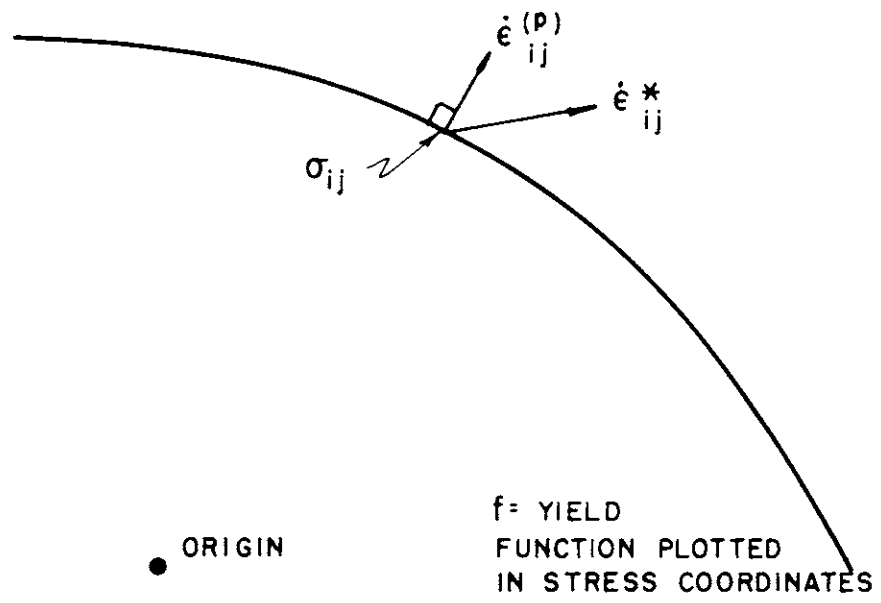


FIG.2 NORMALITY OF PLASTIC STRAIN RATE

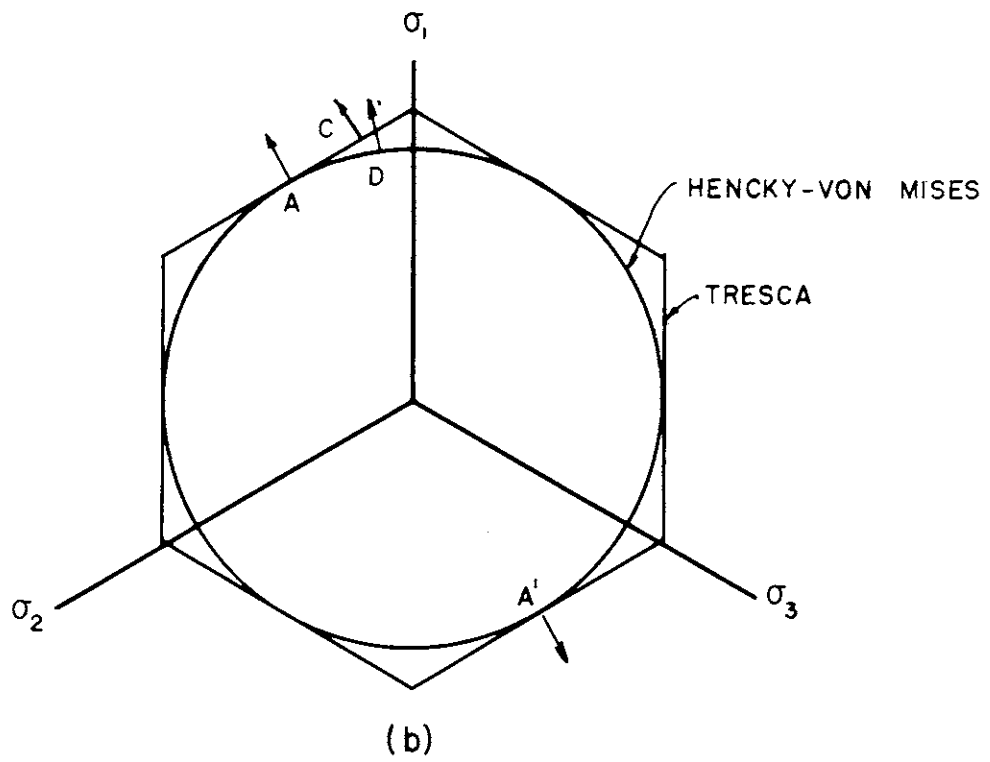
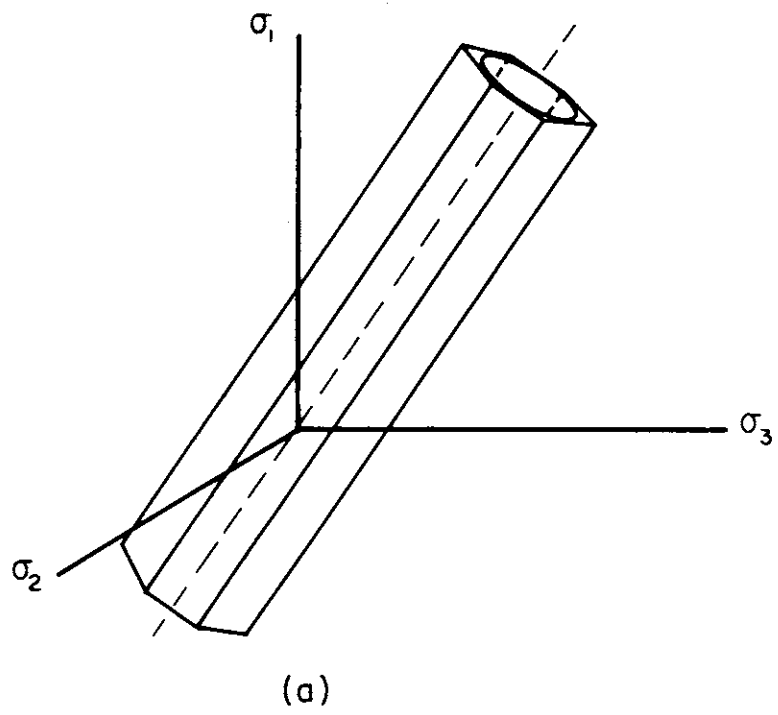


FIG. 3 NON - FRICTIONAL YIELD CRITERIA

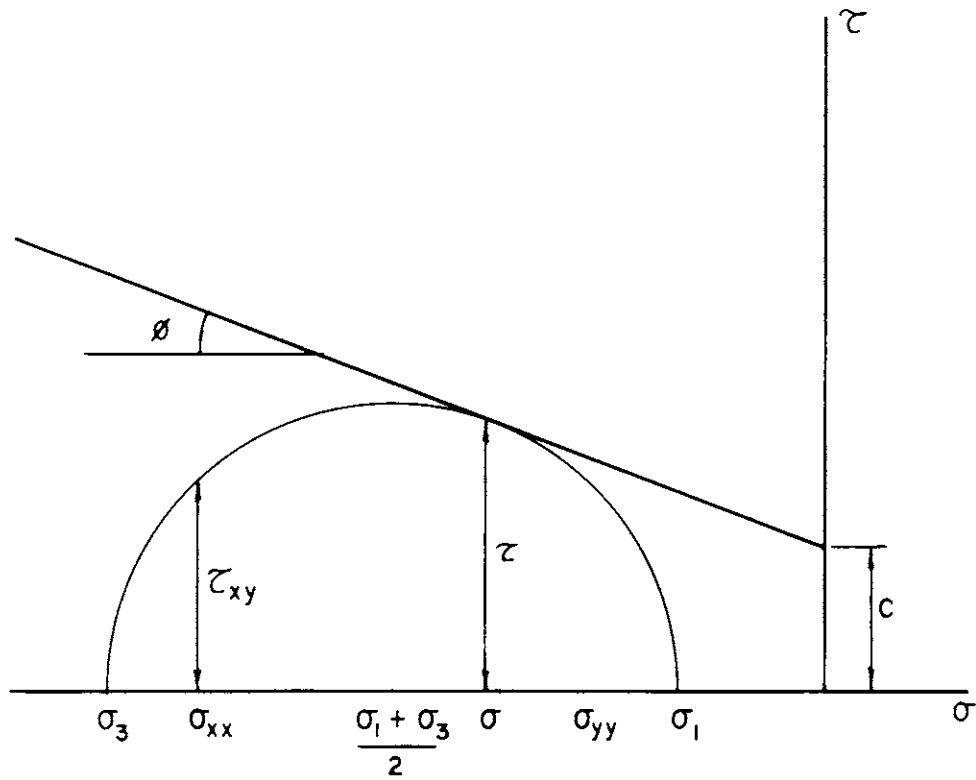


FIG. 4 MOHR-COULOMB LAW

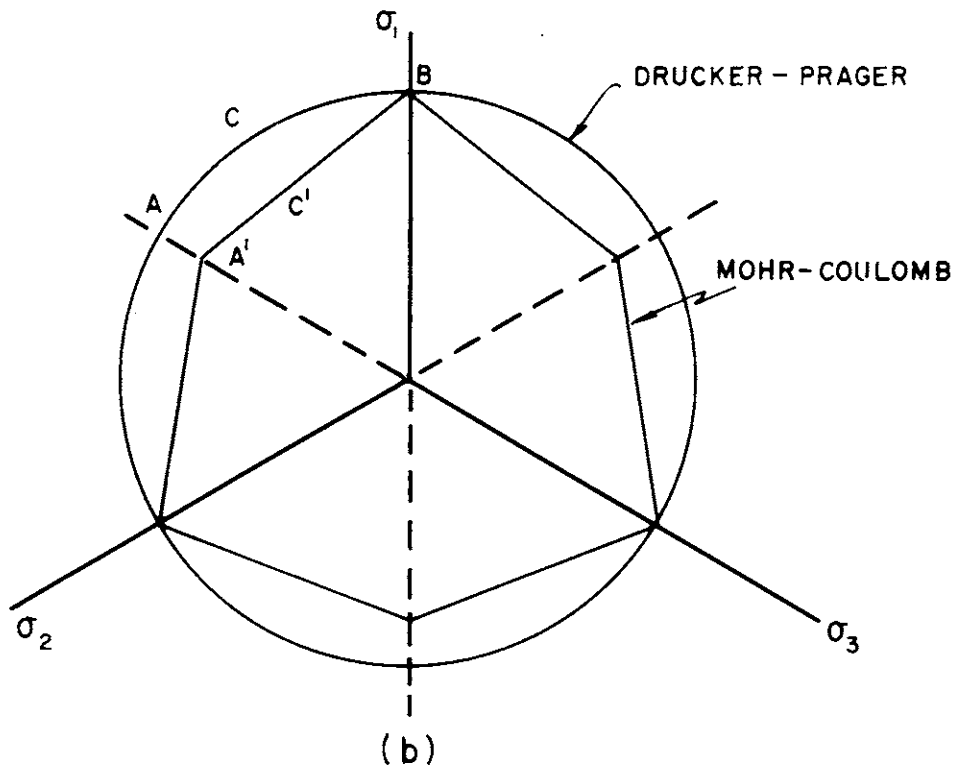
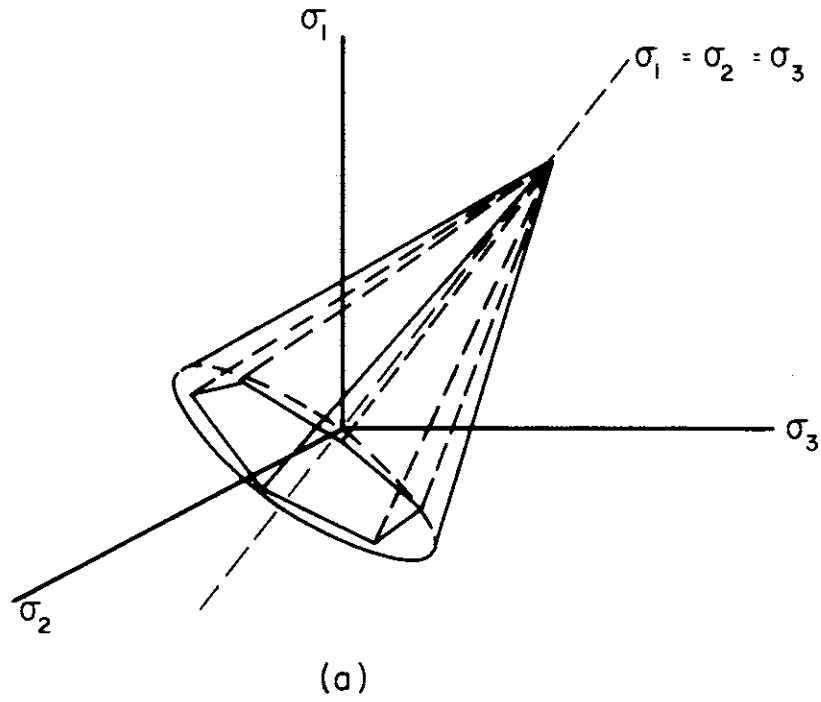


FIG. 5 FRICTIONAL YIELD CRITERIA

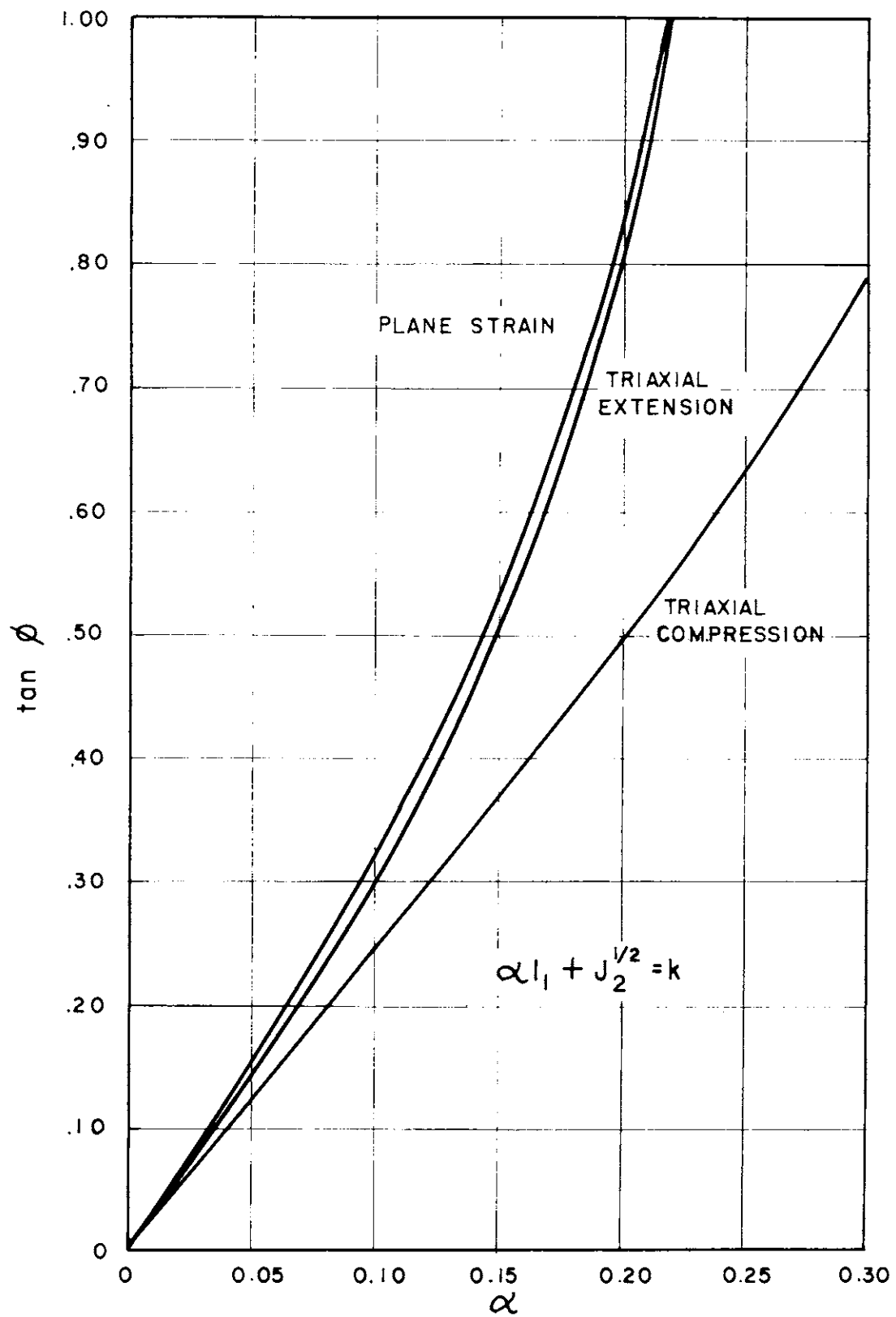


FIG. 6 COULOMB FRICTION FROM DRUCKER-PRAGER CONSTANTS

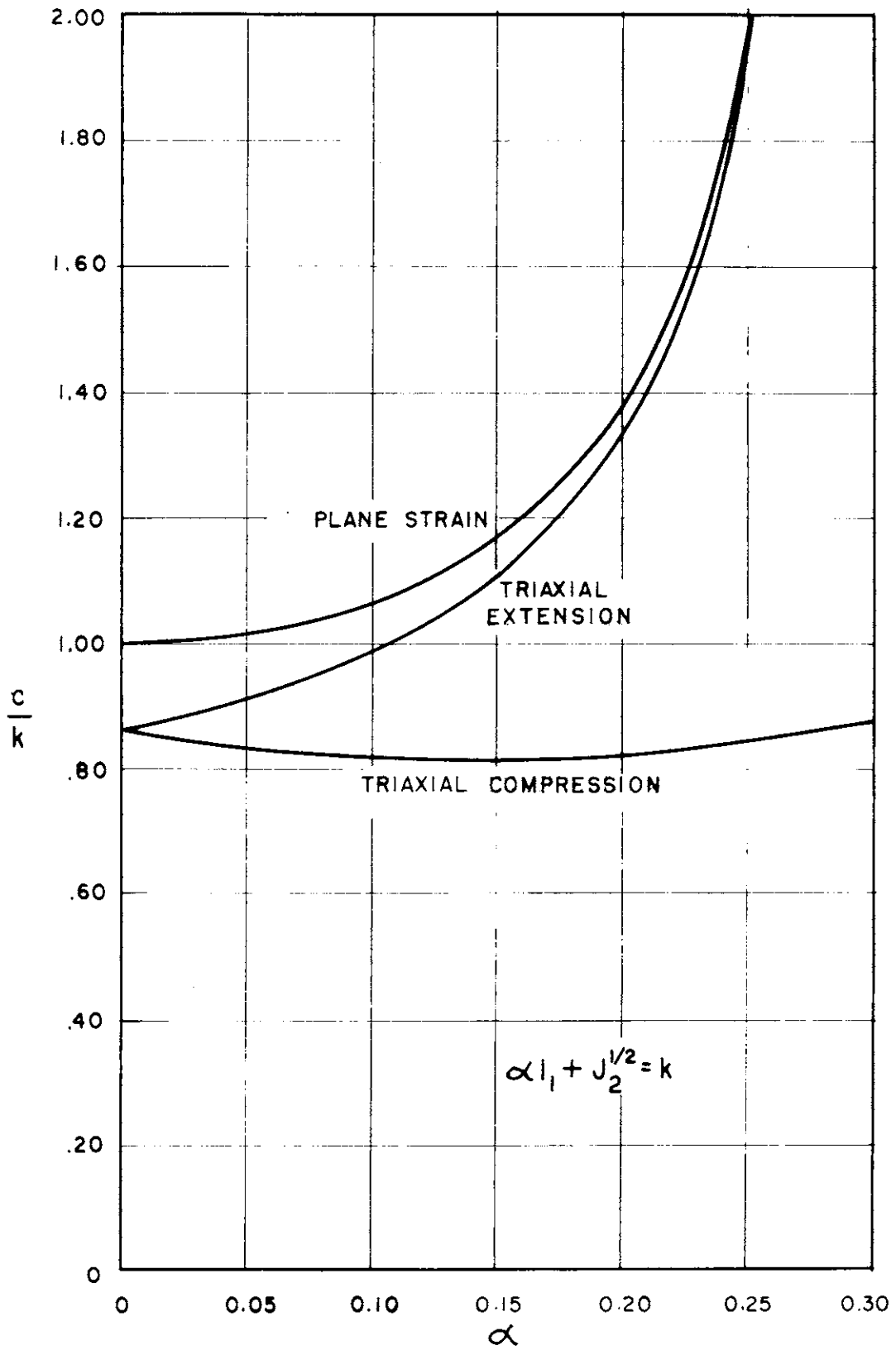


FIG. 7 COULOMB COHESION FROM DRUCKER-PRAGER CONSTANTS

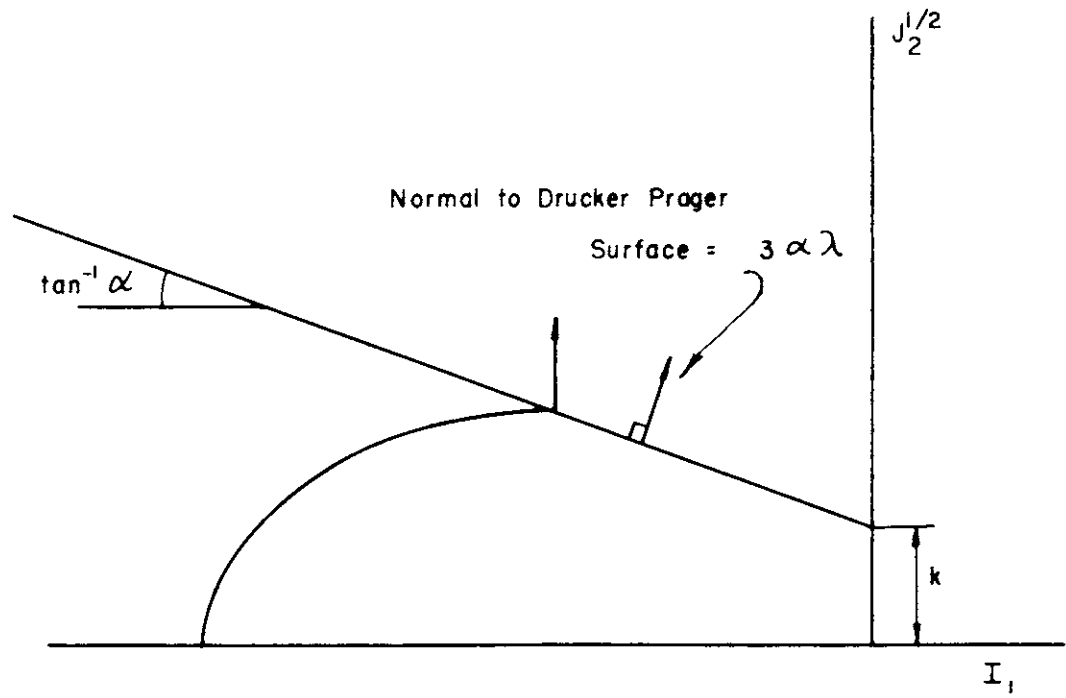


FIG. 8 STRAIN RATES FOR FRICTIONAL MATERIALS

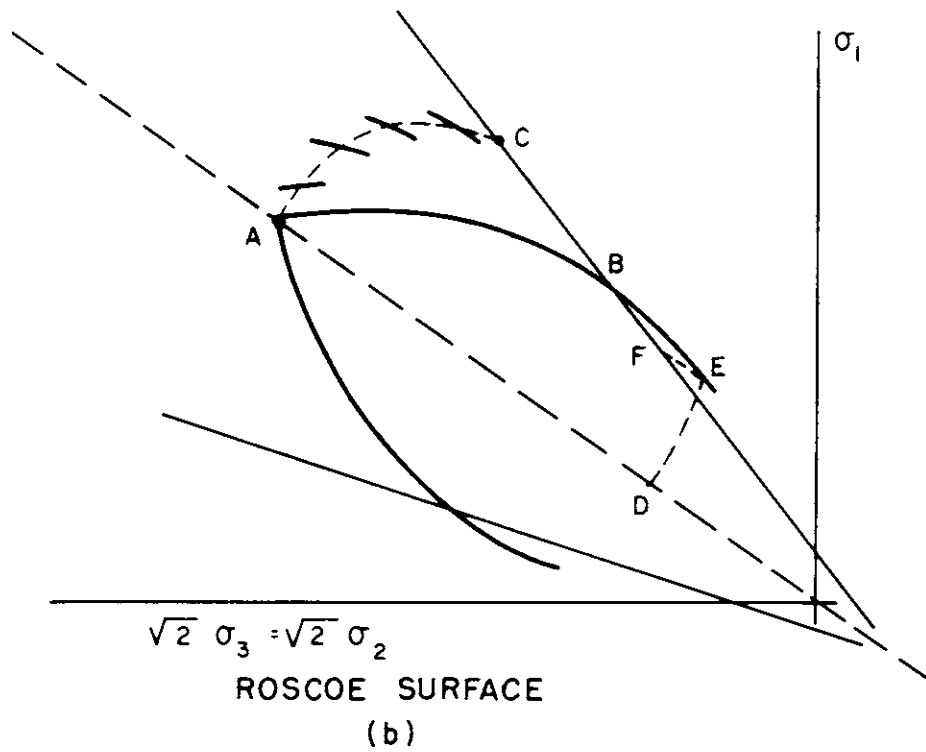
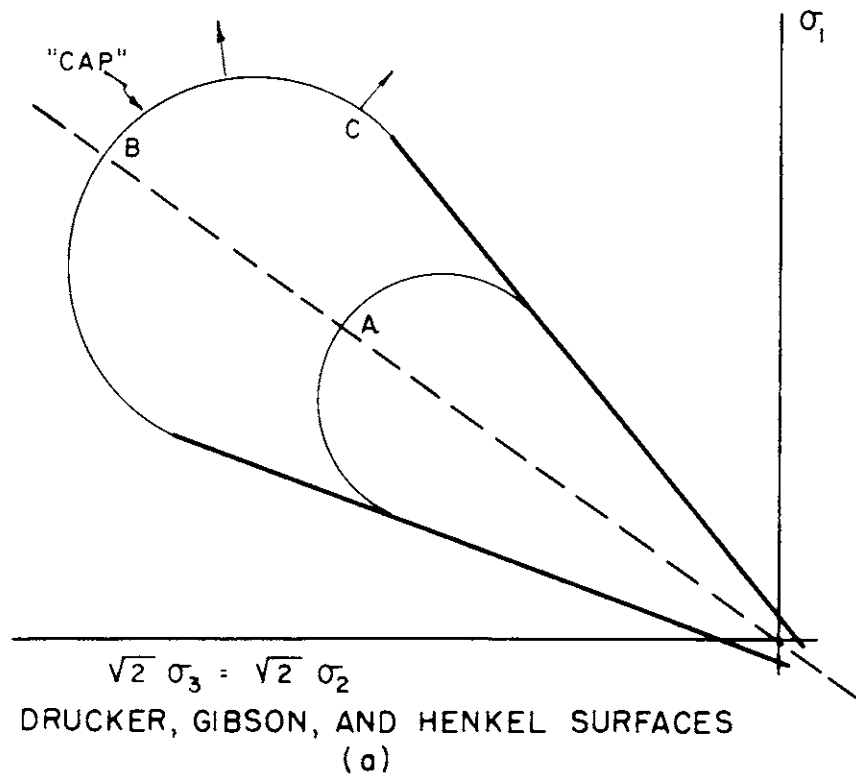


FIG. 9 CAPPED SURFACES



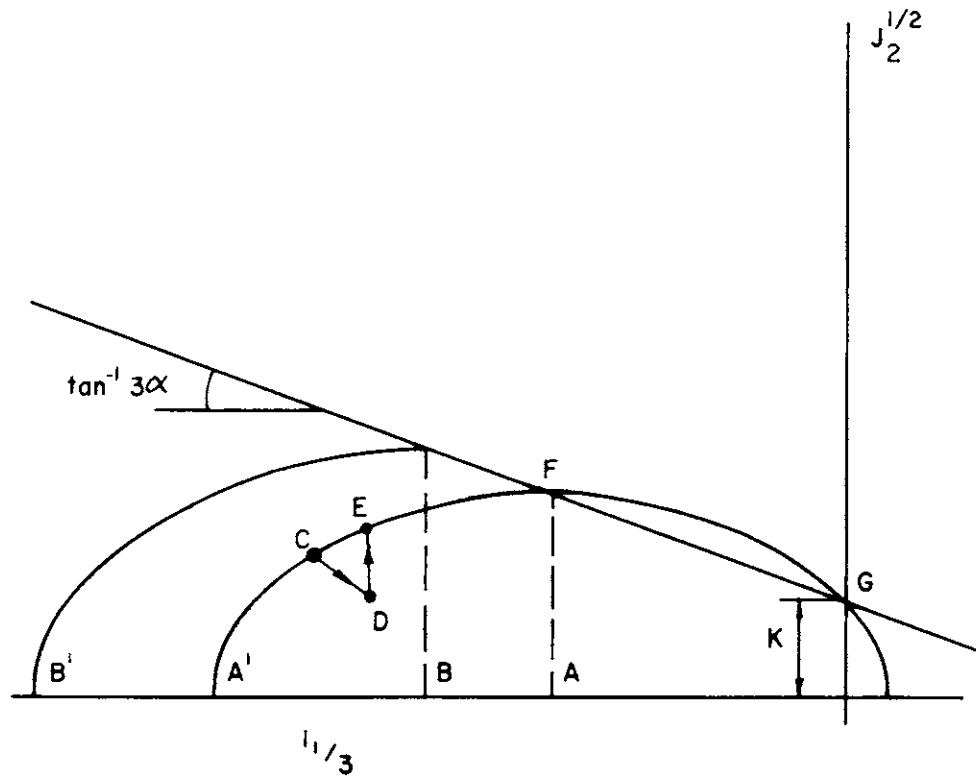
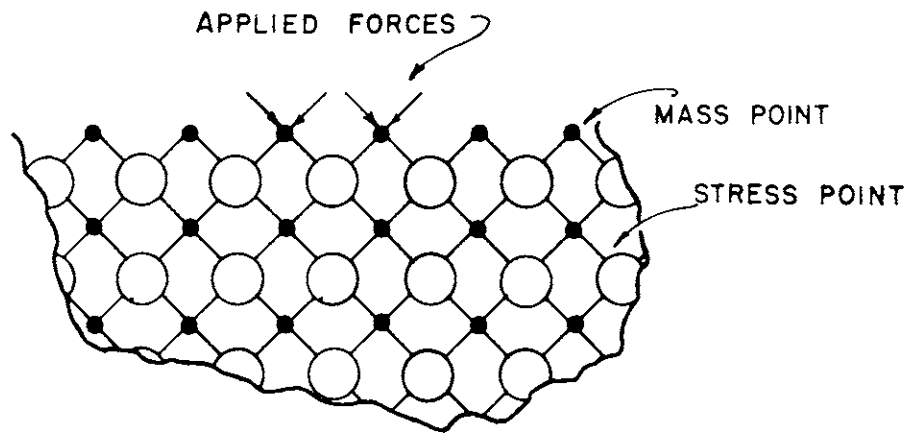
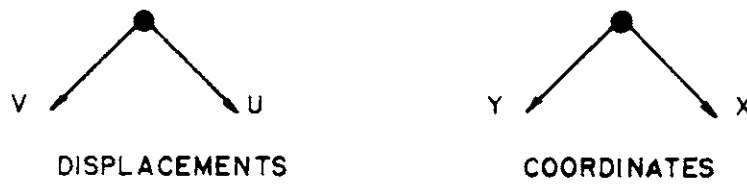


FIG. 10 ELLIPTICAL SURFACE

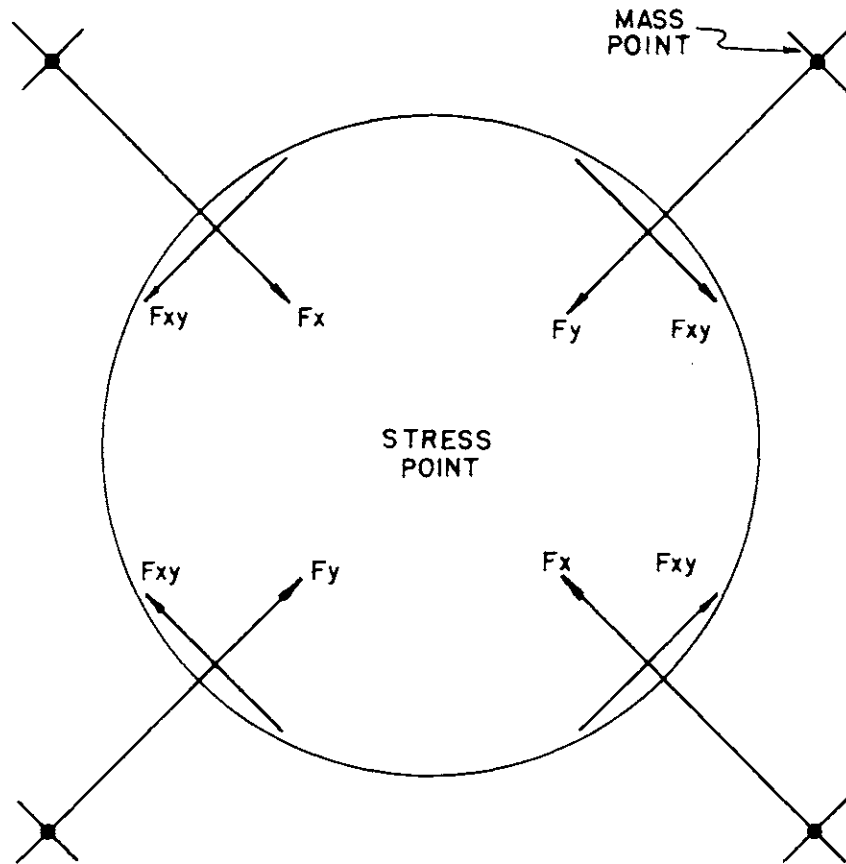


MASS AND STRESS POINT ARRAY  
(a)



POSITIVE SIGN CONVENTIONS  
(b)

FIG. II LUMPED PARAMETER MODEL



FORCES ARE POSITIVE ON MASS POINTS AS SHOWN

FIG. 12 FORCE CONVENTION

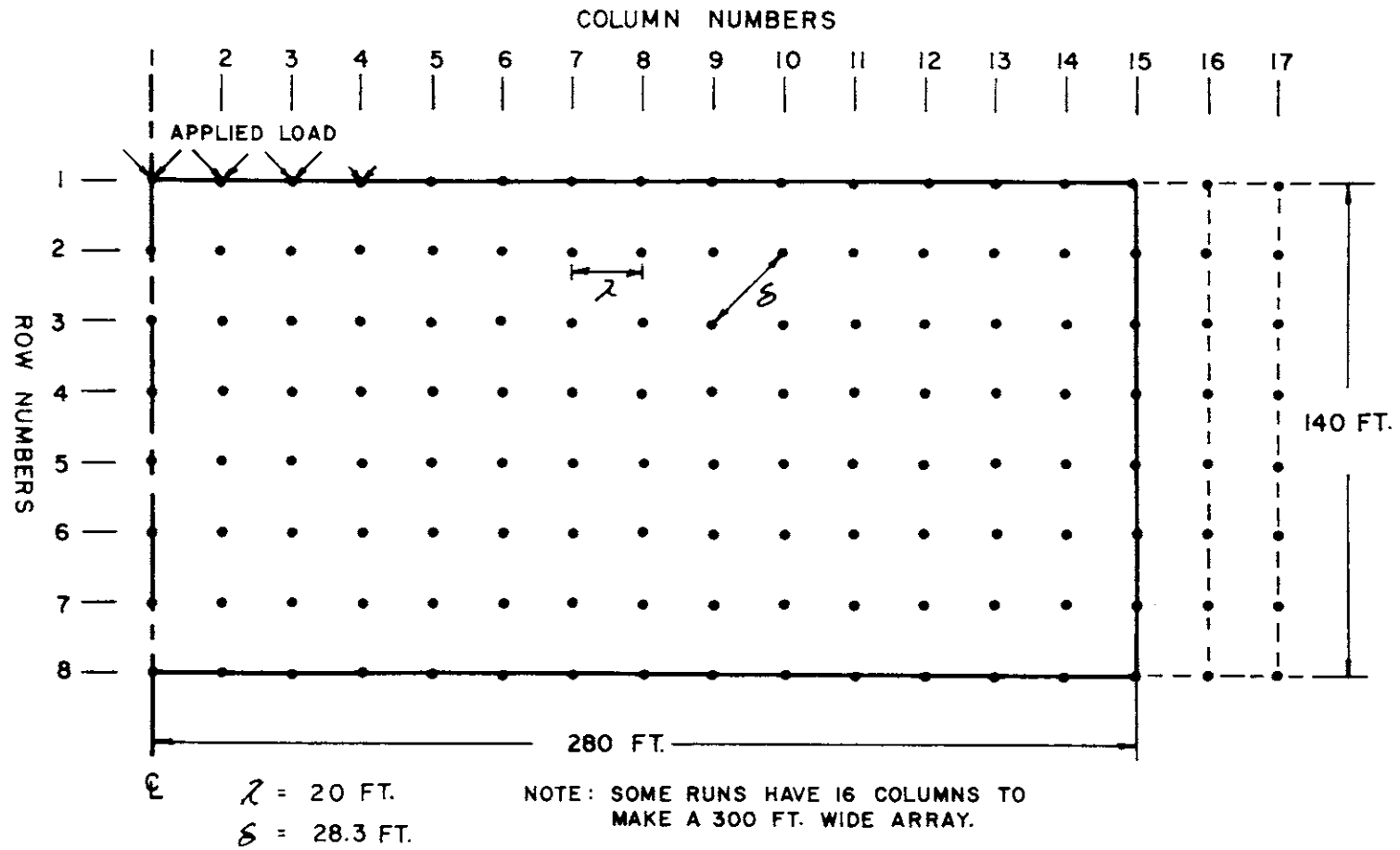


FIG. 13 STANDARD PROBLEM

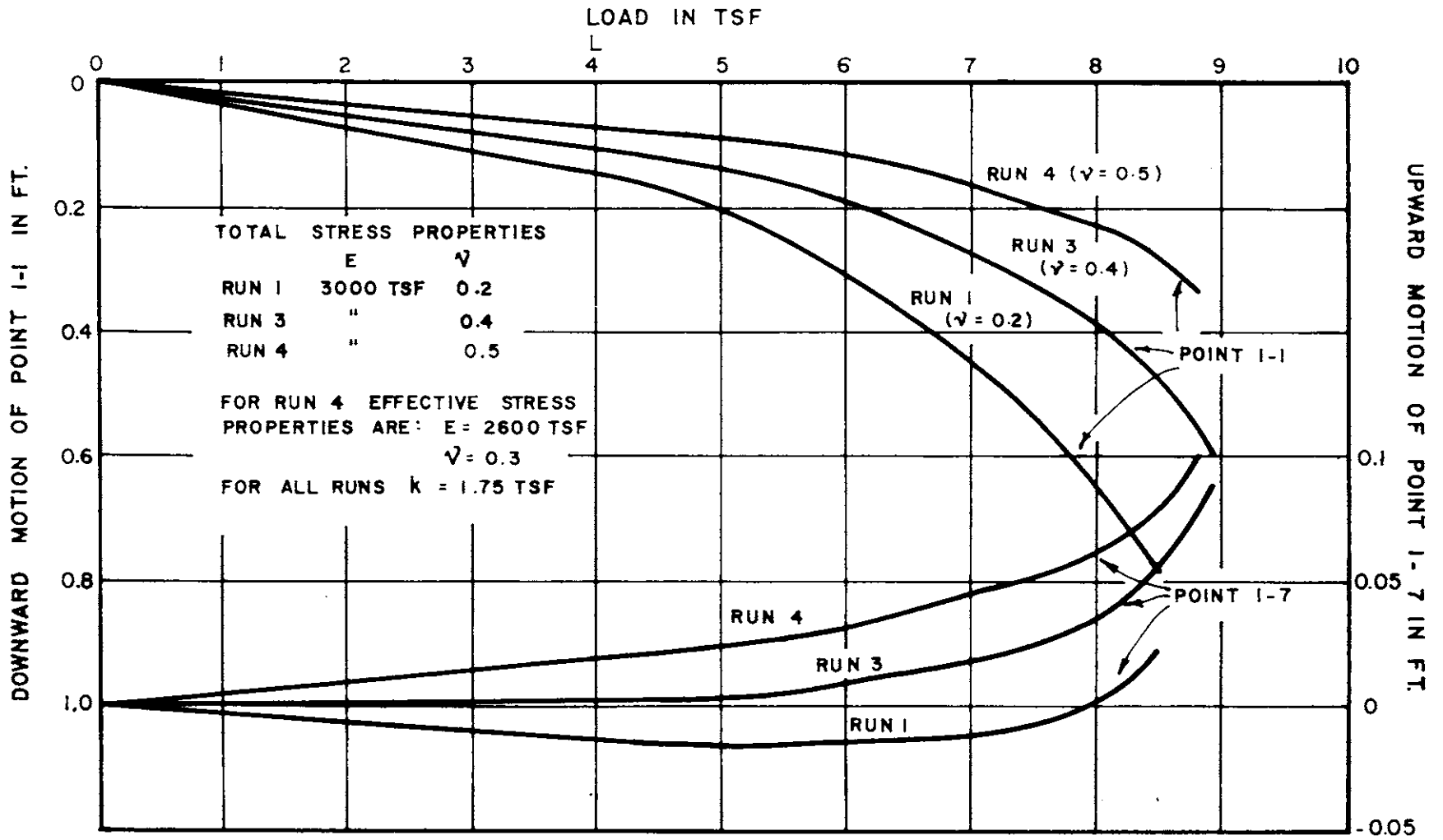


FIG. 14 DISPLACEMENTS IN RUNS 1, 3 AND 4

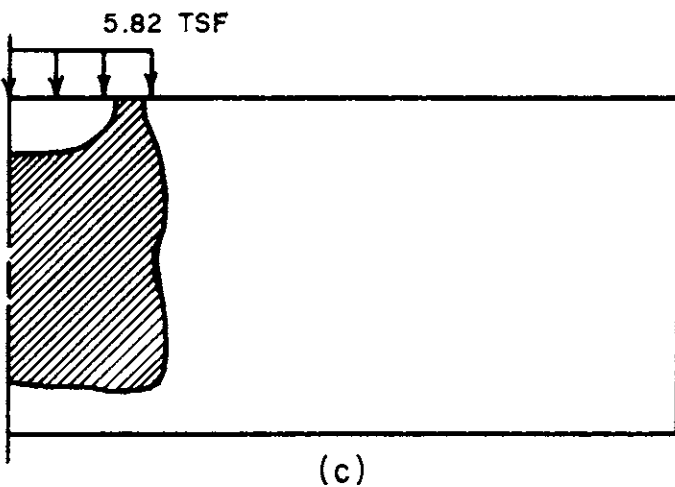
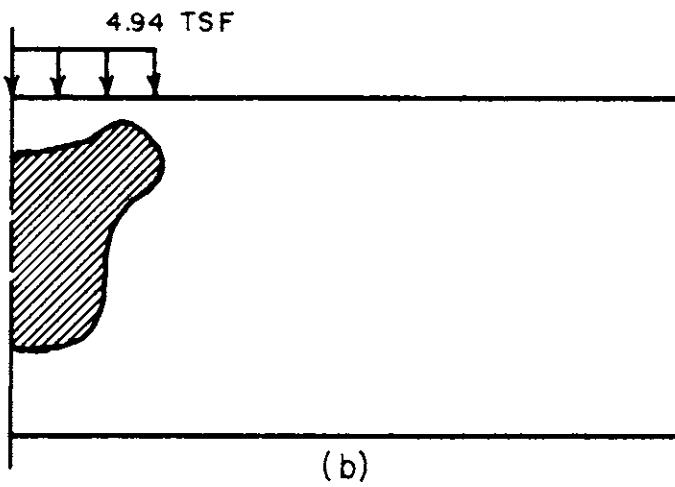
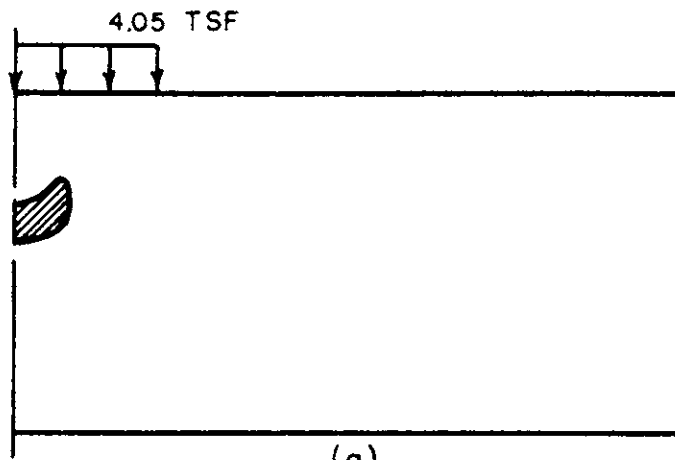


FIG. 15 SPREAD OF PLASTIC ZONE - RUN I

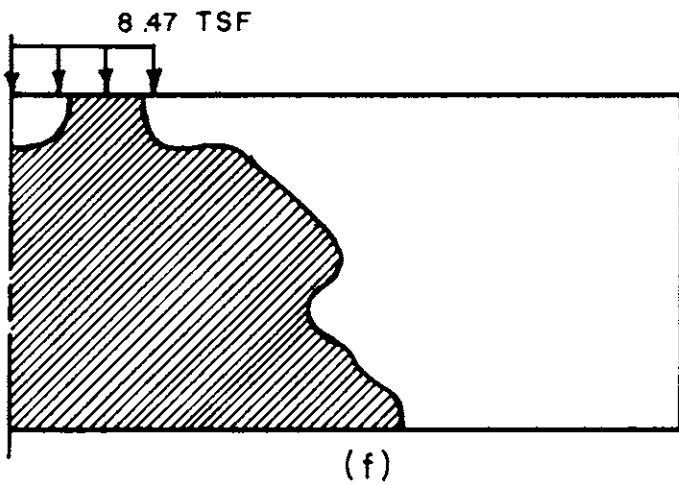
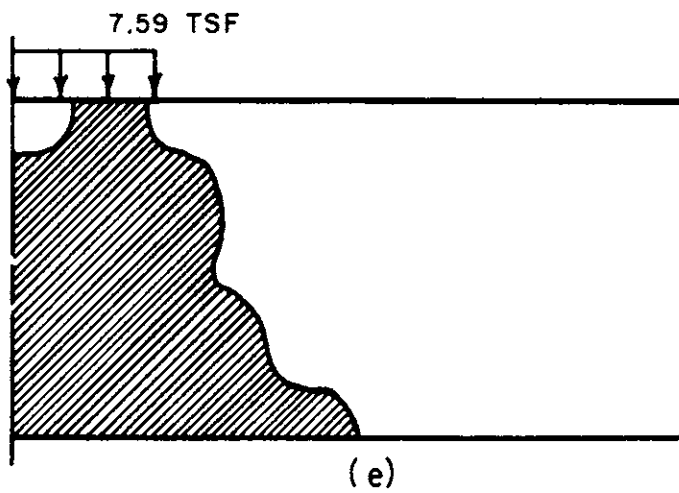
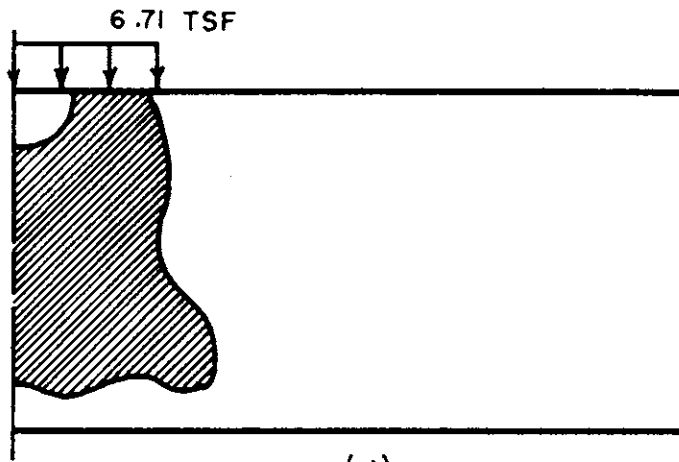


FIG. 15 SPREAD OF PLASTIC ZONE - RUN I

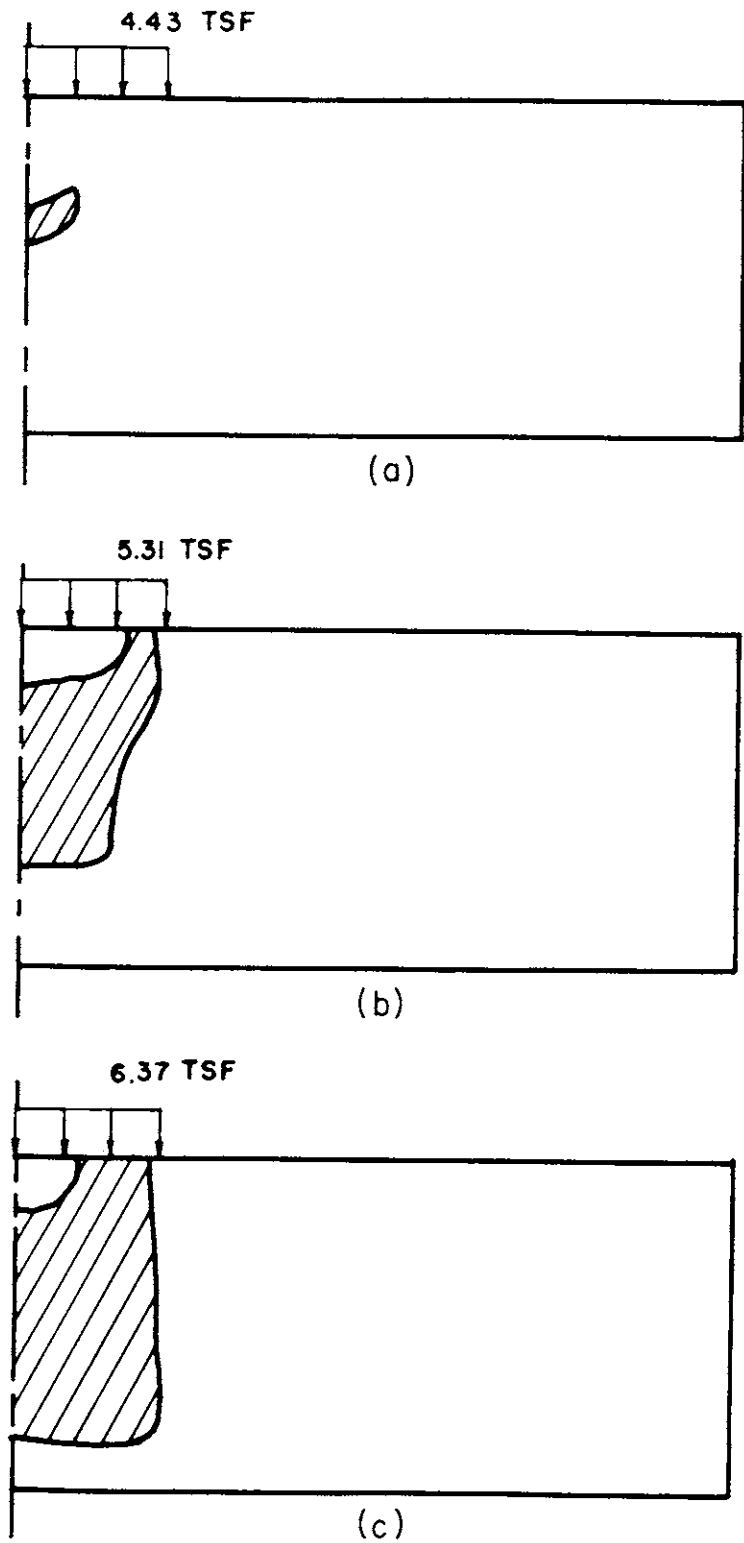


FIG.16 SPREAD OF PLASTIC ZONE - RUN 2



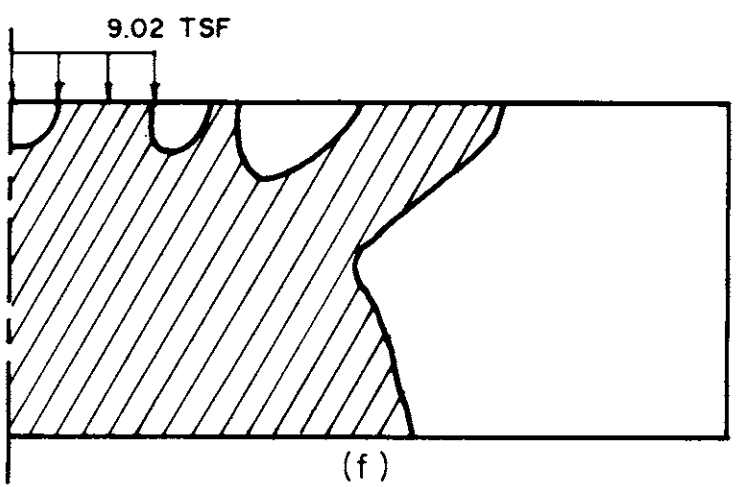
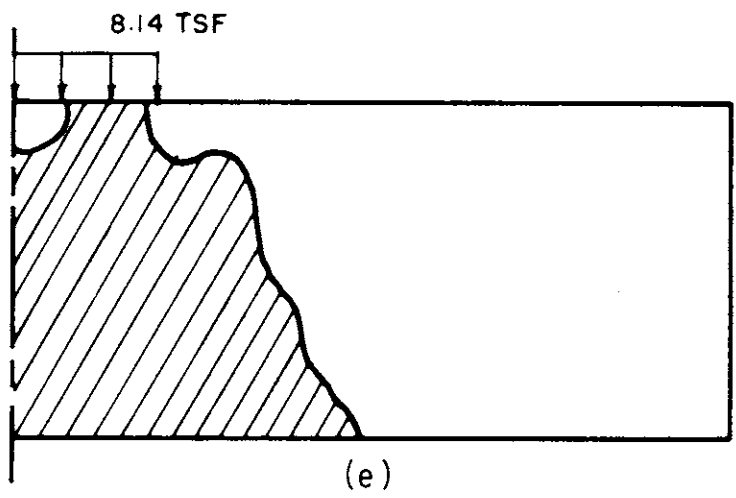
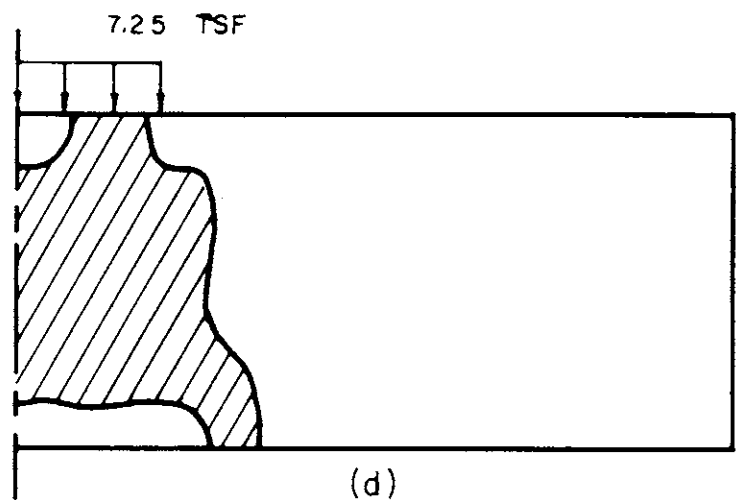


FIG.16 SPREAD OF PLASTIC ZONE - RUN 2

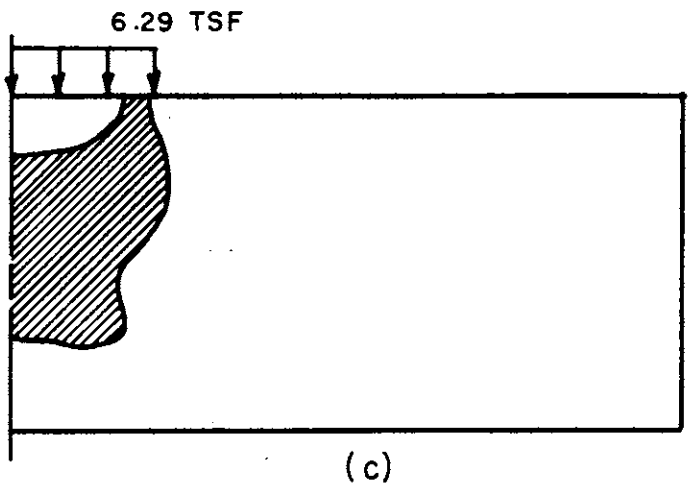
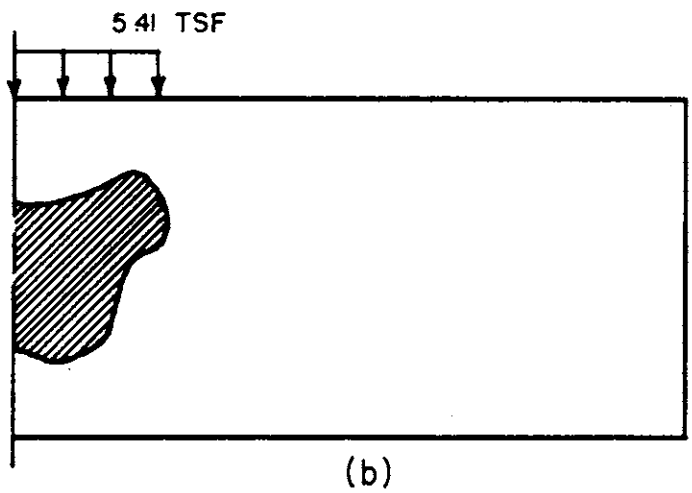
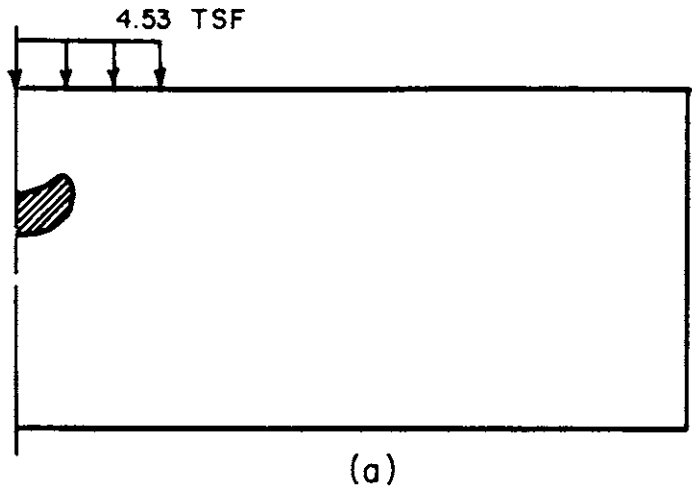


FIG. 17 SPREAD OF PLASTIC ZONE - RUN 3

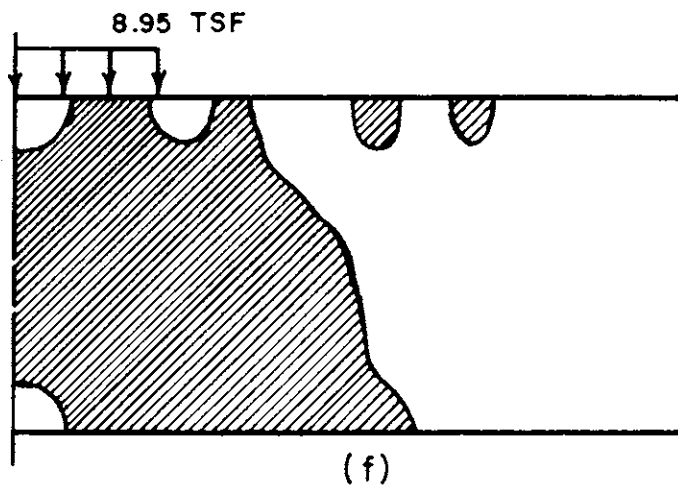
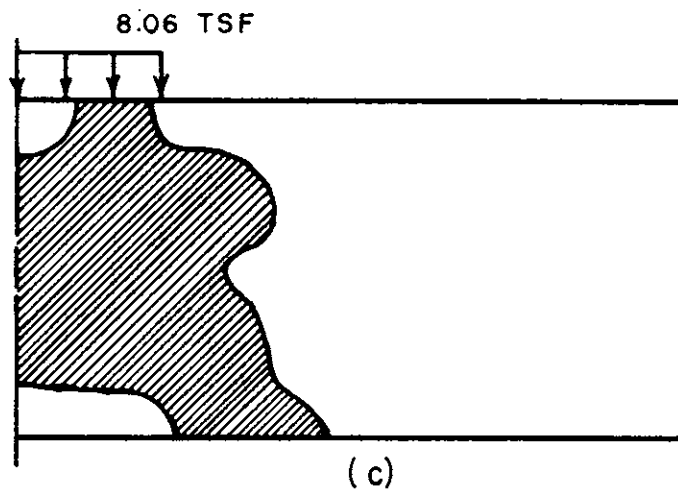
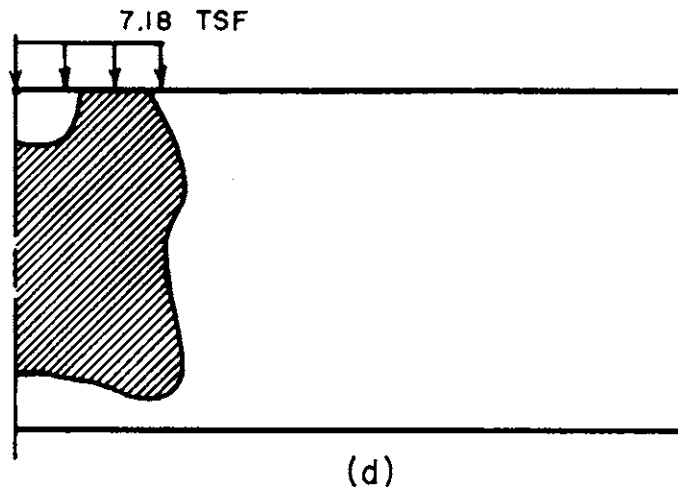


FIG. 17 SPREAD OF PLASTIC ZONE - RUN 3

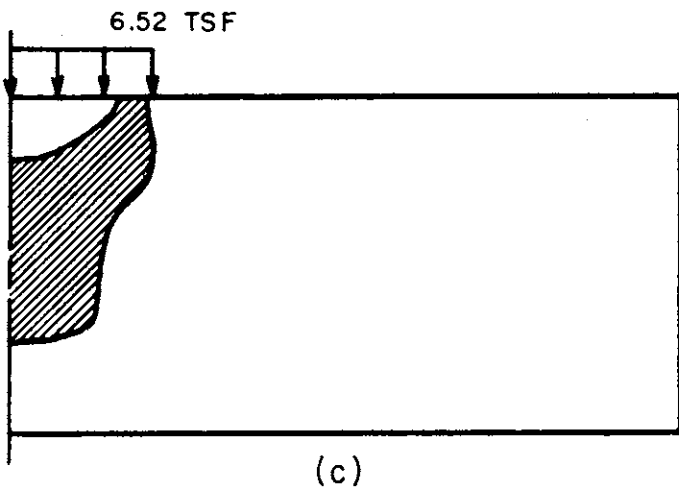
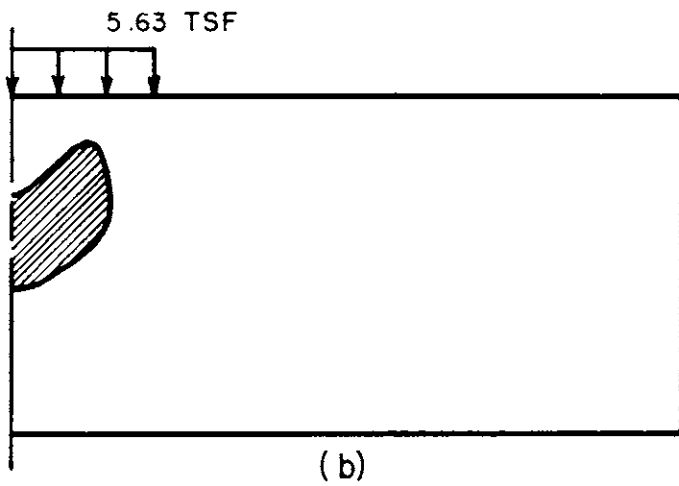
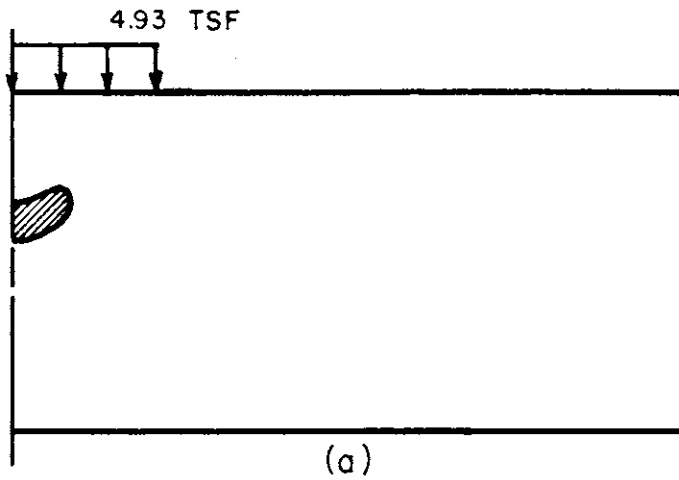


FIG.18 SPREAD OF PLASTIC ZONE - RUN 4

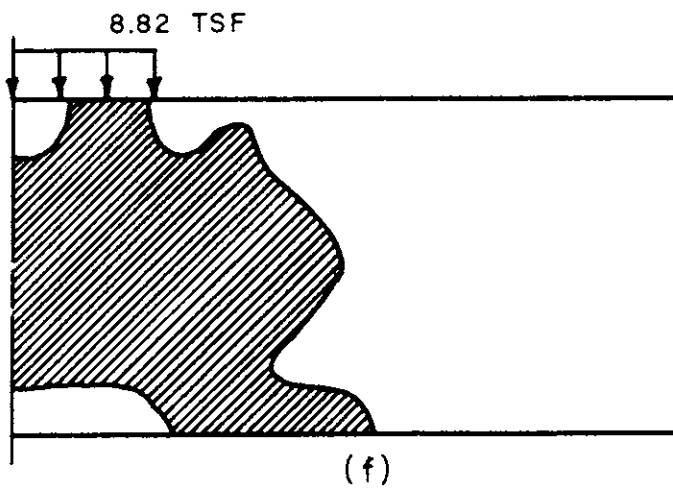
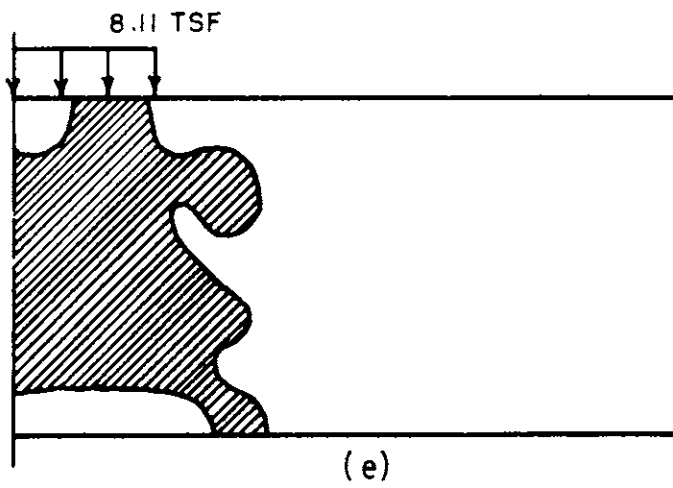
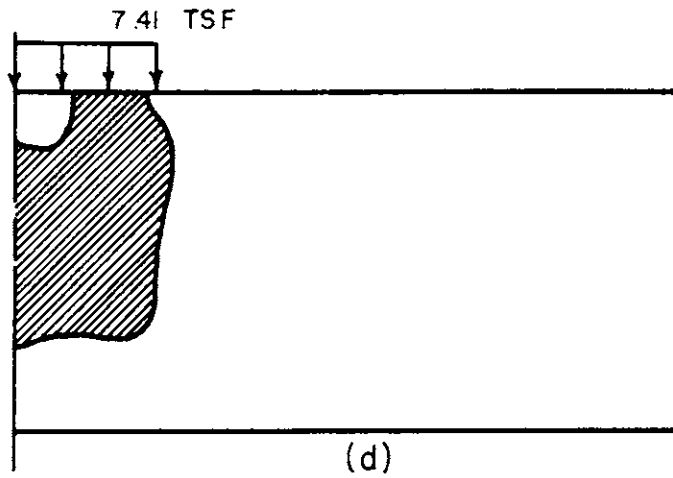
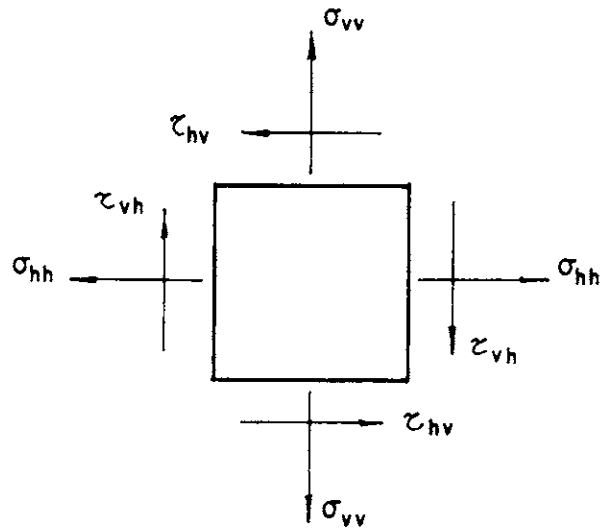
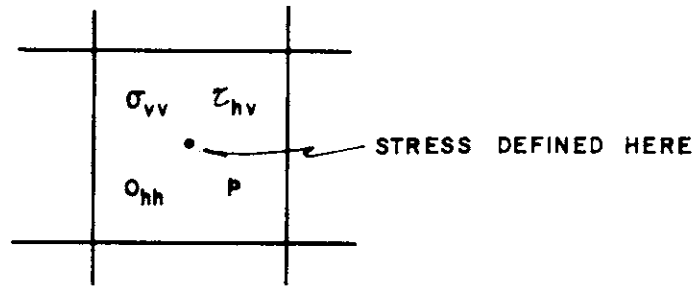


FIG. 18 SPREAD OF PLASTIC ZONE - RUN 4



POSITIVE SIGN CONVENTION  
(a)



$p$  IS PORE PRESSURE POSITIVE IN TENSION

PATTERN USED IN FIGURES  
(b)

FIG. 19 CONVENTIONS IN STRESS FIGURES

-98-01	-102-01	-84-14	-16-14	02 00	-02 00	01 01	-01 01	01 01	00 01	00 01	00 00	00 00	00 00
50	48	33	04	10	11	10	08	07	05	04	02	02	01
-96-01	-94-11	-66-24	-34-24	-07-10	-02-01	-02 00	00 02	00 02	01 02	00 01	01 01	00 01	00 00
23	15	10	18	13	03	01	01	01	01	01	01	01	01
-91-05	-79-15	-62-20	-39-20	-20-16	-07-07	-03-02	-01 00	00 01	00 01	01 01	01 01	01 01	01 00
05	05	10	10	14	12	07	05	03	02	01	01	00	00
-81-05	-73-12	-59-17	-41-18	-25-14	-14-10	-06-05	-03-02	-01-01	00 00	01 00	01 01	01 00	01 00
00	03	04	10	11	12	10	07	06	04	03	02	01	01
-73-03	-67-10	-55-13	-42-14	-29-13	-18-10	-10-07	-02-04	-02-02	00-01	00-01	01 00	01 00	01 00
01	01	06	07	11	10	10	09	06	05	03	03	02	02
-67-03	-62-07	-53-11	-42-12	-31-12	-21-11	-13-08	-07-06	-04-04	-02-03	00-02	00-01	01-01	01 00
03	05	05	09	08	09	08	07	06	04	03	02	02	01
-62-02	-58-07	-51-10	-41-12	-32-12	-22-11	-15-10	-09-07	-05-05	-03-04	-01-03	00-02	00-01	00-01
11	10	11	09	09	07	06	04	03	02	01	01	01	01

LOAD = 4.06 TSF

FIG. 20 NORMALIZED ELASTIC STRESSES - RUN 1

-97-01	-103-01	-84-12	-20-08	08-04	-03-01	01-01	00-00	00-00	00-00	00-00	00-00	-01-00	01-00
-61	-62	-51	-30	-26	-28	-27	-28	-28	-28	-27	-27	-26	-26
-101-02	-93-08	-71-00	-37-00	01-06	01-02	-01-02	01-00	00-01	00-01	00-01	00-01	00-01	00-00
-60	-54	-50	-54	-39	-30	-32	-29	-28	-27	-26	-25	-24	-24
-97-07	-81-13	-67-18	-37-21	-18-15	00-04	00-01	01-04	00-02	00-03	00-02	00-02	-01-01	00-01
-58	-49	-47	-41	-47	-40	-33	-32	-27	-26	-24	-23	-22	-22
-83-06	-79-16	-60-20	-42-20	-22-17	-10-12	02-08	00-06	00-06	00-04	-01-04	-01-03	-01-02	-02-01
-44	-51	-49	-53	-47	-43	-36	-28	-27	-23	-22	-20	-19	-18
-75-02	-69-12	-59-19	-42-21	-26-19	-12-17	-03-14	-01-10	-01-08	-01-08	-02-06	-02-04	-03-03	-03-01
-34	-34	-42	-38	-40	-36	-32	-29	-23	-21	-17	-16	-15	-15
-67-09	-62-10	-52-15	-42-20	-27-21	-16-19	-05-17	-05-15	-02-13	-04-11	-04-08	-05-05	-05-03	-05-01
-27	-26	-24	-32	-29	-30	-29	-24	-20	-14	-13	-11	-10	-10
-60-02	-56-12	-49-15	-37-18	-28-20	-16-21	-08-20	-04-20	-07-18	-07-13	-07-09	-07-06	-07-04	-07-01
-19	-22	-21	-15	-22	-20	-16	-12	-08	-07	-05	-05	-05	-05

LOAD = 8.47 TSF

FIG. 21 NORMALIZED STRESSES - RUN 1



SBT

-99-01	102 01	84-14	16-14	02 00	-02 00	01 01	-01 01	00 01	00 01	00 01	00 00	00 00	00 00	00 00	00 00
-52	-51	-36	-08	07	07	06	04	03	01	-01	-02	-02	-03	-03	
-97 01	94-11	66-24	34-24	03-10	02-01	01 00	00 02	00 02	01 02	00 01	00 01	00 01	00 00	00 00	00 00
-26	-18	-13	-22	-17	-07	-04	-03	-02	-02	-02	-03	-03	-03	-03	
-91-05	80-15	62-20	39-20	20-16	07-07	03-02	01 00	00 01	00 01	01 01	01 01	01 01	01 01	00 00	01 00
-09	-09	-15	-14	-18	-16	-10	-08	-06	-05	-04	-04	-03	-03	-03	
81-05	73-12	58-17	41-18	25-14	14-10	06-05	03-02	01-01	00 00	01 00	01 00	01 00	01 00	01 00	01 00
-05	-08	-09	-15	-15	-16	-14	-11	-09	-07	-06	-04	-04	-03	-03	
73-03	67-10	56-13	42-14	29-14	18-10	10-08	05-05	02-03	00-02	00-01	01-01	01 00	01-01	01 00	01 00
-06	-07	-12	-12	-16	-15	-14	-12	-09	-08	-06	-05	-04	-03	-03	
68-03	62-08	53-11	42-13	30-13	21-12	12-09	07-07	03-05	02-04	00-03	00-02	00-01	00-01	00-01	00 00
-11	-12	-12	-14	-13	-14	-12	-10	-08	-06	-05	-03	-03	-02	-02	
62-03	58-08	51-11	41-14	31-14	22-13	15-11	09-09	05-07	03-05	02-04	01-03	00-02	00-01	00 00	00 00
-20	-18	-18	-15	-14	-11	-09	-07	-05	-04	-02	-02	-01	-01	-01	

LOAD = 4.24 TSF

FIG. 22 NORMALIZED ELASTIC STRESSES - RUN 2

-97-02	-100-03	-88-14	-16-11	03 01	-02 00	01 01	-01 01	01 01	00 01	00 01	00 00	00 00	00 00	00 00	00 00
-51	-46	-29	-04	06	05	04	02	01	-01	-02	-03	-04	-04	-04	-04
-96 00	-90-11	-74-24	-33-23	-05-09	-02 00	-01 00	00 02	00 01	01 02	00 01	01 01	00 01	00 00	00 00	00 00
-30	-28	-28	-31	-20	-09	-07	-05	-04	-04	-04	-04	-04	-04	-04	-04
-90-06	-79-14	-66-20	-39-23	-19-17	-06-07	-03-02	-01-01	00 01	00 01	01 01	00 01	01 01	00 00	01 00	01 00
-25	-19	-19	-20	-23	-19	-13	-11	-08	-07	-06	-05	-05	-05	-05	-04
-77-06	-74-16	-59-19	-42-20	-26-16	-14-12	-06-06	-03-03	-01-02	00 00	00 00	01 00	01 00	01 00	01 00	00 00
-13	-17	-15	-19	-18	-19	-16	-13	-11	-08	-07	-06	-05	-04	-04	-04
-68-03	-67-12	-58-17	-43-17	-30-16	-18-12	-10-09	-05-06	-02-04	-01-03	00-02	00-01	01-01	00 00	01 00	01 00
-02	-05	-13	-14	-17	-16	-16	-13	-11	-09	-07	-06	-04	-04	-04	-04
-61-03	-60-08	-54-13	-44-16	-32-15	-22-13	-13-10	-08-08	-04-06	-02-04	-01-03	00-02	00-01	00-01	00-01	00 00
-07	-09	-10	-15	-14	-15	-13	-11	-09	-07	-06	-04	-04	-03	-03	-03
-57-02	-55-07	-50-12	-42-15	-33-16	-23-14	-16-13	-10-10	-06-08	-03-06	-02-04	-01-03	-01-02	-01-01	-01-01	00 00
-18	-17	-17	-15	-15	-11	-10	-07	-05	-04	-03	-02	-01	-01	-01	-01

LOAD = 5.31 TSF

FIG. 23 NORMALIZED STRESSES - RUN 2

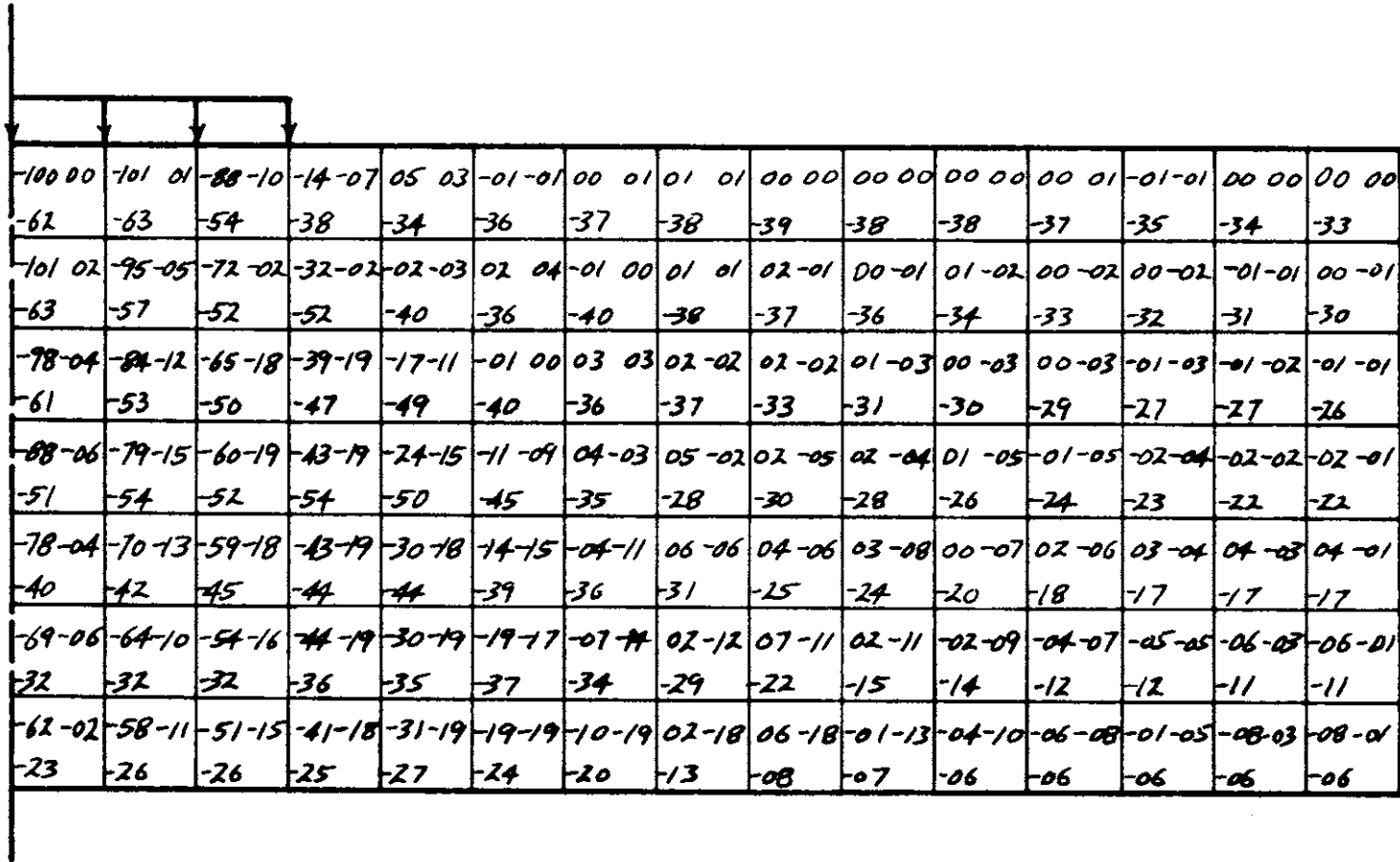


FIG. 24 NORMALIZED STRESSES - RUN 2

-99-01	-102-00	-84-14	-16-14	02-00	-02-00	01-01	-01-01	01-01	00-01	00-01	00-00	00-00	00-00	00-00
-56	-54	-40	-12	02	02	01	-02	-04	-05	-07	-08	-08	-09	
-97-01	-94-11	-66-23	-35-23	-07-09	-02-00	-01-01	00-02	00-02	01-02	00-01	01-01	00-00	01-00	
-31	-23	-18	-27	-22	-12	-10	-08	-08	-08	-08	-08	-08	-08	
-92-05	-80-14	-62-19	-39-19	-20-15	-07-06	-03-01	-01-00	00-01	01-01	01-01	01-01	01-00	01-00	
-15	-15	-20	-19	-23	-21	-16	-14	-11	-10	-09	-09	-08	-08	
-82-08	-74-12	-59-16	-42-17	-25-13	-14-10	-06-05	-03-02	00-01	01-00	01-00	01-00	01-00	01-00	
-11	-15	-15	-21	-21	-21	-20	-16	-14	-11	-10	-09	-08	-08	
-74-03	-68-09	-56-13	-42-14	-29-14	-17-10	-10-08	-04-05	-02-03	00-02	01-01	01-01	01-01	01-00	
-14	-15	-19	-19	-22	-20	-19	-17	-13	-11	-09	-08	-07	-07	
-68-03	-63-08	-54-12	-42-14	-30-13	-20-12	-12-10	-07-08	-03-06	-01-04	00-03	00-02	00-01	00-01	
-20	-22	-20	-22	-20	-20	-17	-14	-12	-09	-07	-06	-05	-05	
-62-03	-58-09	-51-13	-41-15	-31-16	-21-15	-14-13	-09-11	-05-09	-03-06	-02-04	-01-03	-01-02	-01-01	
-32	-30	-29	-24	-21	-16	-13	-10	-07	-05	-04	-03	-02	-02	

LOAD = 4.53 TSF

FIG. 25 NORMALIZED ELASTIC STRESSES - RUN 3

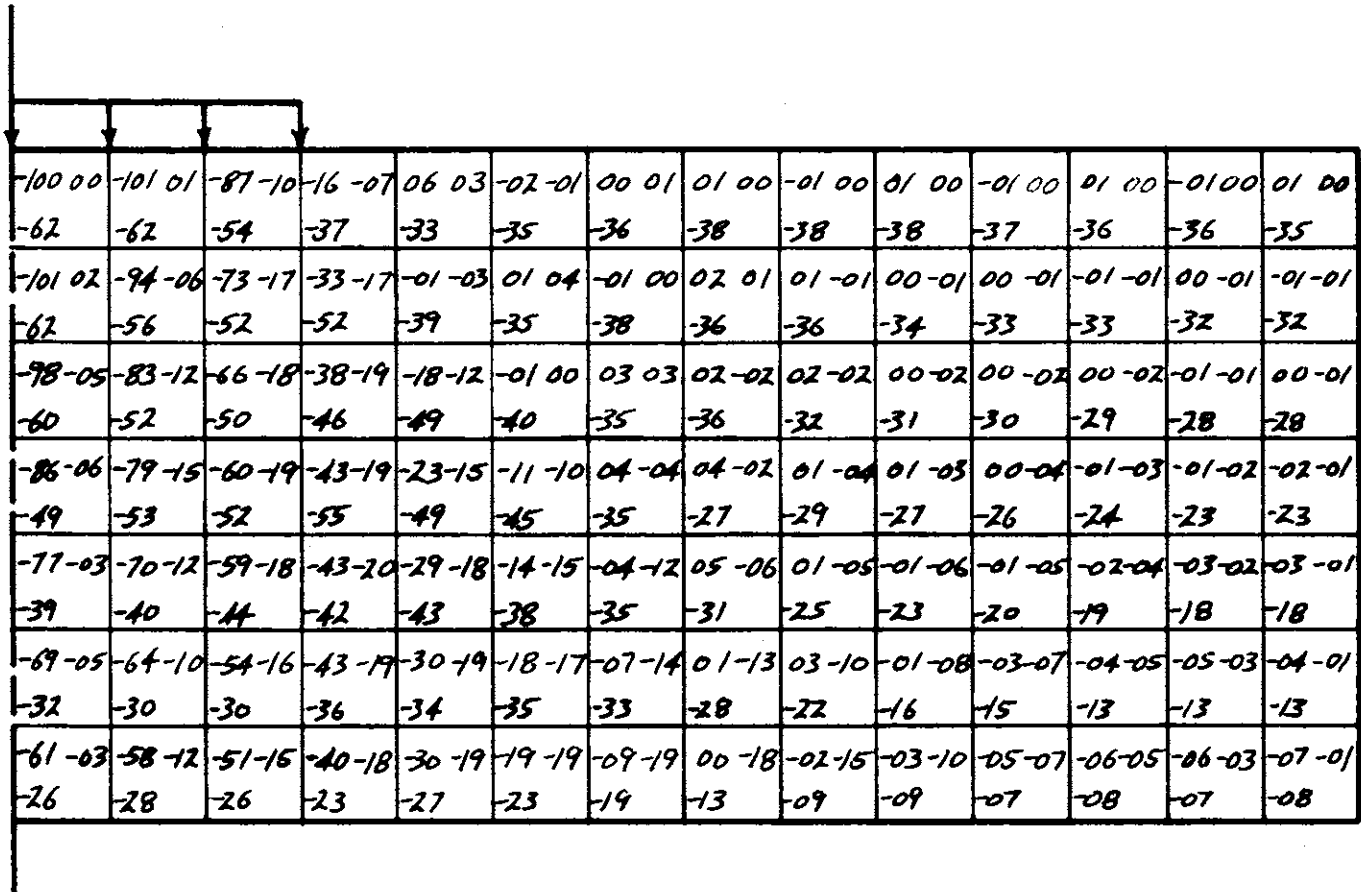


FIG. 26 NORMALIZED STRESSES - RUN 3

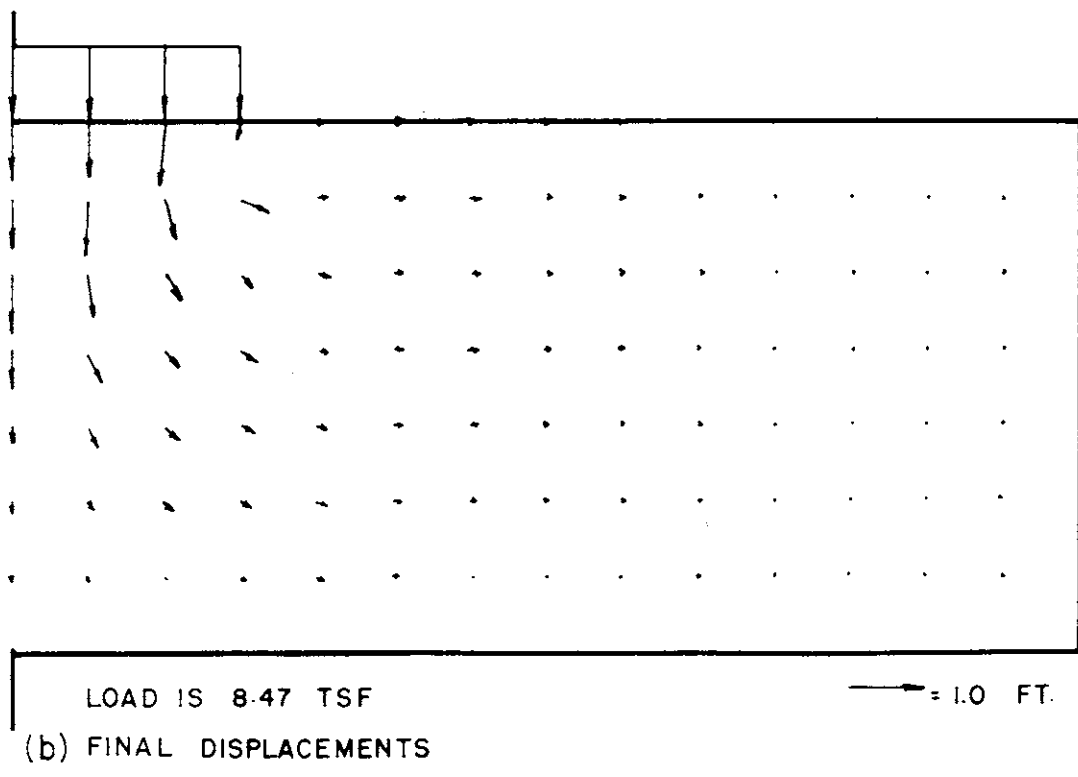
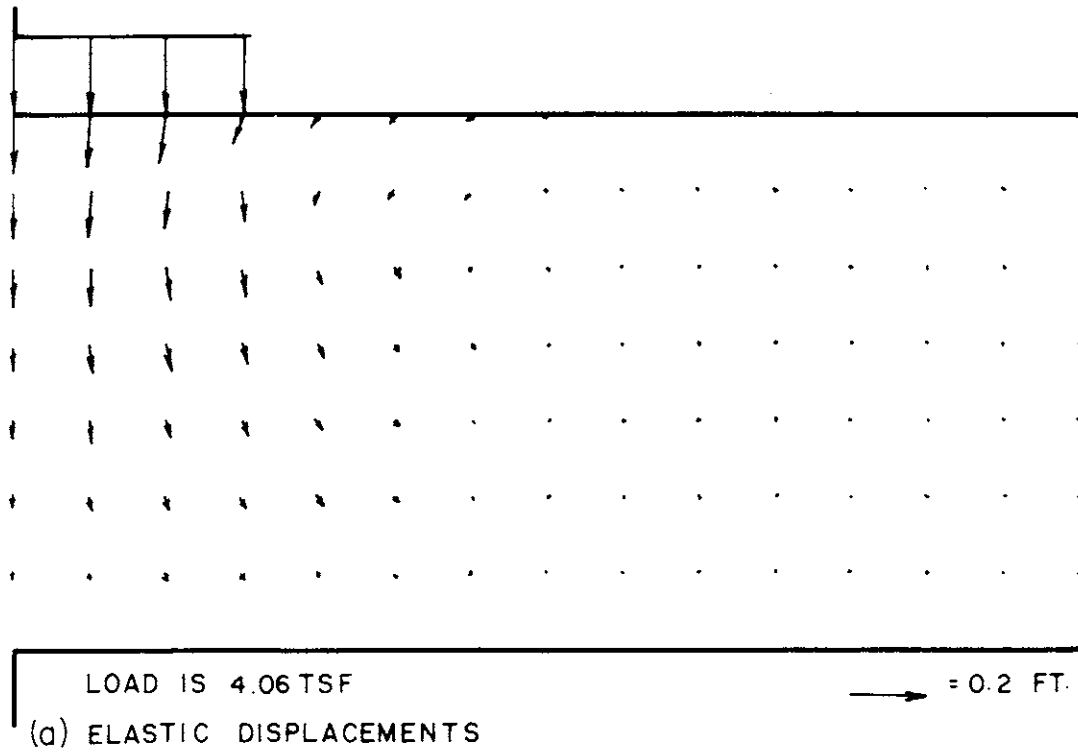


FIG.27 DISPLACEMENT FIELDS RUN I

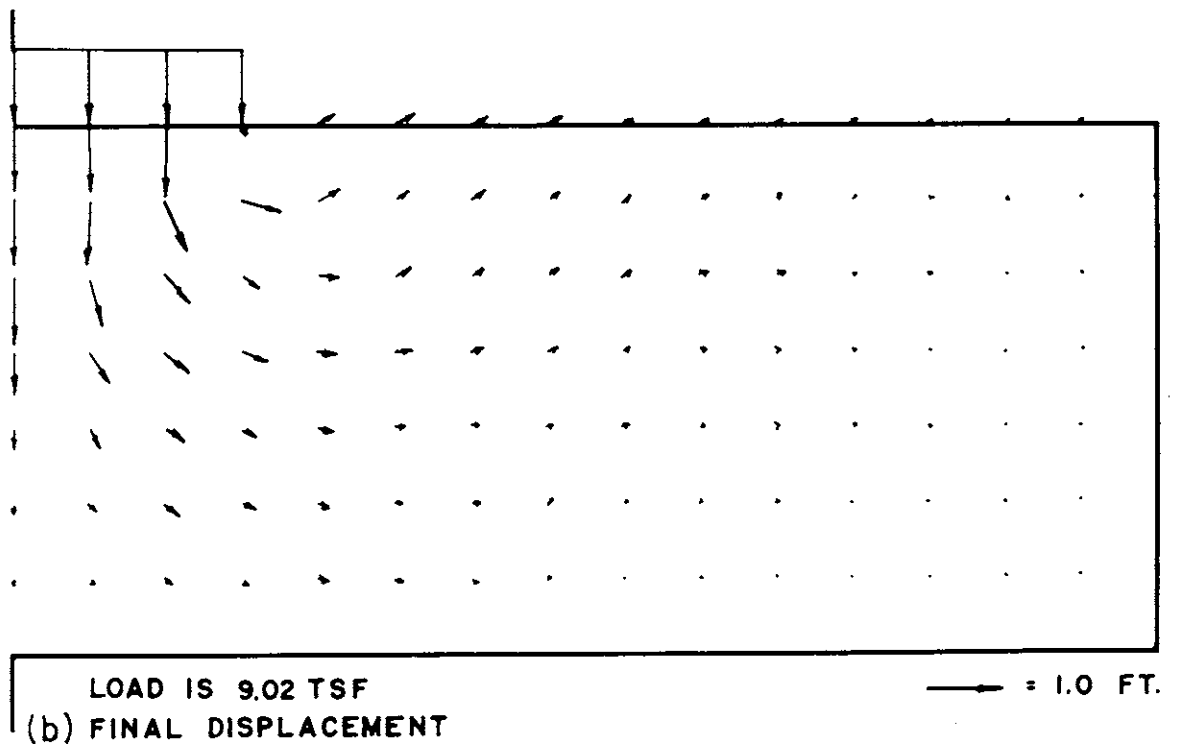
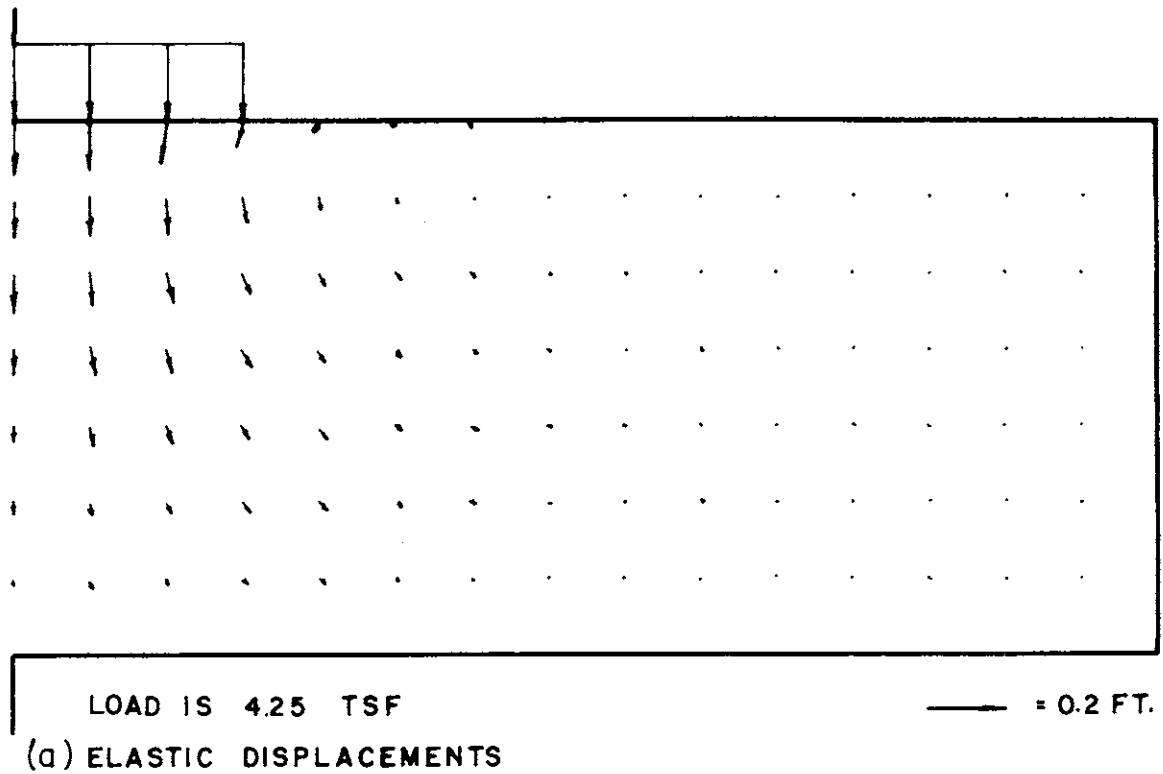


FIG. 28 DISPLACEMENT FIELDS - RUN 2

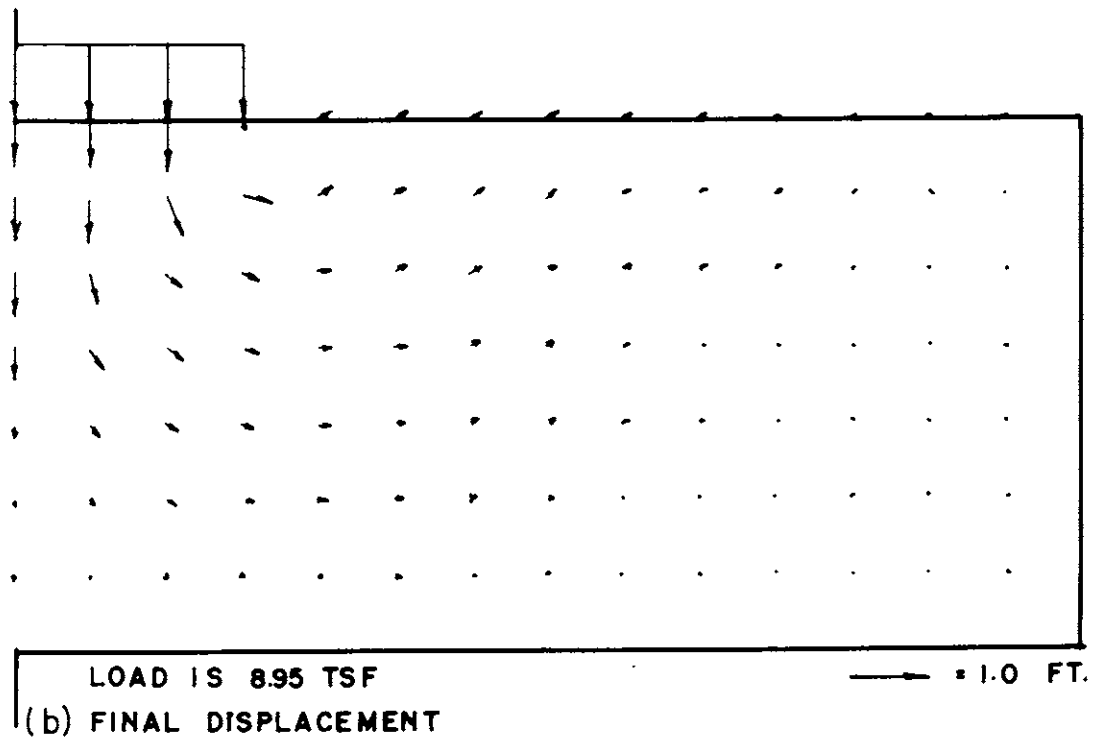
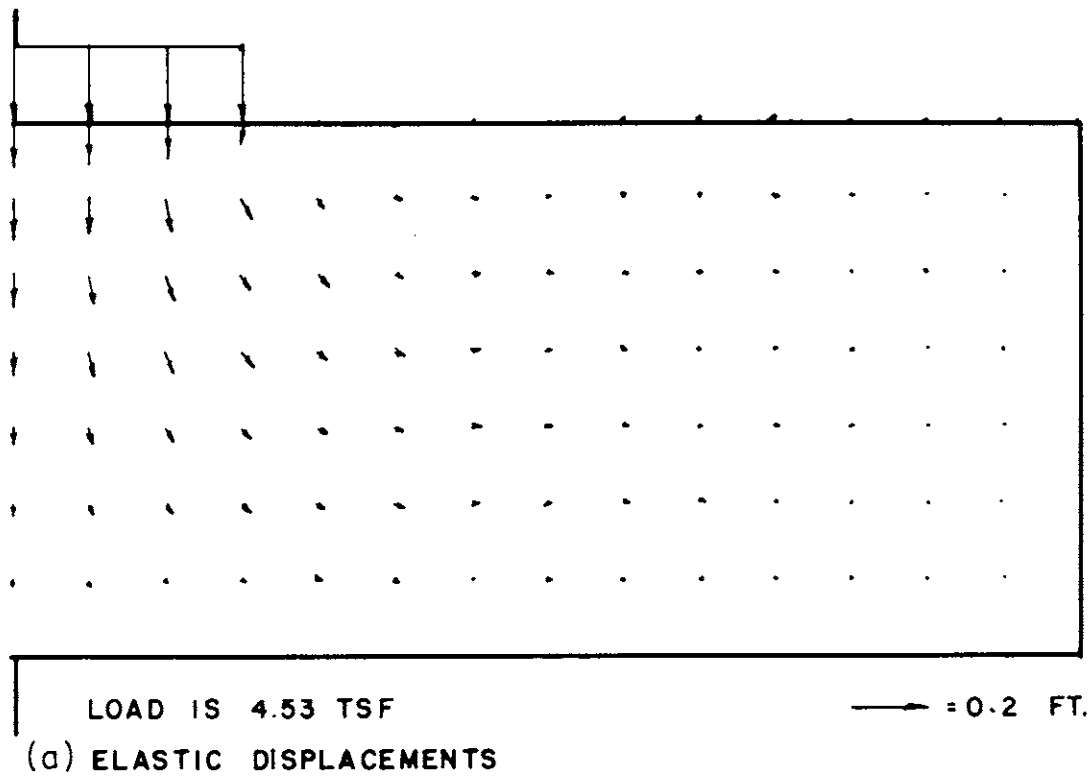
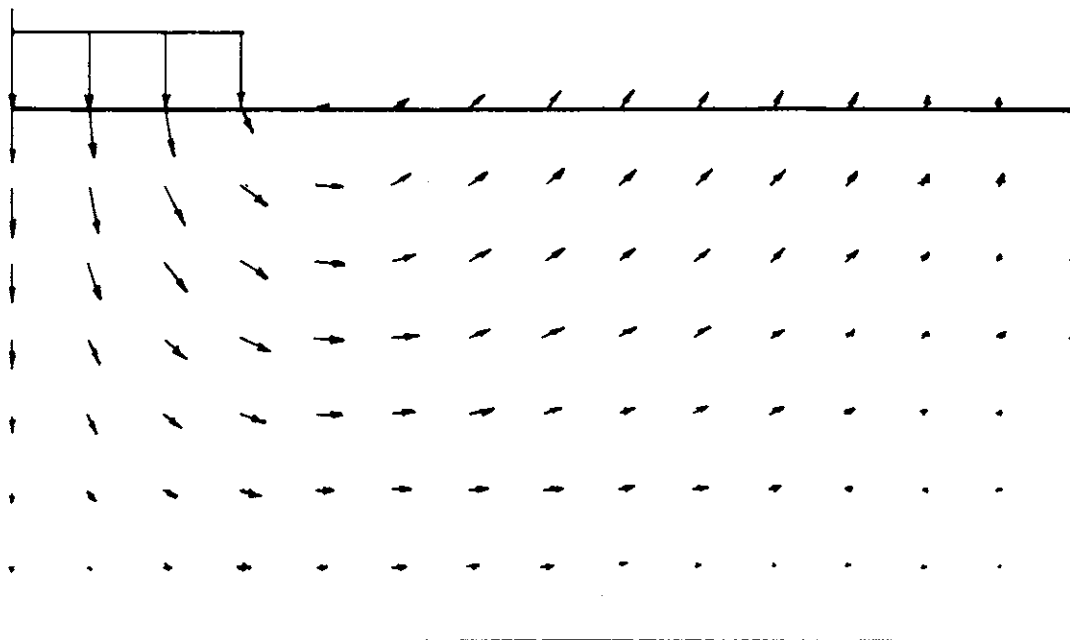


FIG.29 DISPLACEMENT FIELDS - RUN 3

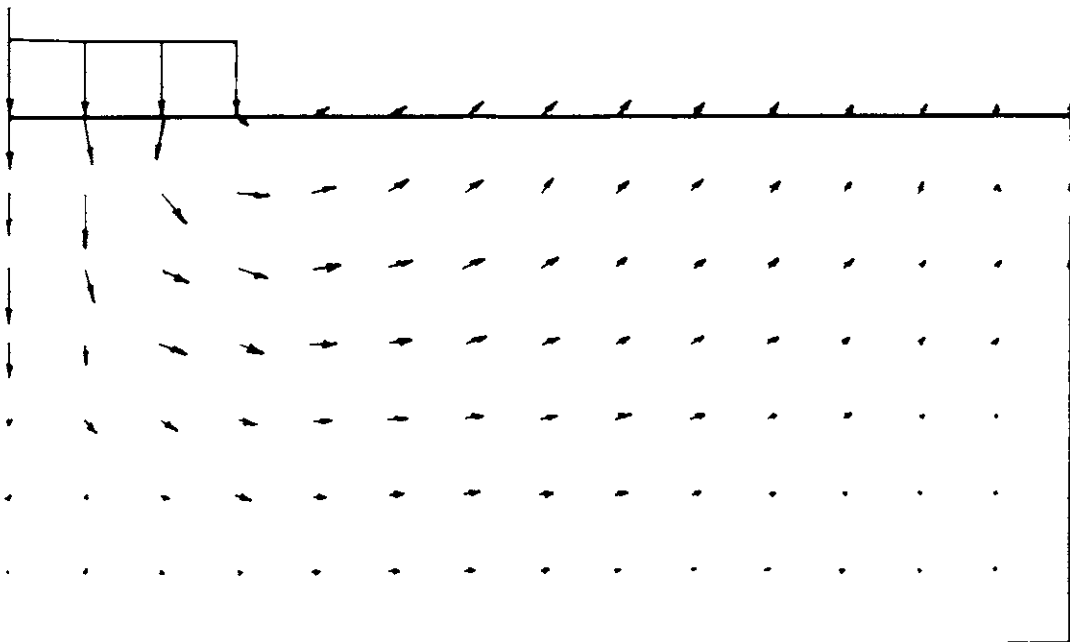




Load = 4.93 TSF

→ = 0.4 FT.

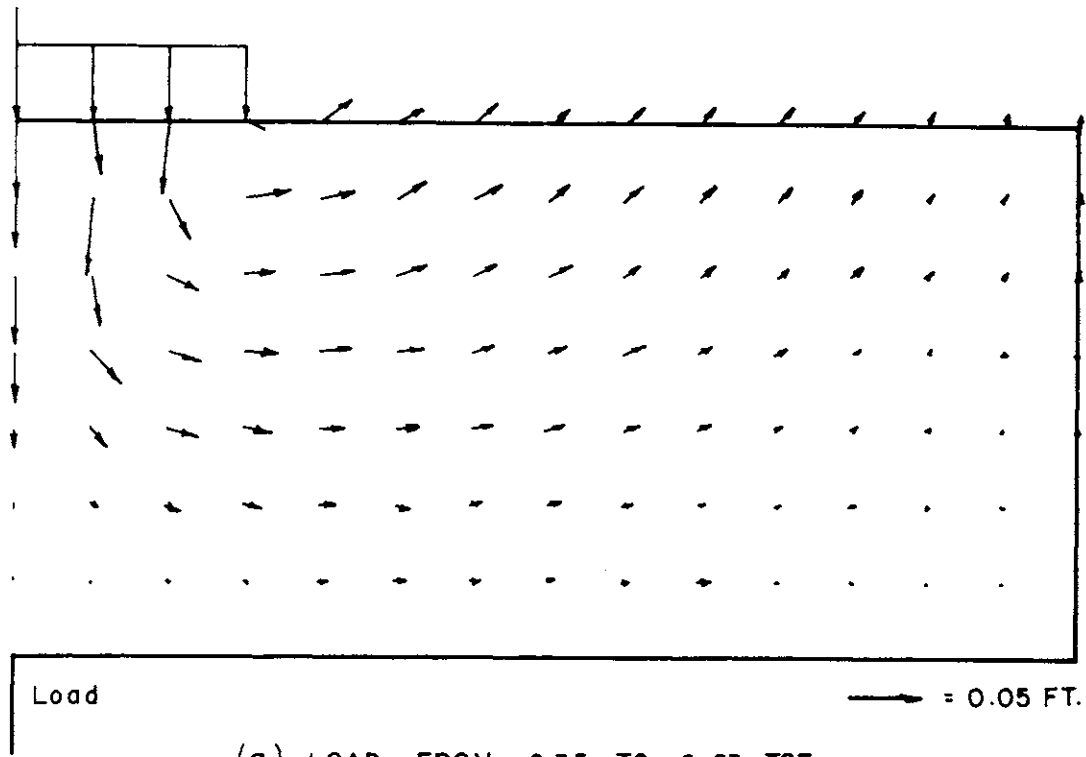
(a) DISPLACEMENTS AT FIRST YIELD



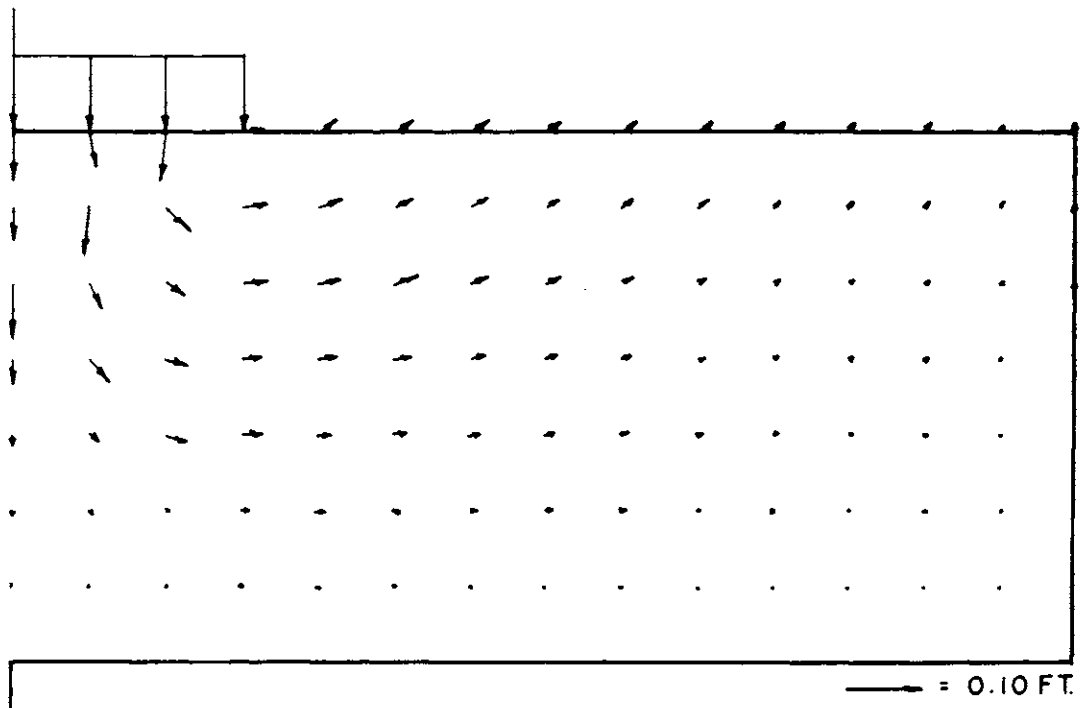
→ = 0.04 FT.

(b) LOAD FROM 5.50 TO 5.78 TSF

FIG. 30 INCREMENTAL DISPLACEMENTS - RUN 5



(a) LOAD FROM 6.35 TO 6.63 TSF



(b) LOAD FROM 7.19 TO 7.48 TSF

FIG. 31 INCREMENTAL DISPLACEMENTS - RUN 5

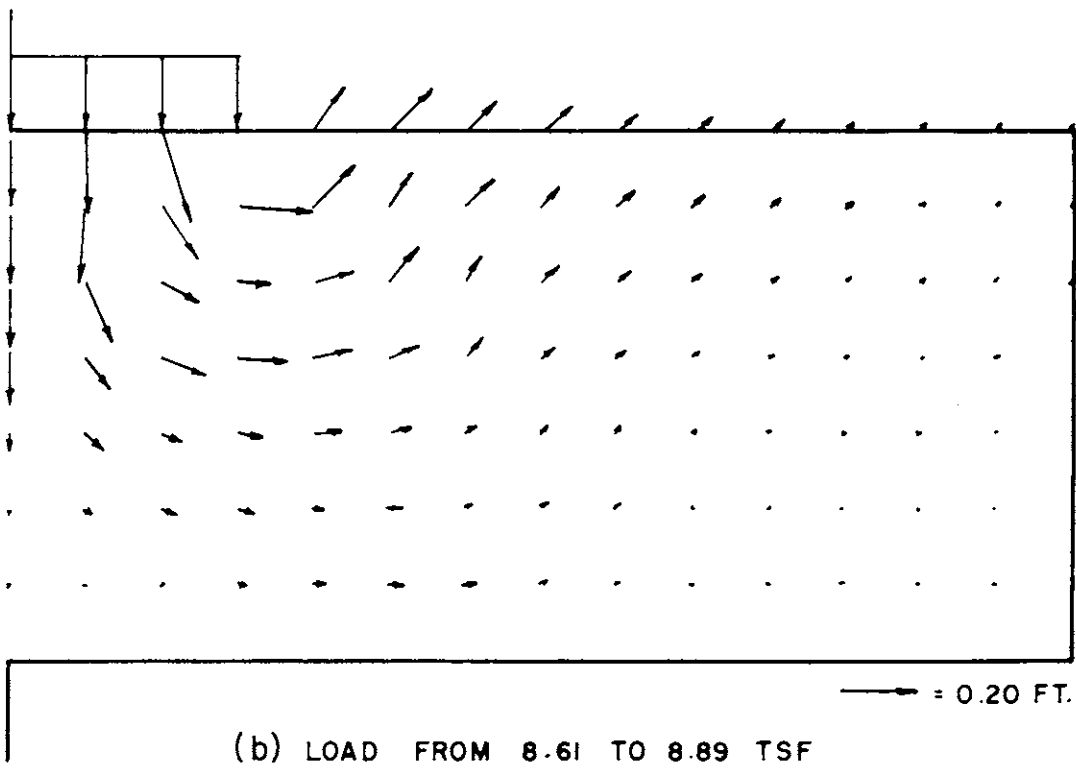
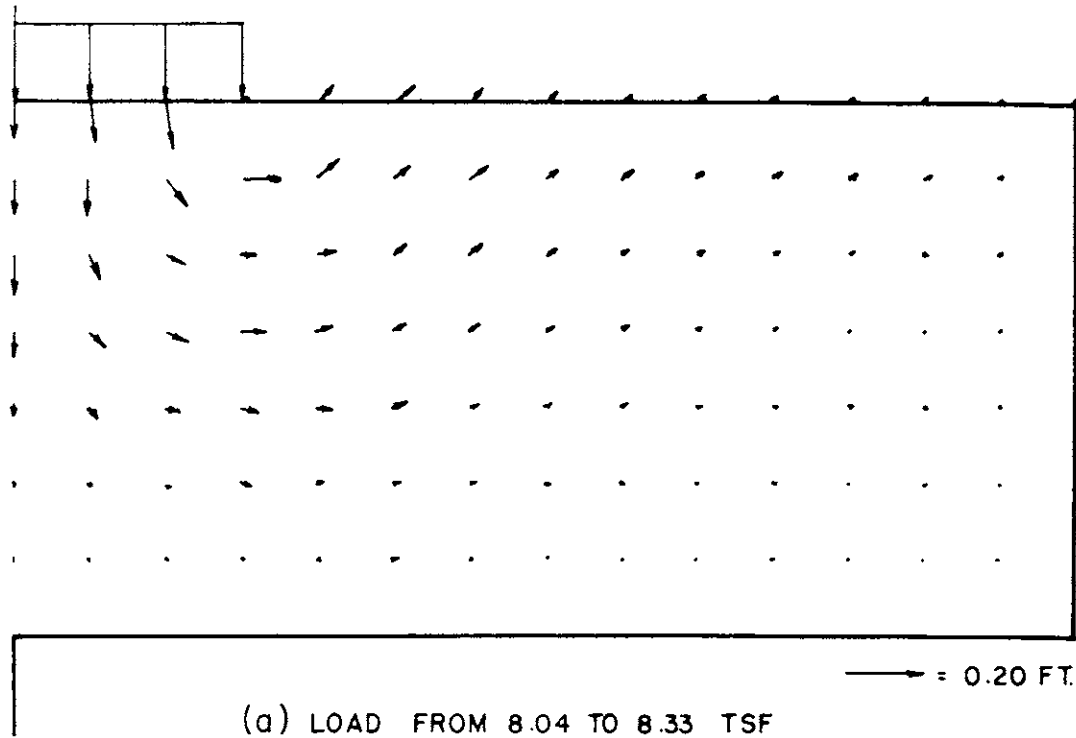


FIG. 32 INCREMENTAL DISPLACEMENTS - RUN 5

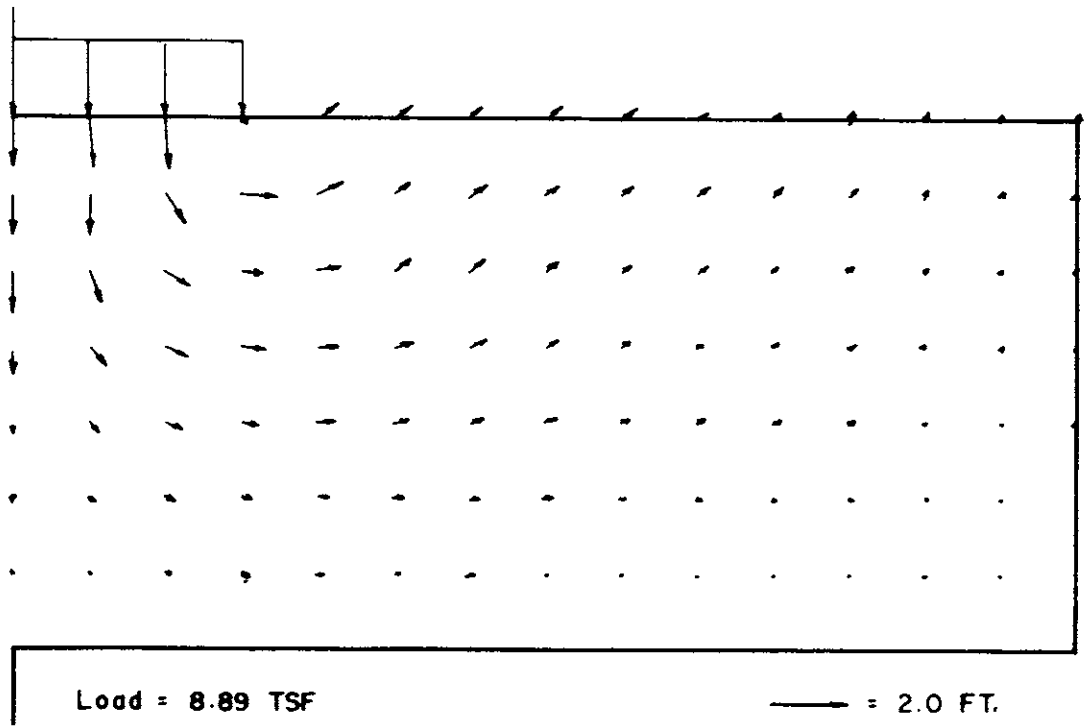


FIG. 33 FINAL DISPLACEMENTS - RUN 5

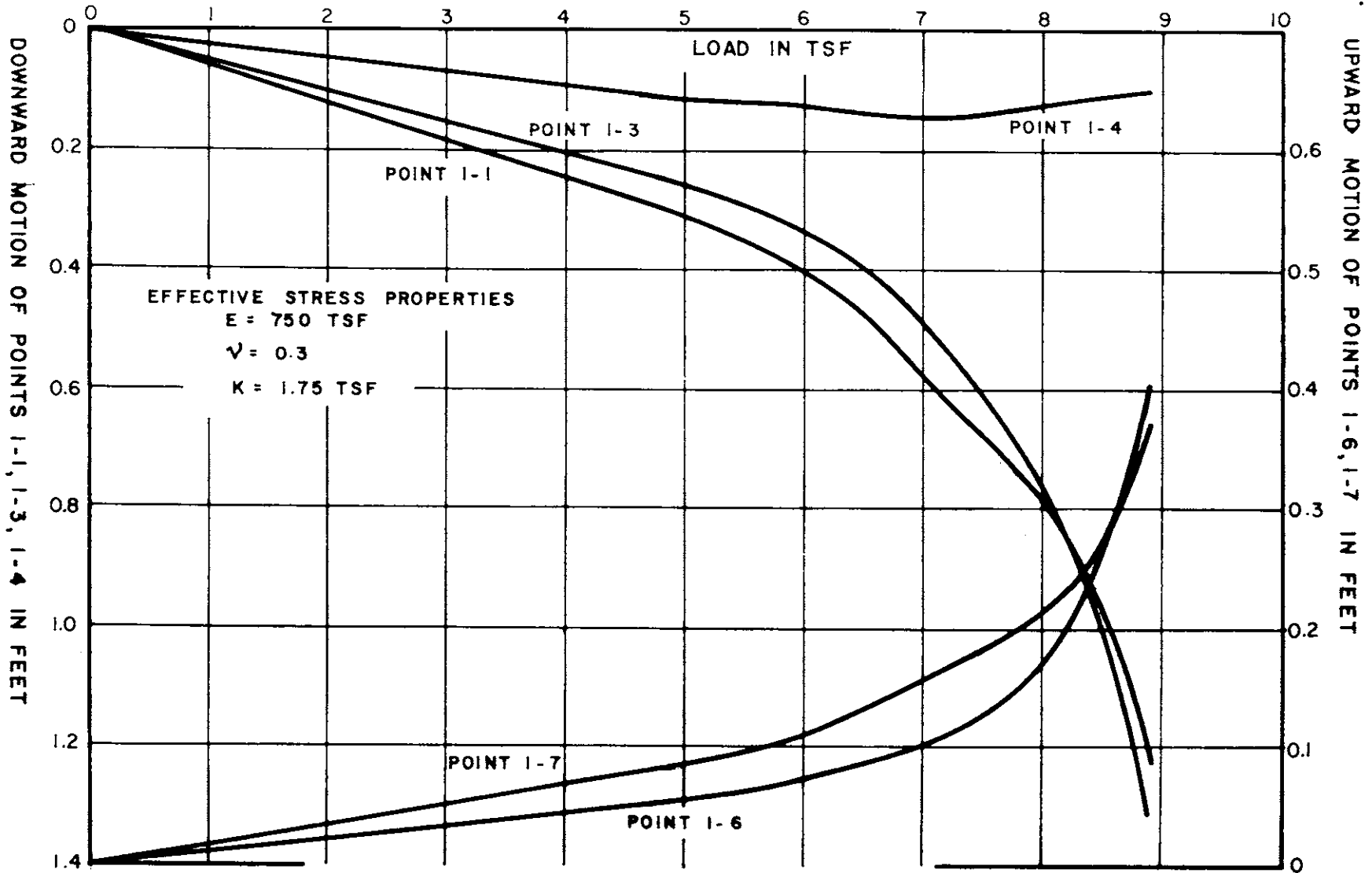


FIG. 34 DISPLACEMENTS IN RUN 5

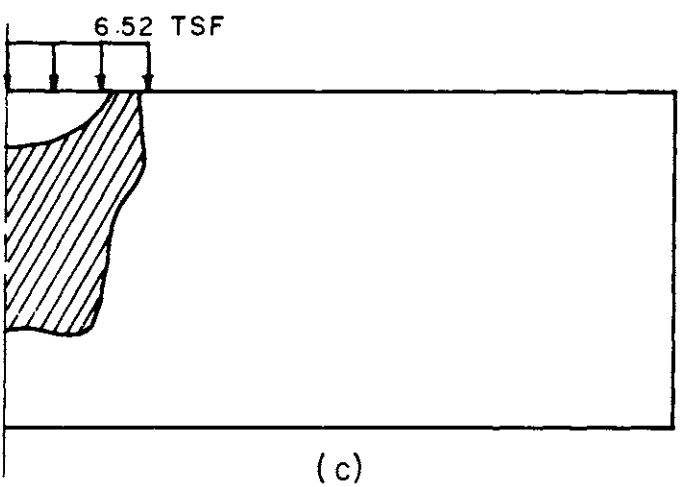
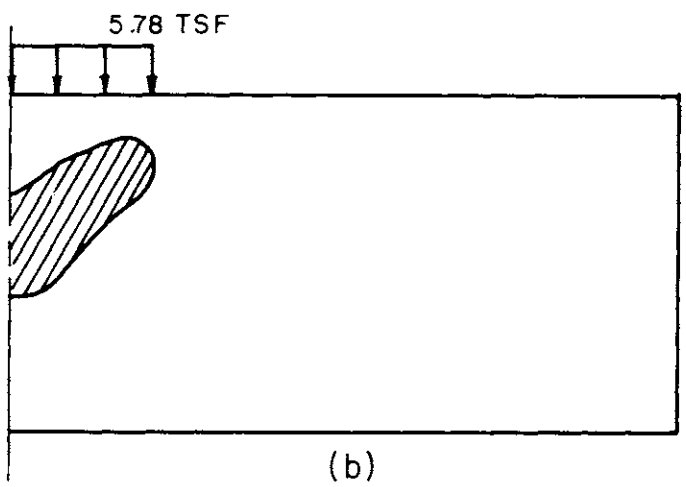
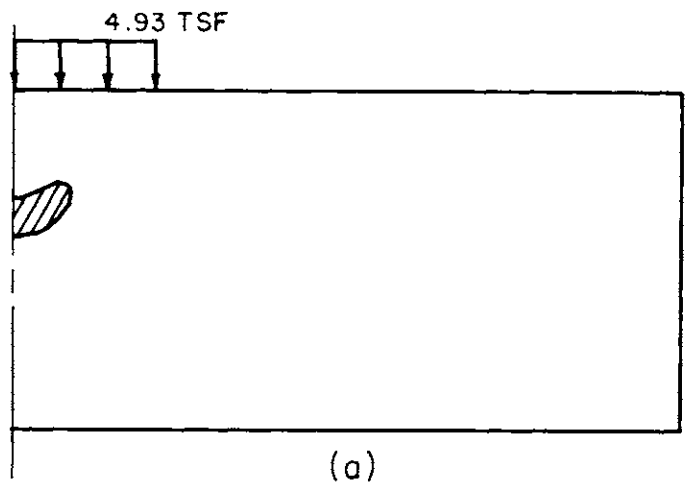


FIG. 35 SPREAD OF PLASTIC ZONE - RUN 5

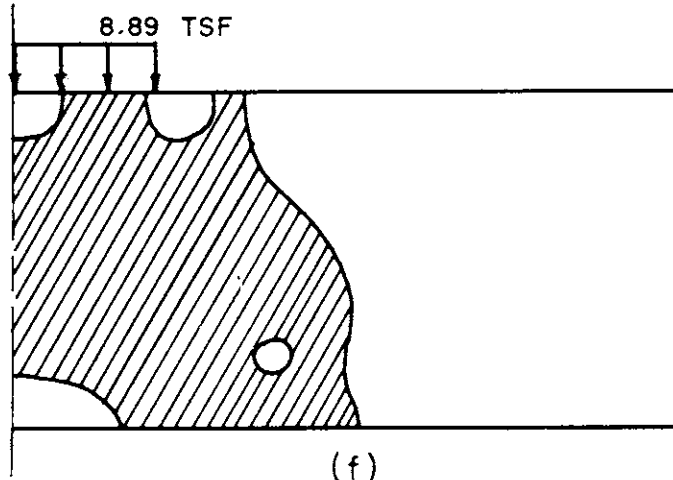
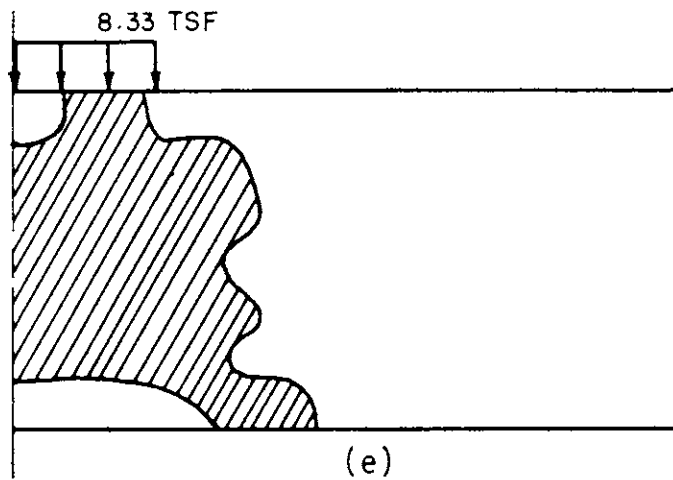
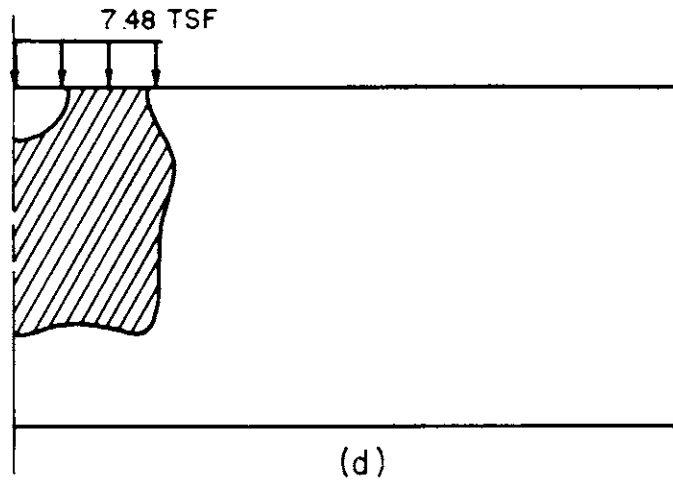


FIG. 35 SPREAD OF PLASTIC ZONE - RUN 5

200

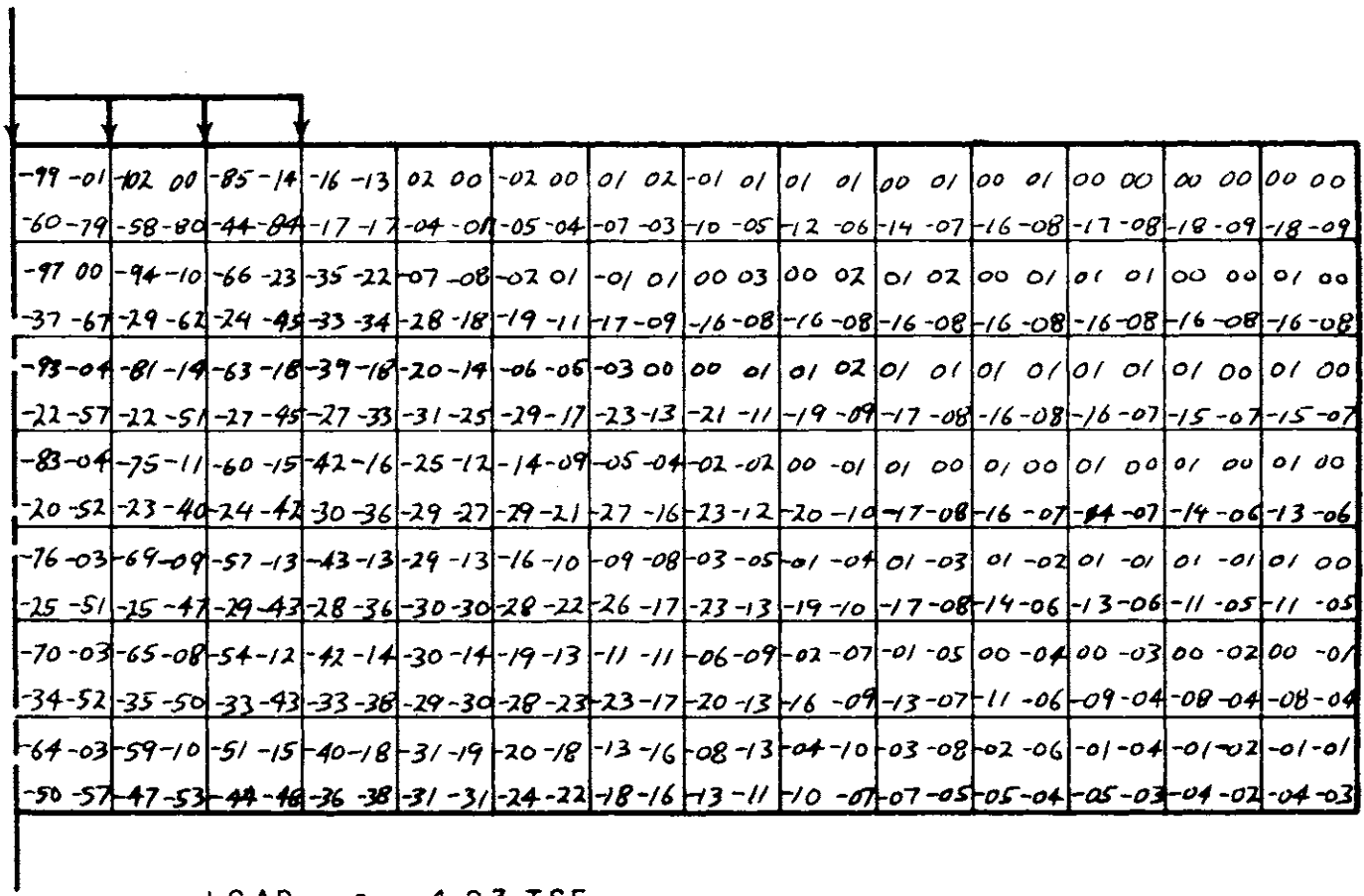


FIG. 36 NORMALIZED STRESSES - RUN 5



201

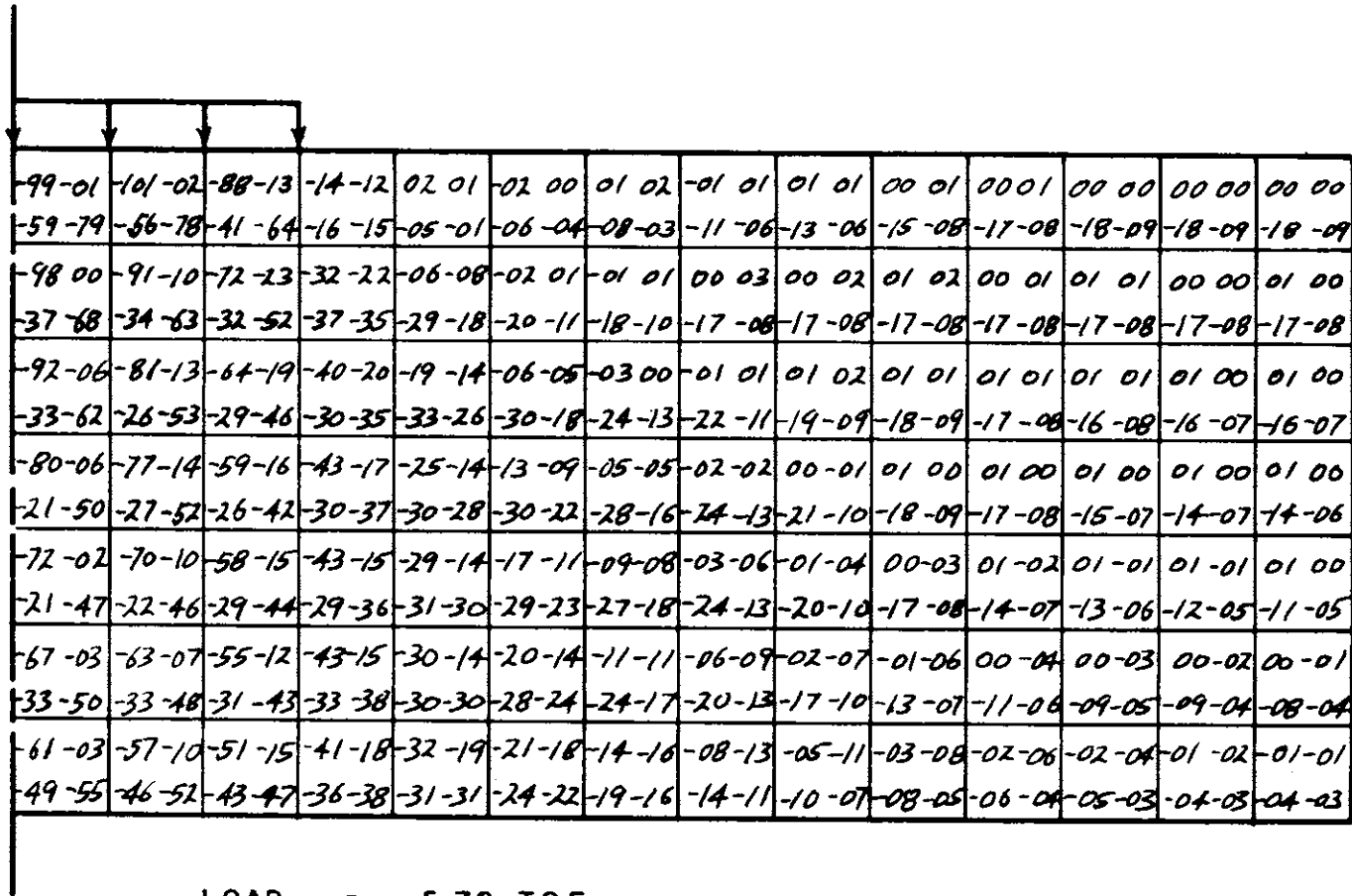
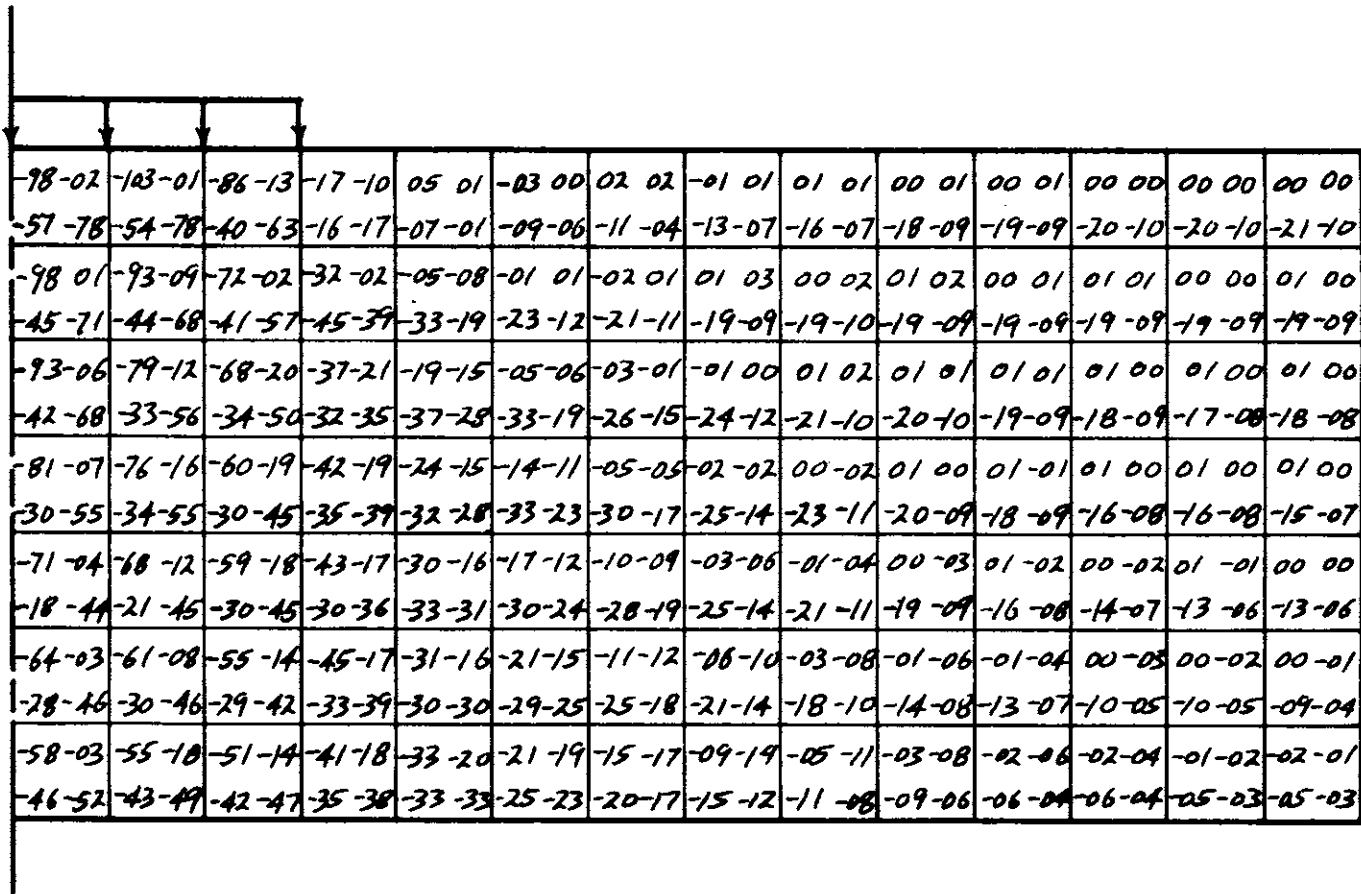


FIG. 37 NORMALIZED STRESSES - RUN 5



LOAD = 6.63 TSF

FIG. 38 NORMALIZED STRESSES - RUN 5

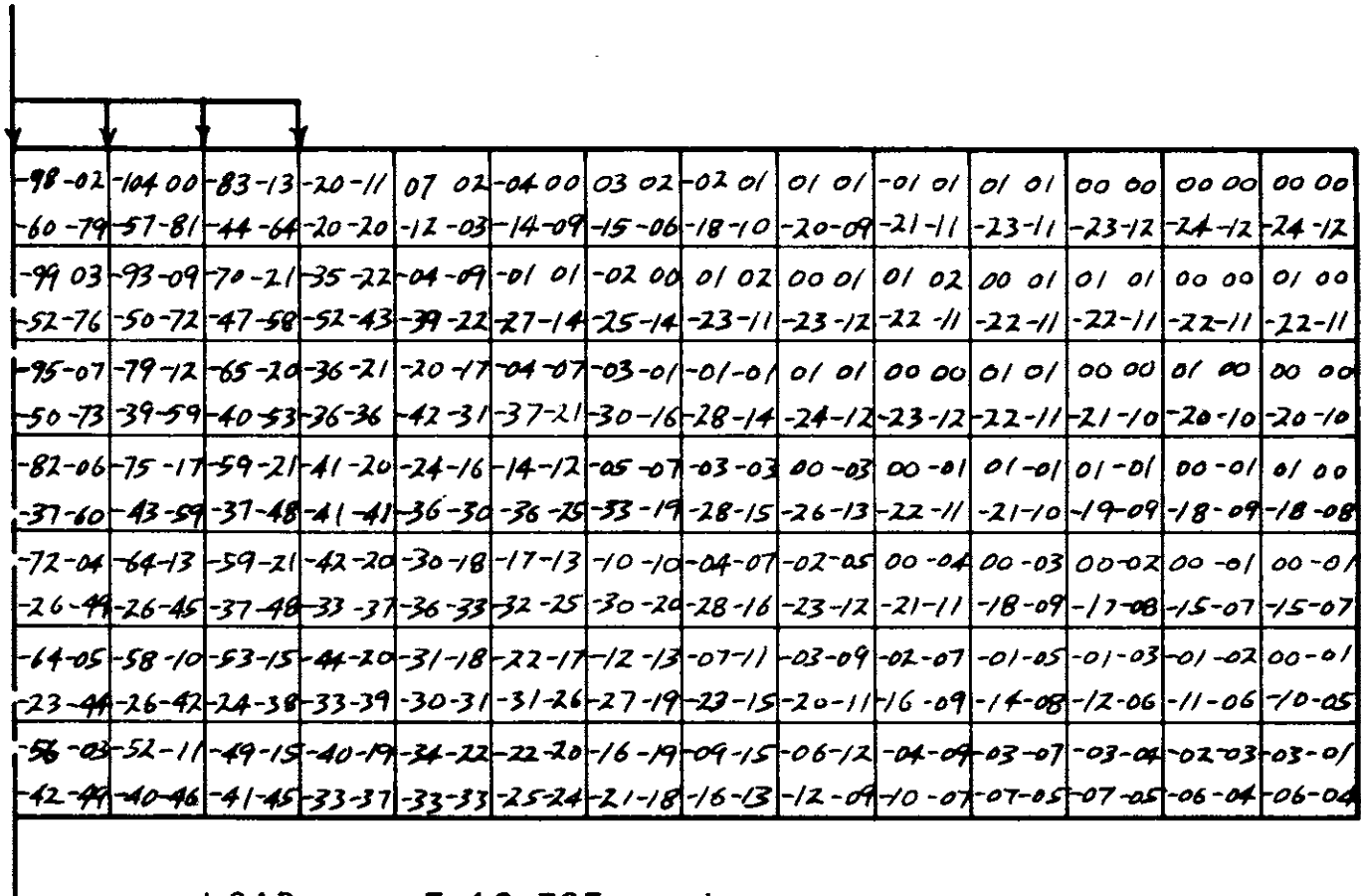


FIG. 39 NORMALIZED STRESSES - RUN 5

-99-01	-103-01	-84-12	-20-09	07-03	-03-01	01-00	-01-00	01-01	00-00	00-00	00-00	00-00	00-00	00-00
-82-80	-61-82	-50-67	-29-24	-23-08	-26-14	-25-12	-26-13	-27-13	-28-14	-28-14	-28-14	-29-14	-28-14	
-100-03	-93-08	-69-19	-37-19	00-07	01-01	-02-01	00-01	00-00	00-01	00-00	00-00	00-00	00-00	00-00
-58-79	-59-74	-51-60	-55-46	-39-20	-29-14	-30-16	-29-14	-28-14	-27-13	-27-13	-27-13	-26-13	-26-13	
-96-06	-80-13	-65-19	-39-21	-16-16	00-05	-02-01	-01-02	00-00	00-01	00-00	00-01	00-00	00-00	00-00
-56-76	-47-61	-46-55	-40-40	-44-30	-40-20	-33-18	-31-16	-28-14	-27-13	-25-13	-25-12	-24-12	-24-12	
-84-06	-77-16	-59-20	-42-21	-22-17	-10-12	-02-07	-03-04	00-03	00-02	00-02	00-02	00-01	00-01	00-00
-44-63	-50-63	-46-52	-51-46	-45-34	-42-26	-36-19	-30-17	-28-14	-25-13	-24-12	-22-11	-21-11	-21-10	
-74-03	-67-13	-58-19	-41-21	-27-20	-14-16	-09-11	-03-08	-02-06	-01-05	-01-04	-01-03	-01-02	-01-01	
-33-54	-34-50	-42-50	-37-39	-39-33	-36-25	-33-21	-30-16	-25-14	-23-12	-20-10	-19-10	-17-09	-17-09	
-66-05	-61-10	-51-16	-41-20	-28-21	-20-18	-10-15	-07-12	-03-09	-03-07	-02-06	-02-04	-02-02	-02-01	
-25-45	-25-43	-23-37	-32-36	-30-29	-31-26	-28-19	-24-15	-21-12	-17-10	-16-09	-14-08	-13-08	-12-07	
-57-03	-56-13	-47-17	-37-20	-31-21	-20-21	-14-20	-09-15	-06-13	-05-09	-04-07	-04-05	-04-03	-04-01	
-42-49	-42-49	-39-43	-29-33	-20-31	-26-23	-20-17	-16-13	-12-09	-11-08	-09-06	-08-06	-07-05	-07-06	

LOAD = 8.33 TSF

FIG. 40 NORMALIZED STRESSES - RUN 5

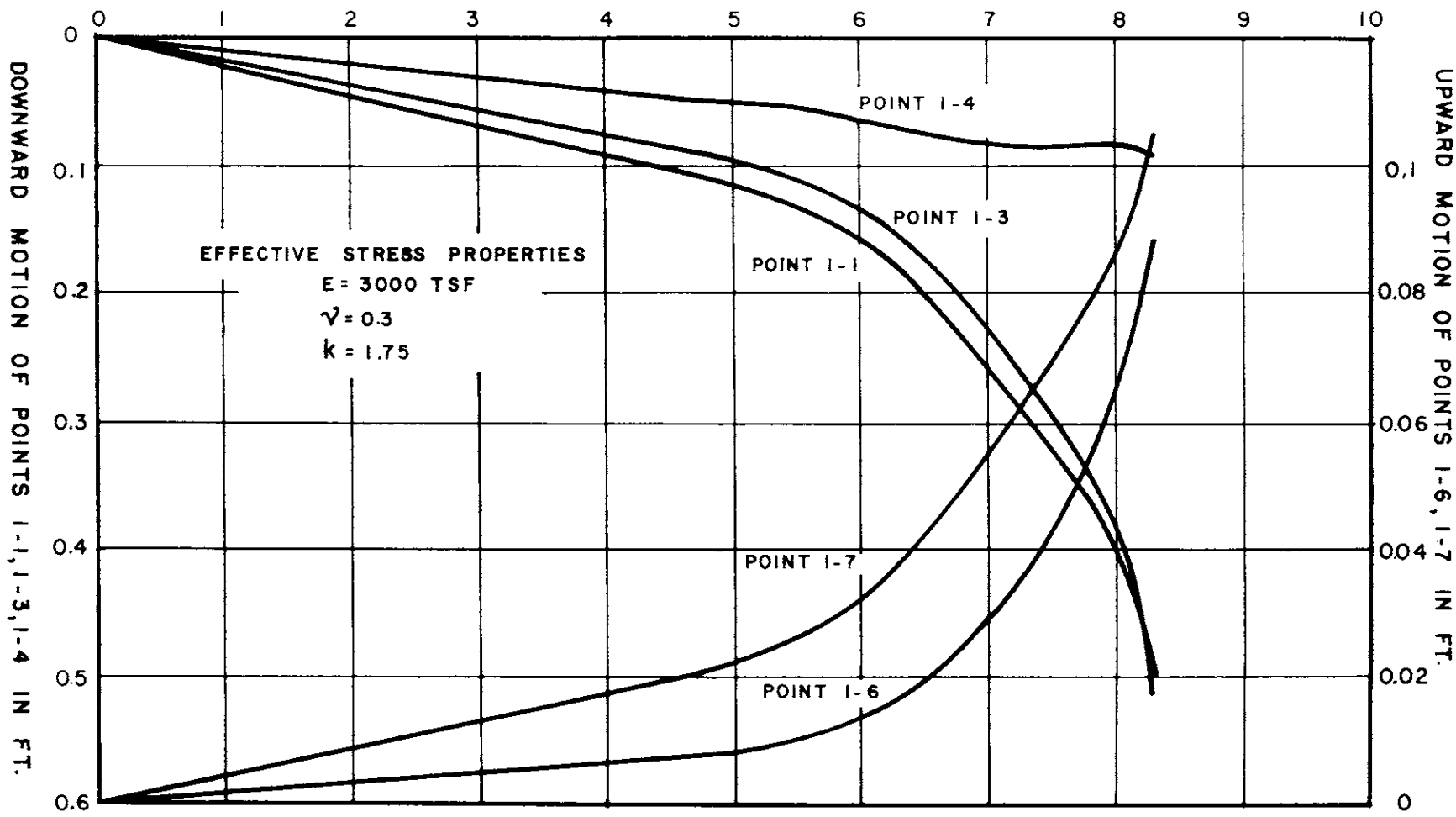
205

-99 00	-101 01	-86 -10	-17 -06	07 03	-03 -01	01 01	00 00	00 00	00 00	00 00	00 00	00 00	00 00	01 00
-62 -80	-62 -82	-53 -70	-36 -26	-32 -13	-35 -19	-35 -17	-37 -18	-37 -19	-37 -18	-37 -19	-36 -18	-36 -18	-35 -17	
-101 02	-93 -06	-72 -17	-33 -17	-01 -03	01 04	-01 00	02 01	00 -01	00 -01	00 -01	00 -01	00 -01	00 -01	00 00
-62 -81	-56 -75	-52 -62	-52 -43	-39 -20	-34 -17	-37 -19	-35 -17	-35 -17	-34 -17	-33 -17	-33 -16	-32 -16	-32 -16	
-97 -06	-83 -12	-66 -18	-38 -19	-17 -12	-01 -01	02 02	01 -02	01 -01	00 -02	00 -01	00 -02	00 -01	00 -01	00 -01
-59 -78	-52 -67	-49 -58	-46 -42	-48 -33	-40 -20	-35 -16	-35 -17	-31 -15	-31 -15	-30 -15	-29 -15	-28 -14	-28 -14	
-86 -05	-79 -15	-60 -19	-42 -19	-23 -15	-11 -10	04 -04	02 -02	00 -03	01 -02	00 -02	-01 -02	-01 -02	-01 -02	-01 -01
-48 -67	-53 -66	-51 -56	-54 -48	-49 -36	-45 -28	-34 -15	-27 -13	-30 -15	-27 -13	-26 -13	-25 -13	-24 -13	-24 -12	
-77 -03	-70 -12	-59 -18	-43 -20	-28 -18	-14 -16	-03 -11	02 -05	00 -04	00 -05	-01 -04	-02 -03	-02 -02	-02 -01	
-38 -58	-38 -54	-44 -52	-41 -42	-42 -35	-38 -26	-35 -19	-32 -15	-26 -13	-24 -12	-21 -11	-20 -11	-19 -11	-19 -11	
-69 -05	-64 -11	-54 -15	-42 -19	-30 -20	-18 -17	-06 -14	-02 -12	01 -09	-01 -07	-02 -06	-03 -04	-04 -02	-03 -01	
-31 -50	-31 -47	-29 -42	-35 -39	-33 -32	-36 -27	-34 -20	-28 -15	-23 -11	-17 -09	-16 -09	-15 -09	-14 -09	-14 -09	
-60 -04	-57 -14	-52 -18	-39 -19	-32 -20	-19 -19	-08 -19	-04 -17	-04 -14	-03 -09	-04 -07	-05 -05	-05 -03	-05 -01	
-43 -52	-41 -49	-37 -44	-28 -34	-31 -31	-25 -22	-20 -14	-15 -09	-12 -08	-10 -07	-09 -06	-09 -07	-09 -07	-09 -07	

LOAD = 8.89 TSF

FIG. 41 NORMALIZED STRESSES - RUN 5

LOAD IN TSF



206

FIG. 42 DISPLACEMENTS IN RUN 6

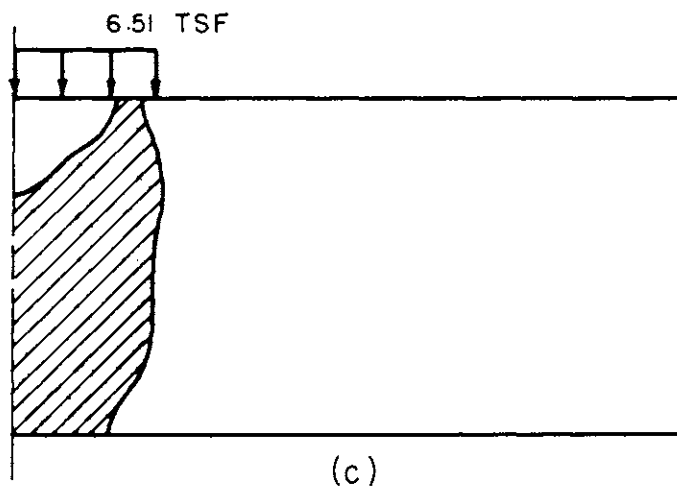
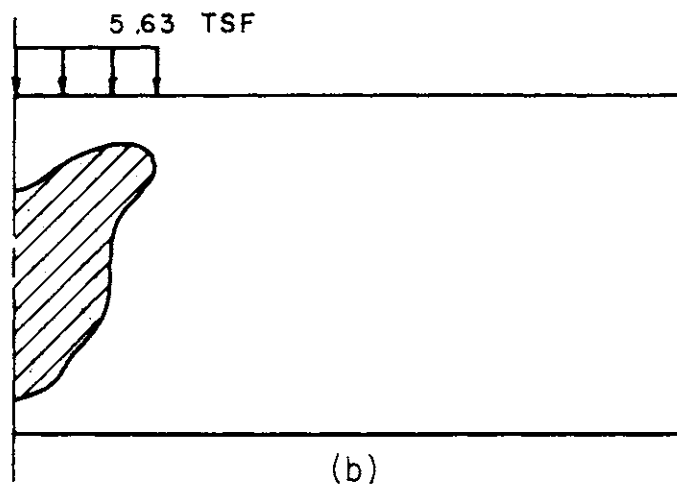
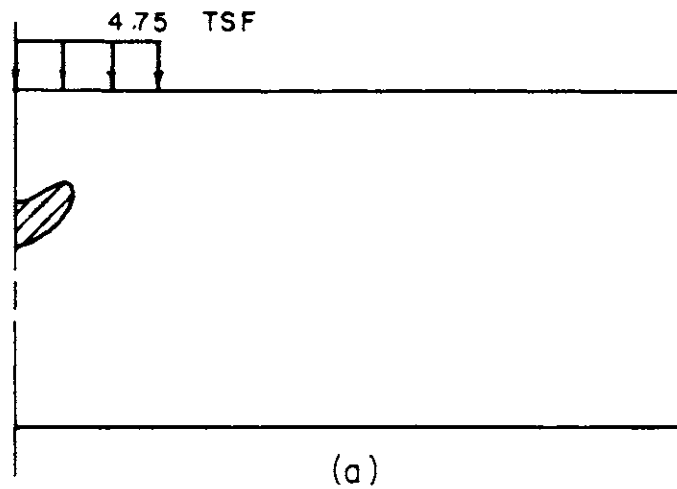


FIG.43 SPREAD OF PLASTIC ZONE - RUN 6

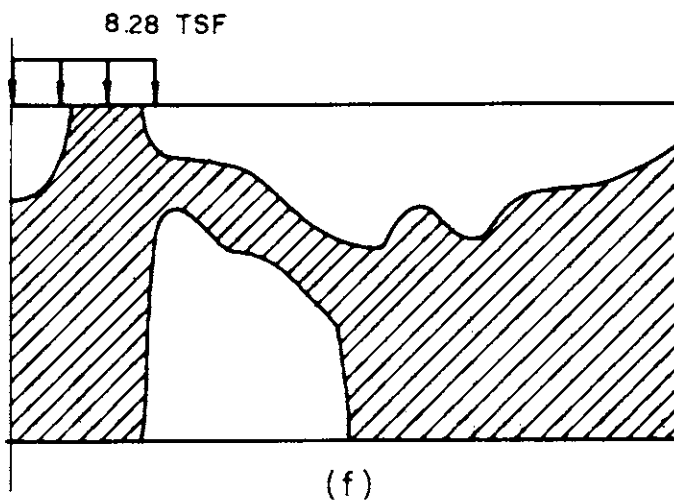
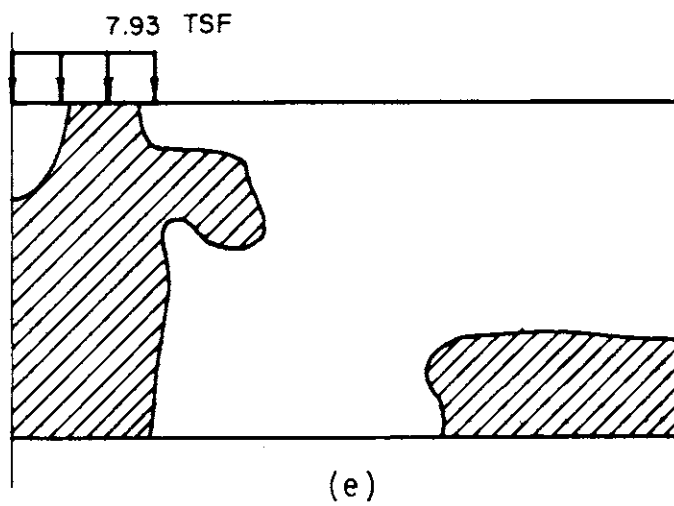
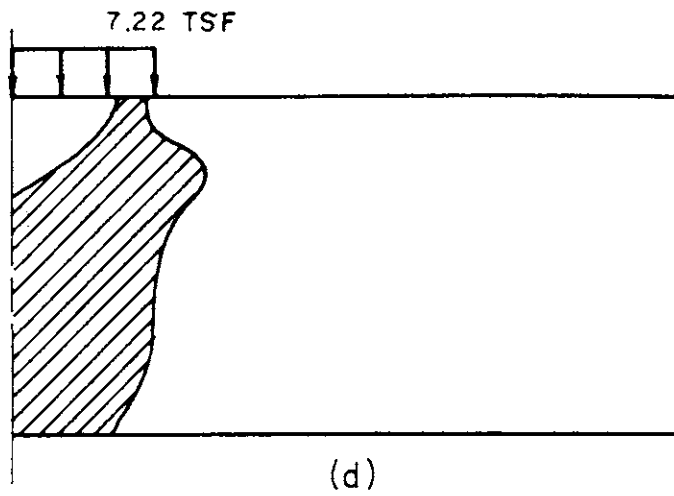


FIG. 43 SPREAD OF PLASTIC ZONE - RUN 6



-99-01	-102-01	-85-14	-16-14	02 00	-02 00	01 01	-01 01	00 01	00 01	00 01	00 01	00 01	00 00	00 00
-66-82	-64-83	-48-66	-20-18	-05-01	-04-03	05-02	-07-04	-09-04	-12-06	-13-07	-15-07	-16-08	-16-08	
-97-01	-94-11	-66-24	-35-24	-07-10	-02-01	-01 00	00 02	00 02	00 03	00 02	01 02	00 01	01 00	
-37-67	-29-61	-24-45	-33-34	-28-17	-18-10	-16-09	-15-07	-15-08	-16-08	-17-08	-17-08	-18-09	-18-09	
-91-05	-80-15	-60-20	-39-20	-21-15	-07-06	-04-01	-02 01	00 03	00 02	01 02	01 02	01 01	01 00	
-18-54	-18-49	-24-43	-23-31	-28-24	-27-17	-23-13	-21-11	-20-10	-20-10	-20-09	-20-09	-20-09	-20-09	
-81-05	-73-12	-59-16	-42-17	-26-12	-15-08	-07-03	-04 00	-01 01	00 02	01 02	02 02	02 01	02 00	
-10-46	-14-44	-16-37	-23-33	-24-25	-27-21	-27-17	-25-14	-24-13	-23-11	-23-11	-22-10	-22-10	-22-10	
-74-03	-68-08	-57-11	-43-11	-30-10	-19-06	-11-04	-05-01	-02 01	00 01	01 02	02 01	03 01	03 00	
-08-41	-09-38	-15-36	-18-31	-24-27	-25-22	-27-19	-27-16	-26-14	-26-13	-24-12	-24-11	-23-10	-23-10	
-69-02	-64-05	-55-07	-44-07	-32-06	-22-05	-13-02	-07-01	-03 00	00 01	01 01	03 01	03 00	03 00	
-06-38	-09-37	-12-33	-18-31	-21-27	-25-24	-27-20	-27-17	-28-15	-27-13	-26-12	-25-11	-25-11	-24-11	
-67 00	-62-01	-55-02	-44-02	-34-02	-23-01	-15-01	-08-01	-03-01	00 00	02 00	02 00	03 00	03 00	
-05-36	-07-35	-12-34	-16-30	-22-28	-25-24	-27-21	-28-19	-28-16	28-14	-26-12	-26-12	-25-11	-25-11	

LOAD = 4.75 TSF

FIG. 44 NORMALIZED STRESSES - RUN 6

-99-02	-101-03	-88-15	-15-12	03 00	-02 00	01 01	-01 01	01 01	00 01	00 01	00 01	00 00	00 00
-66-82	-61-81	-44-66	-17-16	-05-01	-05-04	06-03	-08-05	-11-05	-13-07	-15-07	-16-08	-17-08	-18-09
-96-01	-91-11	-72-24	-33-24	-06-09	-02 00	-02 01	00 03	00 02	01 03	00 02	01 02	00 01	01 00
-37-67	-33-62	-33-53	-39-36	-29-18	-20-11	-18-10	-16-08	-17-08	-17-08	-18-09	-18-09	-19-09	-19-09
-89-06	-80-14	-65-20	-40-21	-20-16	-07-06	-04-01	-01 01	00 03	00 02	01 03	01 02	01 01	01 00
-28-59	-24-52	-26-46	-27-33	-32-26	-29-18	-24-14	-23-12	-21-11	-21-10	-21-10	-21-10	-21-10	-21-10
-77-06	-76-14	-60-17	-43-18	-26-14	-15-09	-07-03	-04 00	-01 01	00 02	01 02	02 02	02 01	02 00
-16-47	-20-48	-20-40	-26-34	-27-26	-29-22	-28-17	-26-15	-26-13	-24-12	-24-11	-23-11	-23-11	-23-10
-69-03	-69-10	-59-14	-44-13	-31-12	-19-07	-12-04	-05-01	-02 01	00 01	01 02	02 01	03 01	03 00
-07-38	-10-39	-17-38	-19-32	-25-28	-27-23	-28-20	-29-17	-27-15	-27-13	-26-12	-26-12	-25-11	-25-11
-64-02	-63-05	-57-08	-46-04	-33-07	-23-05	-13-03	-08-01	-03 00	00 01	01 01	03 01	03 00	03 00
-02-33	-05-34	-09-33	-18-32	-21-27	-26-29	-28-21	-29-18	-29-16	-28-14	-28-13	-27-12	-26-12	-26-11
-63 00	-61-01	-56-02	-45-02	-35-02	-24-01	-15-02	-08-01	-04-01	-01 00	02 00	02 00	03 00	03 00
-02-32	-04-32	-09-33	-14-30	-22-29	-25-24	-28-22	-30-19	-29-16	-29-15	-28-13	-27-13	-26-12	-26-12

LOAD = 5.63 TSF

FIG. 45 NORMALIZED STRESSES - RUN 6

-98-02	-102-02	-85-17	-21-12	07 02	-04 00	02 02	-02 01	01 02	-01 01	01 01	00 01	00 00	00 00
-65-82	-61-81	-42-63	-14-17	-05 01	-07-06	-09-03	-11-06	-14-06	-17-09	-19-09	-20-10	-21-11	-22-11
-97 00	-91-11	-69-24	-41-25	-04-09	01 01	-02 01	01 03	-01 02	01 03	00 02	01 02	00 01	01 00
-45-71	-42-67	-44-56	-52-46	-36-20	-23-12	-21-12	-20-10	-21-11	-21-10	-22-11	-23-11	-23-12	-23-11
-91-06	-77-15	-64-21	-42-22	-22-18	-06-06	-04 00	-01 01	00 03	00 03	01 03	01 02	02 01	01 00
-39-65	-32-54	-30-47	-29-35	-39-30	-35-20	-29-16	-28-15	-26-13	-26-13	-25-12	-26-12	-25-12	-26-12
-78-06	-70-18	-63-21	-44-18	-28-14	-16-10	-06-03	-04 01	-01 02	01 03	01 02	02 02	02 01	03 00
-26-52	-29-50	-28-46	-32-38	-31-29	-35-26	-34-20	-31-17	-31-16	-29-14	-29-14	-28-13	-28-13	-28-13
-66-05	-62-14	-64-18	-47-16	-33-12	-20-08	-12-04	-05-01	-02 01	01 02	01 02	02 01	03 01	03 00
-13-40	-15-38	-24-44	-25-36	-32-32	-32-26	-34-23	-34-20	-33-17	-32-16	-31-14	-31-14	-30-13	-30-14
-57-04	-59-09	-62-10	-51-11	-35-08	-25-06	-14-03	-08-01	-03 00	00 01	02 01	03 01	03 01	04 00
-03-30	-08-33	-12-37	-23-37	-26-31	-32-29	-34-24	-35-21	-35-19	-33-17	-33-16	-32-14	-32-14	-31-13
-52-01	-57-03	-63-02	-49-02	-39-03	-25-01	-16-02	-08 00	-03-01	00 00	02 00	03 00	04 00	04 00
02-25	-03-30	-13-38	-17-33	-28-33	-31-28	-34-25	-35-22	-35-19	-35-17	-33-15	-33-15	-31-14	-32-14

LOAD = 6.51 TSF

FIG. 46 NORMALIZED STRESSES - RUN 6

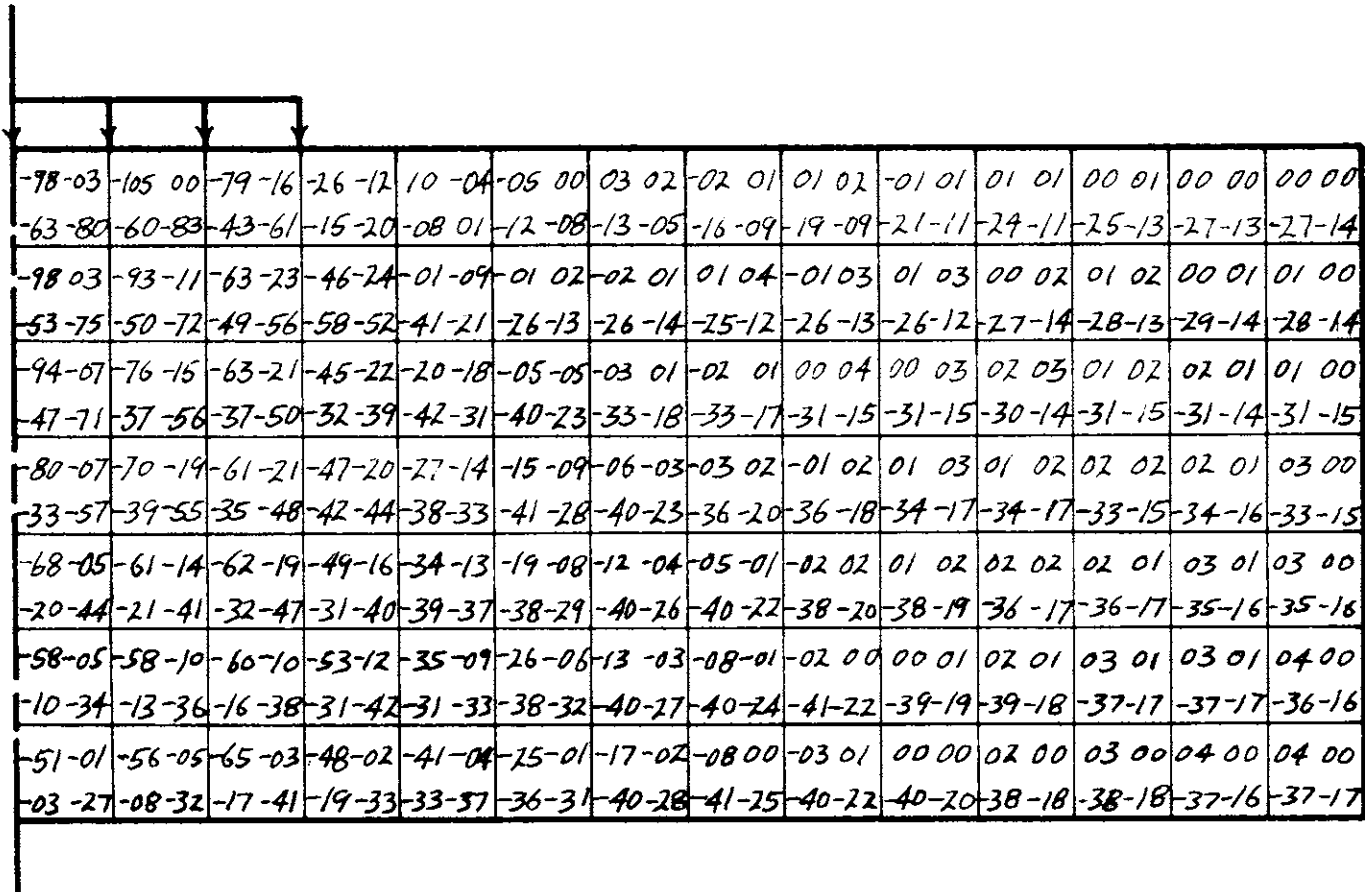


FIG. 47 NORMALIZED STRESSES - RUN 6

-98-02	-105-01	-78-16	-27-11	10-06	-03-01	02-01	-02-01	01-01	-01-01	01-01	00-01	00-00	00-00
-61-80	-61-83	-47-62	-20-24	-16-03	-21-12	-21-10	-23-12	-25-12	-27-14	-29-14	-31-16	-32-16	-33-17
-100-03	-92-10	-62-21	-48-21	00-07	03-03	-04-00	01-03	-01-02	01-03	00-02	01-02	00-01	01-00
-59-79	-53-73	-50-56	-60-54	-41-20	-27-12	-30-17	-30-15	-31-16	-32-15	-33-16	-33-16	-34-17	-34-16
-96-08	-76-15	-63-20	-47-20	-18-17	-02-04	-02-03	-02-01	00-04	00-03	01-03	01-02	02-01	01-00
-55-75	-44-60	-43-53	-35-41	-46-32	-44-23	-36-19	-37-19	-36-18	-36-18	-36-17	-36-18	-36-17	-37-18
-81-07	-71-19	-60-20	-49-20	-25-13	-13-08	-04-02	-03-02	-01-02	01-03	01-02	02-02	02-01	03-00
-39-60	-48-60	-44-52	-51-50	-44-35	-46-29	-45-24	-40-22	-41-21	-39-19	-39-19	-38-18	-39-19	-38-18
-70-04	-62-13	-62-19	-50-16	-33-14	-17-08	-11-03	-04-00	-01-02	01-02	02-02	02-02	03-01	03-00
-27-48	-26-44	-38-50	-36-43	-46-39	-44-30	-45-28	-45-24	-42-22	-43-21	-41-20	-42-20	-40-18	-41-19
-60-05	-59-10	-60-09	-53-11	-35-09	-25-07	-12-02	-07-01	-02-01	01-01	01-01	03-01	03-01	04-00
-18-39	-20-40	-20-40	-36-44	-36-35	-44-34	-45-29	-45-26	-46-24	-43-21	-43-21	-41-19	-41-19	-40-18
-53-02	-56-07	-67-04	-46-01	-41-04	-25-01	-16-02	-07-00	-02-01	00-00	02-00	02-00	04-00	04-00
-10-32	-14-35	-23-45	-23-35	-38-39	-41-33	-45-30	-46-27	-44-23	-44-22	-42-20	-42-20	-40-18	-40-18

LOAD = 7.93 TSF

FIG. 48 NORMALIZED STRESSES - RUN 6

-99-01	-105-02	-79-15	-27-10	10-07	-03-00	02-01	-02-01	01-01	00-01	00-01	00-01	00-00	-01-01
-62-81	-63-84	-49-64	-24-25	-21-06	-28-15	-28-13	-30-16	-32-15	-34-17	-35-17	-37-18	-38-19	-39-20
-101-04	-92-10	-64-20	-47-20	-01-05	06-05	-04-00	02-03	-01-02	01-03	-01-02	01-02	00-02	00-06
-61-81	-55-74	-52-58	-61-54	-43-22	-30-12	-34-19	-35-17	-36-19	-37-18	-40-20	-40-20	-42-21	-42-21
-96-08	-78-15	-64-19	-48-19	-19-16	-01-01	01-05	-02-02	01-05	-01-03	01-04	00-03	02-02	01-01
-57-77	-47-62	-46-55	-39-44	-47-33	-43-22	-38-19	-40-21	-40-19	-41-21	-40-20	-42-21	-41-19	-42-20
-82-05	-72-18	-62-20	-50-19	-27-12	-12-07	-02-01	00-05	-01-01	01-04	00-03	02-03	01-02	04-00
-41-62	-51-62	-47-55	-54-52	-48-36	-50-31	-45-23	-41-21	-43-22	-40-20	-42-21	-40-19	-41-20	-39-17
-72-05	-64-12	-63-18	-53-15	-34-14	-17-06	-08-03	-02-01	01-04	00-02	02-03	01-02	04-01	03-01
-31-51	-28-46	-40-52	-40-46	-48-41	-45-31	-49-28	-44-23	-41-20	-43-22	-40-19	-41-20	-38-17	-40-19
-62-05	-61-11	-61-09	-55-11	-36-08	-25-06	-10-01	-04-01	-02-01	02-03	00-01	05-01	03-00	05-00
-21-41	-24-43	-23-42	-36-46	-38-37	-46-35	-44-27	-47-25	-44-23	-40-19	-42-21	-38-17	-40-19	-37-16
-56-02	-57-06	-68-05	-49-01	-42-04	-23-01	-14-03	-02-00	-03-03	-01-00	05-01	02-00	05-00	03-00
-13-34	-17-37	-27-46	-27-38	-39-40	-41-32	-47-31	-45-24	-45-24	-44-23	-38-17	-41-19	-37-16	-39-18

LOAD = 8.28 TSF

FIG. 49 NORMALIZED STRESSES - RUN 6

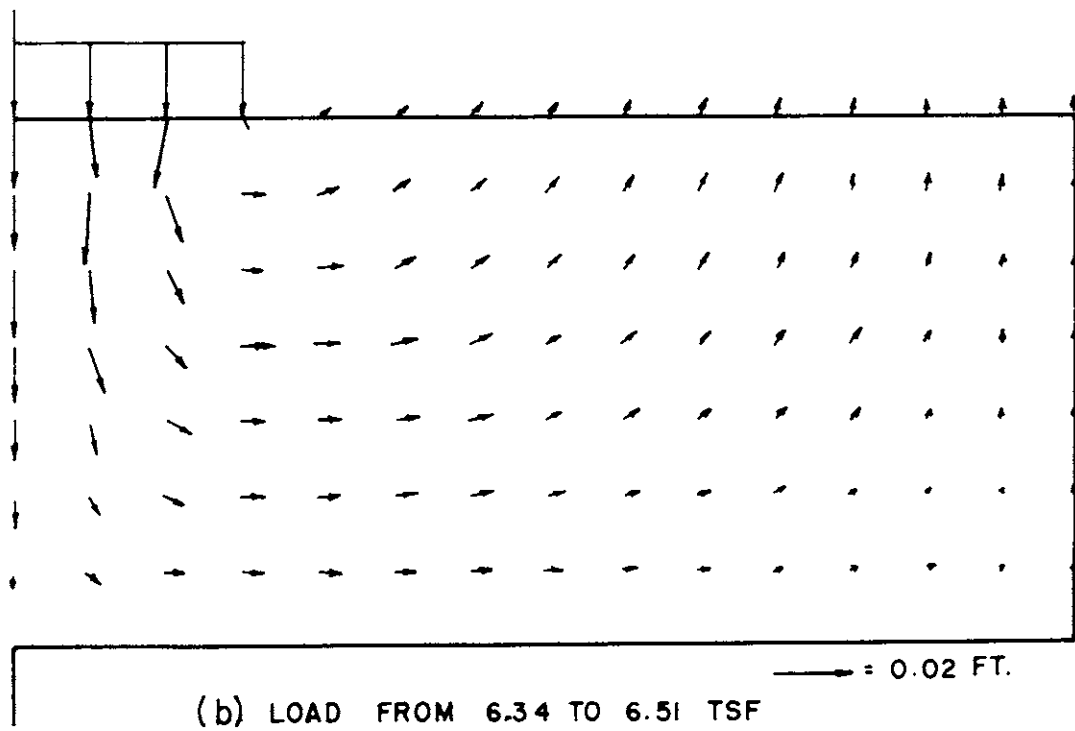
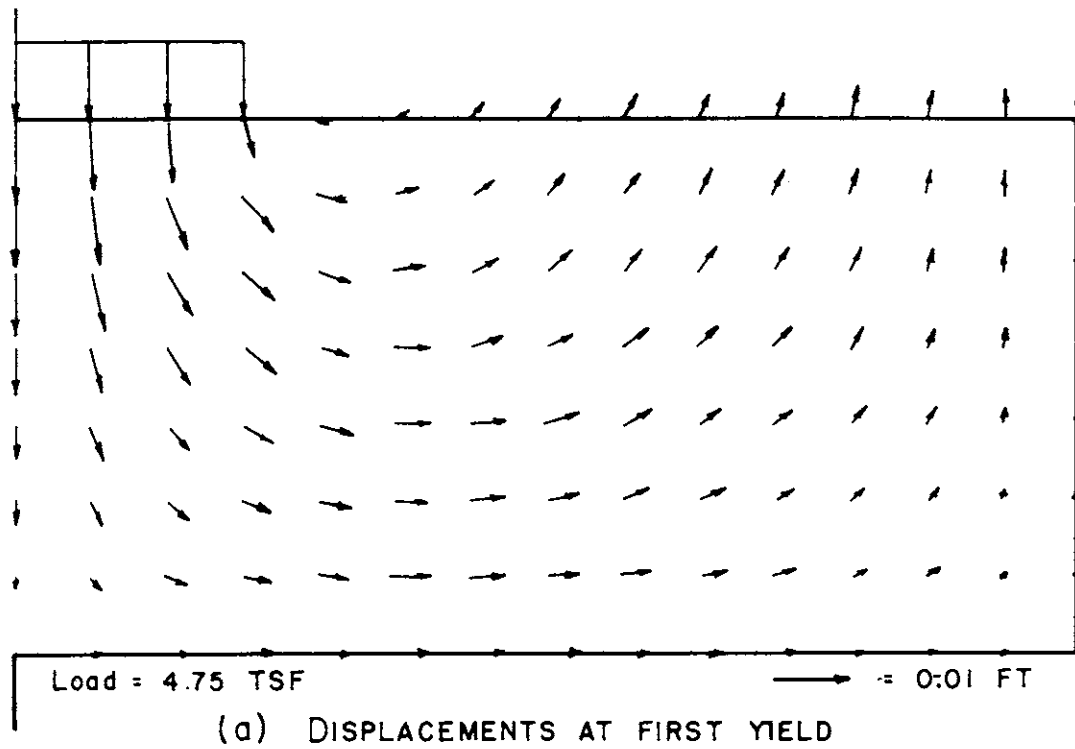


FIG. 50 INCREMENTAL DISPLACEMENTS - RUN 6

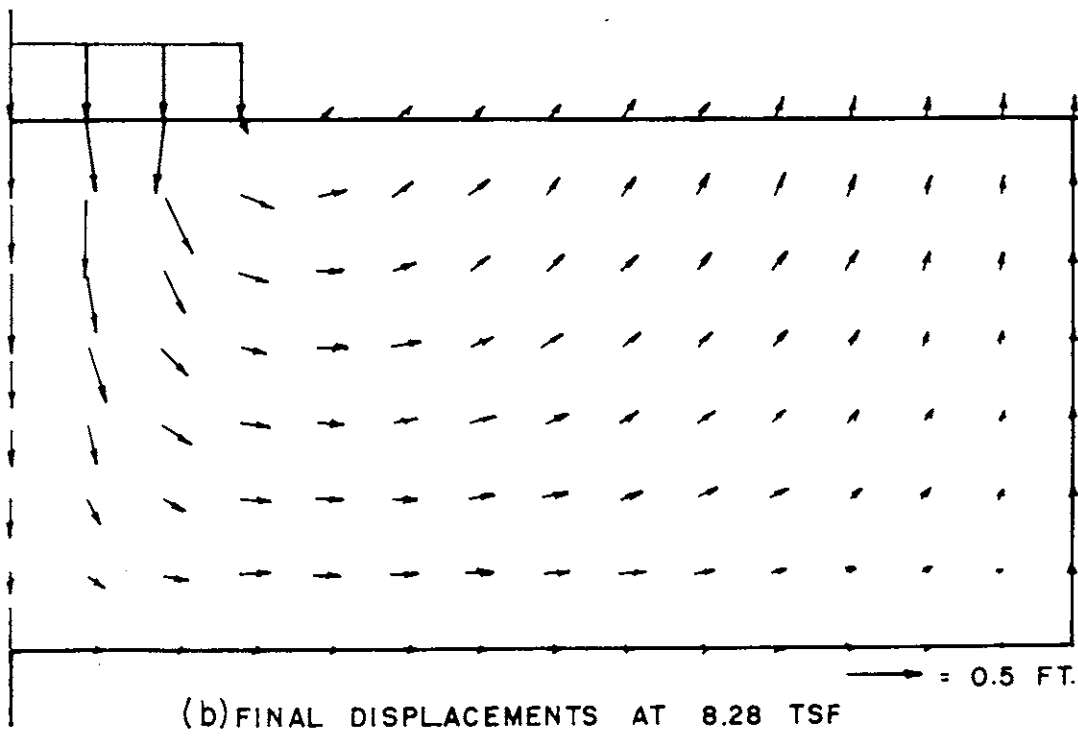
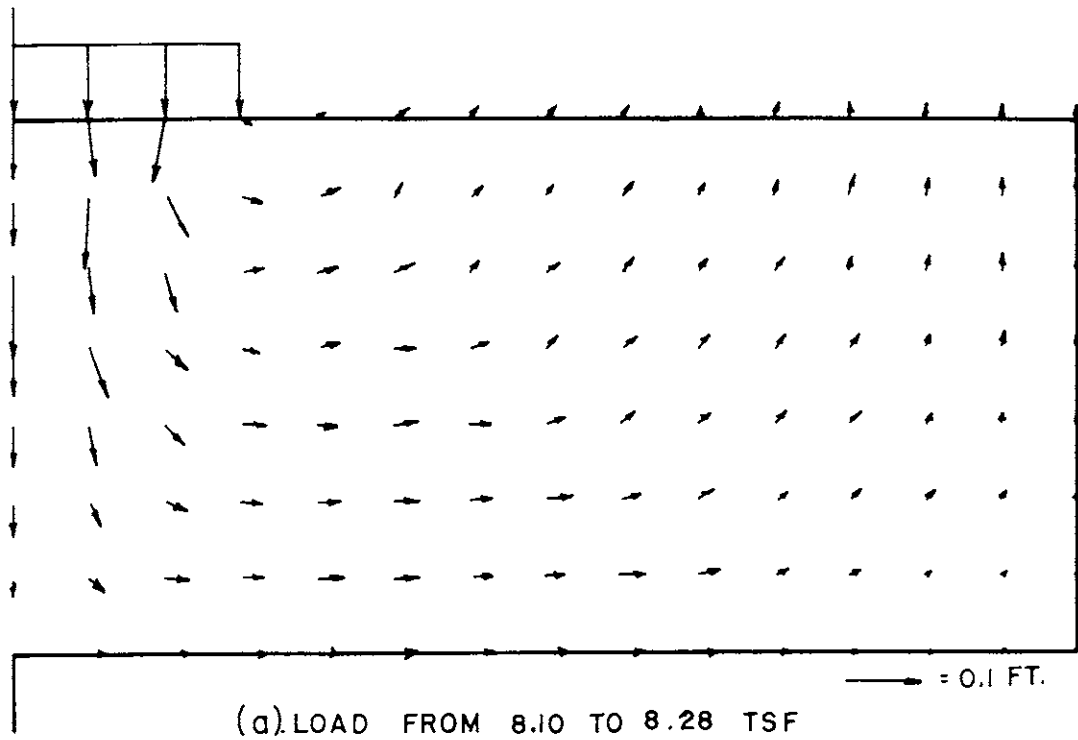


FIG. 51 INCREMENTAL DISPLACEMENTS - RUN 6



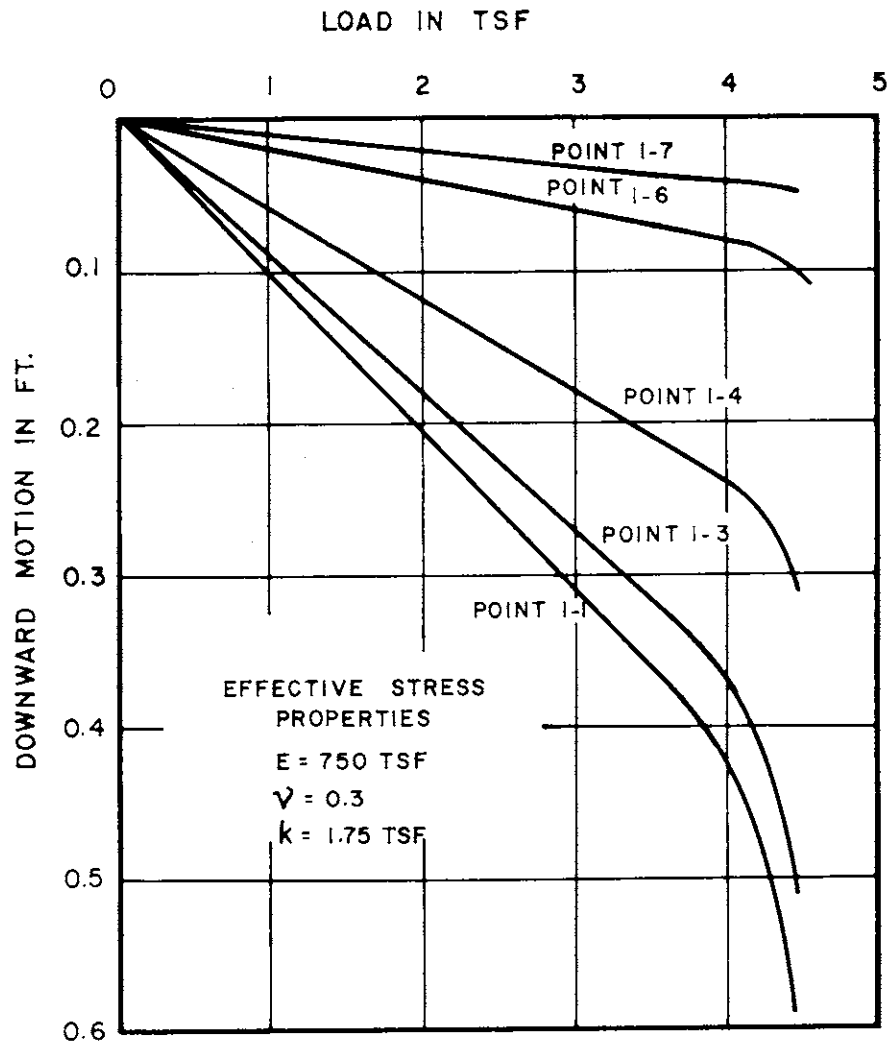


FIG. 52 DISPLACEMENTS IN RUN 7

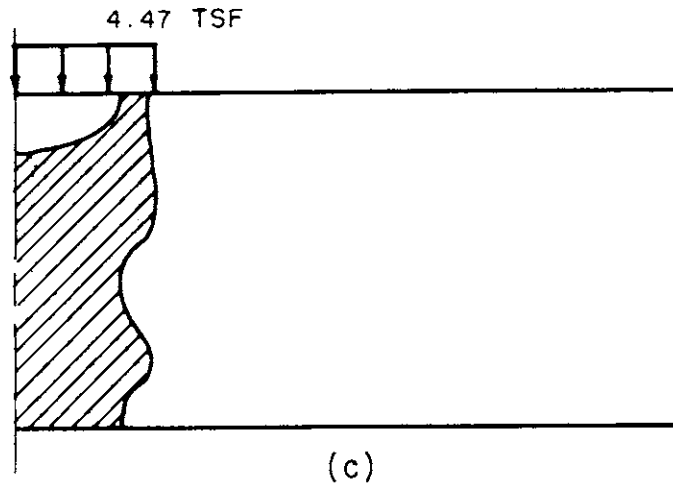
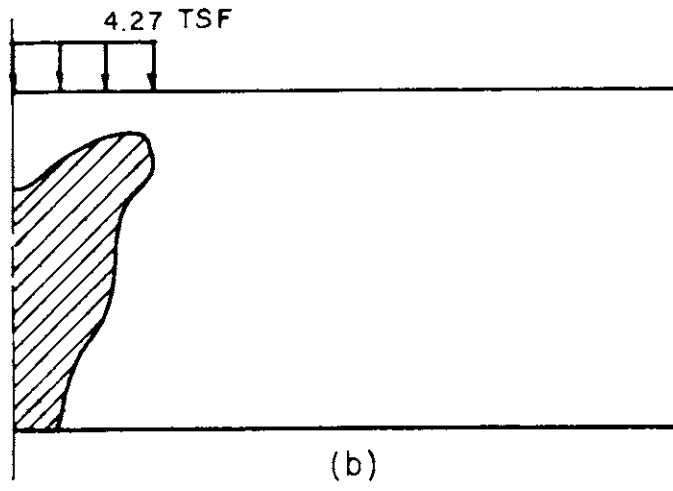
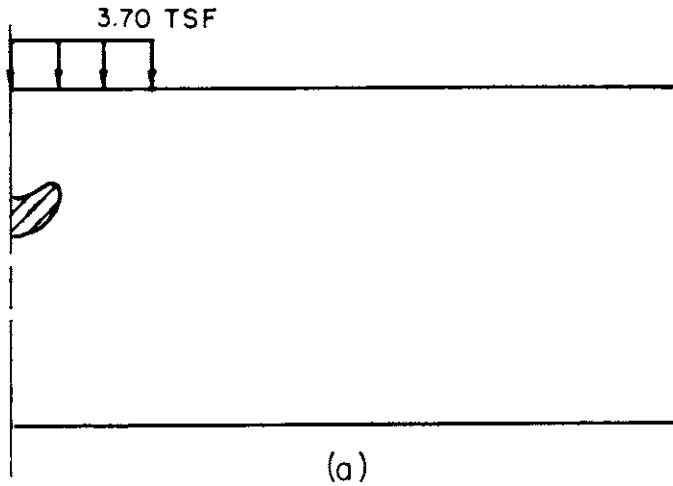



FIG.53 SPREAD OF PLASTIC ZONE - RUN 7



-98-01	-101-01	-84-14	-16-14	02 00	-02 00	01 01	-01 01	00 01	00 01	00 01	00 01	00 01	00 00
-44-71	-42-72	-27-56	01-07	15 09	16 07	15 08	12 06	10 05	07 03	05 02	02 01	01 01	00 00
-96-01	-93-11	-66-24	-34-24	-07-10	-03-01	-02-01	00 03	00 03	00 03	00 03	01 02	01 02	01 01
-16-56	-08-51	-03-35	-12-23	-07-07	02 00	04 01	05 02	05 02	04 02	03 01	02 01	01 01	00 01
-91-05	-79-15	-62-20	-39-19	-21-15	-07-06	-04 00	-02 02	00 04	00 03	01 04	01 03	02 02	02 01
03-44	03-38	-03-32	-03-21	-07-14	-06-07	-02-03	01-01	00 00	-01 00	-01 01	00 01	00 01	00 01
-81-05	-73-11	-59-16	-42-16	-26-12	-15-08	-07-02	-04 01	-01 02	00 03	01 03	02 03	03 02	04 01
11-35	07-33	05-27	-02-22	-03-15	-06-11	-06-06	-04-04	-03-02	-02-01	-01 00	00 01	00 01	00 02
-74-03	-68-08	-57-11	-43-11	-31-10	-19-06	-12-03	-06 00	-03 02	00 02	01 02	02 02	04 02	05 01
13-30	12-28	06-26	03-20	-03-17	-04-12	-05-09	-06-06	-04-03	-04-02	-02-01	-02 00	00 02	00 03
-69-02	-64-04	-55-06	-44-07	-32-06	-22-04	-14-02	-08-01	-03 00	-01 01	01 01	03 01	04 01	06 00
15-27	12-26	09-23	03-21	00-16	-04-13	-05-09	-06-07	-06-05	-04-03	-03-01	-02 00	-01 02	00 03
-67 00	-62-02	-55-02	-44-02	-34-02	-23-01	-15-01	-08-01	-04 00	-01 00	01 00	03 00	05 00	06 00
15-26	14-24	08-23	05-19	01-17	03-13	-06-10	-06-07	-06-05	-05-03	-03-01	-02 00	-01 02	-01 03

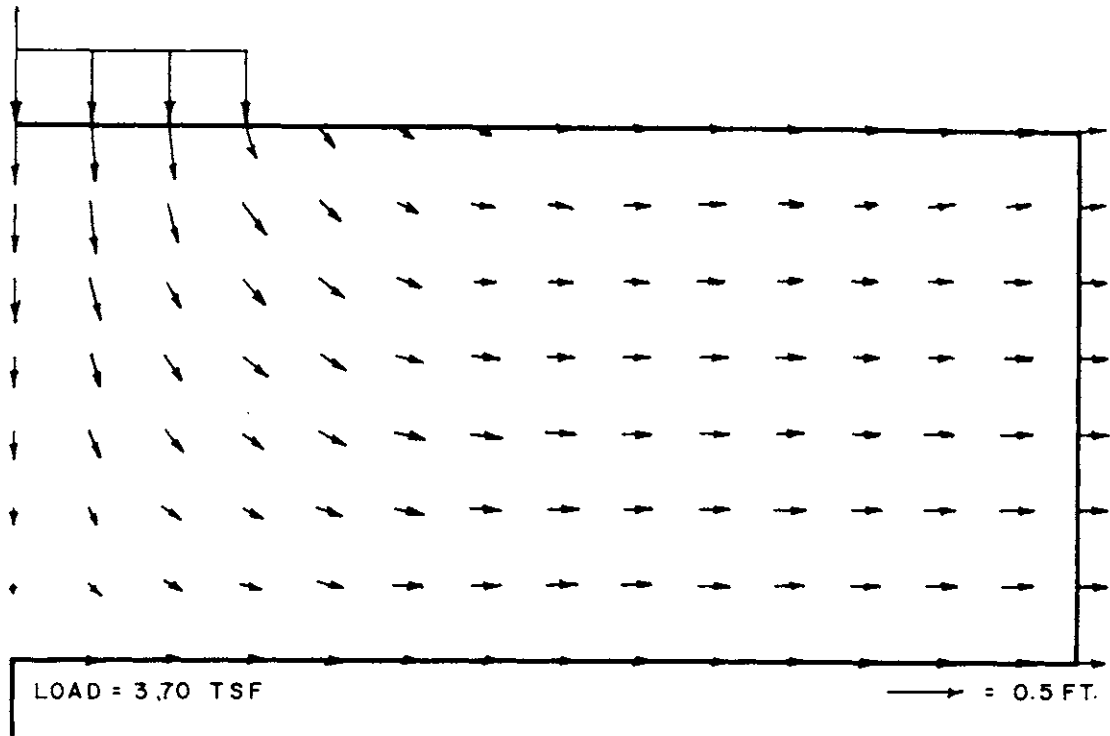
LOAD = 3.70 TSF

FIG. 54 NORMALIZED STRESSES - RUN 7

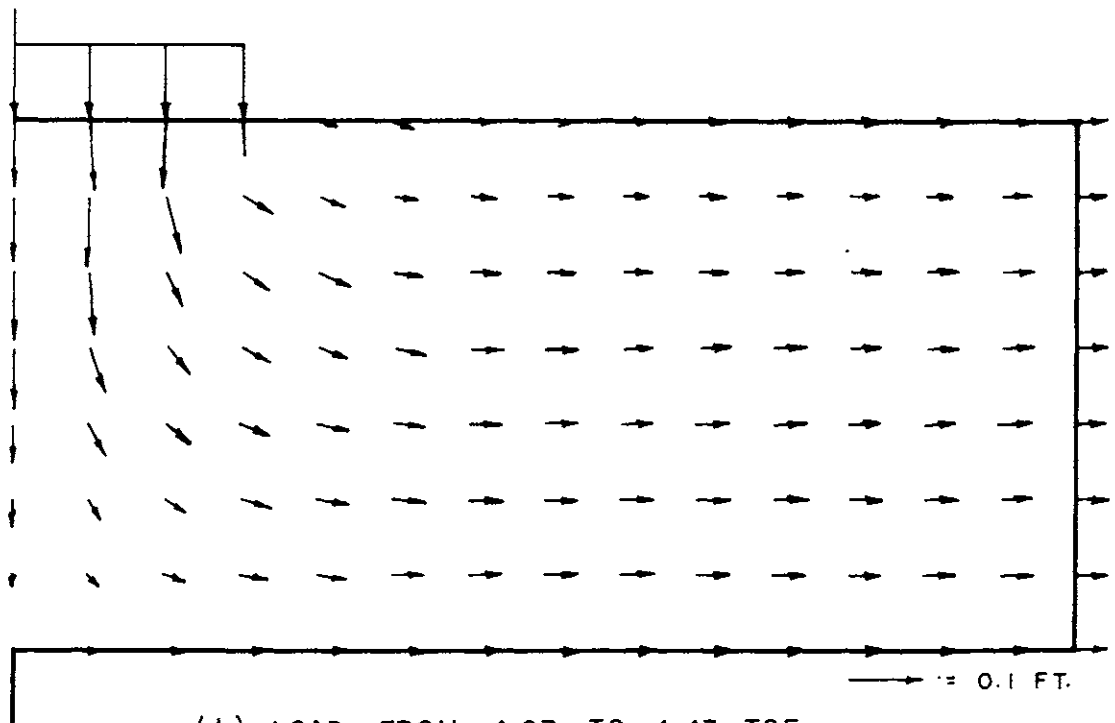
-98-02	-100-04	-87-16	-17-12	04 01	-03 00	02 02	-01 01	01 02	00 01	00 01	00 01	00 01	00 01	00 00
-43-70	-37-68	-17-52	11-03	21 13	20 08	18 10	15 07	11 06	08 04	05 03	03 01	01 01	00 00	
-95-01	-88-13	-74-26	-37-25	-05-08	-02 01	-02 01	00 04	00 03	01 04	00 03	01 03	01 02	01 01	
-17-56	-15-52	-16-45	-21-29	-08-06	03 01	05 02	06 03	05 02	04 02	03 02	02 01	01 01	00 01	
-87-07	-75-16	-68-22	-43-23	-21-17	-07-06	-04 01	-02 02	00 04	00 04	01 04	02 03	02 03	03 01	
-10-49	-03-39	-04-36	-05-24	-12-16	-08-07	-02-03	-01-01	01 00	01 00	01 01	00 01	00 01	00 01	
-73-07	-70-18	-65-20	-46-19	-29-15	-16-09	-07-03	-04 02	-01 03	00 04	01 04	02 03	03 02	04 01	
04-34	00-35	00-32	05-25	05-17	08-12	07-07	04-04	03-02	02-01	01 00	00 01	00 01	00 02	
-61-04	-62-12	-66-17	-48-15	-34-12	-21-08	-13-03	-06 00	-03 02	00 02	01 03	03 02	04 02	06 01	
16-23	12-25	04-31	02-23	-04-19	-05-13	-07-10	-07-06	-05-04	-04-02	-02 00	-02 00	00 02	00 03	
-55-03	-57-06	-62-09	-52-11	-36-08	-26-05	-15-02	-09-01	-03 01	-01 01	02 01	03 01	05 01	07 00	
23-16	20-19	14-24	03-24	01-18	-05-15	-06-11	-07-08	-07-05	-05-03	-04-01	-02 01	-01 02	00 04	
-52 00	-55-02	-61-02	-51-02	-40-03	-26-01	-17-02	-09 00	-04 01	-01 00	02 00	03 00	05 00	07 00	
26-13	23-16	17-22	11-20	-01-20	-03-15	-07-12	-07-08	-07-05	-06-03	-04-01	-03 00	-01 02	-01 03	

LOAD = 4.47 TSF

FIG. 55 NORMALIZED STRESSES - RUN 7



(a) DISPLACEMENTS AT FIRST YIELD



(b) LOAD FROM 4.27 TO 4.47 TSF

FIG. 56 INCREMENTAL DISPLACEMENTS RUN 7

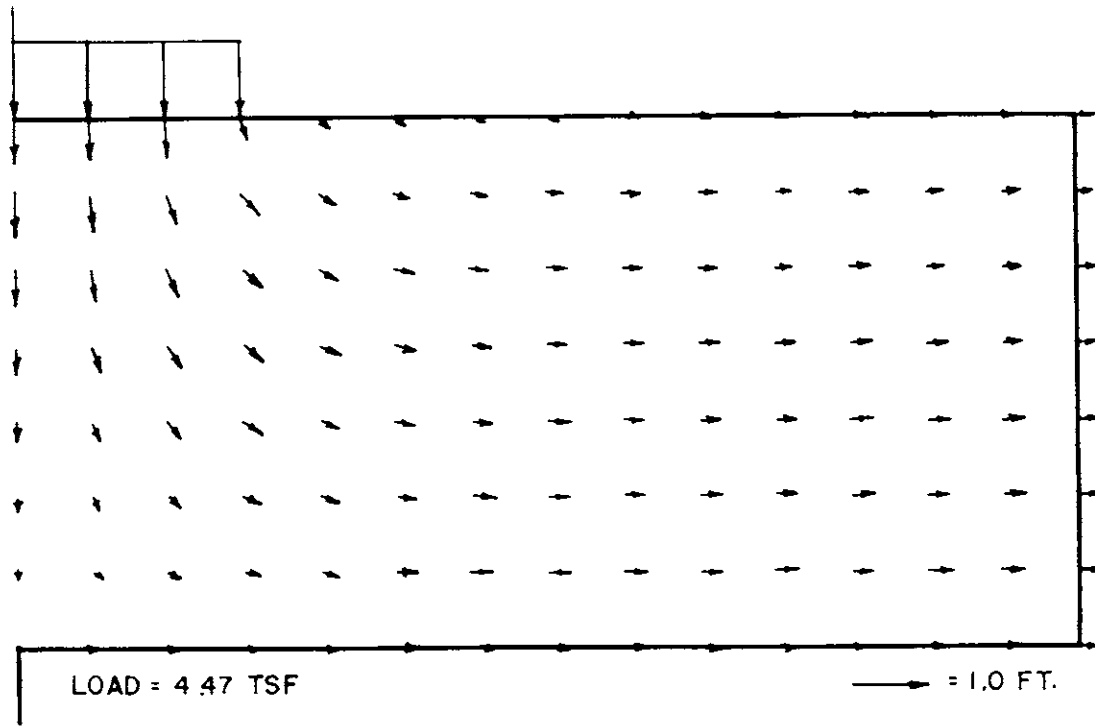


FIG. 57 FINAL DISPLACEMENTS - RUN 7

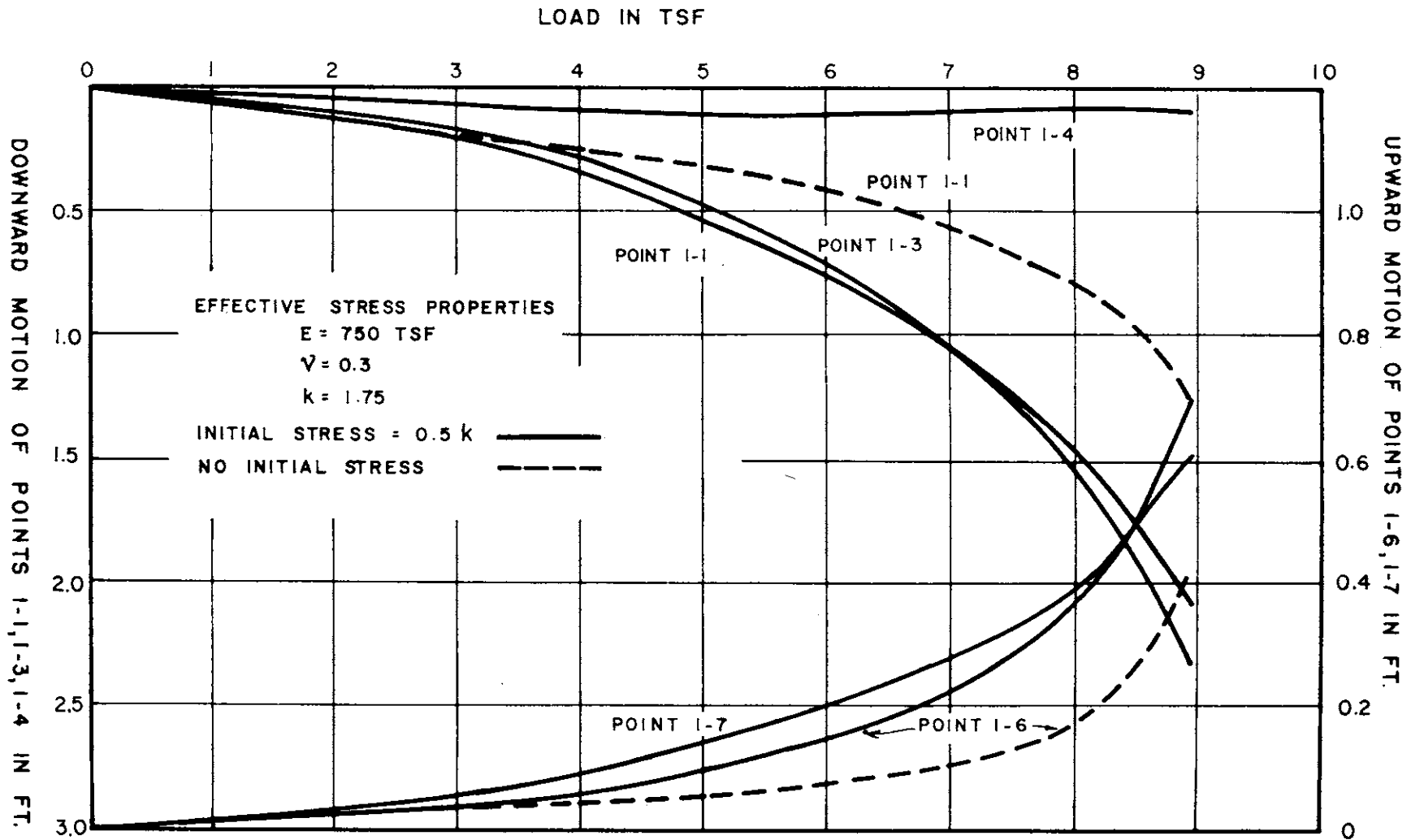


FIG. 58 DISPLACEMENTS IN RUNS 5 AND 8

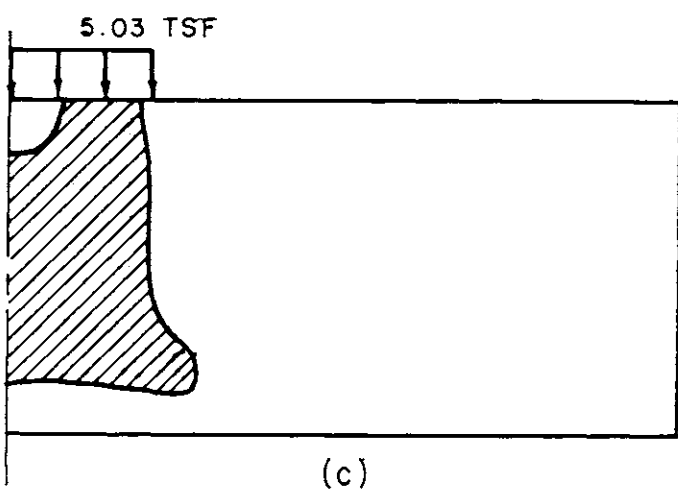
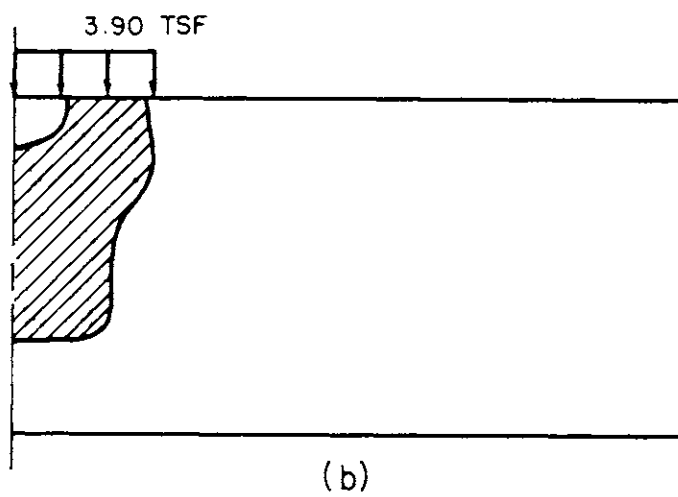
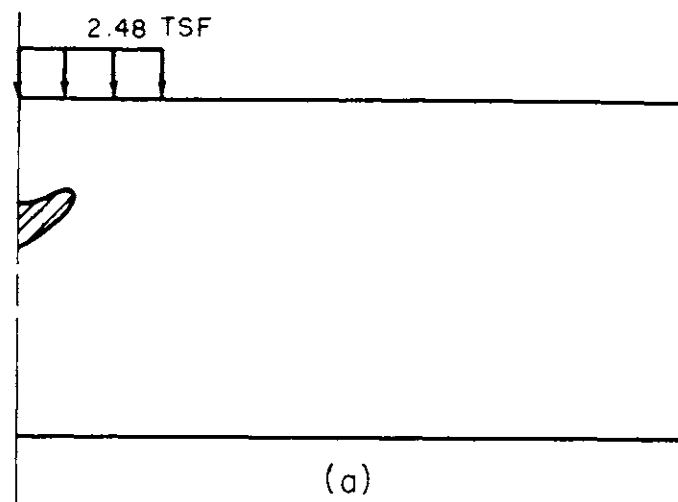


FIG. 59 SPREAD OF PLASTIC ZONE - RUN 8



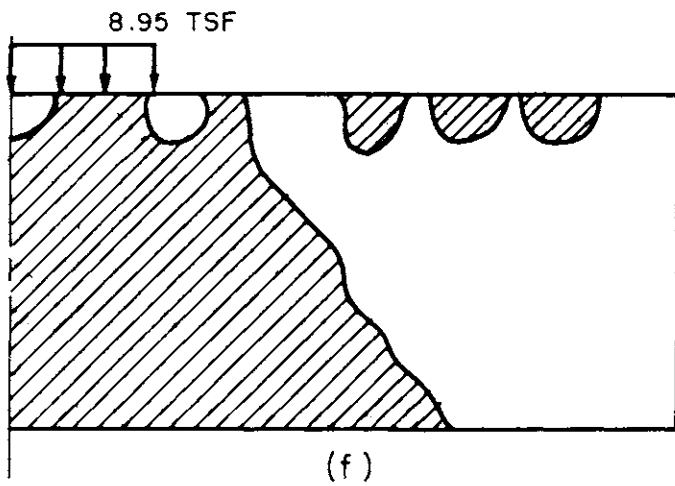
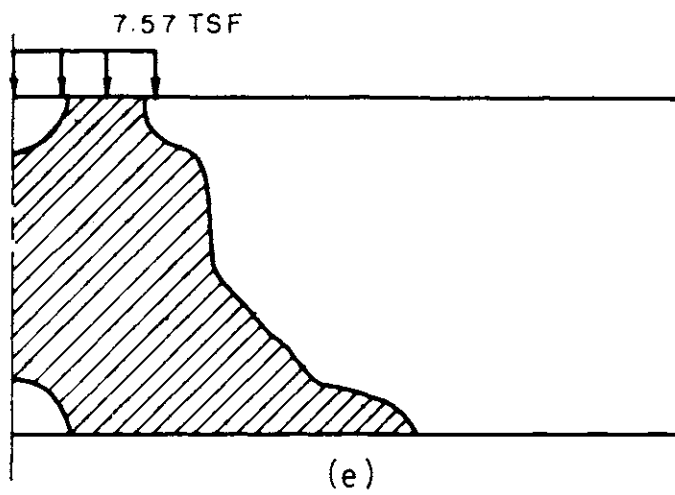
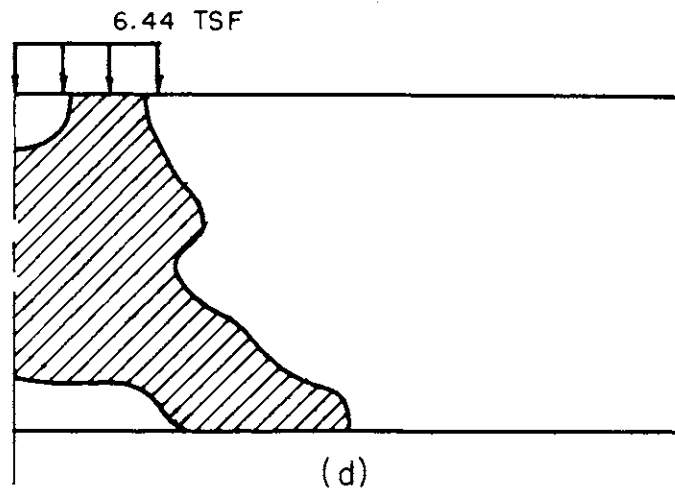


FIG.59 SPREAD OF PLASTIC ZONE - RUN 8

-98-02	-104-00	-81-16	-22-13	07-02	-05-00	03-02	-02-01	01-01	-01-01	01-01	01-01	00-00	00-00	00-00
-72-85	-69-87	-53-67	-25-24	-15-04	-17-11	-19-08	-22-12	-23-11	-25-13	-27-13	-27-14	-28-14	-28-14	-28-14
-98-03	-90-12	-67-25	-39-25	-05-10	-01-01	-02-00	01-03	-01-01	01-02	00-01	01-01	00-00	01-00	01-00
-64-81	-60-75	-54-61	-60-50	-46-26	-33-17	-30-16	-27-13	-27-14	-26-13	-26-13	-26-15	-26-13	-26-13	-26-13
-92-09	-73-17	-65-24	-42-24	-22-19	-05-09	-03-02	-01-02	00-01	00-00	01-01	00-00	01-00	00-00	00-00
-60-76	-47-60	-49-57	-44-43	-50-36	-44-25	-35-19	-32-17	-29-14	-27-14	-25-12	-25-12	-24-11	-24-12	-24-12
-74-09	-70-12	-59-24	-47-24	-27-19	-16-15	-06-08	-03-04	-01-03	00-01	00-02	01-01	00-01	01-00	01-00
-42-58	-50-60	-43-51	-48-48	-43-35	-42-29	-38-22	-32-18	-30-15	-26-13	-24-12	-22-11	-22-11	-21-10	-21-10
-62-04	-59-15	-58-25	-48-24	-33-22	-19-17	-12-12	-05-09	-03-06	-01-05	00-03	00-03	00-01	00-01	00-01
-27-44	-30-44	-44-51	-38-43	-41-37	-37-28	-35-24	-32-18	-27-15	-24-12	-21-10	-20-10	-17-09	-18-09	-18-09
-53-05	-52-09	-48-16	-50-24	-35-22	-26-19	-14-15	-09-13	-04-10	-02-08	-02-06	-01-04	-01-02	-01-01	-01-01
-18-35	-20-36	-21-34	-35-43	-32-34	-34-30	-31-22	-26-17	-23-14	-18-10	-17-09	-14-07	-13-07	-12-06	-12-06
-46-02	-46-10	-44-13	-41-18	-40-24	-26-22	-19-21	-11-17	-07-14	-05-10	-04-08	-04-05	-03-03	-03-01	-03-01
-34-40	-35-41	-36-40	-30-36	-36-38	-29-28	-24-21	-19-16	-14-11	-12-09	-09-06	-08-06	-07-05	-07-05	-07-05

LOAD = 5.03 TSF

FIG. 60 NORMALIZED STRESSES - RUN 8

227

-100-00	-102-01	-88-10	-16-07	06-03	-02-01	00-01	01-01	-01-00	00-00	00-00	00-00	00-00	00-00	01-01
-81-91	-82-92	-73-80	-56-36	-53-23	-55-28	-56-28	-58-28	-58-29	-58-29	-58-29	-58-29	-58-29	-58-29	-67-28
-102-02	-94-06	-73-17	-33-17	-01-04	01-04	01-00	01-01	01-00	-01-01	01-00	-01-00	01-01	00-01	00-01
-82-92	-76-85	-71-72	-72-52	-59-30	-55-27	-58-30	-56-27	-56-27	-56-28	-54-27	-53-27	-53-26	-53-27	
-98-05	-84-12	-67-18	-37-19	-18-12	-01-01	02-03	01-02	01-01	00-02	00-01	01-01	00-01	01-01	
-80-99	-72-78	-69-68	-66-52	-69-43	-60-31	-55-26	-56-27	-51-25	-56-25	-49-25	-48-23	-47-24	-46-23	
-87-06	-80-15	-60-19	-43-19	-23-15	-11-10	03-04	03-02	00-04	00-02	00-03	00-03	00-02	-01-01	
-69-78	-73-77	-72-66	-74-59	-69-46	-65-38	-55-26	-47-22	-48-24	-45-23	-43-22	-42-21	-40-20	-40-20	
-78-03	-70-12	-59-18	-43-20	-29-18	-14-15	-04-12	04-07	00-05	01-06	00-05	-01-05	-02-03	-02-01	
-59-68	-60-65	-64-62	-62-52	-63-46	-58-36	-54-29	-50-23	-43-22	-41-20	-37-19	-34-17	-33-17	-32-17	
-70-06	-64-10	-54-16	-44-19	-29-19	-18-18	-06-14	-01-12	02-12	01-11	-01-10	-03-07	-04-04	-04-02	
-52-61	-50-57	-51-52	-55-50	-53-41	-54-36	-54-30	-51-26	-44-21	-33-17	-28-15	-25-14	-23-14	-23-14	
-62-02	-58-12	-51-15	-41-18	-30-20	-19-19	-10-19	01-19	01-20	03-18	-05-12	06-08	07-05	07-02	
-43-52	-46-52	-45-48	-43-42	-47-29	-44-31	-38-24	-28-14	-21-10	-19-11	-15-10	-14-10	-14-10	-13-10	

LOAD = 8.95 TSF

FIG. 61 NORMALIZED STRESSES - RUN 8

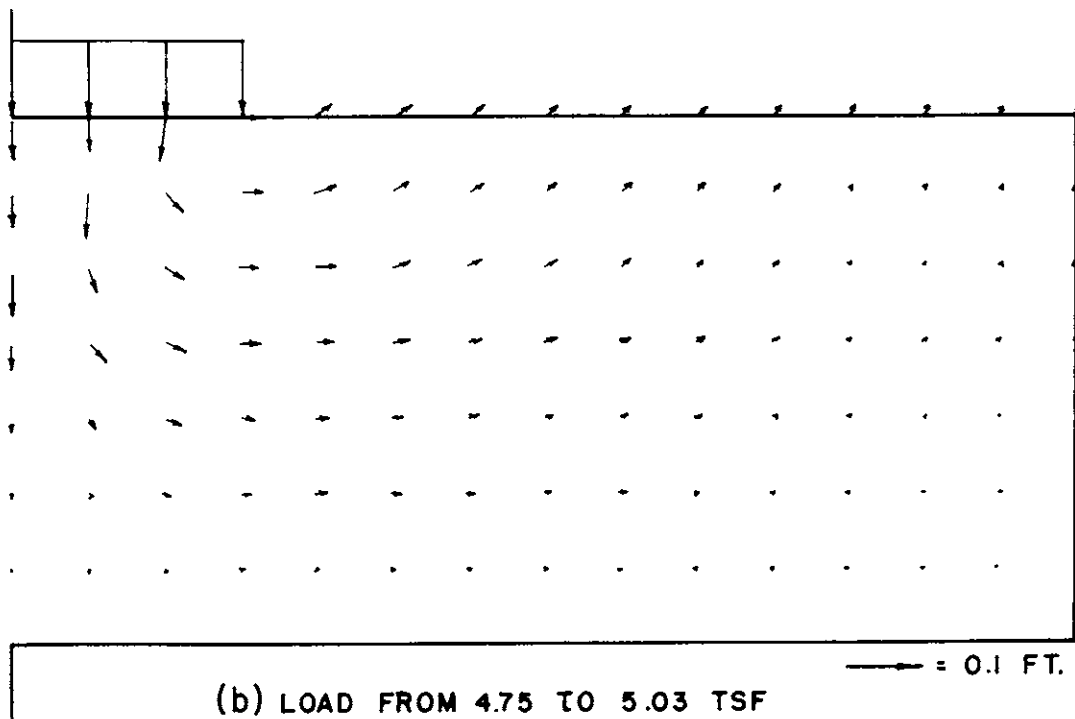
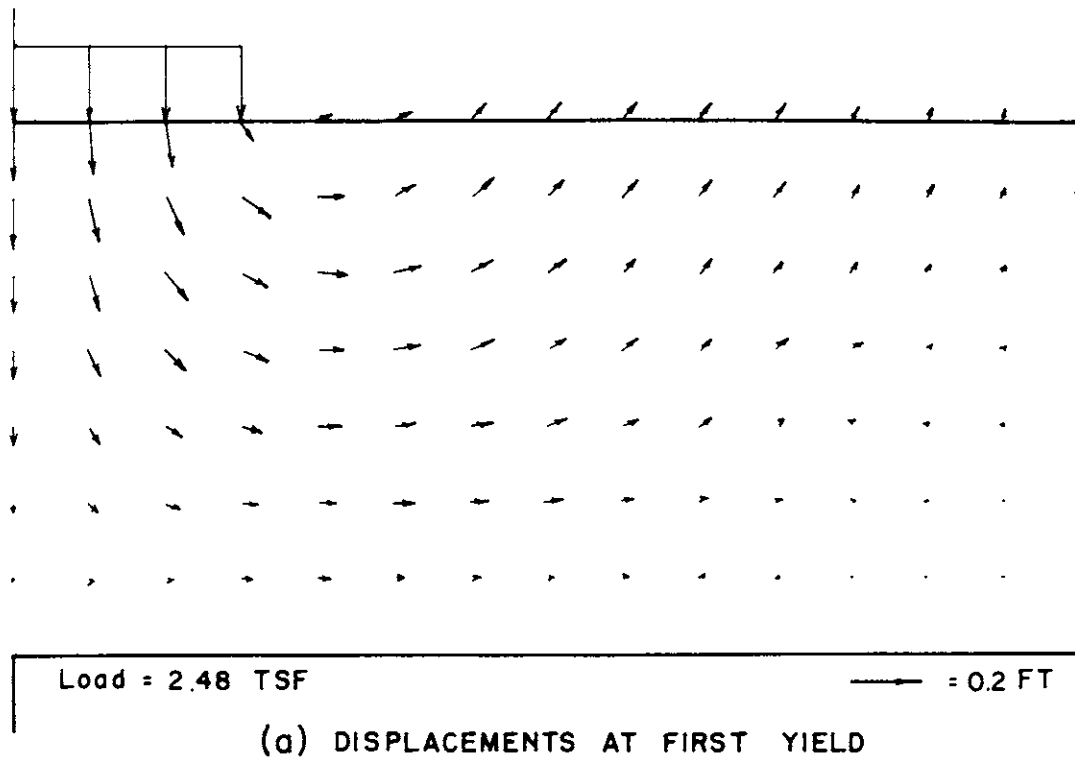


FIG. 62 INCREMENTAL DISPLACEMENTS - RUN 8

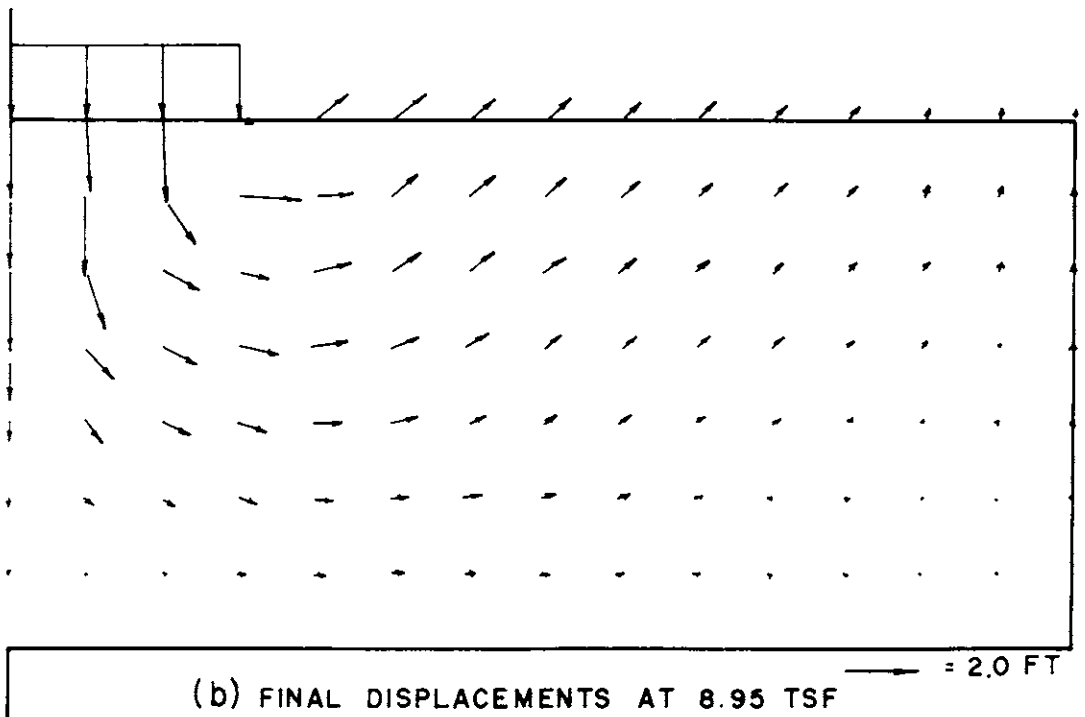
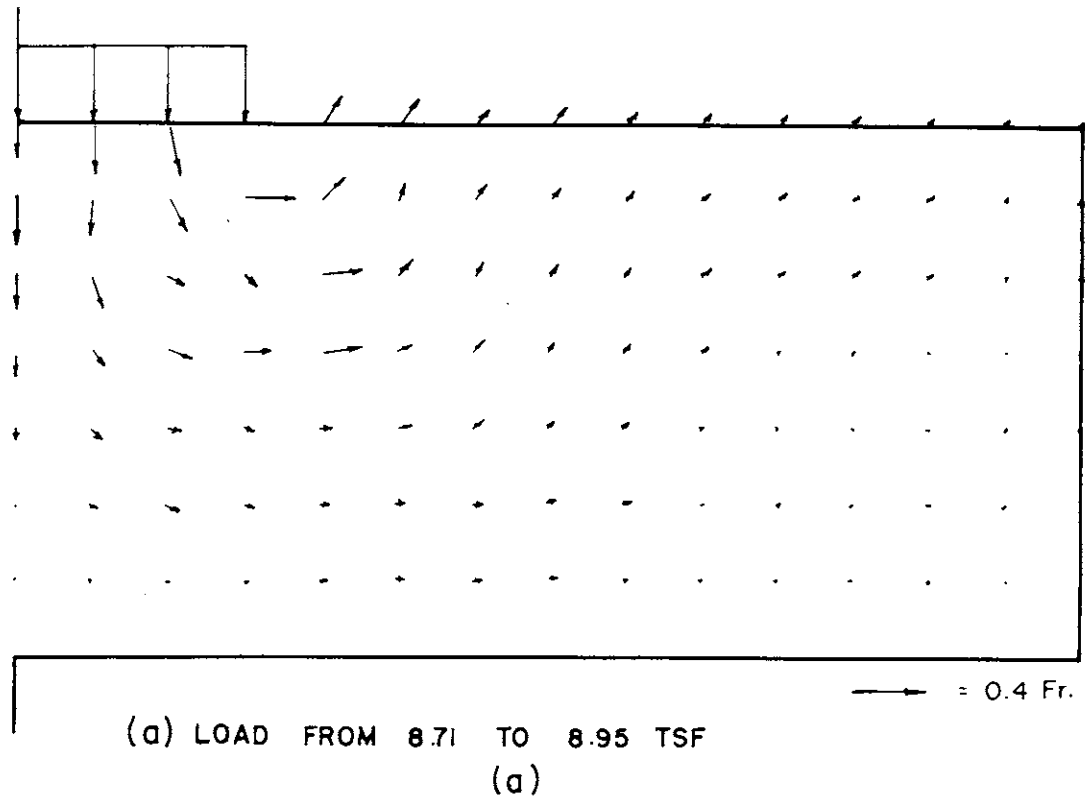


FIG. 63 INCREMENTAL DISPLACEMENTS - RUN 8

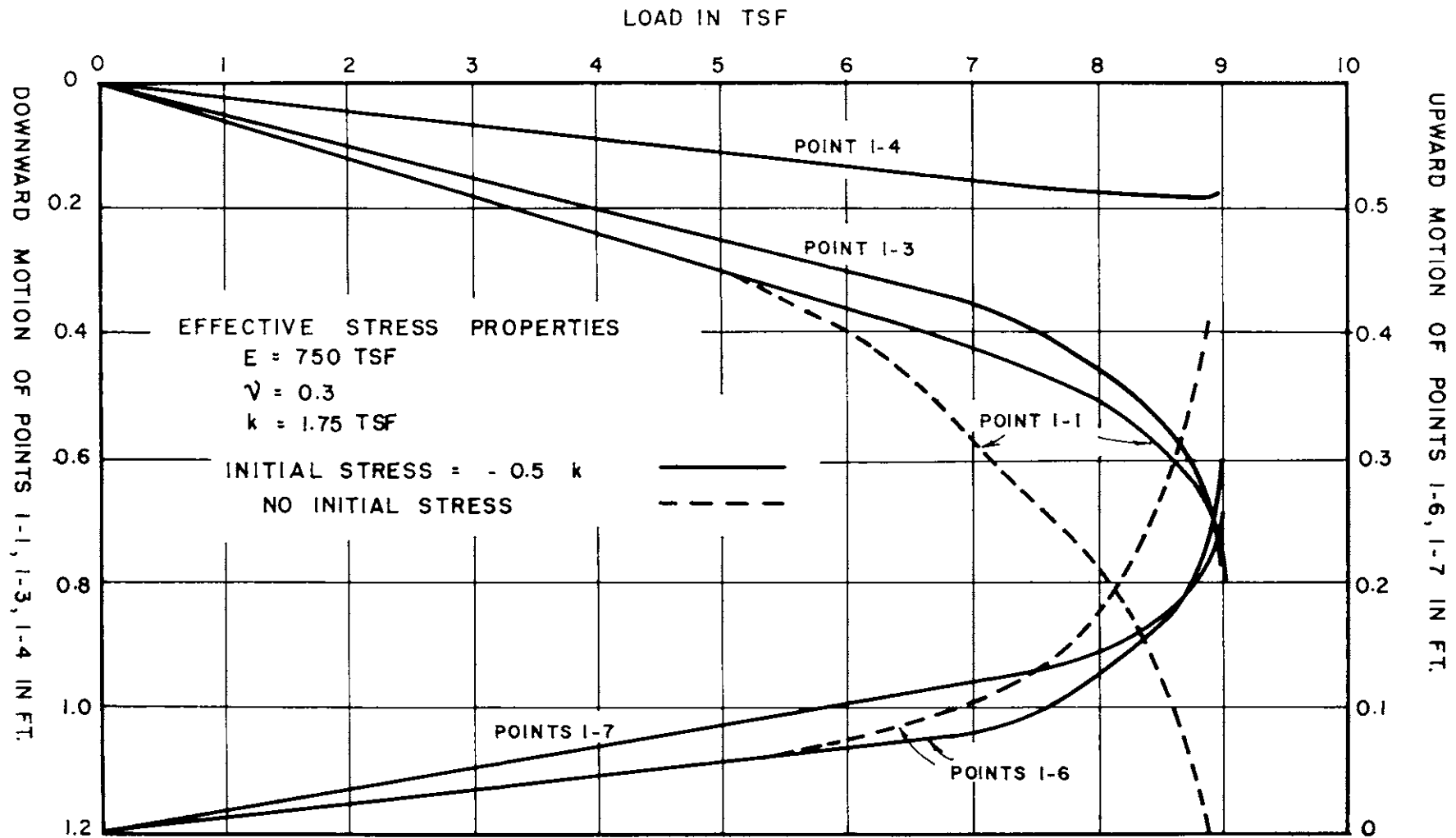


FIG. 64 DISPLACEMENTS IN RUNS 5 AND 10

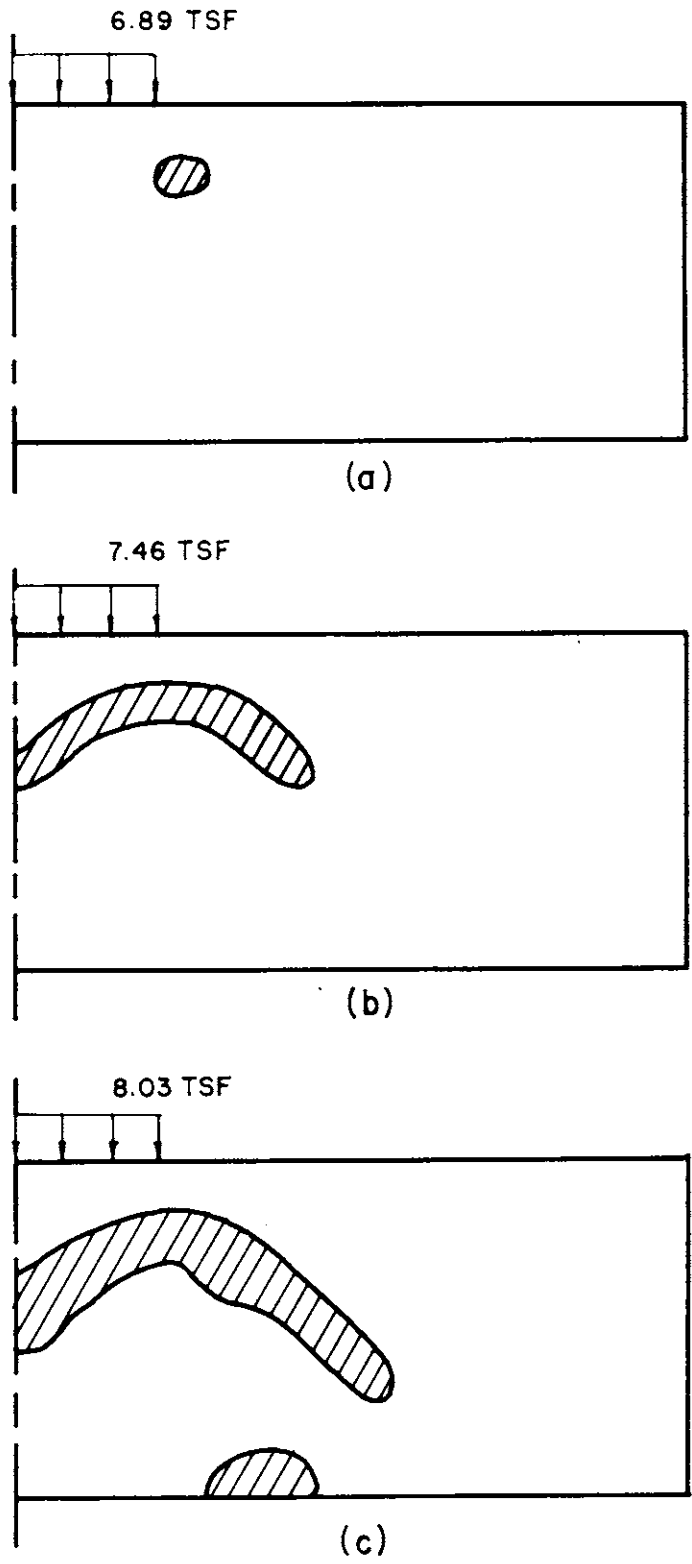


FIG. 65 SPREAD OF PLASTIC ZONE - RUN 10

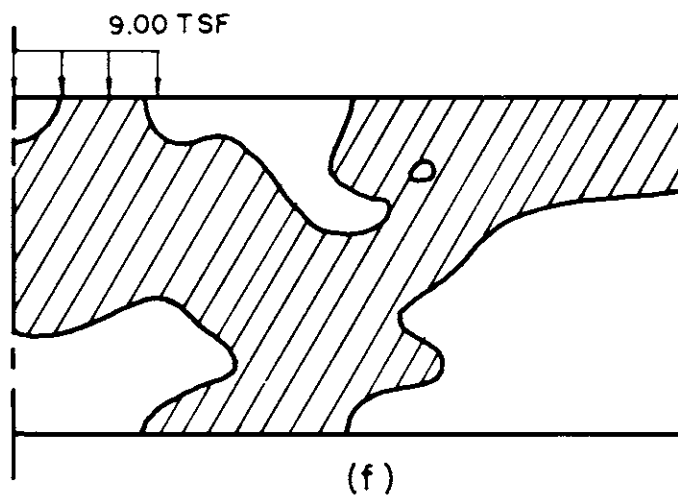
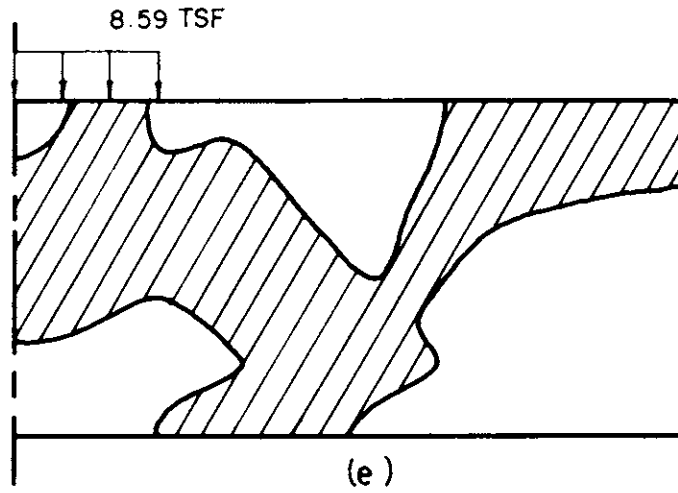
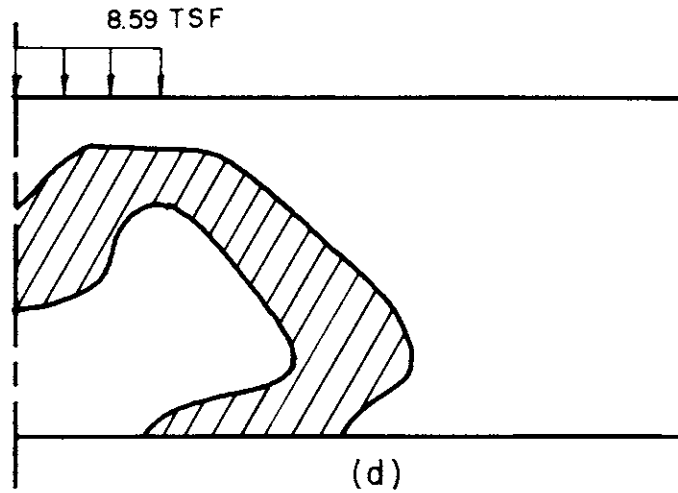
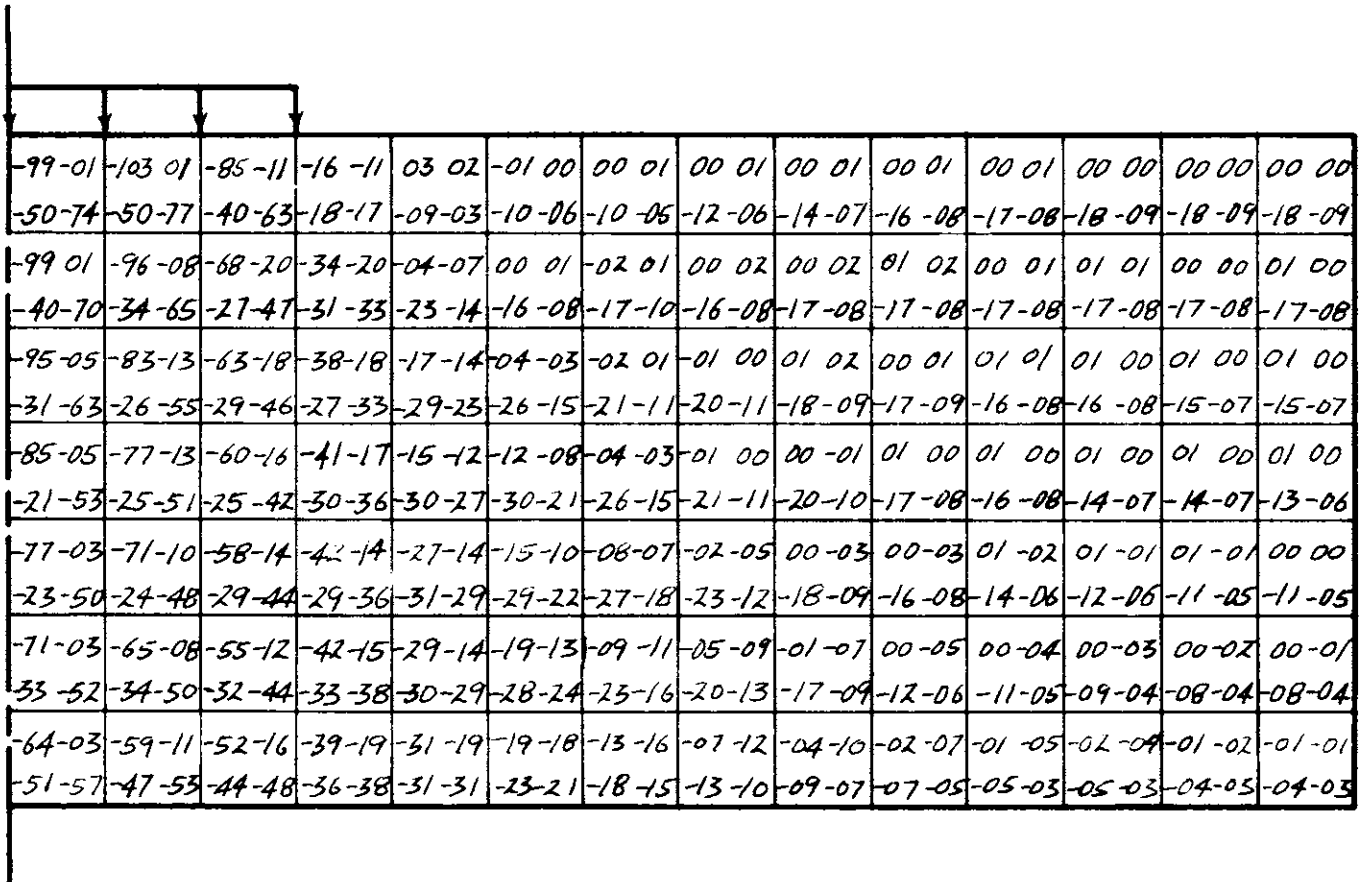


FIG. 65 SPREAD OF PLASTIC ZONE - RUN 10



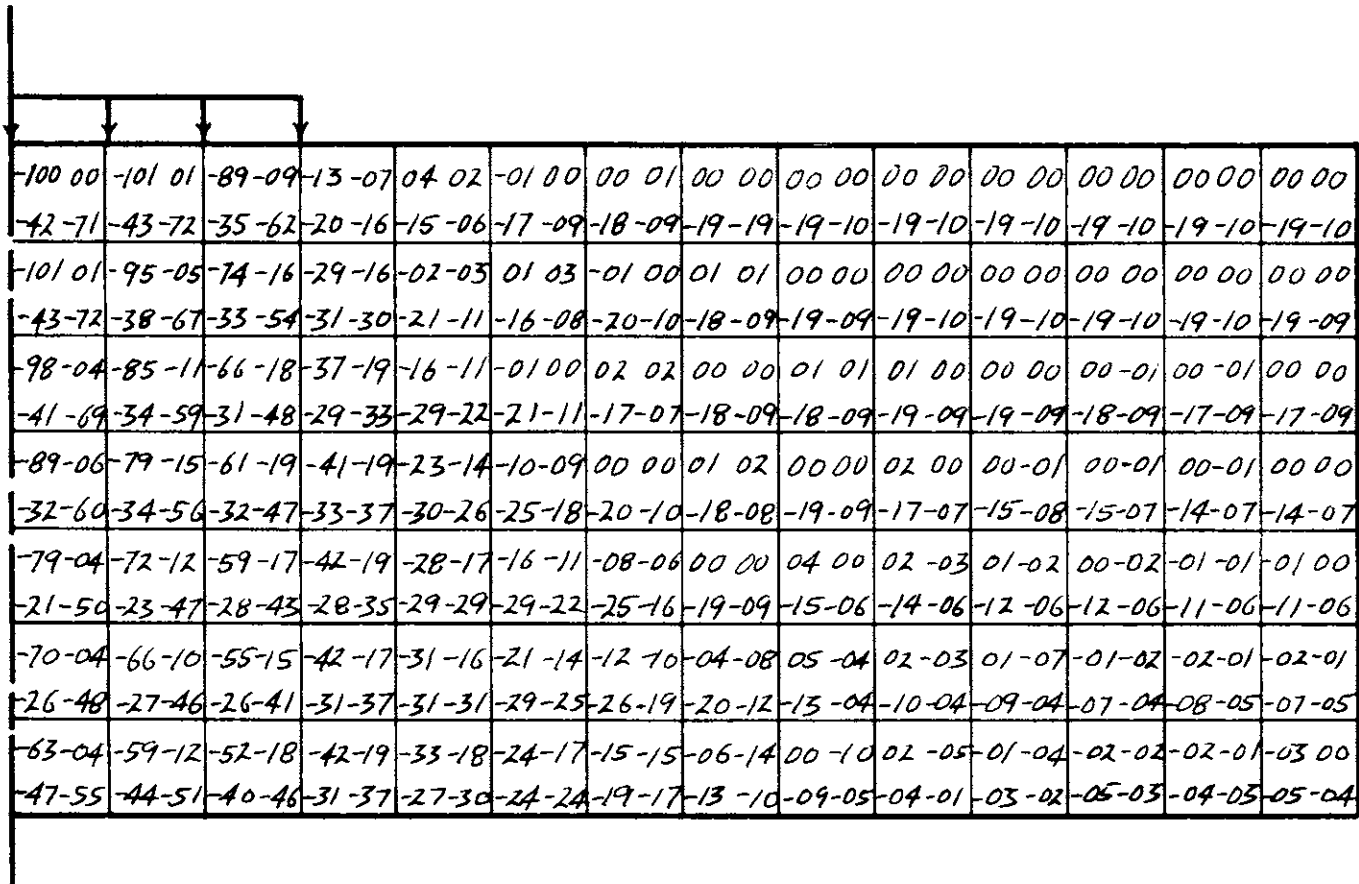
233



LOAD = 8.03 TSF

FIG. 66 NORMALIZED STRESSES - RUN 10

234



LOAD = 9.00 TSF

FIG. 67 NORMALIZED STRESSES - RUN 10

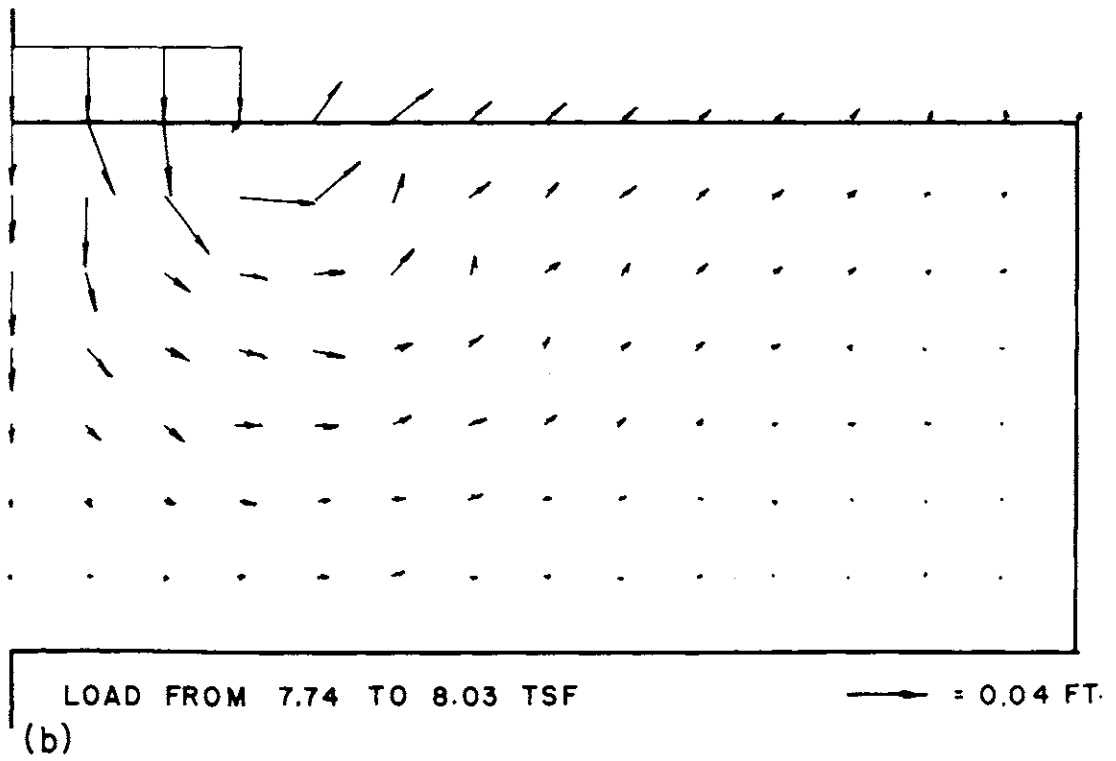
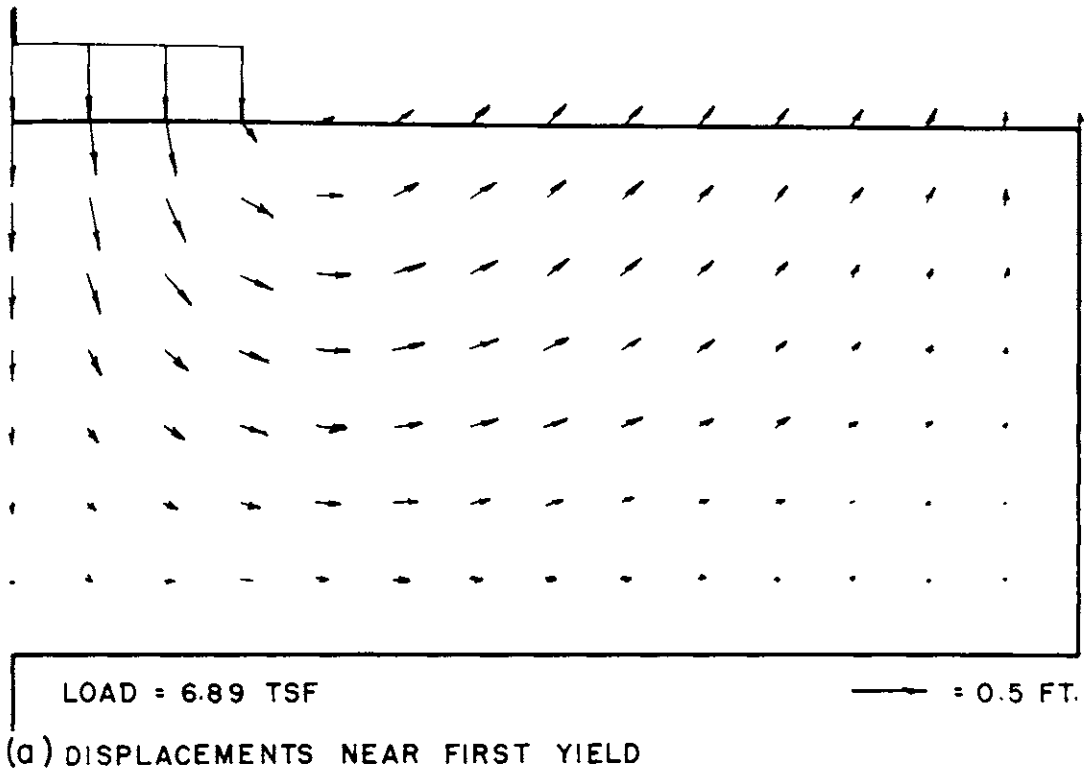


FIG. 68 INCREMENTAL DISPLACEMENTS - RUN 10

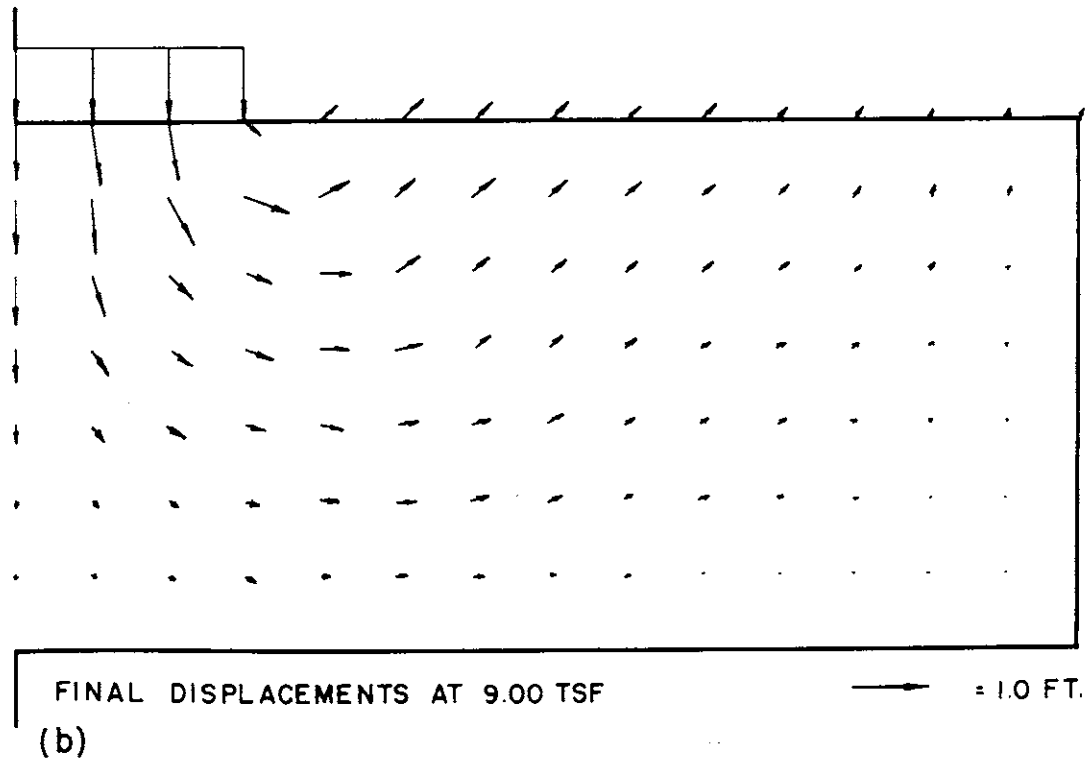
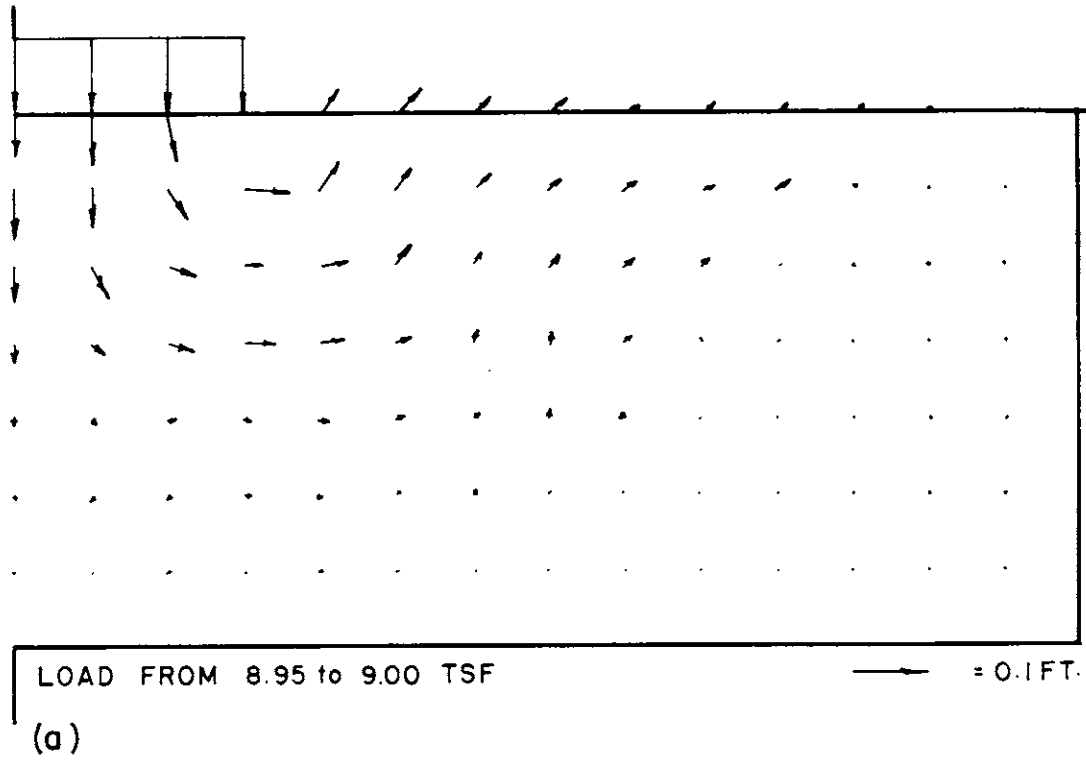


FIG. 69 INCREMENTAL DISPLACEMENTS - RUN 10

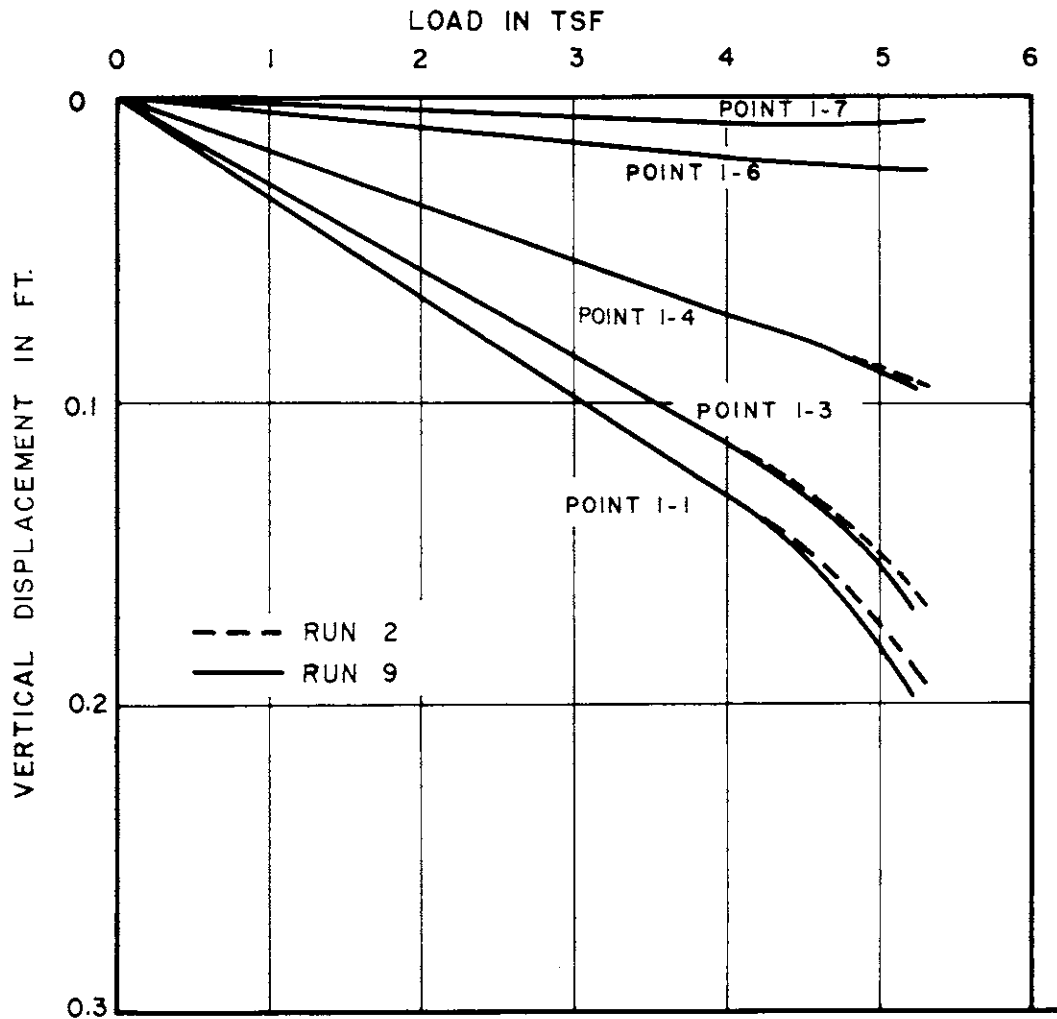


FIG.70 COMPARISON OF TRESCA AND PRANDTL-REUSS DISPLACEMENTS

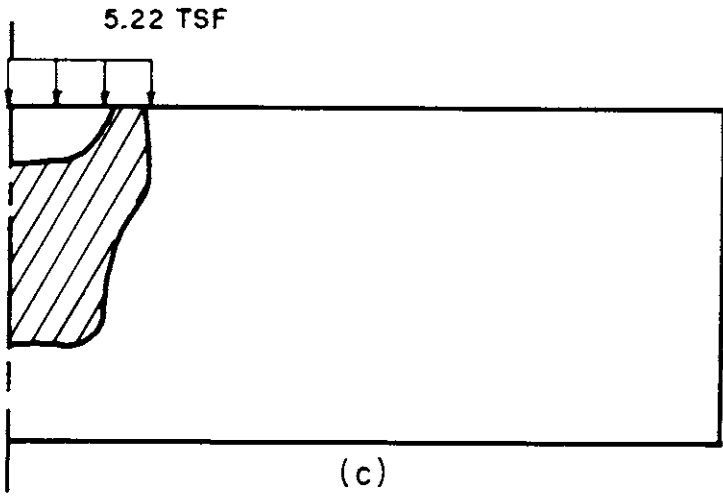
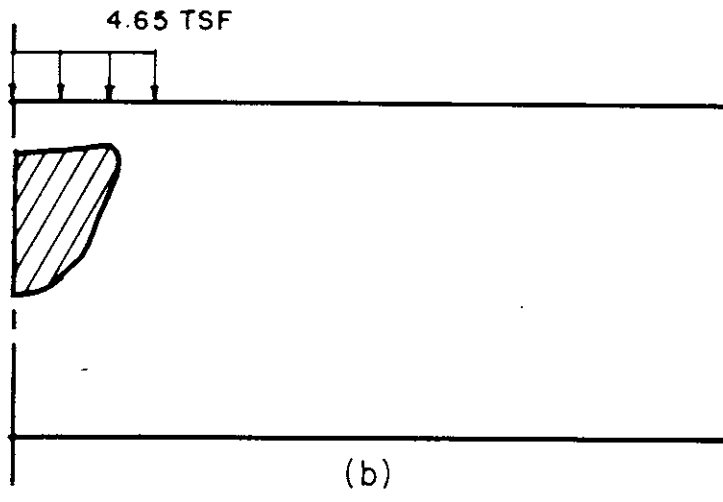
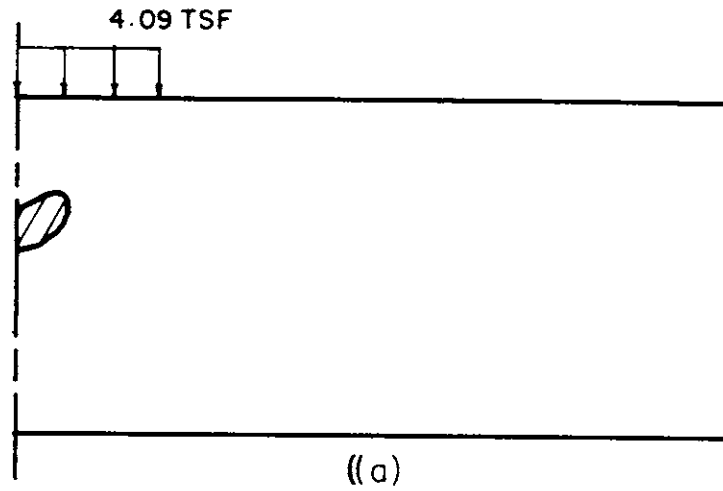


FIG. 71 SPREAD OF PLASTIC ZONE - RUN 9

239

-98-02	-101-03	-87-14	-16-11	04 01	-03 00	01 01	-01 01	01 01	00 01	00 01	00 00	00 00	00 00	00 00	00 00
-51	-46	-29	-04	06	05	04	02	00	-01	-02	-03	-04	-04	-05	
-96 00	-91-11	-73-24	-33-23	-05-09	-02 00	-01 00	00 02	00 01	01 02	00 01	01 01	00 00	01 00	00 00	
-33	-30	-29	-32	-20	-09	-07	-05	-04	-04	-04	-04	-04	-04	-05	
-89-06	-78-14	-67-21	-39-23	-19-17	-06-07	-03-02	-01-01	00 01	00 01	01 01	00 01	01 01	00 00	01 00	
-26	-20	-21	-20	-24	-19	-13	-11	-08	-07	-06	-05	-05	-05	-04	
-77-07	-74-16	-61-20	-43-21	-25-17	-14-12	-06-06	-03-03	-01-02	00 00	00 00	01 00	01 00	01 00	00 00	
-13	-16	-15	-20	-19	-19	-17	-13	-11	-08	-07	-06	-05	-05	-04	
-67-03	-66-12	-58-17	-44-18	-30-17	-18-12	-11-09	-05-06	-02-04	-01-03	00-02	00-01	01-01	00 00	01 00	
-01	-04	-12	-14	-18	-17	-16	-14	-11	-09	-07	-06	-05	-04	-04	
-61-03	-59-07	-54-13	-44-16	-32-15	-22-14	-13-11	-08-08	-04-06	-02-04	-01-03	00-02	00-01	00-01	00 00	
-07	-08	-09	-14	-14	-15	-13	-11	-09	-07	-06	-04	-04	-03	-03	
-56-02	-54-07	-50-11	-42-15	-33-16	-23-15	-16-13	-10-10	-06-08	-04-06	-02-04	-01-03	-01-02	-01-01	00 00	
-18	-17	-17	-14	-15	-12	-10	-07	-05	-04	-03	-02	-02	-01	-01	

LOAD = 5.22 TSF

FIG. 72 NORMALIZED STRESSES - RUN 9

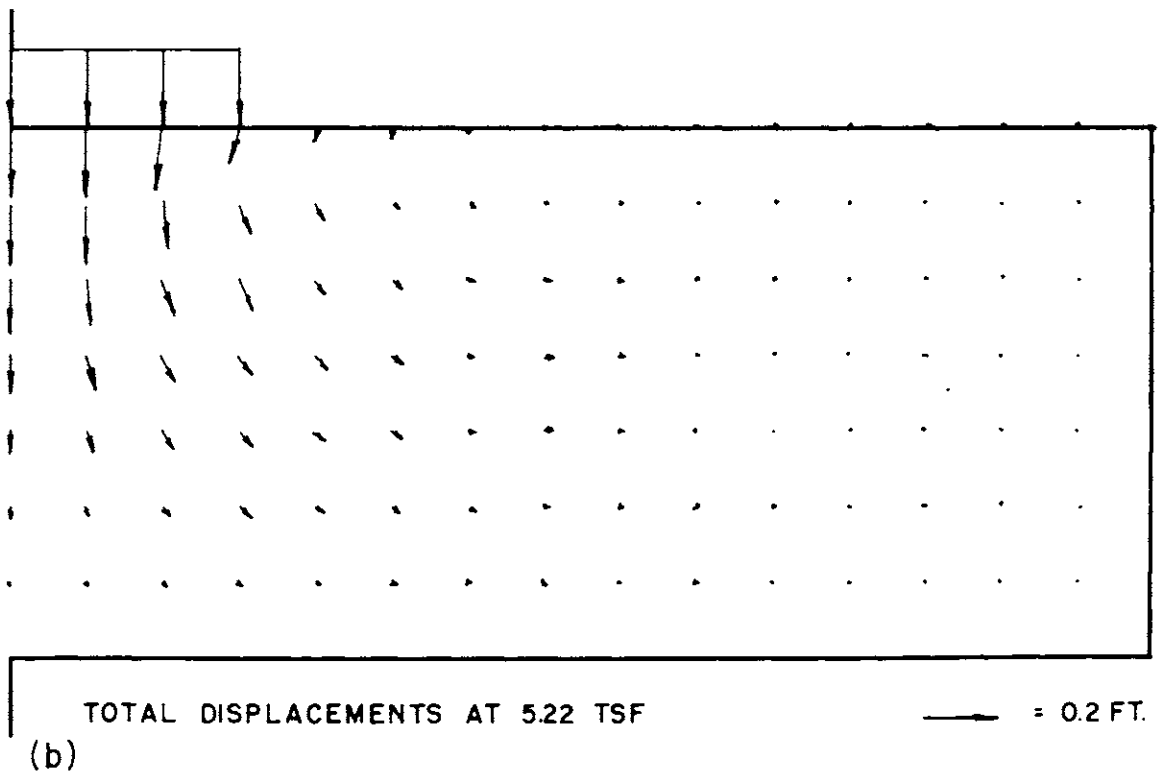
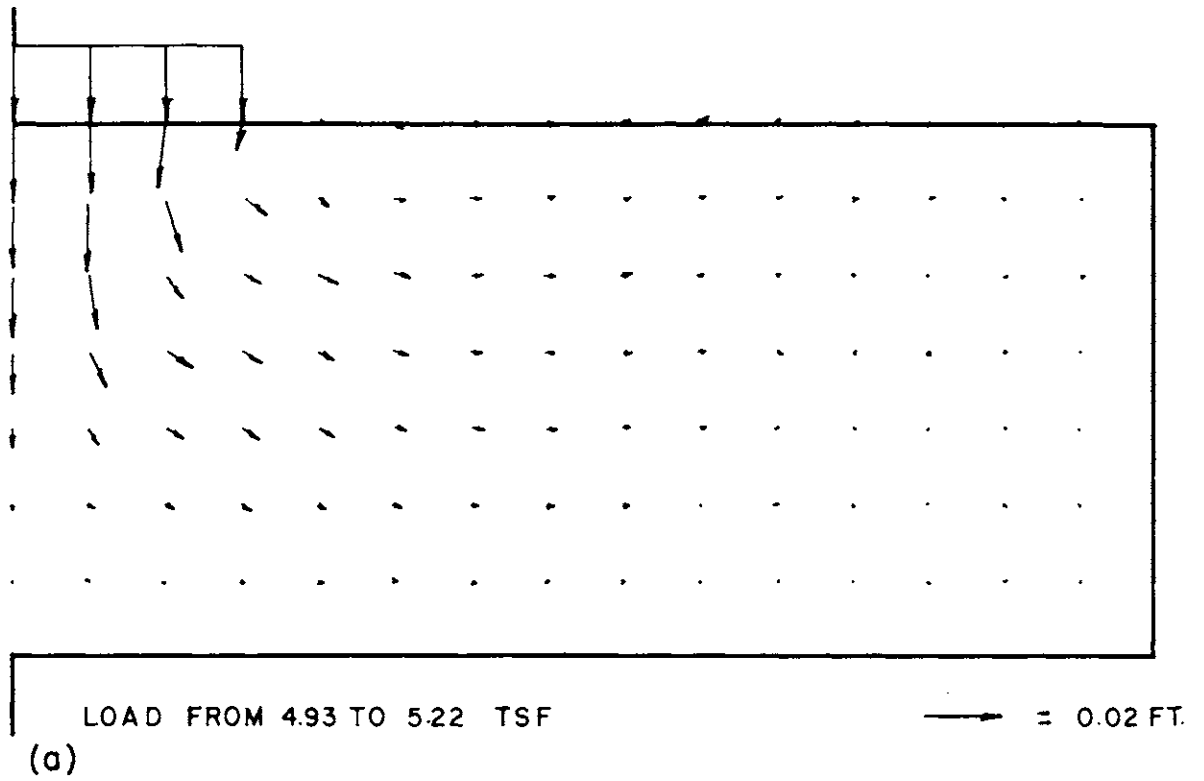


FIG.73 INCREMENTAL DISPLACEMENTS - RUN 9



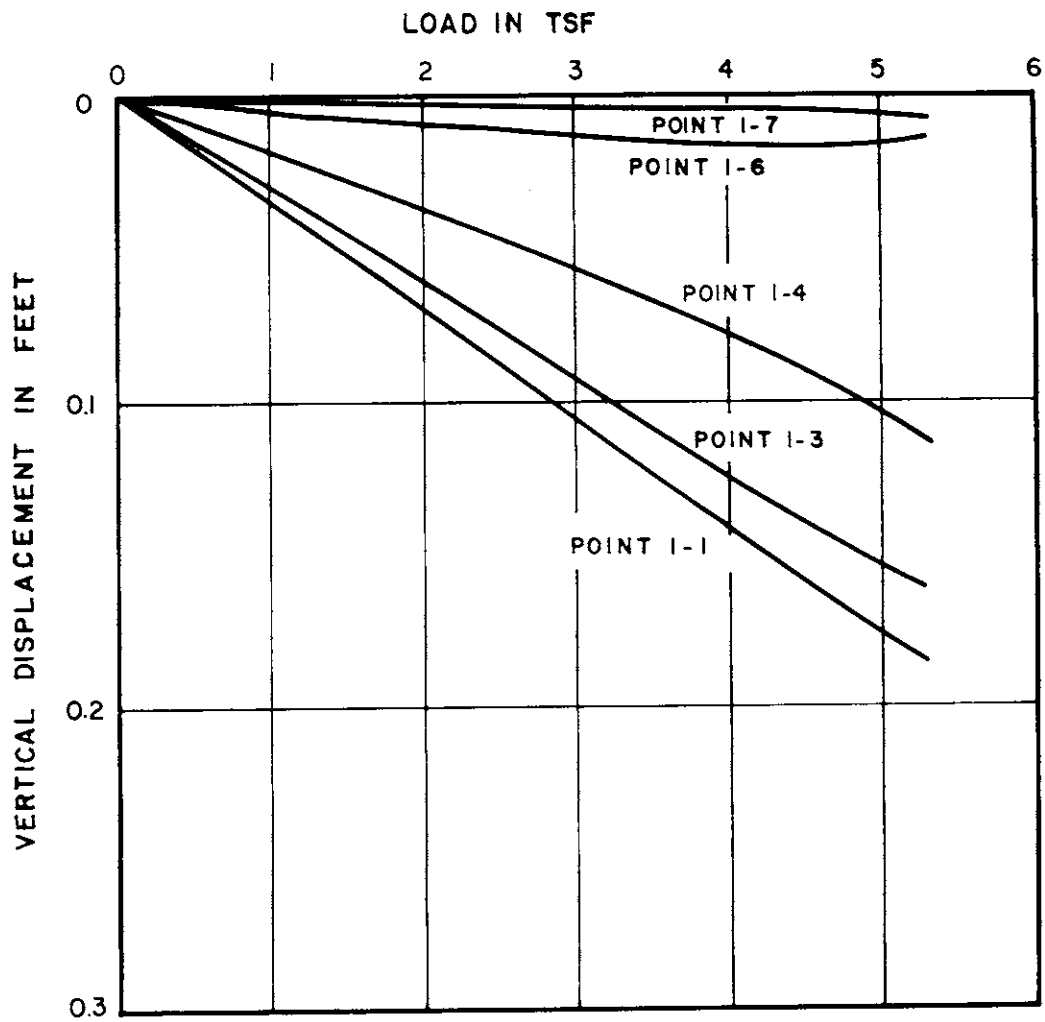


FIG.74 DRUCKER PRAGER DISPLACEMENTS

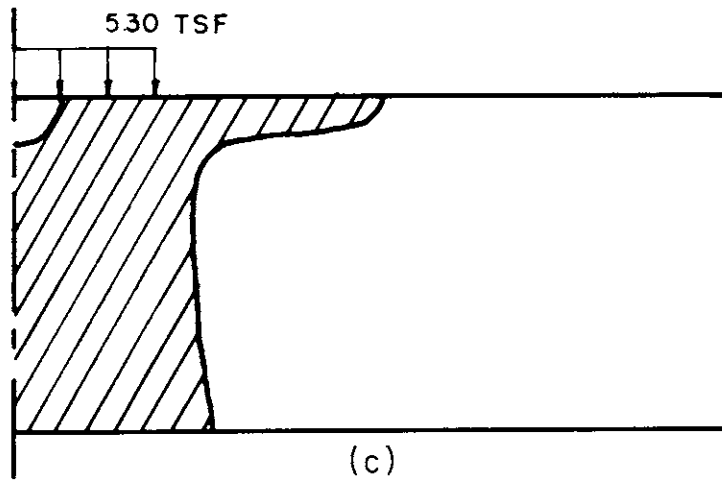
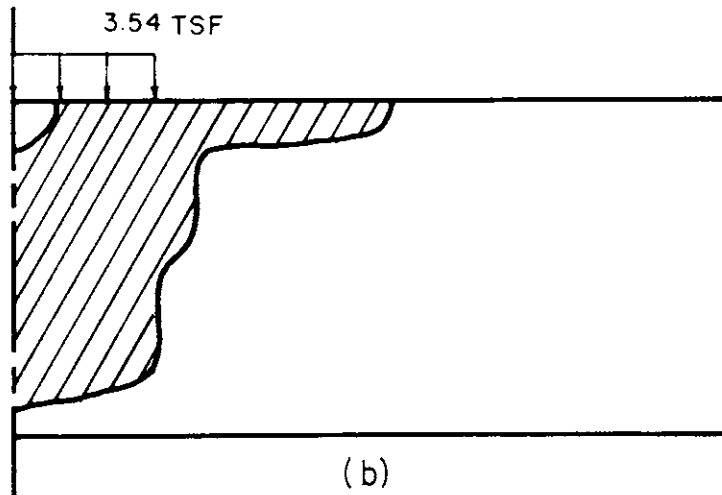
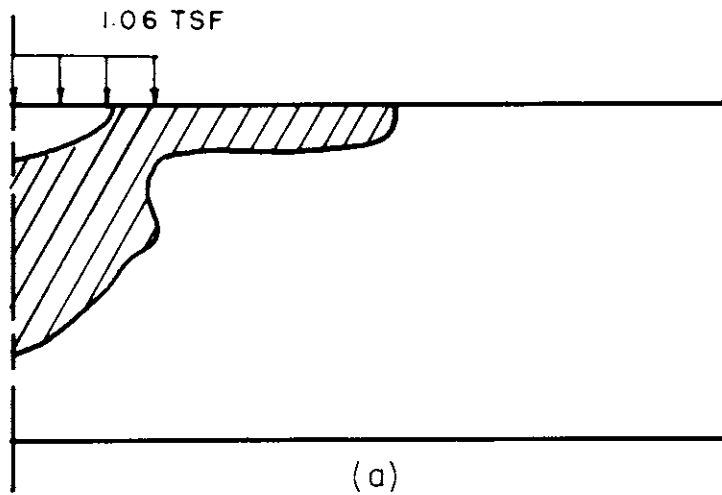


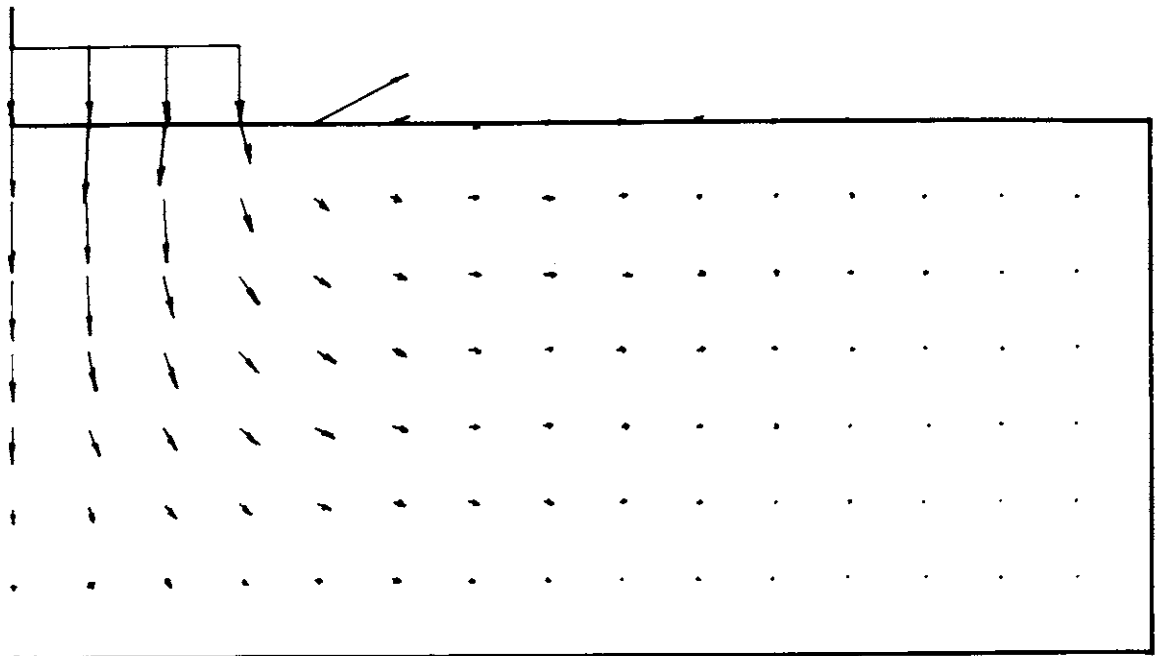
FIG. 75 SPREAD OF PLASTIC ZONE - RUN 12

243

-99-01	-100-01	-90-11	-11-10	01 00	00-01	00 00	00 01	00 01	00 01	00 01	00 00	00 00	00 00	00 00	00 00	00 00
-48-44	-46-44	-34-55	-13-19	04 03	-03 01	-02 01	-03 02	-04-01	-05-02	-06-02	-07-02	-07-02	-08-02	-08-02	-08-02	-08-02
-98-01	-96-07	-71-21	-29-21	-03-08	-01-02	-02-01	00 01	00 01	00 01	00 01	00 00	00 00	00 00	00 00	00 00	00 00
-37-50	-34-56	-30-51	-30-26	-21-07	-13-04	-12-04	-10-03	-09-03	-08-02	-08-02	-08-02	-08-02	-08-02	-08-02	-08-02	-08-02
-94-02	-82-12	-62-20	-38-22	-15-16	-05-07	-03-03	-02-01	00 00	00 00	00 00	00 00	00 00	00 00	00 00	00 00	00 00
-30-55	-27-54	-26-41	-26-24	-27-13	-22-08	-16-06	-14-05	-12-04	-10-03	-09-03	-08-02	-08-02	-08-02	-07-02	-07-02	-07-02
-86-05	-74-14	-57-20	-39-21	-23-17	-12-12	-15-07	-03-04	-01-03	00-02	00-01	00-01	00-01	00-01	00 00	00 00	00 00
-25-55	-23-47	-23-36	-24-20	-24-14	-23-10	-19-07	-16-06	-13-04	-11-03	-09-03	-08-02	-07-02	-07-02	-07-02	-06-02	-06-02
-76-05	-67-14	-64-18	-41-20	-27-18	-17-14	-09-10	-05-07	-02-05	-01-04	00-03	00-02	00-01	00-01	00-01	00 00	00 00
-19-48	-19-40	-20-30	-21-19	-22-14	-20-11	-18-08	-15-06	-13-04	-10-03	-09-03	-07-02	-06-02	-06-02	-06-02	-05-02	-05-02
-66-05	-59-13	-51-18	-41-20	-30-18	-20-15	-12-12	-07-10	-04-07	-02-05	-01-04	-01-03	00-02	00-01	00 00	00 00	00 00
-16-37	-17-32	-18-26	-18-18	-18-14	-17-11	-15-08	-13-06	-10-04	-08-03	-07-02	-05-02	-05-02	-04-01	-04-01	-04-01	-04-01
-56-04	-53-12	-47-17	-40-20	-31-19	-22-17	-15-15	-10-12	-06-09	-04-07	-03-05	-02-04	-01-02	-01-01	-01-01	-01 00	-01 00
-17-25	-18-24	-18-21	-17-18	-16-14	-13-11	-11-08	-08-06	-06-04	-05-03	-04-02	-03-02	-03-02	-02-01	-02-01	-02-01	-02-01

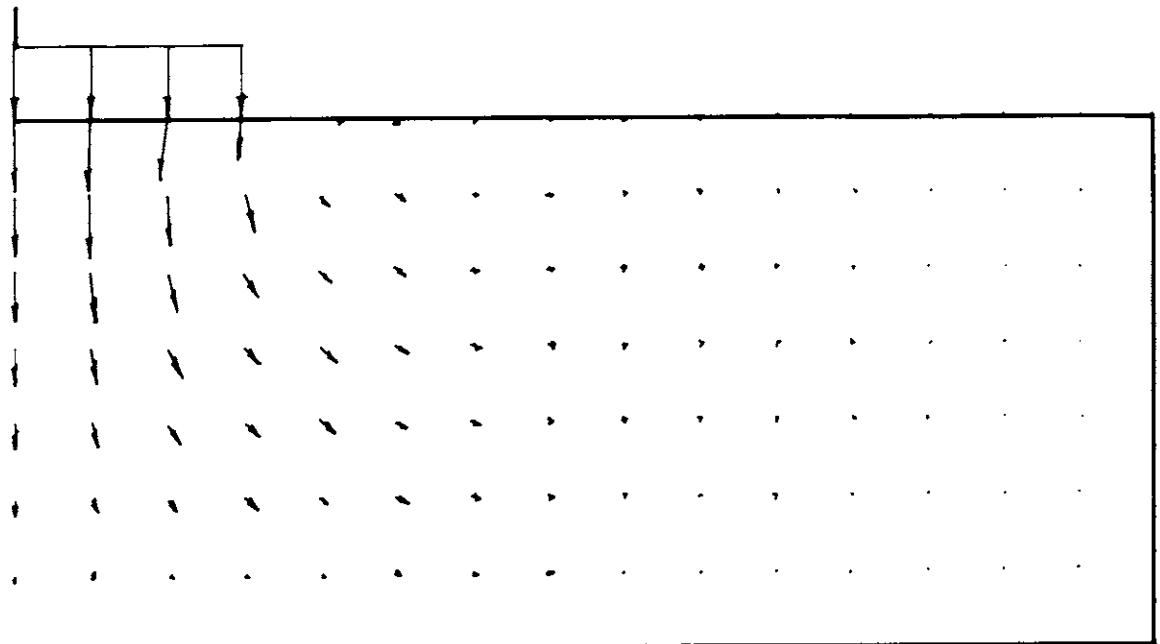
LOAD = 5.30 TSF

FIG. 76 NORMALIZED STRESSES - RUN 12



LOAD FROM 4.60 TO 5.30 TSF  
 (a)

→ = 0.025 FT.



LOAD IS 5.30 TSF  
 (b) FINAL DISPLACEMENTS

→ = 0.2 FT.

FIG.77 DISPLACEMENTS - RUN 12

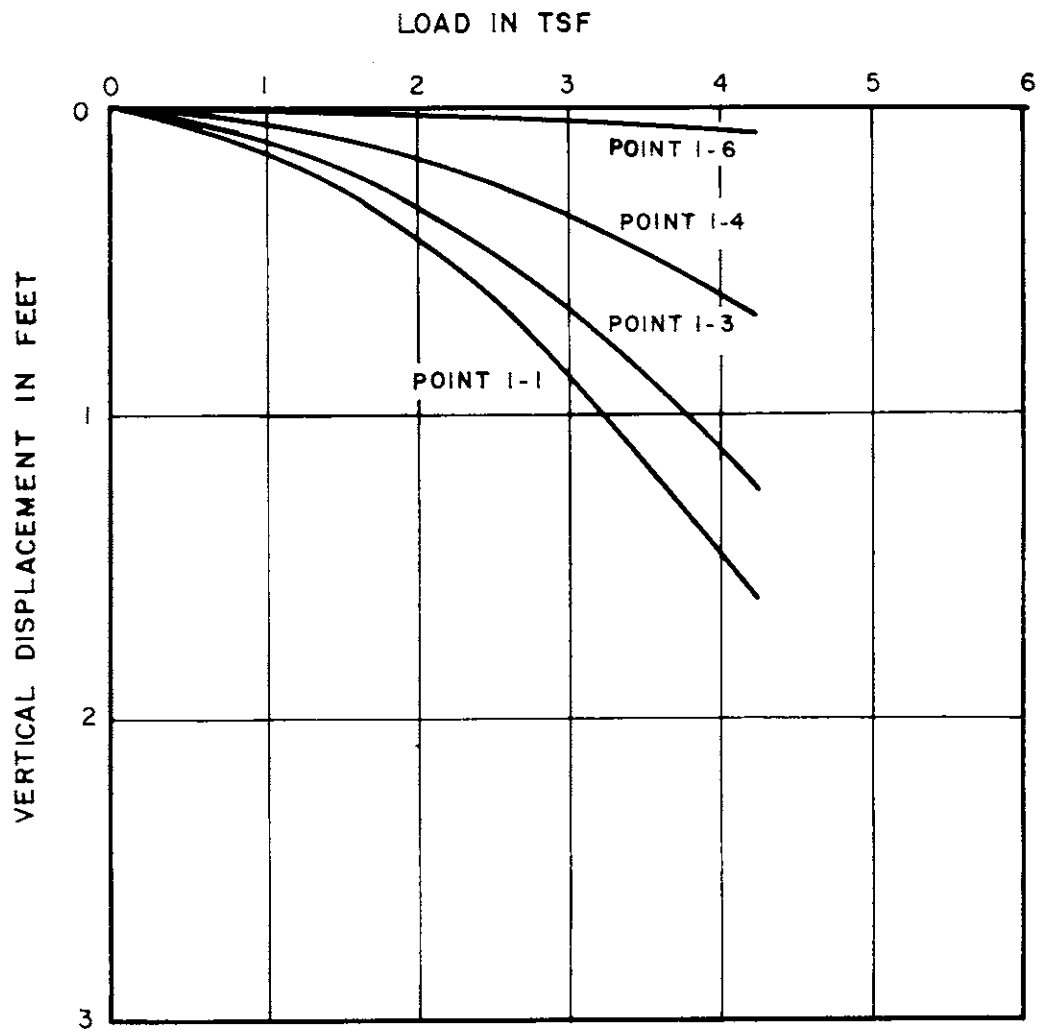
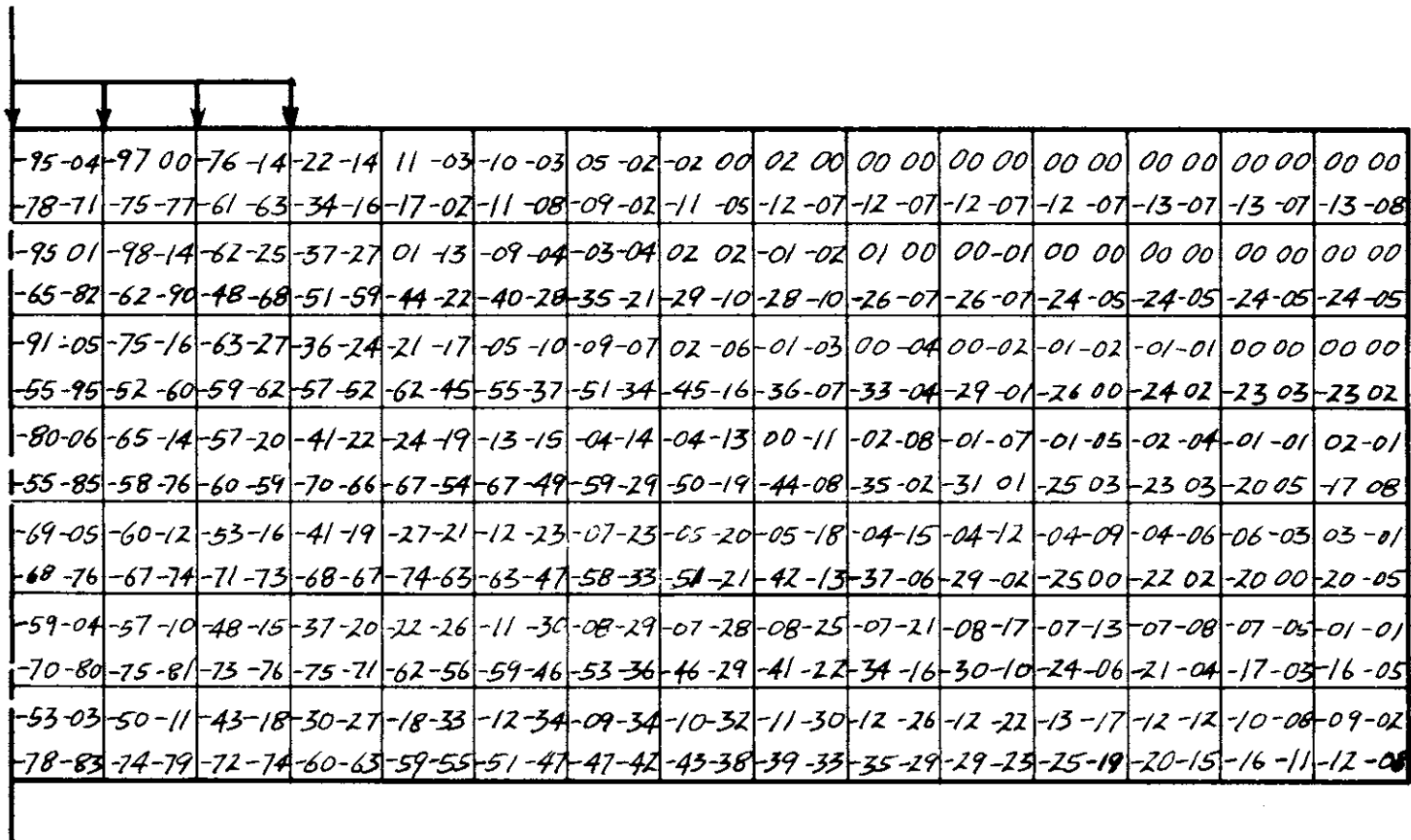


FIG. 78 VERTICAL DISPLACEMENTS - RUN 11



LOAD = 4.24 TSF

FIG. 79 NORMALIZED STRESSES - RUN 11

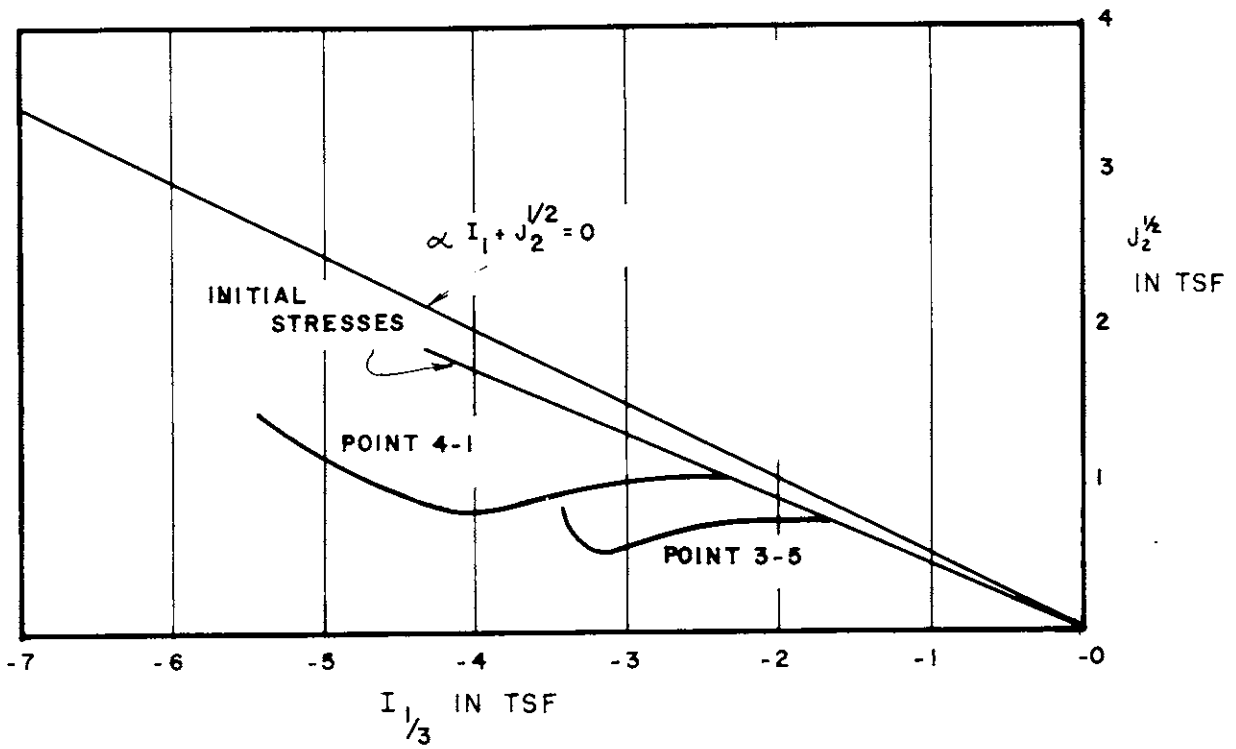


FIG. 80 STRESS PATHS - RUN II

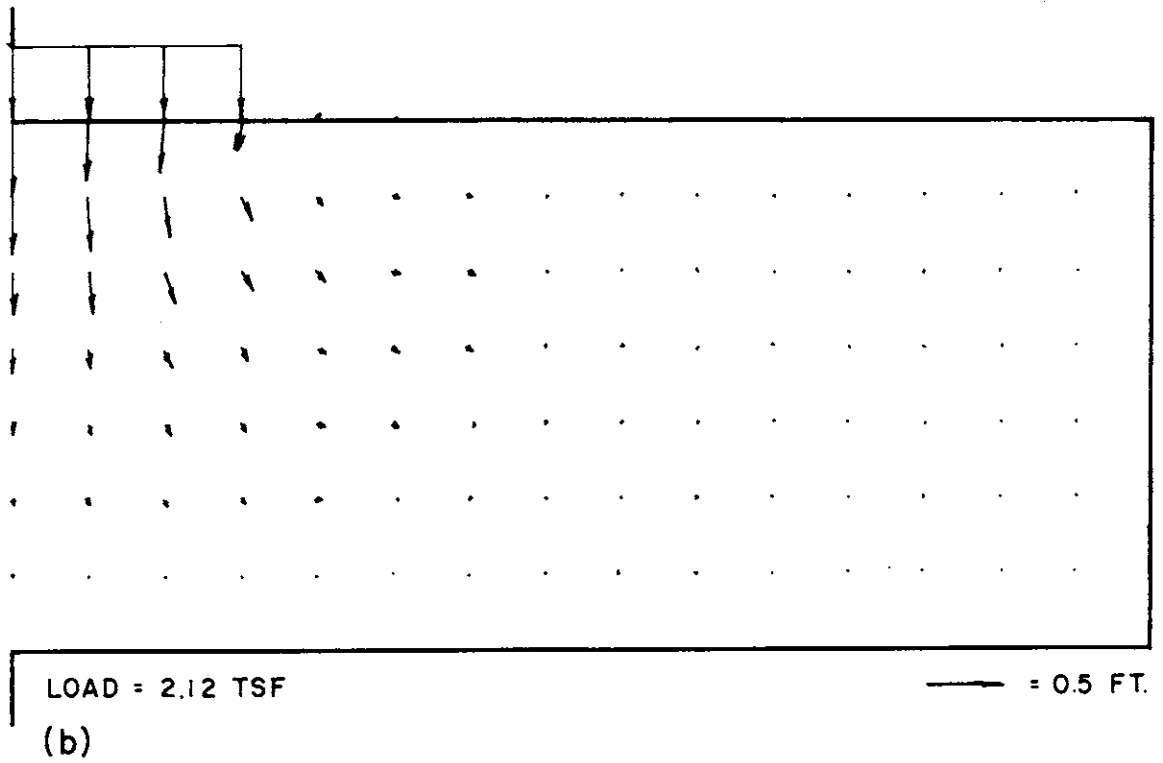
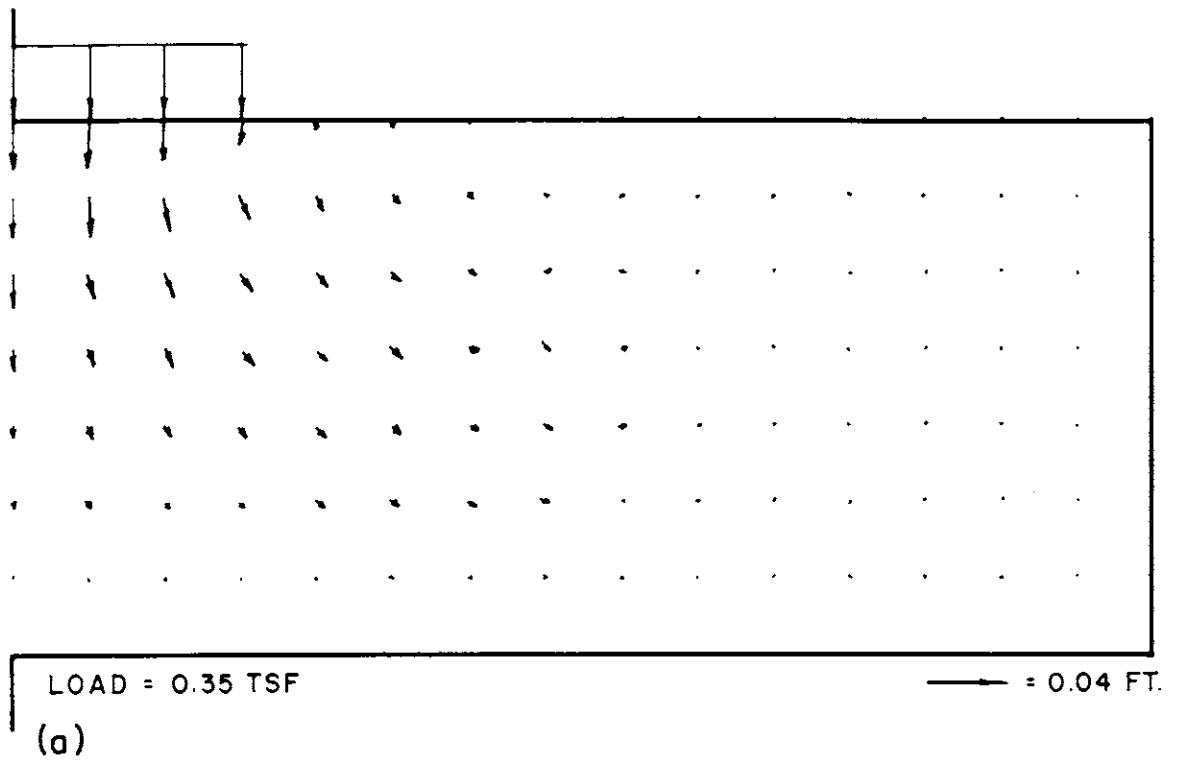


FIG. 81 DISPLACEMENT FIELDS - RUN II



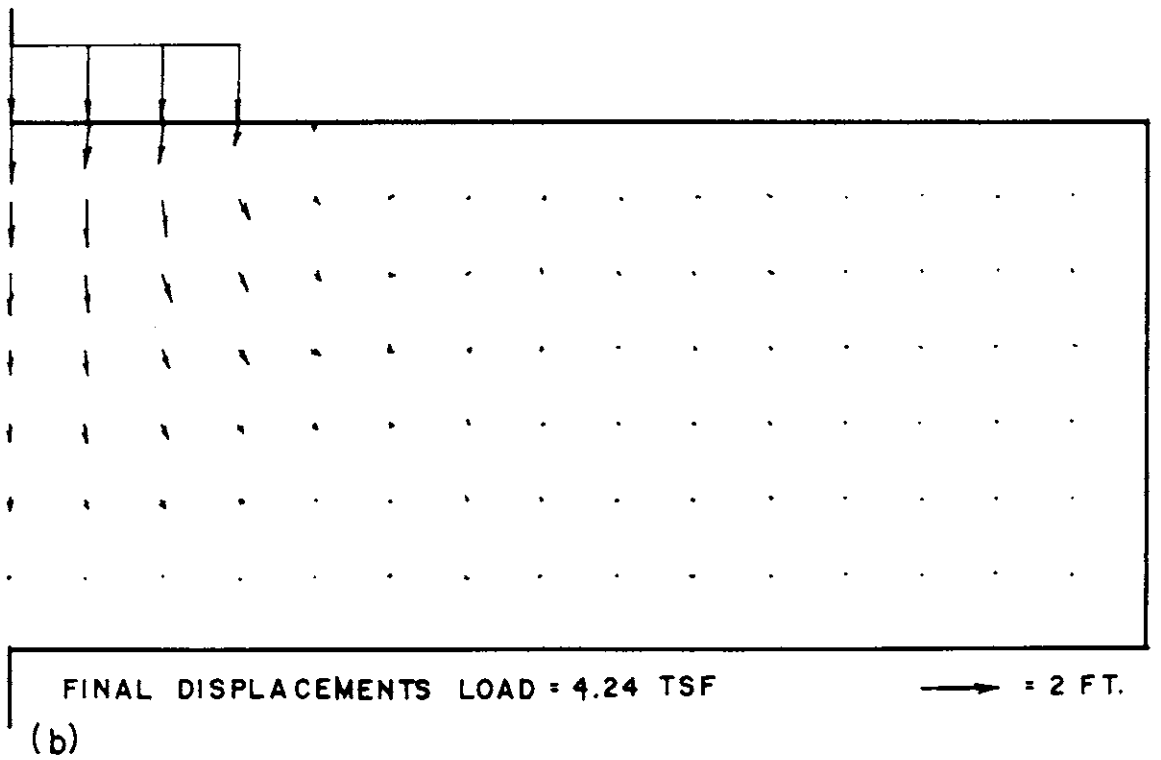
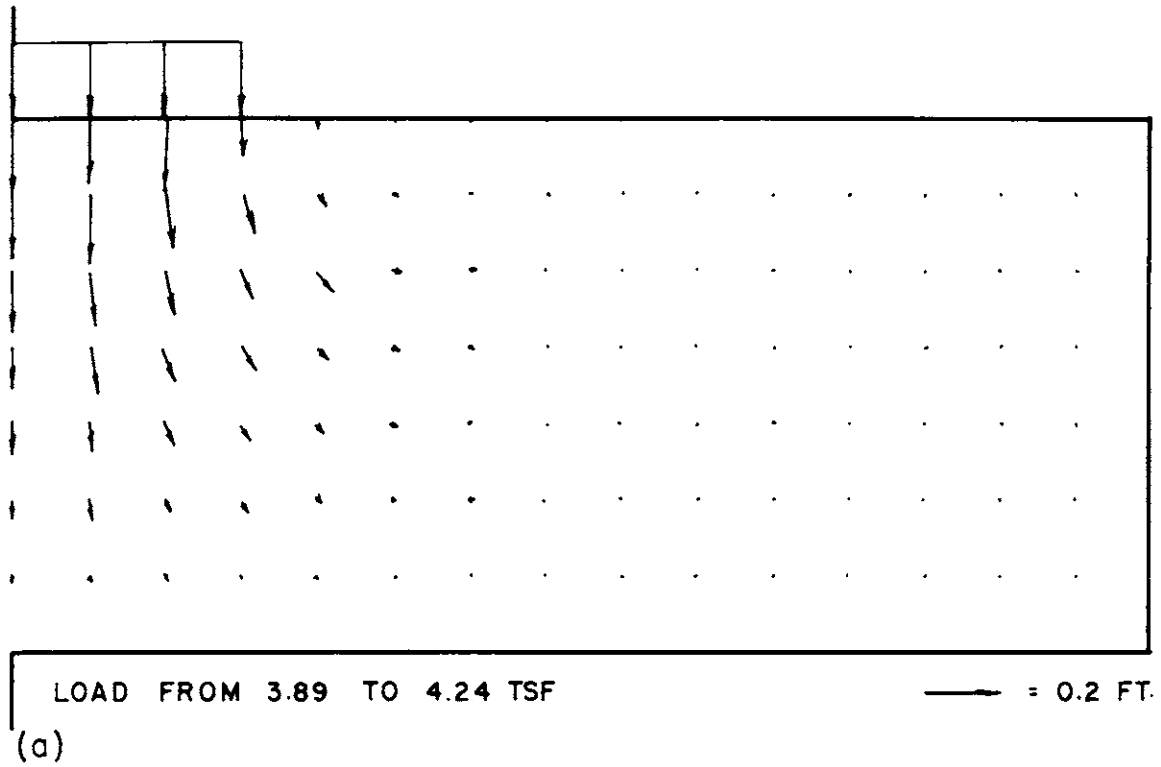


FIG. 82 INCREMENTAL DISPLACEMENTS - RUN II

TABLE I  
COMPUTER PROGRAMS

Program Name	Material/Criterion Name	Yield Function
MASS-TR (PERFPLAS)	Tresca	$ \frac{\sigma_1 - \sigma_3}{2}  - k = 0$
MASS-PR	Prandtl-Reuss/ Hencky-von Mises	$\frac{1}{J_2^2} - k = 0$
PLUSS	Tresca with no Elastic Volume Change	$ \frac{\sigma_1 - \sigma_3}{2}  - k = 0$
MASS-DP	Drucker-Prager	$\alpha I_1 + \frac{1}{J_2^2} - k = 0$
MASS-SH	Strain Hardening	$\frac{(I_1/3 - p_0)^2}{a^2} + \frac{J_2}{b^2} = 0^*$
PLANE	Linearly Elastic- Drained or Un- drained	NONE

\* For the strain hardening material  $a/b = D$  and all ellipsoids are have half axis  $b$  passing through the surface  $\alpha I_1 + \frac{J_2}{2} - k = 0$ .

TABLE II  
RUNS MADE

Run No.	Program	Horizontal Distance From $\zeta$ to Boundary in Ft.	Vertical Depth of Soil in Ft.	Final Load in TSF	E in TSF	$\nu$	k in TSF	$\alpha$	$\gamma$ in TSF	Other
1	MASS-TR	280 Ft.	140 Ft.	8.47	3,000	0.2	1.75	-	-	
2	"	"	"	9.02	3,000	0.3	1.75	-	-	
3	"	300 Ft.	"	8.95	3,000	0.4	1.75	-	-	
4	"	280 Ft.	"	8.82	3,000	0.5	1.75	-	-	
5	PLUSS	"	"	8.89	865	0.5	1.75	-	-	
6	"	"	"	8.28	3,000	0.5	1.75	-	-	Smooth Bottom
7	"	"	"	4.27	865	0.5	1.75	-	-	Smooth Bottom, Free Side
8	"	"	"	8.95	865	0.5	1.75	-	-	Initial Stress = 0.5k
9	MASS-PR	300 Ft.	"	5.22	3,000	0.3	1.75	-	-	Initial
10	PLUSS	280 Ft.	"	9.00	865	0.5	1.75	-	-	Initial Stress = -0.5k
11	MASS-SH	300 Ft.	"	4.24	3,000	0.3	0	0.165	0.05	D=2, k=0.5 C=600 TSF
12	MASS-DP	"	"	5.30	3,000	0.3	0	0.165	0.05	$k_o=0.5$

- Notes:
1. Effective stress  $\nu$  for all PLUSS runs is 0.3. Effective stress E for PLUSS runs is 2,000 TSF when total stress E is 3,000 TSF and 750 TSF when total stress E is 865 TSF.
  2. Bottom is fixed, side is smooth, and top is free unless otherwise noted.